Messengers Outer Space: Exploring Extracellular Vesicles of *Ustilago maydis* and their mRNA Cargo

Inauguraldissertation

zur Erlangung des Doktorgrades
der Mathematisch-Naturwissenschaftlichen Fakultät
der Heinrich-Heine-Universität Düsseldorf

vorgelegt von

Seomun Kwon

aus Seoul, Korea

Düsseldorf, Dezember 2021

aus dem Institut für Mikrobiologie

der Mathematisch-Naturwissenschaftlichen Fakultät

der Heinrich-Heine-Universität Düsseldorf

Gedruckt mit der Genehmigung der

Mathematisch-Naturwissenschaftlichen Fakultät der

Heinrich-Heine-Universität Düsseldorf

Referent: Prof. Dr. Michael Feldbrügge

Korreferent: Prof. Dr. Laura Rose

Tag der mündlichen Prüfung: 02.03.2022

The research presented in this thesis was conducted from April 2016 until March 2021 in Düsseldorf at the Institute for Microbiology, Heinrich Heine University Düsseldorf, under the supervision of Prof. Dr. Michael Feldbrügge.

Düsseldorf, den _____

_____

Seomun Kwon

I hereby confirm that for each published or prepared manuscript included in this thesis, the specific contributions of the doctoral researcher, Seomun Kwon, and the other co-authors have been accurately stated.

Düsseldorf, den _____

_____

Prof. Dr. Michael Feldbrügge

Statutory declaration

I declare under oath that I have produced my thesis independently and without any undue assistance by third parties under consideration of the 'Principles for the Safeguarding of Good Scientific Practice at Heinrich Heine University Düsseldorf. No other person's work has been used without due acknowledgement. Experimental work for this thesis has been conducted at Heinrich Heine University Düsseldorf. This dissertation has not been submitted in the current or similar form to other institutions or faculties. I have not previously failed a doctoral examination procedure.

Eidesstattliche Erklärung

Ich versichere an Eides Statt, dass die Dissertation von mir selbständig und ohne unzulässige fremde Hilfe unter Beachtung der „Grundsätze zur Sicherung guter wissenschaftlicher Praxis an der Heinrich-Heine-Universität Düsseldorf" erstellt worden ist. Keine andere Person wirkte an der Arbeit ohne entsprechende Nennung mit. Experimentelle Arbeiten für diese Dissertation wurden an der Heinrich-Heine-Universität Düsseldorf angefertigt. Die Dissertation wurde in ihrer jetzigen oder ähnlichen Form noch bei keiner anderen Hochschule oder Fakultät eingereicht. Ich habe zuvor keine erfolglosen Promotionsversuche unternommen.

Düsseldorf, den _____

_____

Seomun Kwon

In memory of all the

failed experiments and ideas

that paved way for better ones

Table of Contents

Summary

Extracellular vesicles (EVs) are emerging as important vehicles for molecular plant-pathogen interactions. Examining cargo molecules of EVs produced by phytopathogenic fungi has the potential to discover novel types of effector molecules that alter host plant physiology for the benefit of the pathogen. Presented in this thesis is a pioneering investigation on EV-associated mRNAs from the maize smut fungus *Ustilago maydis*. The project was driven by the original hypothesis that intact fungal mRNAs can be delivered to plant cells via EVs, where they are translated to produce effector proteins using host resources. The strategy was to first study *U. maydis* EVs from axenic culture, then proceed to more complex samples from infected plants. In order to identify EV cargos that are more relevant for infection, a synthetic strain was utilised, where a set of known effectors and infection-associated genes can be induced in axenic culture. A highly reproducible method was established for preparing EVs from such induced cultures of *U. maydis,* resulting in an inventory of EV-associated mRNAs. Initial insights on selective loading and functionality of EV cargo mRNAs could be gained from the *U. maydis* axenic culture system. mRNAs of known virulence proteins were found in the culture-derived EVs, supporting the potential to discover novel virulence-associated mRNAs with this strategy. Several functionally interesting candidate mRNA effectors were identified, that are both enriched in EVs and highly upregulated during infection. Importantly, the top candidate mRNA effectors tested were intact, so they could theoretically be translated into functional proteins in the plant cell. mRNAs encoding proteins with metabolic enzyme activities were especially enriched in EVs, so a single fungal mRNA molecule delivered and translated could produce profound effects in the host cell. For studying *U. maydis* EVs produced during infection, a method was developed to isolate EVs from the apoplastic washing fluid of infected maize plants. Furthermore, a tagged syntaxin marker was designed for *U. maydis* EVs for visualisation and purification from infected plant materials. Using this marker, production of EV-like structures could be observed *in planta*. With the tools and methods developed in this thesis, it is now possible to cross-examine the transcriptome and proteome of both axenic culture-derived EVs and EVs from infected plants to identify high-confidence, biologically interesting cargos for in-depth investigations. The data and methods presented in this thesis should serve as a foundation for future studies on *U. maydis* EV cargos and their role in interaction with the host plant.

Zusammenfassung

Extrazelluläre Vesikel (EVs) gewinnen zunehmend Bedeutung als wichtigen Vehikel für die molekulare Interaktionen zwischen Pflanzen und Pathogenen. Die Untersuchung der Frachtmoleküle von EVs, die von phytopathogenen Pilzen produziert werden, birgt das Potenzial, neue Arten von Effektoren zu entdecken, die die Physiologie der Wirtspflanze zum Nutzen des Pathogens manipulieren. In dieser Pionierarbeit über EVs aus dem Maisbeulenbrandpilz *Ustilago maydis* wird die Untersuchung von EV-assoziierten mRNAs vorgestellt. Das Projekt fußt auf der Hypothese, dass intakte pilzliche mRNAs durch EVs in Pflanzenzellen transportiert werden können, wo sie mittels Wirtsressourcen translatiert werden, um Effektorproteine zu produzieren. Die Strategie bestand darin, zunächst die EVs von *U. maydis* aus axenischen Kulturen zu untersuchen, um anschließend zu komplexeren Proben aus infiziertem Pflanzenmaterial überzugehen. Um die für die Infektion relevanten EV-Fracht zu identifizieren, wurde ein synthetischer Stamm verwendet, bei dem bekannte Effektoren und infektionsassoziierte Gene in axenischer Kultur induziert werden können. Eine hoch reproduzierbare Methode zur Isolation von EVs aus diesen induzierten *U. maydis* Kulturen wurde entwickelt. Mit dieser wurde ein Inventar von EV-assoziierten mRNAs erstellt. Dieses axenische *U. maydis* Kultursystem ermöglichte erste Einblicke in die selektive Beladung und Funktionalität von EV-Fracht-mRNAs. In den aus der Kultur stammenden EVs wurden mRNAs bekannter Virulenzproteine gefunden, was das Potenzial unterstützt, mit dieser Strategie neue virulenzassoziierte mRNAs zu entdecken. Es wurden weiterhin mehrere, funktionell interessante mRNA-Effektorkandidaten identifiziert, die sowohl in EVs angereichert, als auch während der Infektion hochreguliert sind. Wichtig ist, dass intakte mRNAs in voller Länge für alle getesteten Kandidaten nachgewiesen werden konnten, sodass sie theoretischin von der Pflanzenzelle in funktionelle Proteine translatiert werden könnten. Stoffwechselenzym-kodierende mRNAs waren in EVs besonders angereichert, was darauf hindeutet, dass ein einzelnes in die Wirtszelle übertragenes und translatiertes Pilz-mRNA-Molekül potentiell tiefgreifende Auswirkungen auf die Wirtsphysiologie haben könnte. Zur Untersuchung der während der Infektion von *U. maydis* produzierten EVs, wurden Methoden zur EV-Isolation aus apoplastischer Waschflüssigkeit infizierter Maispflanzen angewandt. Zur Visualisierung und Anreicherung von Pilz-EVs aus infiziertem Pflanzenmaterial, wurde ein Marker für *U. maydis*-EVs entwickelt. Mit diesem Marker konnte die Produktion von EV-ähnlichen Strukturen *in planta* beobachtet werden. Mit den in dieser Arbeit entwickelten Werkzeugen und Methoden ist es nun möglich, das Transkriptom und Proteom von EVs zu untersuchen, die aus axenischer Kultur und aus infizierten Pflanzen gewonnen wurden. Die in dieser Arbeit vorgestellten Daten und Methoden sollten als Grundlage für künftige Studien über *U. maydis*-EVs und ihre Rolle bei der Interaktion mit der Wirtspflanze dienen.

Abbreviations

AWF	Apoplastic washing fluid	**ml**	Millilitre
bp	Basepair	**mm**	Millimetre
cDNA	Complementary DNA	**mM**	Millimolar
CDS	Coding DNA sequence	**mRNA**	Messenger RNA
cm	Centimetre	**MVE**	Multivesicular endosome
CM	Complete medium	**MWCO**	Molecular weight cut-off
DIC	Differential interference contrast	**µg**	Microgram
DNA	Deoxyribonucleic acid	**µl**	Microlitre
DNase	Deoxyribonuclease	**µm**	Micrometre
dpi	Days post inoculation	**µM**	Micromolar
dsRNA	Double-stranded RNA	**NA**	Numerical aperture
eGFP	Enhanced green fluorescent protein	**NLS**	Nuclear localisation signal
ESCRT	endosomal sorting complex required for transport	**nm**	Nanometer
EV	Extracellular vesicle	**NM**	Nitrate minimal medium
g	Gram	**nt**	Nucleotide(s)
HIGS	Host-induced gene silencing	**OD**	Optical density
hpi	Hours post inoculation	**padj**	Adjusted p-value
kb	Kilobase	**PIGS**	Pathogen-induced gene silencing
kDa	Kilodalton	**PoC**	Proof of concept
ILV	Intraluminal vesicle	**RBP**	RNA-binding protein
l	Litre	**RNA**	Ribonucleic acid
Log2FC	Log2 fold change	**RNAi**	RNA interference
M	molar	**RNase**	Ribonuclease
mbar	Millibar	**RNP**	Ribonucleoprotein
mg	Milligram	**rpm**	Revolutions per minute

rRNA	Ribosomal RNA	**TEM**	Transmission electron microscopy
RT-PCR	Reverse transcription polymerase chain reaction	**TPM**	Transcripts per million
RT-qPCR	Reverse transcription-quantitative polymerase chain reaction	**tRNA**	Transfer RNA
SA	Salicylic acid	**UPR**	Unfolded protein response
SEC	Size-exclusion chromatography	**UTR**	Untranslated region
siRNA	Small interfering RNA	**v/v**	Volume per volume
sRNA	Small RNA	**w/v**	Weight per volume
tasiRNA	Trans-acting small interfering RNA	**x g**	Times gravity (relative centrifugal force)

1. Introduction

1.1. Definition of extracellular vesicles (EVs)

Biological membranes serve the fundamental function of delimiting cells and compartmentalising them into organelles. Vesicles are membrane-bound structures that can transport molecules both inside and outside a cell. For example, within a cell, endocytic and secretory vesicles are formed for uptake and secretion of molecules and are trafficked throughout the cell. Extracellular vesicles (EVs), on the other hand, are released from cells into the extracellular milieu. Besides the constituent membrane lipids, EVs carry diverse proteins (Choi et al., 2020), RNA (O'Brien et al., 2020), DNA (Malkin and Bratman, 2020), polysaccharides (Rodrigues et al., 2007), as well as metabolites (Williams et al., 2019) (Figure 1-1A). Importantly, EVs represent a means of protected, bulk transport of otherwise intracellular components across the extracellular space, and can deliver the cargo molecules to recipient cells. Thus, cells can influence the external environment and communicate with other cells via EVs. In this thesis, EVs produced by a plant-pathogenic fungus, *Ustilago maydis*, will be explored with a special focus on the mRNA cargo of EVs.

"EVs" is an umbrella term for membrane-bound nanoparticles of diverse origin (van Niel et al., 2018). Based on their mechanism of biogenesis, EVs can be largely subcategorized into exosomes and microvesicles (Figure 1-1B). Exosomes are intraluminal vesicles (ILVs) within maturing, multivesicular endosomes (MVEs; also called multivesicular bodies) that are released upon fusion of the MVE with the plasma membrane, while microvesicles are formed by direct budding of the plasma membrane (van Niel et al., 2018). Exosomes are smaller, with diameters of 50 - 150 nm, due to space limitation within MVEs, and microvesicles generally range between 50 - 500 nm (van Niel et al., 2018). While different EV subtypes have typical protein compositions (Kowal et al., 2016), there is substantial overlap between proteomes of exosomes and microvesicles, in part due to shared biogenesis factors such as the endosomal sorting complex required for transport (ESCRT) complex (van Niel et al., 2018). There are additional names for EV subtypes specific to certain cellular states or identities: for example, apoptotic bodies produced from cell disassembly during apoptosis (Caruso and Poon, 2018) and outer membrane vesicles are specific to gram-negative bacteria (Jan, 2017). A recently defined group of smaller extracellular particles (< 50 nm) called exomeres are sometimes considered a subtype of EVs, although they are allegedly membraneless and their route of biogenesis is unknown (Zhang et al., 2018).
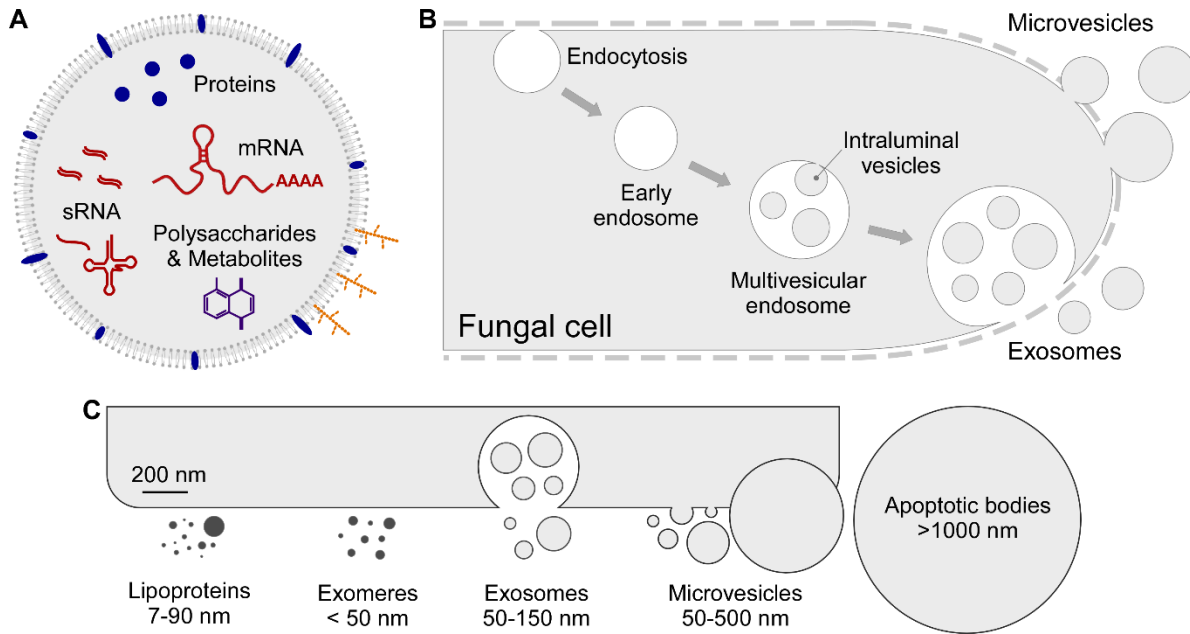
Figure 1-1. Extracellular vesicle (EVs): molecular cargos and biogenesis.
A. EVs are composed of a lipid bilayer enclosing diverse molecules from cells. EVs typically carry proteins, sRNAs, and both intact and fragmented mRNAs. Fungal EVs may additionally contain secondary metabolites (Bleackley et al., 2020) or be decorated with polysaccharides (Rizzo et al., 2021b). **B.** Biogenesis of two major EV subtypes, microvesicles and exosomes. Microvesicles bud directly from the plasma membrane. Exosomes are originally intraluminal vesicles inside multivesicular endosomes (MVEs) that are released upon MVE fusion with the plasma membrane. In fungi, EVs are secreted through the cell wall by an as yet unknown mechanism. **C.** Size range of EVs and co-purified particles. Typical EV subtypes, exosomes and microvesicles, range from 50 – 500 nm diameter (van Niel et al., 2018), but EVs produced during apoptosis can be much larger (Caruso and Poon, 2018). Exomeres (Zhang et al., 2018) and lipoproteins (German et al., 2006) are smaller particles that overlap in size with EVs and are often co-purified.

A confounding problem in the EV field is the difficulty to isolate specific EV subtypes due to their overlapping biophysical characteristics (Figure 1-1C) and the lack of highly specific markers found consistently across different studies and different organisms (Théry et al., 2018). This is further complicated by the variability arising from the use of different cell types, culture conditions and EV isolation methods. While most standards for EV research have been set in the mammalian field (Théry et al., 2018), the study of fungal EVs is in its infancy and this thesis is one of the first documentations on EVs of the maize smut fungus *Ustilago maydis* (details on the system is covered in section 1.6.). Therefore, due to the paucity of data to distinguish between subtypes, this thesis will deal with a heterogeneous population of *U. maydis* EVs as a whole.

1.2.   Biological functions of EVs and how they deliver cargos to recipient cells

Once considered to be artefacts or a mere cellular disposal mechanism, an ever-growing body of evidence illustrates diverse biological functions of EVs (Harding et al., 2013). A particularly interesting function of EVs is in mediating intercellular communication. EVs secreted by one cell can be taken up by another, and the delivered molecules can bring about a physiological effect on the recipient cell.

Here I will consider four non-mutually exclusive reasons why cells produce EVs:

1. as by-products of cellular processes
2. for disposal or sequestration of molecules
3. for formation and remodelling of external structures
4. for intercellular communication

The first notion assumes passive, non-specific loading of EVs, only representing the state of the source cells or the subcellular environment at the site of EV formation. The latter three assume active loading with a degree of specificity in cargo selection for a biological purpose. Given that EV populations are highly heterogeneous in their origin and their cargos, the reality is a combination of the above. Even apoptotic bodies, which would at first sight fit the first category, were found to disseminate signals to promote clearance of apoptotic cells, as well as having immunomodulatory effects like other mammalian EV subtypes (Caruso and Poon, 2018).

The role of EVs in disposal of unneeded components was first illustrated by shedding of unneeded transferrin receptors via exosomes during maturation of red blood cells (Harding and Stahl, 1983, Pan and Johnstone, 1983). Furthermore, as a mechanism of resistance against the bacterial Shiga toxin, blood cells can shed the toxin at the plasma membrane via microvesicles before internalisation (Willysson et al., 2020). Similarly, drug resistance of cancer cells (Maacha et al., 2019) and parasites (Davis et al., 2020) can be facilitated by drug sequestration and export in EVs. Interestingly, outer membrane vesicles of pathogenic gram-negative bacteria can act as protective decoys that sequester membrane-targeting antibiotic drugs outside the cells (Sabnis et al., 2018).

EVs have also been implicated in formation of external protective structures. For example, EVs of the clinically important fungus *Cryptococcus neoformans* carry the macromolecular polysaccharide glucuronoxylomannan, which is both a constituent of the protective external capsule structure (Rodrigues et al., 2007). Acapsular strains can form capsules when supplied with EVs from a capsule-forming strain, suggesting that EVs are the mechanism by which glucuronoxylomannan is delivered beyond the cell wall

for capsule growth (Rodrigues et al., 2007). In plants, exosomes harbouring syntaxin PEN1/ROR2 have been linked to formation of defense structures called papillae and encasements against invading pathogens (Hansen and Nielsen, 2017). Furthermore, cell wall-related proteins are commonly found in both plant (Regente et al., 2017, Rutter and Innes, 2017) and fungal EVs (Zhao et al., 2019), suggesting a role of EVs in cell wall remodelling.
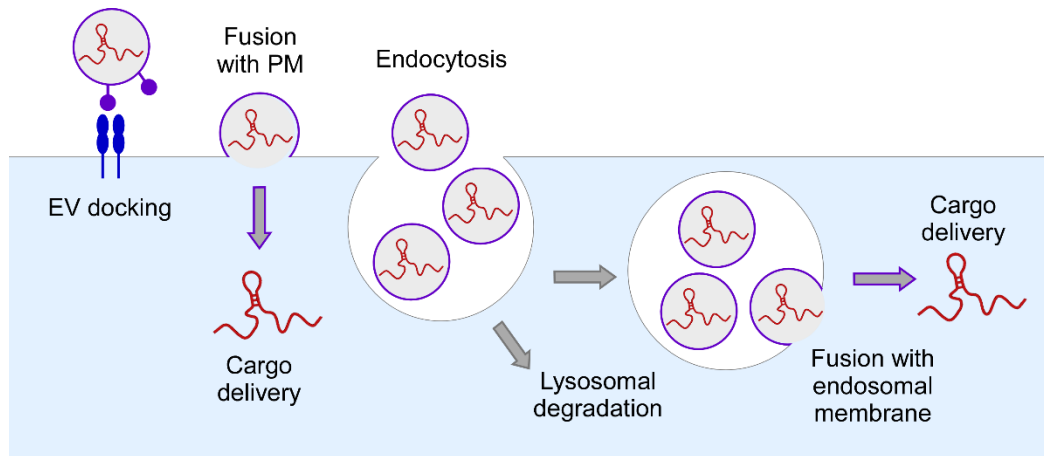

Figure 1-2. Model of EV cargo delivery into recipient cells.
For intercellular communication, EVs from one cell can deliver their cargos to another recipient cell. EVs can be targeted to and bind the plasma membrane (PM) of the recipient cell via surface molecules. This may facilitate fusion of the EV with the PM or uptake of EVs by endocytosis (van Niel et al., 2018). Intraluminal cargo of EVs can be delivered to the cytosol of the recipient cell by fusion of the EV membrane with either the PM at the cell surface, or with the endosomal membrane following endocytosis (van Niel et al., 2018).

EV-mediated communication can occur at both intra- (Zarnowski et al., 2018) and interspecies (Cai et al., 2018) levels. Transfer of EVs can take place both locally between nearby cells and long-distance in multicellular organisms (Maas et al., 2017). Then how do EVs deliver their cargos into recipient cells? Surface molecules on EVs can bind plasma membrane proteins on recipient cells to allow docking and uptake of EVs (Figure 1-2). For example, in mammalian systems, EV docking is mediated by interactions between membrane-bound proteins such as integrins and tetraspanins with intercellular adhesion molecules and extracellular matrix proteins, or between lectins and proteoglycans (van Niel et al., 2018). Tetraspanins and lectins are also present in plants and fungi and may play similar roles (Cai et al., 2018, Lambou et al., 2008). Composition of membrane proteins may also influence targeting of EVs to certain recipient cells, as illustrated by the integrin combination-dependent organotropism of metastatic cancer EVs (Hoshino et al., 2015).

Intraluminal contents of EVs, such as RNA, can be delivered into recipient cells by direct fusion with the plasma membrane or by uptake of entire EVs by endocytosis (Figure 1-2; (van Niel et al., 2018)). If endocytosed, endosomal escape is required for release of intact, intraluminal EV cargo molecules into the cytosol (Figure 1-2). Otherwise, the recipient cell endosomes containing exogenous EVs are targeted for lysosomal degradation. In mammalian cells, back fusion of ILVs is dependent on the presence of the lipid lysobisphosphatidic acid (LBPA) in the late endosome and its interaction with ALIX and ESCRT (Bissig and Gruenberg, 2014). This process seems to involve acidification of the MVE lumen, as well as the accumulation of anionic lipids in the MVE membrane (Joshi et al., 2020). These proposed mechanisms are supported by endosomal escape of bacterial toxins and enveloped viruses, and cycling of cellular proteins such as MHC class II and mannose 6-phosphate receptors (Gruenberg and van der Goot, 2006).

1.3. Fungal EVs: passage through the cell wall and functionality

Since this thesis deals with EVs from a phytopathogenic fungus, the question of how EVs cross the cell wall arises. The fungal cell wall is a highly dynamic and elastic network of fibrils that is permeable even to macromolecules and can be rapidly remodelled within seconds (Coelho and Casadevall, 2019). For example, pores in the cell wall of *Saccharomyces cerevisiae* can range from 50 – 500 nm, which is in the same range as the diameter of EVs and should permit their passage (Brown et al., 2015). Electron microscopy has shown paramural vesicles between the cell wall and the plasma membrane, as well as EVs and similar structures protruding beyond the cell wall (Wolf et al., 2014, Roth et al., 2019). Sites with high cell wall dynamics, tied to cell growth and division, such as the septa, growing hyphal tips, and bud sites in yeast cells may be more conducive to EV secretion. Supporting that EV secretion is an active process, it was demonstrated in *C. neoformans* that viable cells are required to obtain EVs from culture supernatants; cells killed with heat or sodium azide did not release appreciable EV-like structures (Rodrigues et al., 2007).

Three non-mutually exclusive models of EV secretion through the cell wall have been proposed (Brown et al., 2015) (Figure 1-3A). First, EVs could be pushed through the cell wall by turgor pressure. Second, cell wall-modifying enzymes locally enable loosening of the cell wall for EV passage. This notion is supported by the common presence of cell wall modifying enzymes in fungal (Nimrichter et al., 2016, Zhao et al., 2019), bacterial (Lee et al., 2009), and plant (de la Canal and Pinedo, 2018) EV preparations, although it is uncertain whether these are simply co-purified or truly integral to EVs. The third and the least convincing idea is that protein channels and extracellular cytoskeletal elements guide EVs through the cell wall (Brown et al., 2015).
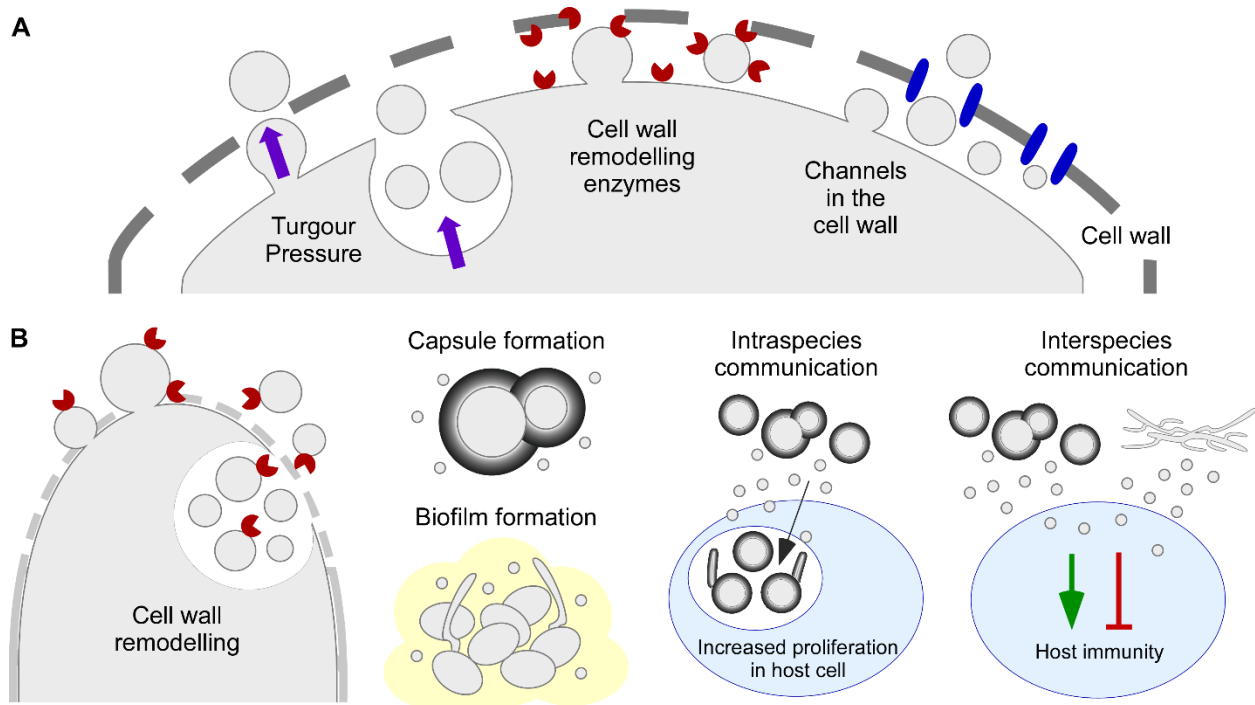
Figure 1-3. Secretion and functionality of fungal EVs.
A. Models of fungal EV secretion through the cell wall. EVs could be pushed through the pores in the cell wall by turgour pressure of the cell. Alternatively, cell wall remodelling enzymes locally loosen the cell wall to allow EV passage, or EVs are secreted through channels in the cell wall (Brown et al., 2015).
B. Biological functions of fungal EVs. Fungal EVs can contribute to formation and remodelling of external structures such as the cell wall (Zhao et al., 2019), glucuronoxylomannan capsule (Rodrigues et al., 2007), or biofilm matrix (Zarnowski et al., 2018). Fungal EVs can also mediate communication at both intra- and interspecies levels. EVs from a highly virulent fungal strain can increase proliferation of a less virulent strain in the host cell (Bielska et al., 2018). Fungal EVs can also stimulate or suppress host immune responses, depending on the context (Rizzo et al., 2021a).

As with EVs produced by other organisms, fungal EVs contain lipids, proteins, RNA, polysaccharides, and various small molecules (Rizzo et al., 2021a). EVs of pathogenic fungi can carry virulence factors or virulence-associated enzymes (Ikeda et al., 2018, Rodrigues et al., 2008), pigments (Bleackley et al., 2020), and mycotoxins (Costa et al., 2021). While many studies have catalogued RNAs associated with fungal EVs, clear functionality of these molecules has yet to be demonstrated (Peres da Silva et al., 2015, Alves et al., 2019, Liu et al., 2020). Especially for fungal EVs, polysaccharides seem to be integral and functionally important cargos. A recent high-resolution cryo-EM study has shown that most EVs produced by *Cryptococcus spp.* and *S. cerevisiae* are decorated with fibrillar structures, which were proposed to be mannoproteins (Rizzo et al., 2021b).

Pertaining to the third major function of EVs proposed above in section 1.2., fungal EVs participate in formation and remodelling of external structures, such as the cell wall (Rizzo et al., 2020, Zhao et al., 2019), the capsule (Rodrigues et al., 2007), and the biofilm matrix (Zarnowski et al., 2018) (Figure 1-3B). Regeneration of *Aspergillus fumigatus* protoplasts is associated with increased EV secretion, and these EVs are carry glycans and cell wall associated enzymes (Rizzo et al., 2020). Furthermore, microscopic evidence showed close association of regenerating cell wall fibrils with the EVs, supporting that the EVs deliver the required building blocks and the biosynthetic machinery. In *S. cerevisiae*, EVs increase resistance to cell wall stress induced by the 1,3-β-glucan synthase inhibitor caspofungin, at least in part by delivering glucan and chitin synthases (Zhao et al., 2019). Given that the protective effect is still present after removal of EVs that have not been taken up by the cells, EVs are actively contributing to cell wall integrity maintenance rather than just acting as decoys for caspofungin binding.

In populations of pathogenic fungi, EVs can contribute to biofilm formation (Zarnowski et al., 2018) and sharing of molecules to enhance virulence (Bielska et al., 2018). Several *Candida albicans* ESCRT mutants with reduced EV production are more sensitive to the antifungal fluconazole and showed reduced biofilm matrix deposition (Zarnowski et al., 2018). Recovery of both biofilm matrix and fluconazole resistance following application of wild-type biofilm-derived EVs, and the presence of matrix polysaccharide-modifying enzymes in EVs indicate their role in biofilm formation (Zarnowski et al., 2018). EVs were also proposed to mediate communication between fungal cells during infection (Bielska et al., 2018) (Figure 1-3B). EVs from a highly virulent outbreak strain of *Cryptococcus gattii* enhance the intracellular proliferation rate of less virulent strains inside macrophages via their RNA and protein cargo (Bielska et al., 2018). It is however unclear how pathogen EVs can be released from an infected macrophage and taken up by another to reach the cryptococcal phagosome *in vivo* (Bielska et al., 2018).

In the context of host-pathogen interactions, EVs of pathogenic fungi appear to be mixed bags, carrying both virulence factors that support fungal infections as well as immunogenic molecules that can prevent successful infection (Freitas et al., 2019) (Figure 1-3B). In clinically important fungi, evidences that support stimulation of host immunity by fungal EVs seemingly outweigh those that underpin the role of EVs in virulence. Treatment of immune cells with EVs from different clinical fungal pathogens stimulate innate immunity and improve macrophage killing of fungal cells (Oliveira et al., 2010, da Silva et al., 2016, Bitencourt et al., 2018, Brauer et al., 2020). Furthermore, *in vivo*, pre-treatment with EVs of pathogenic fungi have a protective effect on the host, suggesting potential use of fungal EVs as vaccines (Vargas et al., 2015, Brauer et al., 2020, Colombo et al., 2019).

However, in some fungi, clear virulence-promoting functions of EVs were observed alongside immunogenicity. EVs of *Candida auris* promote both adhesion to host epithelial cells and survival in macrophages, while also inducing immune responses (Zamith-Miranda et al., 2021). *Sporothorix brasiliensis* EVs stimulate phagocytosis and cytokine production *in vitro*, but increase fungal load and lesion size when applied *in vivo* (Ikeda et al., 2018). So far, for phytopathogenic fungal EVs, the only known effect on the host plant is induction of necrosis, which suggests a virulence function for the necrotrophic *Fusarium* species (Bleackley et al., 2020). Hence, fungal EVs seem to have opposing influences on pathogenesis in the host and the overall effect is probably context-dependent.

1.4. EVs in plant-fungus interactions and cross-kingdom RNA transfer

EV-like structures have long been observed at various plant-microbe interfaces, hinting that they may be functionally important in these interactions (Snetselaar and Mims, 1994, Mims et al., 2004, An et al., 2006). EVs at the extrahaustorial matrices in powdery mildew infections are better-studied examples and currently more is known about plant EVs than on the side of the pathogens. MVEs are abundantly observed inside both haustoria of powdery mildews and the host plant cells they are colonising (Micali et al., 2011). It is probable that intimate contact sites between the fungus and the plant plasma membrane, such as haustorial interfaces (Bozkurt and Kamoun, 2020, Micali et al., 2011) or the biotrophic interfacial complex (Giraldo et al., 2013), where both parties are actively secreting in a molecular warfare, are also prime locations of EV-mediated exchange.

As mentioned in section 1.2., accumulation of syntaxin PEN1/ROR2-positive plant exosomes at sites of encasement or papilla formation is a conserved defence response against powdery mildews in both *A. thaliana* and barley (An et al., 2006, Collins et al., 2003). Loss of PEN1/ROR2 and factors that affect release of PEN1/ROR2-positive exosomes block papilla formation (Hansen and Nielsen, 2017). Although callose itself was not detectable in these exosomes, H_2O_2 and osmiophilic phenolic compounds were present, which are typical defence molecules found in cell wall appositions against the invading pathogen (An et al., 2006) (Figure 1-4). In addition to formation of defence structures, PEN1-positive EV secretion is also increased in *A. thaliana* both when challenged with the bacterial pathogen *Pseudomonas syringae* and when treated with the defence hormone salicylic acid (SA), indicating a general involvement of EVs in plant defence (Rutter and Innes, 2017).
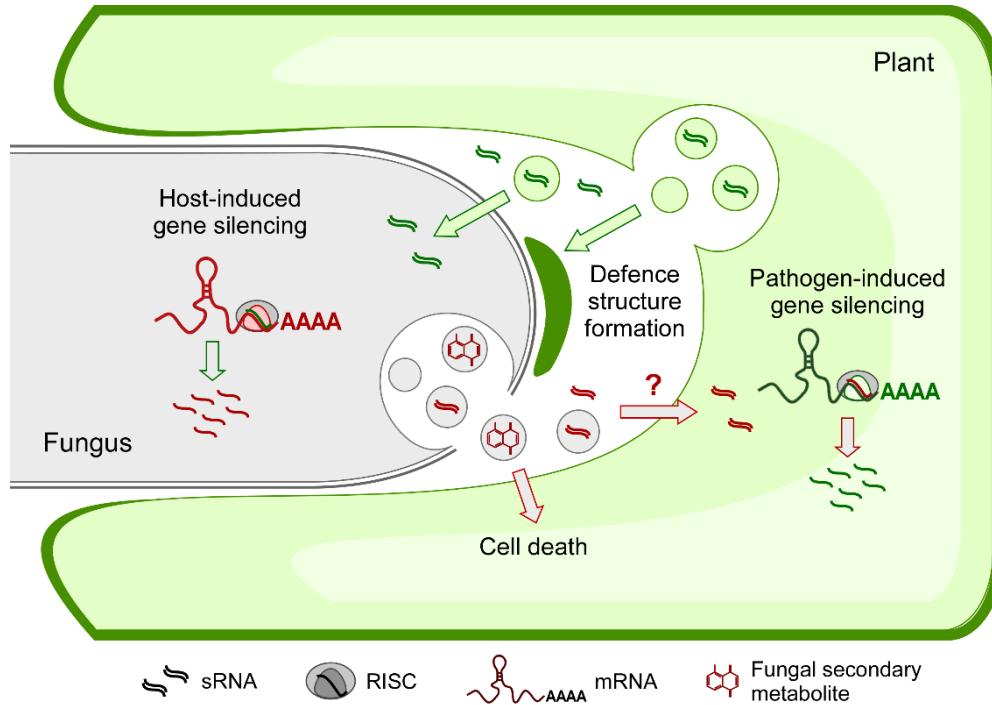
Figure 1-4. EVs in plant-fungus interactions.
Plant exosomes participate in formation of defence structures, such as papillae and encasements, against invading filamentous pathogens (Hansen and Nielsen, 2017). As another defence mechanism, plant sRNAs can be delivered to fungal pathogens via EVs to bring about host-induced gene silencing (HIGS) to compromise the pathogen (Cai et al., 2018). Reciprocally, filamentous pathogens also send sRNA effectors to plants for pathogen-induced gene silencing (PIGS) (Weiberg et al., 2013), but whether the sRNA effectors are delivered by pathogen EVs remains to be confirmed (question mark). In this figure, post-transcriptional gene silencing, rather than transcriptional gene silencing is assumed. Additionally, EVs of fungal pathogens can cause hypersensitive cell death in plants (Bleackley et al., 2020). This phytotoxic effect has been linked to secondary metabolite cargos of fungal EVs but needs to be tested. The precise mechanism of EV uptake and cargo delivery in plants and pathogenic fungi has not been elucidated so far.

More recently, isolation of EVs from plant apoplastic washing fluids (AWF) have enabled -omics analyses and studies on the effect of plant EVs on pathogens. Proteins involved in responses to biotic and abiotic stress are overrepresented in EVs compared to the whole *A. thaliana* proteome (Rutter and Innes, 2017). Supporting the hypothesis that EVs are vehicles for delivering weapons in plant-pathogen warfare, EVs from sunflower AWF are taken up by the *Sclerotinia scletiorum* ascospores and inhibit hyphal growth from the spores and reduce viability of the fungus (Regente et al., 2017). Similarly, EVs isolated from tomato root exudates also inhibit spore germination of *Fusarium oxysporum*, *Botrytis cinerea*, and *Alternaria alternata* (De Palma et al., 2020).

A noteworthy function of EVs in plant-pathogen interaction is mediating RNA transfer between the partners (Cai et al., 2018). Plants secrete sRNAs that silence genes in fungal pathogens, in a phenomenon termed host-induced gene silencing (HIGS; Figure 1-4) (Nowara et al., 2010). *A. thaliana* tetraspanin TET8-positive EVs deliver trans-acting small interfering RNAs (tasiRNAs) that target and silence genes encoding components of vesicle trafficking, important for virulence in *B. cinerea* (Cai et al., 2018). Given that sRNAs abundant in the total leaf tissue are not necessarily abundant in EVs or detectible in fungal cells, there seems to be a selective mechanism for EV loading and delivery (Cai et al., 2018). This selectivity can be partially explained by RNA-binding proteins (RBPs). In *A. thaliana*, individual deletions of AGO1, RNA helicase, or annexin all partially affect EV loading of the miRNA and tasiRNAs tested (He et al., 2021). Thus RNA targeting to EVs likely occurs at the level of ribonucleoproteins (RNPs), determined by the combination of proteins bound to a given RNA. In addition to sRNAs of conventional sizes (21-24 nt), a large proportion of RNAs found in PEN1-positive *A. thaliana* EVs are single-stranded tiny RNAs (10-17 nt) derived from diverse regions in the genome (Baldrich et al., 2019). In such EVs, shorter tiny RNAs of unknown function are predominant in EVs while the tasiRNAs are underrepresented (Baldrich et al., 2019). Secretion of different types of sRNA in plant EV populations is still under debate but the differences in starting material, EV marker choice and EV isolation method may explain the conflicting findings.

In the opposite direction, pathogen-induced gene silencing (PIGS; Figure 1-4) of host defence-related genes by sRNA effectors has been observed in various filamentous pathogens (Weiberg et al., 2013, Wang et al., 2017, Jian and Liang, 2019, Dunker et al., 2020, Ji et al., 2021). In a pioneering study, it was shown that small interfering RNA (siRNA) effectors of the fungus *B. cinerea* "hijack" the argonaute protein AGO1 of *A. thaliana* and silence plant genes that encode stress and defence signalling-related proteins (Weiberg et al., 2013). These siRNA effectors in *B. cinerea* are likely to be transferred in the mature form, rather than being processed in the plant, as their production and functionality depend on the fungal dicer-like proteins (Weiberg et al., 2013). It has not yet been verified that such sRNA effectors are truly translocated via pathogen EVs.

So far, only protein and metabolite cargos have been addressed in EVs of a few fungal phytopathogens and their effect on virulence is unclear. EV proteomes from axenic cultures of the wheat pathogen *Zymoseptoria tritici* (Hill and Solomon, 2020) and the cotton pathogen *Fusarium oxysporum* f.sp. *vasinfectum* (*Fov*) (Bleackley et al., 2020) have been characterised to date. Interestingly, *Fov* EVs are associated with polyketite synthases for secondary metabolite biosynthesis and an unknown purple pigment (Bleackley et al., 2020). Treatment of leaves with of fractions enriched in *Fov* EVs triggers

hypersensitive cell death (Bleackley et al., 2020). For now, the cell death inducing effect of *Fov* EVs can be interpreted in two ways: 1. *Fov* EVs trigger plant defence responses, or 2. *Fov* EV-induced plant cell death promotes necrotrophic infection and reflects the mycotoxin-producing nature of *Fov*. Similarly, EVs of the citrus pathogen *Penicillium digitatum* inhibit seed germination and carry various secondary metabolites including toxic tryptoquialanines and fungisporin, the former of which is likely accountable for the inhibitory effect (Costa et al., 2021). It requires further investigation to ascertain whether EVs of plant pathogenic fungi support infection and increase pathogen fitness, or are a liability to the pathogen, harbouring PAMPs that trigger host immunity.

To the best of my knowledge, RNAs associated with EVs of phytopathogenic fungi had not been characterised in a publication prior to the work presented in this thesis (Kwon et al., 2021). The role of EVs in transfer of fungal sRNAs to plants for PIGs is highly probable and is now actively being investigated in various pathogens (personal communication, DFG FOR5116). The future research avenue linking fungal endosomal RNA transport with EVs is addressed in the review paper in the Appendix to Chapter 1 (Section 1.9. (Kwon et al., 2020)). Here I will explore in depth an overlooked but fascinating possibility that mRNAs are transferred between plants and pathogens.

1.5. Functionality of mRNAs in EVs

All common types of RNA in a cell can be secreted in EVs, including intact mRNAs that can be translated if delivered correctly (O'Brien et al., 2020). RNA composition of EVs is generally quite different from that of the secreting cells, although they still reflect the source cell status (O'Brien et al., 2020). EV-associated RNAs tends to be more fragmented and overrepresented in shorter sequences derived from rRNA and other non-coding RNA (Hinger et al., 2018, Wei et al., 2017). The space limitation inside EVs also seem to pose a restriction on loading of larger RNA molecules. Presumably due to their larger size range, microvesicles tend to carry a greater proportion of longer RNAs and hence more intact mRNAs than do exosomes (Skog et al., 2008, Wei et al., 2017). Most intact mRNAs in EVs are around 1000 nt but much longer RNAs can still be carried by microvesicles (Hinger et al., 2018, Wei et al., 2017).

The proportion of intact mRNAs is likely to be low in EVs. According to a conservative estimate which doesn't account for sample losses during processing steps, only a single copy of intact or fragmented mRNA would be present per ~10 EVs (Wei et al., 2017). This raises the question of functional relevance of mRNAs in EVs. However, a single mRNA molecule delivered to the recipient cell can have an amplifiable physiological effect, potentially yielding multiple copies of protein. A few studies in mammalian systems

strongly support EV-mediated transfer and translation of mRNAs in recipient cells by means of fluorescent or luminescent reporter systems (Ridder et al., 2015, Zomer et al., 2015, Lai et al., 2015). Additionally, several papers suggest that the mRNA in EVs from cancer cells promote proliferation, metastasis, or metabolic changes in the recipient cells (Skog et al., 2008, Zomer et al., 2015, Zeng et al., 2020). Current challenge is to effectively rule out that the protein signal detected as a readout in EV-recipient cells is truly from de novo translation of mRNAs and not ready-made protein delivered via EVs.

mRNAs and mRNA fragments associated with EVs of clinically important fungi have also been characterised (Peres da Silva et al., 2019, Alves et al., 2019, Liu et al., 2020, Zamith-Miranda et al., 2021). Although there is no obvious commonality between the EV-associated mRNAs from different fungi, the RNA isolation method may be a critical factor accounting for the number of different mRNA species identified, which can range from as few as ~30-93 using a kit (Peres da Silva et al., 2019, Alves et al., 2019, Zamith-Miranda et al., 2021) and thousands using Trizol™ (Liu et al., 2020, Kwon et al., 2021). The presence of mRNAs in EVs of pathogenic fungi raises the following question: can mRNAs from a fungus be translated properly in a metazoan or plant host cell? In vitro translation of RNA isolated from *Paracoccidiodes brasiliensis* EVs with rabbit reticulocyte system yielded proteins, indicating that the mRNAs associated with the EVs are indeed translation-competent (Peres da Silva et al., 2019). This further supports the possibility of cross-kingdom transfer of pathogen mRNAs and translation using the host machinery and resources.

mRNAs transferred via EVs could meet different fates in recipient cells. Endocytosis is thought to be the dominant route of EV cargo delivery (van Niel et al., 2018). The aforementioned endosomal escape would be essential for intact RNAs to be released for functionality in the host cell cytoplasm; otherwise they would face lysosomal degradation (see Figure 1-2, Section 1.2.). Assuming that an EV cargo mRNA has escaped the endosome, it can be translated with the recipient cell translation machinery, or if they have special codon usage, may require co-delivery of tRNAs and other translation factors from the source cells. While tRNAs are generally abundant in EVs, intact ribosomes are somewhat unlikely to be delivered in sufficient quantities (O'Brien et al., 2020), although transiently intact extracellular ribosomes independent of EVs have been detected in one exceptional case (Tosar et al., 2020). Alternatively, mRNA fragments complementary to recipient cell transcripts could be further cleaved and function as tasiRNAs that silence genes in the recipient cell.

1.6. *Ustilago maydis* as a system for studying EVs

In this thesis, the organism of choice to investigate EV-associated mRNAs relevant for fungal pathogenesis in plants is the maize smut pathogen, *Ustilago maydis*. It is a basidiomycete fungus with a biotrophic lifestyle, that infects all aerial parts of a maize plant and causes characteristic tumours filled with sooty, black teliospores, which gave it the moniker "smut" fungus (Brefort et al., 2009). Due to its culturability and genetic tractability, it has been used extensively to study plant-pathogen interactions (Dean et al., 2012), and as a model system where the Holliday junction (Holliday, 1964) and the microtubule-dependent endosome-associated mRNA transport (Baumann et al., 2012) were discovered.
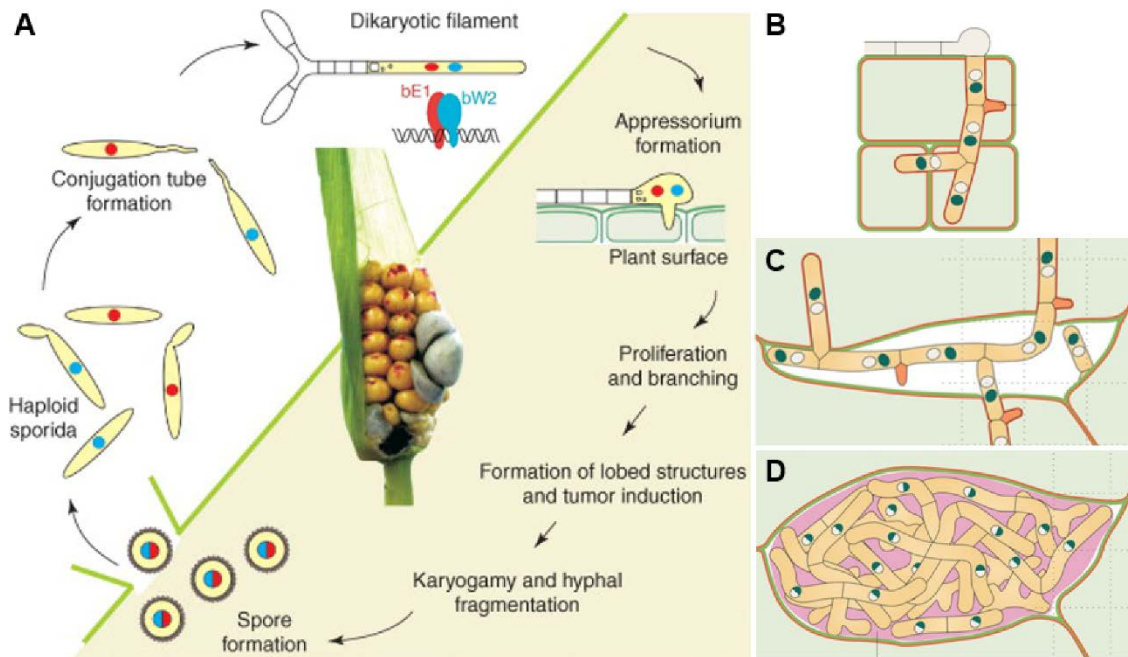
Figure 1-5. Life cycle and infection stages of the maize smut pathogen *Ustilago maydis*.
A. Life cycle of *U. maydis* (from (Feldbrügge et al., 2004)). **B-D.** *U. maydis* hyphae in maize during different stages of infection (schematic from (Lanver et al., 2017), Figure 1). During early infection, dikaryotic hyphae are mostly surrounded by the plant plasma membrane (**B**). Hyphae gradually proliferate more in the apoplastic space between plant cells (**C**), inducing tumour in the plant tissue. Eventually, the dikaryotic cells undergo karyogamy and become true diploid hyphae, then proliferate to form massive hyphal aggregates in the apoplastic cavity in tumour tissues, surrounded by a polysaccharide matrix (**D**). These dikaryotic hyphae fragment to form teliospores. Original images from the cited sources have been reproduced with permissions.

In nature, *U. maydis* begins its lifecycle as haploid sporidia, released from diploid teliospores following meiosis (Figure 1-5A). These sporidia can multiply by yeast-like budding and are culturable. When two sporidia of compatible mating types detect each other by pheromone sensing, which is dependent on the biallelic *a-locus*, they grow conjugation tubes towards each other, and fuse to form a dikaryotic filament (Bölker et al., 1992). Here, the heterodimerisation of compatible bE and bW homeodomain transcription factors from the multiallelic *b-locus* in each nucleus of the dikaryon, culminates in a transcriptional cascade for switch to infectious filamentous development (Kämper et al., 1995). The dikaryotic hypha is then able to infect the plant and proliferate predominantly in the apoplastic space, inducing tumour in the colonised tissue (Figure 1-5B-D). Eventually the two nuclei in each cell undergo karyogamy to form a diploid and the hyphae fragment to form teliospores, which are released to complete the lifecycle.

EV-like structures have long been observed at the interface between *U. maydis* and maize during infection (Snetselaar and Mims, 1994). Interestingly, the hyphae proliferating in tumour cells are said to be embedded in a vesicular or mucilaginous matrix prior to teliospore formation (Banuett and Herskowitz, 1996, Brefort et al., 2009). Whether *U. maydis* EVs play a role in formation of this matrix and whether it serves as a protective barrier remains to be tested. More recently, paramural membrane tubules have been observed in both the arbuscular mycorrhiza *Rhizophagus irregularis* and *U. maydis* during plant colonisation (Roth et al., 2019). The function of the membrane tubules in *U. maydis* is unclear. Furthermore, membrane protrusions or "membrane chunks" harbouring the translocon-like Stp complex were found extending beyond the *U. maydis* cell wall and interacting with the channel-forming protein aquaporin on the maize plasma membrane (Ludwig et al., 2021). It will be interesting to find out if EVs and such membrane extensions serve distinct functions or are related structures.

Of particular importance for EV isolation is the culturability of *U. maydis* and the possibility to obtain its EVs from the apoplastic washing fluid of infected maize (Figure 1-5C). Culturability is especially important for studying fungal EVs in isolation before moving on to more complex infection samples. Another advantage of using *U. maydis* is the availability of synthetic laboratory strains where infectious filamentous growth can be induced in culture without mating (Brachmann et al., 2001). For example, in the strain AB33, compatible bE and bW genes are placed under a promoter that is inducible by changing the nitrogen source in the medium (Brachmann et al., 2001). This allows expression of several genes relevant for filamentous growth and infection in axenic culture (Wahl et al., 2010, Heimel et al., 2010), whose mRNAs may then be secreted in EVs. Furthermore, since such inducible strains are haploid, it is simpler to test EV markers and study genes important for EV biogenesis by genetic manipulation.
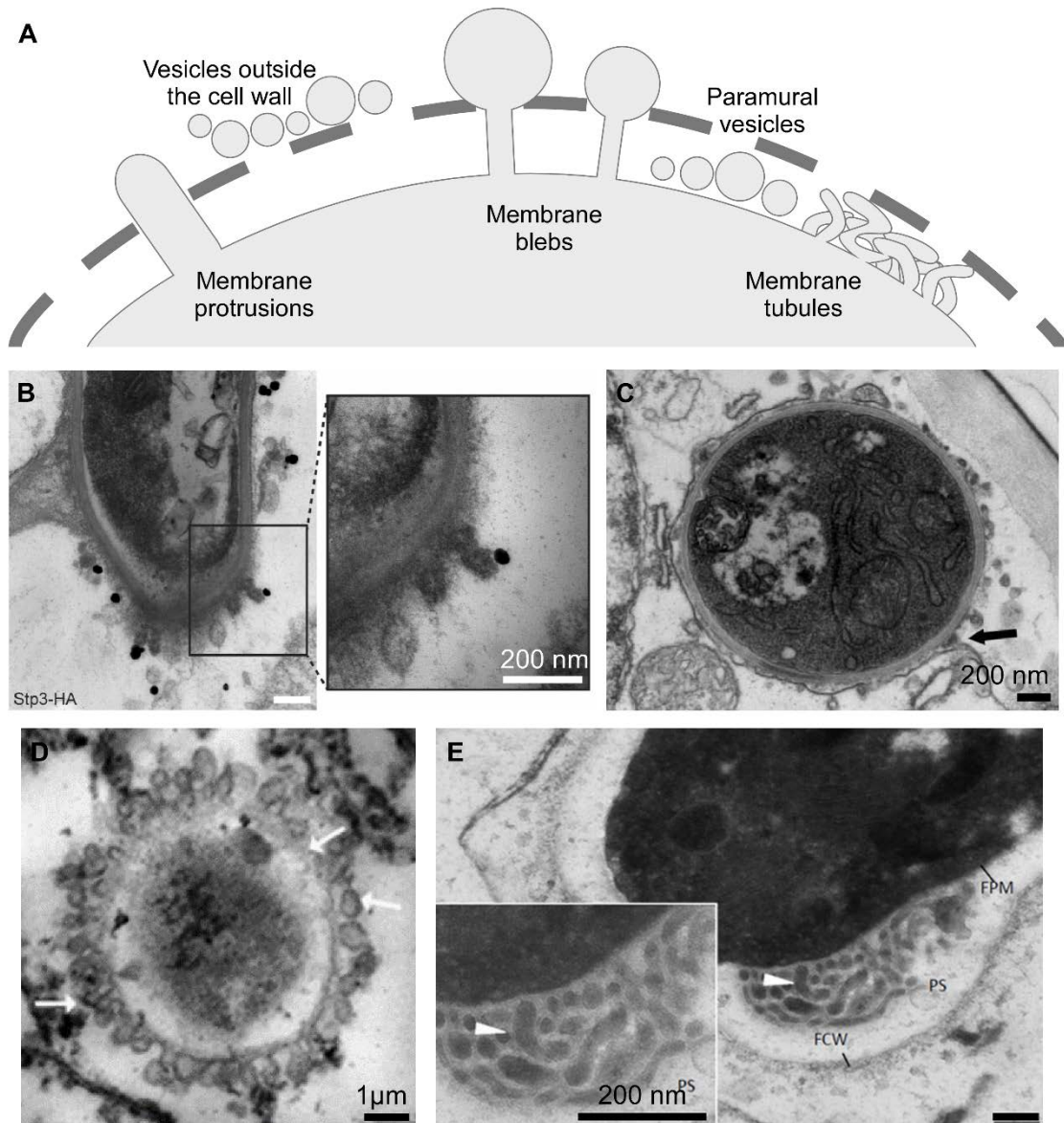
Figure 1-6. Structures akin to EVs observed in *U. maydis*.

A. Different types of membrane structures observed in *U. maydis.* **B.** Membrane protrusions harbouring the Stp complex (labelled with gold particle; from (Ludwig et al., 2021), Extended Data Figure 7). **C.** Electron-dense EV-like structures surrounding the hypha (black arrow; from (Ludwig et al., 2021), Extended Data Figure 7). **D.** Membrane blebs produced following treatment of sporidial cells with chitosan (white arrows; from (Olicón-Hernández et al., 2015), Figure 4). **E.** Membrane tubules (white arrowhead) in the paramural space (PS), continuous with the fungal plasma membrane (FPM), within the fungal cell wall (FCW) (from (Roth et al., 2019), Supplementary Figure 5). **B**, **C**, and **E** are micrographs of hyphae *in planta* and **D** shows a sporidium from axenic culture*.* Original images from the cited sources have been reproduced with permissions.

Another notable feature of *U. maydis* is the secondary loss of the RNAi machinery (Laurie et al., 2008). One hypothesis is that like *S. cerevisiae*, cells that lack RNAi would have had a selective advantage by harbouring a dsRNA virus that confers the ability to produce a killer toxin to outcompete the neighbouring cells while being immune to it (Drinnenberg et al., 2011). Hence RNAs other than canonical miRNAs or siRNAs may be more enriched in *U. maydis* EVs and perhaps mRNAs or tRNAs may be more functionally important. Moreover, Rrm4, the key RBP for endosome-associated mRNA transport, is known to bind over 3000 mRNAs (Olgeiser et al., 2019). Since exosomes are derived from MVEs, close association of so many mRNAs with endosomes is promising and RBPs such as Rrm4 may facilitate their loading into exosomes. Thus *U. maydis* is a particularly fascinating system for studying EV-associated mRNAs.

Pathogen effectors are molecules that are secreted to bring about physiological changes in a host plant, usually to the benefit of the pathogen. So far, due to the narrow criteria set for attempts to search for effectors in the post-genomic era (Kämper et al., 2006), only conventionally secreted protein effectors have been characterised as *bona fide* effectors in *U. maydis* (Lanver et al., 2017). Examining EVs would not only open up the possibility to discover RNA effectors, but also a diverse range of other molecules that are otherwise intracellular.

1.7.   Aims and Hypotheses

The following points have been established in above subchapters:

1.2.   EVs are not artefacts and have diverse functions e.g. mediating intercellular communication

1.3.   Fungi secrete EVs through the cell wall

1.4.   EVs are likely to play an important role in plant-pathogen interactions

1.5.   EVs carry intact mRNAs that are translatable

1.6.   *Ustilago maydis* produces EV-like structures

The main hypotheses are as follows:

1.   *U. maydis* secretes EVs with intact mRNAs

2.   Certain mRNAs are selectively loaded into EVs for a specific function

3.   EV cargo mRNAs can be delivered to and translated in plant cells

4.   The protein products of the EV-mRNAs serve a virulence function as effectors
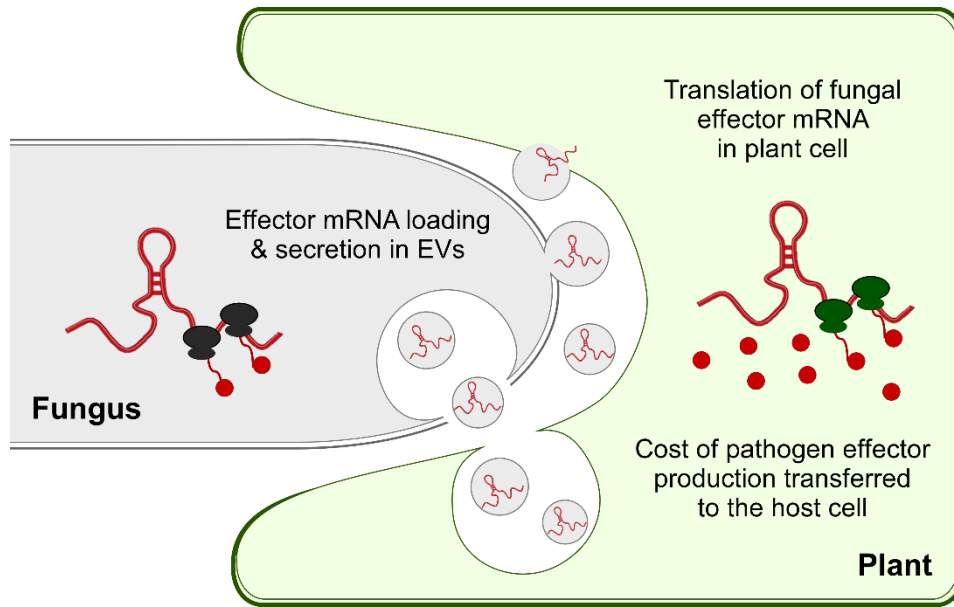
Figure 1-7. EV cargo mRNA effector hypothesis
Intact fungal mRNAs encoding effector proteins are selectively secreted via EVs during plant infection. EVs deliver the cargo mRNA effectors to the cytosol of the host plant cell, where these mRNAs are translated to produce multiple copies of effector protein using host resources. Thus the cost of pathogen effector production is transferred to the host cell.

EV-associated mRNAs that are hypothetically translated in maize to function as effectors will be hereafter called mRNA effector candidates. Another non-mutually exclusive possibility is that mRNAs fragments act as tasiRNAs to silence plant genes. There is of course also the possibility that EV cargo mRNAs are are biologically insignificant, passively released by chance or simply disposed of via EVs.

As a pioneering study on EVs of phytopathogenic fungi, and the first in *U. maydis*, the aims of this thesis are as follows:

1. Establish a method for EV isolation from axenic culture
2. Demonstrate protection of extracellular RNA within EVs
3. Catalogue EV-associated mRNAs
4. Select promising mRNA effector candidates
5. Establish methods to further investigate mRNA effector candidates

1.8. References

ALVES, L. R., PERES DA SILVA, R., SANCHEZ, D. A., ZAMITH-MIRANDA, D., RODRIGUES, M. L., GOLDENBERG, S., PUCCIA, R. & NOSANCHUK, J. D. 2019. Extracellular Vesicle-Mediated RNA Release in Histoplasma capsulatum. *mSphere,* 4.

AN, Q., HÜCKELHOVEN, R., KOGEL, K.-H. & VAN BEL, A. J. E. 2006. Multivesicular bodies participate in a cell wall-associated defence response in barley leaves attacked by the pathogenic powdery mildew fungus. *Cellular Microbiology,* 8**,** 1009-1019.

BALDRICH, P., RUTTER, B. D., KARIMI, H. Z., PODICHETI, R., MEYERS, B. C. & INNES, R. W. 2019. Plant Extracellular Vesicles Contain Diverse Small RNA Species and Are Enriched in 10-to 17-Nucleotide "Tiny" RNAs. *Plant Cell,* 31**,** 315-324.

BANUETT, F. & HERSKOWITZ, I. 1996. Discrete developmental stages during teliospore formation in the corn smut fungus, Ustilago maydis. *Development,* 122**,** 2965-2976.

BAUMANN, S., POHLMANN, T., JUNGBLUTH, M., BRACHMANN, A. & FELDBRÜGGE, M. 2012. Kinesin-3 and dynein mediate microtubule-dependent co-transport of mRNPs and endosomes. *Journal of Cell Science,* 125**,** 2740-2752.

BIELSKA, E., SISQUELLA, M. A., ALDEIEG, M., BIRCH, C., O'DONOGHUE, E. J. & MAY, R. C. 2018. Pathogen-derived extracellular vesicles mediate virulence in the fatal human pathogen *Cryptococcus gattii*. *Nature Communications,* 9.

BISSIG, C. & GRUENBERG, J. 2014. ALIX and the multivesicular endosome: ALIX in Wonderland. *Trends Cell Biol,* 24**,** 19-25.

BITENCOURT, T. A., REZENDE, C. P., QUARESEMIN, N. R., MORENO, P., HATANAKA, O., ROSSI, A., MARTINEZ-ROSSI, N. M. & ALMEIDA, F. 2018. Extracellular Vesicles From the Dermatophyte Trichophyton interdigitale Modulate Macrophage and Keratinocyte Functions. *Frontiers in Immunology,* 9.

BLEACKLEY, M., SAMUEL, M., GARCIA-CERON, D., MCKENNA, J. A., LOWE, R. G. T., PATHAN, M., ZHAO, K. N., ANG, C. S., MATHIVANAN, S. & ANDERSON, M. A. 2020. Extracellular Vesicles From the Cotton Pathogen *Fusarium oxysporum* f. sp. *vasinfectum* Induce a Phytotoxic Response in Plants. *Frontiers in Plant Science,* 10.

BÖLKER, M., URBAN, M. & KAHMANN, R. 1992. The a mating type locus of U. maydis specifies cell signaling components. *Cell,* 68**,** 441-50.

BOZKURT, T. O. & KAMOUN, S. 2020. The plant–pathogen haustorial interface at a glance. *Journal of Cell Science,* 133.

BRACHMANN, A., WEINZIERL, G., KAMPER, J. & KAHMANN, R. 2001. Identification of genes in the bW/bE regulatory cascade in *Ustilago maydis*. *Molecular Microbiology,* 42**,** 1047-1063.

BRAUER, V. S., PESSONI, A. M., BITENCOURT, T. A., PAULA, R. G. D., ROCHA, L. D. O., GOLDMAN, G. H., ALMEIDA, F. & MITCHELL, A. P. 2020. Extracellular Vesicles from Aspergillus flavus Induce M1 Polarization <i>In Vitro</i>. *mSphere,* 5**,** e00190-20.

BREFORT, T., DOEHLEMANN, G., MENDOZA-MENDOZA, A., REISSMANN, S., DJAMEI, A. & KAHMANN, R. 2009. *Ustilago maydis* as a Pathogen. *Annual Review of Phytopathology,* 47**,** 423-445.

BROWN, L., WOLF, J. M., PRADOS-ROSALES, R. & CASADEVALL, A. 2015. Through the wall: extracellular vesicles in Gram-positive bacteria, mycobacteria and fungi. *Nature Reviews Microbiology,* 13**,** 620-630.

CAI, Q., QIAO, L., WANG, M., HE, B., LIN, F. M., PALMQUIST, J., HUANG, S. D. & JIN, H. 2018. Plants send small RNAs in extracellular vesicles to fungal pathogen to silence virulence genes. *Science,* 360**,** 1126-1129.

CARUSO, S. & POON, I. K. H. 2018. Apoptotic Cell-Derived Extracellular Vesicles: More Than Just Debris. *Frontiers in Immunology,* 9.

CHOI, D., GO, G., KIM, D. K., LEE, J., PARK, S. M., DI VIZIO, D. & GHO, Y. S. 2020. Quantitative proteomic analysis of trypsin-treated extracellular vesicles to identify the real-vesicular proteins. *J Extracell Vesicles,* 9**,** 1757209.

COELHO, C. & CASADEVALL, A. 2019. Answers to naysayers regarding microbial extracellular vesicles. *Biochem Soc Trans,* 47**,** 1005-1012.

COLLINS, N. C., THORDAL-CHRISTENSEN, H., LIPKA, V., BAU, S., KOMBRINK, E., QIU, J.-L., HÜCKELHOVEN, R., STEIN, M., FREIALDENHOVEN, A., SOMERVILLE, S. C. & SCHULZE-LEFERT, P. 2003. SNARE-protein-mediated disease resistance at the plant cell wall. *Nature,* 425**,** 973-977.

COLOMBO, A. C., RELLA, A., NORMILE, T., JOFFE, L. S., TAVARES, P. M., ARAÚJO, G. R. D. S., FRASES, S., ORNER, E. P., FARNOUD, A. M., FRIES, B. C., SHERIDAN, B., NIMRICHTER, L., RODRIGUES, M. L., POETA, M. D. & DOERING, T. L. 2019. <i>Cryptococcus neoformans</i> Glucuronoxylomannan and Sterylglucoside Are Required for Host Protection in an Animal Vaccination Model. *mBio,* 10**,** e02909-18.

COSTA, J. H., BAZIOLI, J. M., BARBOSA, L. D., JÚNIOR, P. L. T. D. S., REIS, F. C. G., KLIMECK, T., CRNKOVIC, C. M., BERLINCK, R. G. S., SUSSULINI, A., RODRIGUES, M. L., FILL, T. P. & KRONSTAD, J. W. 2021. Phytotoxic Tryptoquialanines Produced <i>In Vivo</i> by <i>Penicillium digitatum</i> Are Exported in Extracellular Vesicles. *mBio,* 12**,** e03393-20.

DA SILVA, T. A., ROQUE-BARREIRA, M. C., CASADEVALL, A. & ALMEIDA, F. 2016. Extracellular vesicles from Paracoccidioides brasiliensis induced M1 polarization in vitro. *Scientific Reports,* 6**,** 35867.

DAVIS, C. N., WINTERS, A., MILIC, I., DEVITT, A., COOKSON, A., BROPHY, P. M. & MORPHEW, R. M. 2020. Evidence of sequestration of triclabendazole and associated metabolites by extracellular vesicles of Fasciola hepatica. *Scientific Reports,* 10**,** 13445.

DE LA CANAL, L. & PINEDO, M. 2018. Extracellular vesicles: a missing component in plant cell wall remodeling. *Journal of Experimental Botany,* 69**,** 4655-4658.

DE PALMA, M., AMBROSONE, A., LEONE, A., DEL GAUDIO, P., RUOCCO, M., TURIÁK, L., BOKKA, R., FIUME, I., TUCCI, M. & POCSFALVI, G. 2020. Plant Roots Release Small Extracellular Vesicles with Antifungal Activity. *Plants,* 9**,** 1777.

DEAN, R., VAN KAN, J. A. L., PRETORIUS, Z. A., HAMMOND-KOSACK, K. E., DI PIETRO, A., SPANU, P. D., RUDD, J. J., DICKMAN, M., KAHMANN, R., ELLIS, J. & FOSTER, G. D. 2012. The Top 10 fungal pathogens in molecular plant pathology. *Molecular Plant Pathology,* 13**,** 414-430.

DRINNENBERG, I. A., FINK, G. R. & BARTEL, D. P. 2011. Compatibility with killer explains the rise of RNAi-deficient fungi. *Science,* 333**,** 1592.

DUNKER, F., TRUTZENBERG, A., ROTHENPIELER, J. S., KUHN, S., PROLS, R., SCHREIBER, T., TISSIER, A., KEMEN, A., KEMEN, E., HUCKELHOVEN, R. & WEIBERG, A. 2020. Oomycete small RNAs bind to the plant RNA-induced silencing complex for virulence. *Elife,* 9.

FELDBRÜGGE, M., KÄMPER, J., STEINBERG, G. & KAHMANN, R. 2004. Regulation of mating and pathogenic development in Ustilago maydis. *Current Opinion in Microbiology,* 7**,** 666-672.

FREITAS, M. S., BONATO, V. L. D., PESSONI, A. M., RODRIGUES, M. L., CASADEVALL, A. & ALMEIDAA, F. 2019. Fungal Extracellular Vesicles as Potential Targets for Immune Interventions. *Msphere,* 4.

GERMAN, J. B., SMILOWITZ, J. T. & ZIVKOVIC, A. M. 2006. Lipoproteins: When size really matters. *Current opinion in colloid & interface science,* 11**,** 171-183.

GIRALDO, M. C., DAGDAS, Y. F., GUPTA, Y. K., MENTLAK, T. A., YI, M., MARTINEZ-ROCHA, A. L., SAITOH, H., TERAUCHI, R., TALBOT, N. J. & VALENT, B. 2013. Two distinct secretion systems facilitate tissue invasion by the rice blast fungus Magnaporthe oryzae. *Nature Communications,* 4**,** 1996.

GRUENBERG, J. & VAN DER GOOT, F. G. 2006. Mechanisms of pathogen entry through the endosomal compartments. *Nature Reviews Molecular Cell Biology,* 7**,** 495-504.

HANSEN, L. L. & NIELSEN, M. E. 2017. Plant exosomes: using an unconventional exit to prevent pathogen entry? *Journal of Experimental Botany,* 69**,** 59-68.

HARDING, C. & STAHL, P. 1983. Transferrin recycling in reticulocytes: pH and iron are important determinants of ligand binding and processing. *Biochem Biophys Res Commun,* 113**,** 650-8.

HARDING, C. V., HEUSER, J. E. & STAHL, P. D. 2013. Exosomes: looking back three decades and into the future. *J Cell Biol,* 200**,** 367-71.

HE, B., CAI, Q., QIAO, L., HUANG, C.-Y., WANG, S., MIAO, W., HA, T., WANG, Y. & JIN, H. 2021. RNA-binding proteins contribute to small RNA loading in plant extracellular vesicles. *Nature Plants,* 7**,** 342-352.

HEIMEL, K., SCHERER, M., VRANES, M., WAHL, R., POTHIRATANA, C., SCHULER, D., VINCON, V., FINKERNAGEL, F., FLOR-PARRA, I. & KAMPER, J. 2010. The Transcription Factor Rbf1 Is the Master Regulator for b-Mating Type Controlled Pathogenic Development in *Ustilago maydis*. *Plos Pathogens,* 6.

HILL, E. H. & SOLOMON, P. S. 2020. Extracellular vesicles from the apoplastic fungal wheat pathogen *Zymoseptoria tritici*. *Fungal Biol Biotechnol,* 7**,** 13.

HINGER, S. A., CHA, D. J., FRANKLIN, J. L., HIGGINBOTHAM, J. N., DOU, Y., PING, J., SHU, L., PRASAD, N., LEVY, S., ZHANG, B., LIU, Q., WEAVER, A. M., COFFEY, R. J. & PATTON, J. G. 2018. Diverse Long RNAs Are Differentially Sorted into Extracellular Vesicles Secreted by Colorectal Cancer Cells. *Cell reports,* 25**,** 715-725.e4.

HOLLIDAY, R. 1964. A mechanism for gene conversion in fungi. *Genetical Research,* 5**,** 282-304.

HOSHINO, A., COSTA-SILVA, B., SHEN, T. L., RODRIGUES, G., HASHIMOTO, A., TESIC MARK, M., MOLINA, H., KOHSAKA, S., DI GIANNATALE, A., CEDER, S., SINGH, S., WILLIAMS, C., SOPLOP, N., URYU, K., PHARMER, L., KING, T., BOJMAR, L., DAVIES, A. E., ARARSO, Y., ZHANG, T., ZHANG, H., HERNANDEZ, J., WEISS, J. M., DUMONT-COLE, V. D., KRAMER, K., WEXLER, L. H., NARENDRAN, A., SCHWARTZ, G. K., HEALEY, J. H., SANDSTROM, P., LABORI, K. J., KURE, E. H., GRANDGENETT, P. M., HOLLINGSWORTH, M. A., DE SOUSA, M., KAUR, S., JAIN, M., MALLYA, K., BATRA, S. K., JARNAGIN, W. R., BRADY, M. S., FODSTAD, O., MULLER, V., PANTEL, K., MINN, A. J., BISSELL, M. J., GARCIA, B. A., KANG, Y., RAJASEKHAR, V. K., GHAJAR, C. M., MATEI, I., PEINADO, H., BROMBERG, J. & LYDEN, D. 2015. Tumour exosome integrins determine organotropic metastasis. *Nature,* 527**,** 329-35.

IKEDA, M. A. K., DE ALMEIDA, J. R. F., JANNUZZI, G. P., CRONEMBERGER-ANDRADE, A., TORRECILHAS, A. C. T., MORETTI, N. S., DA CUNHA, J. P. C., DE ALMEIDA, S. R. & FERREIRA, K. S. 2018. Extracellular Vesicles From *Sporothrix brasiliensis* Are an Important Virulence Factor That Induce an Increase in Fungal Burden in Experimental Sporotrichosis. *Frontiers in Microbiology,* 9.

JAN, A. T. 2017. Outer Membrane Vesicles (OMVs) of Gram-negative Bacteria: A Perspective Update. *Frontiers in Microbiology,* 8.

JI, H.-M., MAO, H.-Y., LI, S.-J., FENG, T., ZHANG, Z.-Y., CHENG, L., LUO, S.-J., BORKOVICH, K. A. & OUYANG, S.-Q. 2021. Fol-milR1, a pathogenicity factor of Fusarium oxysporum, confers tomato wilt disease resistance by impairing host immune responses. *New Phytologist,* n/a.

JIAN, J. & LIANG, X. 2019. One Small RNA of *Fusarium graminearum* Targets and Silences CEBiP Gene in Common Wheat. *Microorganisms,* 7.

JOSHI, B. S., DE BEER, M. A., GIEPMANS, B. N. G. & ZUHORN, I. S. 2020. Endocytosis of Extracellular Vesicles and Release of Their Cargo from Endosomes. *ACS Nano,* 14**,** 4444-4455.

KÄMPER, J., KAHMANN, R., BÖLKER, M., MA, L.-J., BREFORT, T., SAVILLE, B. J., BANUETT, F., KRONSTAD, J. W., GOLD, S. E., MÜLLER, O., PERLIN, M. H., WÖSTEN, H. A. B., DE VRIES, R., RUIZ-HERRERA, J., REYNAGA-PEÑA, C. G., SNETSELAAR, K., MCCANN, M., PÉREZ-MARTÍN, J., FELDBRÜGGE, M., BASSE, C. W., STEINBERG, G., IBEAS, J. I., HOLLOMAN, W., GUZMAN, P., FARMAN, M., STAJICH, J. E., SENTANDREU, R., GONZÁLEZ-PRIETO, J. M., KENNELL, J. C., MOLINA, L., SCHIRAWSKI, J., MENDOZA-MENDOZA, A., GREILINGER, D., MÜNCH, K., RÖSSEL, N., SCHERER, M., VRANEŠ, M., LADENDORF, O., VINCON, V., FUCHS, U., SANDROCK, B., MENG, S., HO, E. C. H., CAHILL, M. J., BOYCE, K. J., KLOSE, J., KLOSTERMAN, S. J., DEELSTRA, H. J., ORTIZ-CASTELLANOS, L., LI, W., SANCHEZ-ALONSO, P., SCHREIER, P. H., HÄUSER-HAHN, I., VAUPEL, M., KOOPMANN, E.,

FRIEDRICH, G., VOSS, H., SCHLÜTER, T., MARGOLIS, J., PLATT, D., SWIMMER, C., GNIRKE, A., CHEN, F., VYSOTSKAIA, V., MANNHAUPT, G., GÜLDENER, U., MÜNSTERKÖTTER, M., HAASE, D., OESTERHELD, M., MEWES, H.-W., MAUCELI, E. W., DECAPRIO, D., WADE, C. M., BUTLER, J., YOUNG, S., JAFFE, D. B., CALVO, S., NUSBAUM, C., GALAGAN, J. & BIRREN, B. W. 2006. Insights from the genome of the biotrophic fungal plant pathogen Ustilago maydis. *Nature,* 444**,** 97-101.

KÄMPER, J., REICHMANN, M., ROMEIS, T., BÖLKER, M. & KAHMANN, R. 1995. Multiallelic recognition: nonself-dependent dimerization of the bE and bW homeodomain proteins in Ustilago maydis. *Cell,* 81**,** 73-83.

KOWAL, J., ARRAS, G., COLOMBO, M., JOUVE, M., MORATH, J. P., PRIMDAL-BENGTSON, B., DINGLI, F., LOEW, D., TKACH, M. & THERY, C. 2016. Proteomic comparison defines novel markers to characterize heterogeneous populations of extracellular vesicle subtypes. *Proceedings of the National Academy of Sciences of the United States of America,* 113**,** E968-E977.

KWON, S., RUPP, O., BRACHMANN, A., BLUM, C. F., KRAEGE, A., GOESMANN, A. & FELDBRÜGGE, M. 2021. mRNA Inventory of Extracellular Vesicles from Ustilago maydis. *Journal of Fungi,* 7**,** 562.

KWON, S., TISSERANT, C., TULINSKI, M., WEIBERG, A. & FELDBRUGGE, M. 2020. Inside-out: from endosomes to extracellular vesicles in fungal RNA transport. *Fungal Biology Reviews,* 34**,** 89-99.

LAI, C. P., KIM, E. Y., BADR, C. E., WEISSLEDER, R., MEMPEL, T. R., TANNOUS, B. A. & BREAKEFIELD, X. O. 2015. Visualization and tracking of tumour extracellular vesicle delivery and RNA translation using multiplexed reporters. *Nature Communications,* 6.

LAMBOU, K., THARREAU, D., KOHLER, A., SIRVEN, C., MARGUERETTAZ, M., BARBISAN, C., SEXTON, A. C., KELLNER, E. M., MARTIN, F., HOWLETT, B. J., ORBACH, M. J. & LEBRUN, M.-H. 2008. Fungi have three tetraspanin families with distinct functions. *BMC Genomics,* 9**,** 63.

LANVER, D., TOLLOT, M., SCHWEIZER, G., LO PRESTI, L., REISSMANN, S., MA, L. S., SCHUSTER, M., TANAKA, S., LIANG, L., LUDWIG, N. & KAHMANN, R. 2017. Ustilago maydis effectors and their impact on virulence. *Nat Rev Microbiol,* 15**,** 409-421.

LAURIE, J. D., LINNING, R. & BAKKEREN, G. 2008. Hallmarks of RNA silencing are found in the smut fungus *Ustilago hordei* but not in its close relative *Ustilago maydis*. *Current Genetics,* 53**,** 49-58.

LEE, E.-Y., CHOI, D.-Y., KIM, D.-K., KIM, J.-W., PARK, J. O., KIM, S., KIM, S.-H., DESIDERIO, D. M., KIM, Y.-K., KIM, K.-P. & GHO, Y. S. 2009. Gram-positive bacteria produce membrane vesicles: Proteomics-based characterization of Staphylococcus aureus-derived membrane vesicles. *PROTEOMICS,* 9**,** 5425-5436.

LIU, M., ZHANG, Z., DING, C., WANG, T., KELLY, B. & WANG, P. 2020. Transcriptomic Analysis of Extracellular RNA Governed by the Endocytic Adaptor Protein Cin1 of Cryptococcus deneoformans. *Frontiers in Cellular and Infection Microbiology,* 10.

LUDWIG, N., REISSMANN, S., SCHIPPER, K., GONZALEZ, C., ASSMANN, D., GLATTER, T., MORETTI, M., MA, L. S., REXER, K. H., SNETSELAAR, K. & KAHMANN, R. 2021. A cell surface-exposed protein complex with an essential virulence function in *Ustilago maydis*. *Nature Microbiology*.

MAACHA, S., BHAT, A. A., JIMENEZ, L., RAZA, A., HARIS, M., UDDIN, S. & GRIVEL, J.-C. 2019. Extracellular vesicles-mediated intercellular communication: roles in the tumor microenvironment and anti-cancer drug resistance. *Molecular Cancer,* 18**,** 55.

MAAS, S. L. N., BREAKEFIELD, X. O. & WEAVER, A. M. 2017. Extracellular Vesicles: Unique Intercellular Delivery Vehicles. *Trends in Cell Biology,* 27**,** 172-188.

MALKIN, E. Z. & BRATMAN, S. V. 2020. Bioactive DNA from extracellular vesicles and particles. *Cell Death & Disease,* 11**,** 584.

MICALI, C. O., NEUMANN, U., GRUNEWALD, D., PANSTRUGA, R. & O'CONNELL, R. 2011. Biogenesis of a specialized plant–fungal interface during host cell internalization of Golovinomyces orontii haustoria. *Cellular Microbiology,* 13**,** 210-226.

MIMS, C., RICHARDSON, E., HOLT, B. & DANGL, J. 2004. Ultrastructure of the host-pathogen interface in Arabidopsis leaves infected with the downy mildew Hyaloperonospora parasitica. *Canadian Journal of Botany-revue Canadienne De Botanique - CAN J BOT,* 82**,** 1001-1008.

NIMRICHTER, L., DE SOUZA, M. M., DEL POETA, M., NOSANCHUK, J. D., JOFFE, L., TAVARES, P. D. M. & RODRIGUES, M. L. 2016. Extracellular Vesicle-Associated Transitory Cell Wall Components and Their Impact on the Interaction of Fungi with Host Cells. *Frontiers in Microbiology,* 7.

NOWARA, D., GAY, A., LACOMME, C., SHAW, J., RIDOUT, C., DOUCHKOV, D., HENSEL, G., KUMLEHN, J. & SCHWEIZER, P. 2010. HIGS: Host-Induced Gene Silencing in the Obligate Biotrophic Fungal Pathogen Blumeria graminis *The Plant Cell,* 22**,** 3130-3141.

O'BRIEN, K., BREYNE, K., UGHETTO, S., LAURENT, L. C. & BREAKEFIELD, X. O. 2020. RNA delivery by extracellular vesicles in mammalian cells and its applications. *Nature Reviews Molecular Cell Biology,* 21**,** 585-606.

O'BRIEN, K., BREYNE, K., UGHETTO, S., LAURENT, L. C. & BREAKEFIELD, X. O. 2020. RNA delivery by extracellular vesicles in mammalian cells and its applications. *Nature Reviews Molecular Cell Biology,* 21**,** 585-606.

OLGEISER, L., HAAG, C., BOERNER, S., ULE, J., BUSCH, A., KOEPKE, J., KONIG, J., FELDBRUGGE, M. & ZARNACK, K. 2019. The key protein of endosomal mRNP transport Rrm4 binds translational landmark sites of cargo mRNAs. *Embo Reports,* 20.

OLICÓN-HERNÁNDEZ, D. R., HERNÁNDEZ-LAUZARDO, A. N., PARDO, J. P., PEÑA, A., VELÁZQUEZ-DEL VALLE, M. G. & GUERRA-SÁNCHEZ, G. 2015. Influence of chitosan and its derivatives on cell development and physiology of Ustilago maydis. *Int J Biol Macromol,* 79**,** 654-60.

OLIVEIRA, D. L., FREIRE-DE-LIMA, C. G., NOSANCHUK, J. D., CASADEVALL, A., RODRIGUES, M. L. & NIMRICHTER, L. 2010. Extracellular vesicles from Cryptococcus neoformans modulate macrophage functions. *Infect Immun,* 78**,** 1601-9.

PAN, B. T. & JOHNSTONE, R. M. 1983. Fate of the transferrin receptor during maturation of sheep reticulocytes in vitro: selective externalization of the receptor. *Cell,* 33**,** 967-78.

PERES DA SILVA, R., LONGO, L. G. V., CUNHA, J., SOBREIRA, T. J. P., RODRIGUES, M. L., FAORO, H., GOLDENBERG, S., ALVES, L. R. & PUCCIA, R. 2019. Comparison of the RNA Content of Extracellular Vesicles Derived from *Paracoccidioides brasiliensis* and *Paracoccidioides lutzii*. *Cells,* 8.

PERES DA SILVA, R., PUCCIA, R., RODRIGUES, M. L., OLIVEIRA, D. L., JOFFE, L. S., CÉSAR, G. V., NIMRICHTER, L., GOLDENBERG, S. & ALVES, L. R. 2015. Extracellular vesicle-mediated export of fungal RNA. *Scientific Reports,* 5**,** 7763.

REGENTE, M., PINEDO, M., SAN CLEMENTE, H., BALLIAU, T., JAMET, E. & DE LA CANAL, L. 2017. Plant extracellular vesicles are incorporated by a fungal pathogen and inhibit its growth. *J Exp Bot,* 68**,** 5485-5495.

RIDDER, K., SEVKO, A., HEIDE, J., DAMS, M., RUPP, A. K., MACAS, J., STARMANN, J., TJWA, M., PLATE, K. H., SULTMANN, H., ALTEVOGT, P., UMANSKY, V. & MOMMA, S. 2015. Extracellular vesicle-mediated transfer of functional RNA in the tumor microenvironment. *Oncoimmunology,* 4.

RIZZO, J., CHAZE, T., MIRANDA, K., ROBERSON, R. W., GORGETTE, O., NIMRICHTER, L., MATONDO, M., LATGÉ, J.-P., BEAUVAIS, A., RODRIGUES, M. L. & MITCHELL, A. P. 2020. Characterization of Extracellular Vesicles Produced by Aspergillus fumigatus Protoplasts. *mSphere,* 5**,** e00476-20.

RIZZO, J., TAHERALY, A. & JANBON, G. 2021a. Structure, composition and biological properties of fungal extracellular vesicles. *microLife,* 2.

RIZZO, J., WONG, S. S. W., GAZI, A. D., MOYRAND, F., CHAZE, T., COMMERE, P.-H., NOVAULT, S., MATONDO, M., PÉHAU-ARNAUDET, G., REIS, F. C. G., VOS, M., ALVES, L. R., MAY, R. C., NIMRICHTER, L., RODRIGUES, M. L., AIMANIANDA, V. & JANBON, G. 2021b. Cryptococcus extracellular vesicles properties and their use as vaccine platforms. *Journal of Extracellular Vesicles,* 10**,** e12129.

RODRIGUES, M. L., NAKAYASU, E. S., OLIVEIRA, D. L., NIMRICHTER, L., NOSANCHUK, J. D., ALMEIDA, I. C. & CASADEVALL, A. 2008. Extracellular vesicles produced by *Cryptococcus neoformans* contain protein components associated with virulence. *Eukaryotic Cell,* 7**,** 58-67.

RODRIGUES, M. L., NIMRICHTER, L., OLIVEIRA, D. L., FRASES, S., MIRANDA, K., ZARAGOZA, O., ALVAREZ, M., NAKOUZI, A., FELDMESSER, M. & CASADEVALL, A. 2007. Vesicular polysaccharide export in *Cryptococcus neoformans* is a eukaryotic solution to the problem of fungal trans-cell wall transport. *Eukaryotic Cell,* 6**,** 48-59.

ROTH, R., HILLMER, S., FUNAYA, C., CHIAPELLO, M., SCHUMACHER, K., LO PRESTI, L., KAHMANN, R. & PASZKOWSKI, U. 2019. Arbuscular cell invasion coincides with extracellular vesicles and membrane tubules. *Nat Plants,* 5**,** 204-211.

RUTTER, B. D. & INNES, R. W. 2017. Extracellular Vesicles Isolated from the Leaf Apoplast Carry Stress-Response Proteins. *Plant Physiology,* 173**,** 728-741.

SABNIS, A., LEDGER, E. V. K., PADER, V. & EDWARDS, A. M. 2018. Antibiotic interceptors: Creating safe spaces for bacteria. *PLOS Pathogens,* 14**,** e1006924.

SKOG, J., WÜRDINGER, T., VAN RIJN, S., MEIJER, D. H., GAINCHE, L., CURRY, W. T., CARTER, B. S., KRICHEVSKY, A. M. & BREAKEFIELD, X. O. 2008. Glioblastoma microvesicles transport RNA and proteins that promote tumour growth and provide diagnostic biomarkers. *Nature Cell Biology,* 10**,** 1470-1476.

SNETSELAAR, K. M. & MIMS, C. W. 1994. Light and Electron-Microscopy of *Ustilago maydis* Hyphae in Maize. *Mycological Research,* 98**,** 347-355.

THÉRY, C., WITWER, K. W., AIKAWA, E., ALCARAZ, M. J., ANDERSON, J. D., ANDRIANTSITOHAINA, R., ANTONIOU, A., ARAB, T., ARCHER, F., ATKIN-SMITH, G. K., AYRE, D. C., BACH, J.-M., BACHURSKI, D., BAHARVAND, H., BALAJ, L., BALDACCHINO, S., BAUER, N. N., BAXTER, A. A., BEBAWY, M., BECKHAM, C., BEDINA ZAVEC, A., BENMOUSSA, A., BERARDI, A. C., BERGESE, P., BIELSKA, E., BLENKIRON, C., BOBIS-WOZOWICZ, S., BOILARD, E., BOIREAU, W., BONGIOVANNI, A., BORRÀS, F. E., BOSCH, S., BOULANGER, C. M., BREAKEFIELD, X., BREGLIO, A. M., BRENNAN, M. Á., BRIGSTOCK, D. R., BRISSON, A., BROEKMAN, M. L. D., BROMBERG, J. F., BRYL-GÓRECKA, P., BUCH, S., BUCK, A. H., BURGER, D., BUSATTO, S., BUSCHMANN, D., BUSSOLATI, B., BUZÁS, E. I., BYRD, J. B., CAMUSSI, G., CARTER, D. R. F., CARUSO, S., CHAMLEY, L. W., CHANG, Y.-T., CHEN, C., CHEN, S., CHENG, L., CHIN, A. R., CLAYTON, A., CLERICI, S. P., COCKS, A., COCUCCI, E., COFFEY, R. J., CORDEIRO-DA-SILVA, A., COUCH, Y., COUMANS, F. A. W., COYLE, B., CRESCITELLI, R., CRIADO, M. F., D'SOUZA-SCHOREY, C., DAS, S., DATTA CHAUDHURI, A., DE CANDIA, P., DE SANTANA, E. F., DE WEVER, O., DEL PORTILLO, H. A., DEMARET, T., DEVILLE, S., DEVITT, A., DHONDT, B., DI VIZIO, D., DIETERICH, L. C., DOLO, V., DOMINGUEZ RUBIO, A. P., DOMINICI, M., DOURADO, M. R., DRIEDONKS, T. A. P., DUARTE, F. V., DUNCAN, H. M., EICHENBERGER, R. M., EKSTRÖM, K., EL ANDALOUSSI, S., ELIE-CAILLE, C., ERDBRÜGGER, U., FALCÓN-PÉREZ, J. M., FATIMA, F., FISH, J. E., FLORES-BELLVER, M., FÖRSÖNITS, A., FRELET-BARRAND, A., et al. 2018. Minimal information for studies of extracellular vesicles 2018 (MISEV2018): a position statement of the International Society for Extracellular Vesicles and update of the MISEV2014 guidelines. *Journal of Extracellular Vesicles,* 7**,** 1535750.

TOSAR, J. P., SEGOVIA, M., CASTELLANO, M., GÁMBARO, F., AKIYAMA, Y., FAGÚNDEZ, P., OLIVERA, Á., COSTA, B., POSSI, T., HILL, M., IVANOV, P. & CAYOTA, A. 2020. Fragmentation of extracellular ribosomes and tRNAs shapes the extracellular RNAome. *Nucleic Acids Research,* 48**,** 12874-12888.

VAN NIEL, G., D'ANGELO, G. & RAPOSO, G. 2018. Shedding light on the cell biology of extracellular vesicles. *Nature Reviews Molecular Cell Biology,* 19**,** 213-228.

VARGAS, G., ROCHA, J. D., OLIVEIRA, D. L., ALBUQUERQUE, P. C., FRASES, S., SANTOS, S. S., NOSANCHUK, J. D., GOMES, A. M., MEDEIROS, L. C., MIRANDA, K., SOBREIRA, T. J., NAKAYASU, E. S., ARIGI, E. A., CASADEVALL, A., GUIMARAES, A. J., RODRIGUES, M. L., FREIRE-DE-LIMA, C. G., ALMEIDA, I. C. &

NIMRICHTER, L. 2015. Compositional and immunobiological analyses of extracellular vesicles released by Candida albicans. *Cell Microbiol,* 17**,** 389-407.

WAHL, R., ZAHIRI, A. & KAMPER, J. 2010. The Ustilago maydis b mating type locus controls hyphal proliferation and expression of secreted virulence factors in planta. *Molecular Microbiology,* 75**,** 208-220.

WANG, B., SUN, Y., SONG, N., ZHAO, M., LIU, R., FENG, H., WANG, X. & KANG, Z. 2017. *Puccinia striiformis* f. sp. *tritici* microRNA-like RNA 1 (*Pst*-milR1), an important pathogenicity factor of *Pst*, impairs wheat resistance to *Pst* by suppressing the wheat pathogenesis-related 2 gene. *New Phytologist,* 215**,** 338-350.

WEI, Z., BATAGOV, A. O., SCHINELLI, S., WANG, J., WANG, Y., EL FATIMY, R., RABINOVSKY, R., BALAJ, L., CHEN, C. C., HOCHBERG, F., CARTER, B., BREAKEFIELD, X. O. & KRICHEVSKY, A. M. 2017. Coding and noncoding landscape of extracellular RNA released by human glioma stem cells. *Nature Communications,* 8**,** 1145.

WEIBERG, A., WANG, M., LIN, F. M., ZHAO, H. W., ZHANG, Z. H., KALOSHIAN, I., HUANG, H. D. & JIN, H. L. 2013. Fungal Small RNAs Suppress Plant Immunity by Hijacking Host RNA Interference Pathways. *Science,* 342**,** 118-123.

WILLIAMS, C., PALVIAINEN, M., REICHARDT, N. C., SILJANDER, P. R. & FALCÓN-PÉREZ, J. M. 2019. Metabolomics Applied to the Study of Extracellular Vesicles. *Metabolites,* 9.

WILLYSSON, A., STÅHL, A.-L., GILLET, D., BARBIER, J., CINTRAT, J.-C., CHAMBON, V., BILLET, A., JOHANNES, L. & KARPMAN, D. 2020. Shiga Toxin Uptake and Sequestration in Extracellular Vesicles Is Mediated by Its B-Subunit. *Toxins,* 12**,** 449.

WOLF, J. M., ESPADAS-MORENO, J., LUQUE-GARCIA, J. L. & CASADEVALL, A. 2014. Interaction of Cryptococcus neoformans extracellular vesicles with the cell wall. *Eukaryot Cell,* 13**,** 1484-93.

ZAMITH-MIRANDA, D., HEYMAN, H. M., COUVILLION, S. P., CORDERO, R. J. B., RODRIGUES, M. L., NIMRICHTER, L., CASADEVALL, A., AMATUZZI, R. F., ALVES, L. R., NAKAYASU, E. S. & NOSANCHUK, J. D. 2021. Comparative Molecular and Immunoregulatory Analysis of Extracellular Vesicles from Candida albicans and Candida auris. *mSystems***,** e0082221.

ZARNOWSKI, R., SANCHEZ, H., COVELLI, A. S., DOMINGUEZ, E., JAROMIN, A., BERNHARDT, J., MITCHELL, K. F., HEISS, C., AZADI, P., MITCHELL, A. & ANDES, D. R. 2018. *Candida albicans* biofilm-induced vesicles confer drug resistance through matrix biogenesis. *Plos Biology,* 16.

ZENG, A., WEI, Z., RABINOVSKY, R., JUN, H. J., EL FATIMY, R., DEFORZH, E., ARORA, R., YAO, Y., YAO, S., YAN, W., UHLMANN, E. J., CHAREST, A., YOU, Y. & KRICHEVSKY, A. M. 2020. Glioblastoma-Derived Extracellular Vesicles Facilitate Transformation of Astrocytes via Reprogramming Oncogenic Metabolism. *iScience,* 23**,** 101420.

ZHANG, H., FREITAS, D., KIM, H. S., FABIJANIC, K., LI, Z., CHEN, H., MARK, M. T., MOLINA, H., MARTIN, A. B., BOJMAR, L., FANG, J., RAMPERSAUD, S., HOSHINO, A., MATEI, I., KENIFIC, C. M., NAKAJIMA, M., MUTVEI, A. P., SANSONE, P., BUEHRING, W., WANG, H., JIMENEZ, J. P., COHEN-GOULD, L., PAKNEJAD, N., BRENDEL, M., MANOVA-TODOROVA, K., MAGALHÃES, A., FERREIRA, J. A., OSÓRIO, H., SILVA, A. M., MASSEY, A., CUBILLOS-RUIZ, J. R., GALLETTI, G., GIANNAKAKOU, P., CUERVO, A. M., BLENIS, J., SCHWARTZ, R., BRADY, M. S., PEINADO, H., BROMBERG, J., MATSUI, H., REIS, C. A. & LYDEN, D. 2018. Identification of distinct nanoparticles and subsets of extracellular vesicles by asymmetric flow field-flow fractionation. *Nature Cell Biology,* 20**,** 332-343.

ZHAO, K. N., BLEACKLEY, M., CHISANGA, D., GANGODA, L., FONSEKA, P., LIEM, M., KALRA, H., AL SAFFAR, H., KEERTHIKUMAR, S., ANG, C. S., ADDA, C. G., JIANG, L. Z., YAP, K., POON, I. K., LOCK, P., BULONE, V., ANDERSON, M. & MATHIVANAN, S. 2019. Extracellular vesicles secreted by *Saccharomyces cerevisiae* are involved in cell wall remodelling. *Communications Biology,* 2.

ZOMER, A., MAYNARD, C., VERWEIJ, F. J., KAMERMANS, A., SCHÄFER, R., BEERLING, E., SCHIFFELERS, R. M., DE WIT, E., BERENGUER, J., ELLENBROEK, S. I. J., WURDINGER, T., PEGTEL, D. M. & VAN

RHEENEN, J. 2015. In Vivo imaging reveals extracellular vesicle-mediated phenocopying of metastatic behavior. *Cell,* 161**,** 1046-1057.

1.9.   Appendix to Chapter 1

Disclaimer

This manuscript has been published in Fungal Biology Reviews(https://doi.org/10.1016/j.fbr.2020.01.001). Author contributions are stated in the manuscript and all contents of the submission package and the final published materials have been confirmed by the authors. The latest published version of the manuscript is reproduced here with permissions according to the Elsevier Author Rights.

Personal Contribution

I have contributed extensively in writing of the manuscript, especially Sections 1, 2, and 4. I have earned an independent scholarship from the Deutscher Akademischer Austausch Dienst with own proposal on EVs to fund this project.

Review

Inside-out: from endosomes to extracellular vesicles in fungal RNA transport

Seomun KWON[a], Constance TISSERANT[b], Markus TULINSKI[a], Arne WEIBERG[b,**], Michael FELDBRÜGGE[a,*]

[a]Heinrich Heine University Düsseldorf, Institute for Microbiology, Cluster of Excellence on Plant Sciences, 40204 Düsseldorf, Germany
[b]Ludwig Maximilians University Munich, Department of Biology I, 82152 Planegg-Martinsried, Germany

ABSTRACT

Membrane-coupled RNA transport is an emerging theme in fungal biology. This review focuses on the RNA cargo and mechanistic details of transport via two inter-related sets of organelles: endosomes and extracellular vesicles for intra- and intercellular RNA transfer. Simultaneous transport and translation of messenger RNAs (mRNAs) on the surface of shuttling endosomes is a conserved process pertinent to highly polarised eukaryotic cells, such as hyphae or neurons. Here we detail the endosomal mRNA transport machinery components and mRNA targets of the core RNA-binding protein Rrm4. Extracellular vesicles (EVs) are newly garnering interest as mediators of intercellular communication, especially between pathogenic fungi and their hosts. Landmark studies in plant–fungus interactions indicate EVs as a means of delivering various cargos, most notably small RNAs (sRNAs), for cross-kingdom RNA interference. Recent advances and implications of the nascent field of fungal EVs are discussed and potential links between endosomal and EV-mediated RNA transport are proposed.

© 2020 British Mycological Society. Published by Elsevier Ltd. All rights reserved.

1. Introduction

The vast majority of fungi grow by forming hyphae. Characteristic for these fungal filaments is a high degree of polarity: they expand at the tip and insert septa in the basal region (Harris, 2019; Riquelme et al., 2018). To achieve this exquisite polar growth, building blocks like lipids, proteins and cell wall material need to be transported efficiently towards the growth pole. Therefore, sophisticated long-distance transport is essential for hyphal growth. Important components are molecular motors that actively transport endosomes and vesicles along microtubules (Riquelme et al., 2018; Steinberg, 2014).

While the exact orchestration of intracellular processes is key for polar growth, intense communication of the growing hyphae with the environment is a second substantial process to guarantee survival. The polar growing cells sense nutrients and utilise them by secreting hydrolytic enzymes from the growing tip. Furthermore, hyphae also exchange information

with other organisms like microbes, plants and animals. A well-studied example is the role of fungi as pathogens. Evidence is accumulating that also in this case membranous carriers like extracellular vesicles are crucial delivery vehicles. Intriguingly, for intra- as well as for intercellular transport, functionally important links between membranous transport vehicles and RNA trafficking has been disclosed.

RNA molecules figure fundamentally in mediating protein production from the genetic blueprint. They serve both as components of the translation machinery as well as adaptable regulators. In this review, we focus on messenger RNAs (mRNAs) and small regulatory RNAs (sRNAs) transported in association with intracellular and extracellular organelles, namely endosomes and extracellular vesicles (EVs).

A molecule of mRNA contains, apart from the protein-coding sequence, cis-acting regulatory elements for interaction with cognate trans-acting factors. These fine-tune timing, localisation and amplitude of translation in a combinatorial manner. Thus, each mRNA molecule interacts with various factors during its lifetime (Eliscovich and Singer, 2017; Singh et al., 2015), including small RNAs (sRNAs) and a plethora of RNA-binding proteins (Hentze et al., 2018).

Small RNAs regulate gene expression at the transcriptional and post-transcriptional level in a process known as RNA silencing or RNA interference (RNAi) in eukaryotes (Bologna and Voinnet, 2014; Chang et al., 2012; Wilson and Doudna, 2013). Dicer-like proteins (DCR, Drosha, DCL) are core factors in sRNA biogenesis that process double-strand RNA precursors into mature 20−30 nucleotide (nt) duplex sRNAs, which include microRNAs (miRNAs), small-interfering RNAs (siRNAs) and PIWI-interacting RNAs (piRNAs). The guide strand of sRNAs is loaded into an active Argonaute (AGO) core of the RNA-induced silencing complex (RISC) to direct sequence-specific gene silencing.

RNA-binding proteins (RBPs) play important roles in escorting and transporting cargo RNAs and thus contain designated domains to interact with specific elements in their targets. For example, the RNA recognition motifs (RRMs) of the poly(A)-binding protein recognises the poly(A) tail of almost all mRNAs (Brambilla et al., 2019; Hogan et al., 2008). Conversely, RNA elements with defined secondary and tertiary structures are bound by specific RNA-binding proteins that influence the stability, functionality and localisation of RNA molecules. Pertinent to intracellular RNA transport are complexes containing RBPs that link them to molecular motors to determine where and when the mRNA should be translated (Martin and Ephrussi, 2009; Niessing et al., 2018).

In recent years, a close link between RNA transport and membrane trafficking has become apparent (Béthune et al., 2019; Jansen et al., 2014). Endosomes, for example, carry mRNA along the microtubule cytoskeleton (Baumann et al., 2012). Moreover, translation of mRNA on the surface of mobile endosomes has been demonstrated as a novel mechanism to load protein cargo on endosomes for long distance transport (Baumann et al., 2012; Haag et al., 2015).

Another emerging theme is extracellular vesicle (EV)-mediated RNA transport. Various RNA species have been found in the lumen of EVs that may participate in intercellular communication. In light of the breakthrough discoveries of cross-kingdom RNAi between pathogenic fungi and their host plants (Nowara et al., 2010; Weiberg et al., 2013), EVs are emerging as probable vehicles mediating this process (Cai et al., 2018). The membrane-associated RBPs, such as the endosome-associated RNAi components (Gibbings et al., 2009; Lee et al., 2009) are predicted to facilitate selective targeting of RNA cargo into extracellular vesicles. Here, we summarise the current knowledge and carefully speculate on the mechanisms of endosomal and EV-mediated RNA transport in fungi, with respect to their development and lifestyle: from endosomal transport of mRNA during polar growth of hyphae to secretion of sRNA in extracellular vesicles at the fungal−plant interface.

2.   Endosomal mRNA transport

Fungal endosomes on the move

The endosomal pathway is an evolutionarily conserved membrane trafficking mechanism important for recycling and degradation of plasma membrane proteins. Starting with endocytosis, early endosomes are formed by inward budding of the plasma membrane and mature into late endosomes. Along the path of maturation, intraluminal vesicles bud inwards forming multivesicular endosomes (MVEs) (Huotari and Helenius, 2011). Maturing endosomes have different fates: they fuse with the vacuole for cargo degradation or they fuse with the plasma membrane, releasing its luminal contents. The intraluminal vesicles of MVEs are released as exosomes. Important regulators of intracellular membrane trafficking are small GTPases, specific subsets of which mark membrane compartment identity. Early and late endosomes, for example, are associated with Rab5- and Rab7-type GTPases, respectively (Huotari and Helenius, 2011).

Among the best-studied examples for endosomal transport in fungi is the basidiomycete *Ustilago maydis* (Haag et al., 2015; Steinberg, 2012). This corn pathogen switches from yeast-like budding to unipolar growth in order to form infectious hyphae for plant colonisation (Lanver et al., 2017). Prior to invading the plant, the cell cycle is temporarily arrested and hyphae begin to grow with a defined axis of polarity. The hyphae expand at the apical pole and insert septa at the basal pole (Fig. 1A; Vollmeister et al., 2012). Studying endocytosis during this phase of the life cycle uncovered extensive bidirectional movement of Rab5a-positive early endosomes along microtubules (Steinberg, 2012, 2014). Endosomal shuttling is achieved by the concerted action of the plus end-directed Kinesin-3-type motor Kin3 towards the hyphal tip and the minus end-directed motor dynein Dyn1/2 towards the central nucleus. Loss of Kin3 results in the formation of aberrant bipolar hyphae, suggesting that endosomal transport is needed for efficient unipolar hyphal growth (Schuster et al., 2011). It has been speculated that endosomes deliver cargo proteins to the basal vacuole or transport signalling components over long distances to allow communication between the nucleus and the growing apex (Bielska et al., 2014; Steinberg, 2012, 2014).
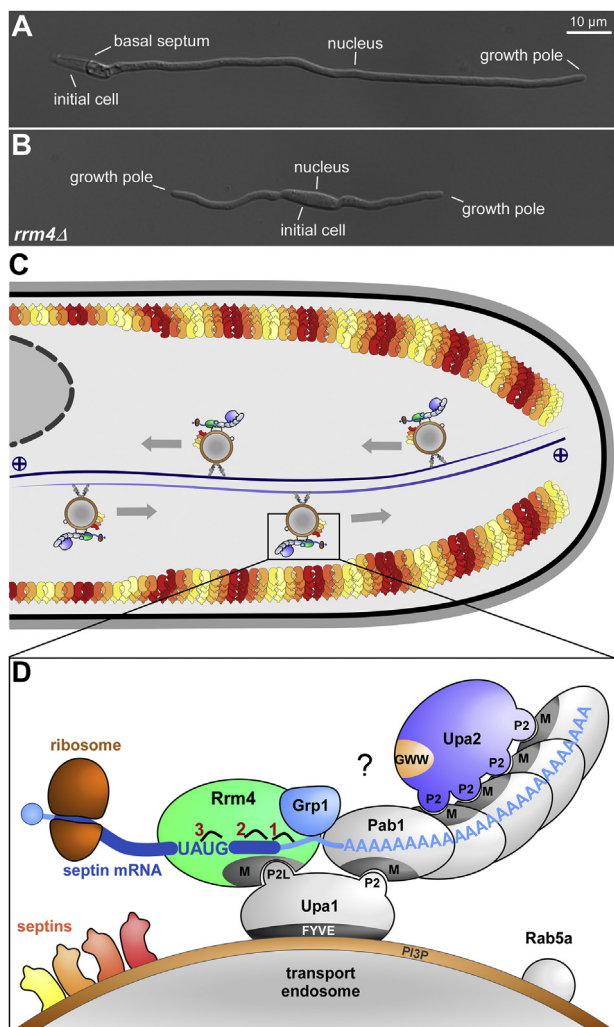
Fig. 1 — Endosomal RNA transport machinery in *Ustilago maydis*. (A) Unipolar filamentous growth of *U. maydis* laboratory strain AB33, engineered to facilitate genetic studies on filamentous growth (Brachmann et al., 2001). **(B)** Bipolar filamentous growth of *rrm4Δ* strain in AB33 background. Aberrant cell polarity in the absence of the endosome-associated mRNA-binding protein Rrm4 indicates the importance of mRNA transport in polarity maintenance in hyphal cells. **(C)** Model of bi-directional, endosome-associated mRNA transport along microtubules in *U. maydis* hypha (growth pole at the right, nucleus in grey). Depicted are cortical septin filaments formed by septin heterooctamers (yellow, orange and red subunits). An array of antiparallel microtubules with shuttling endosomes is drawn in the center (plus ends [+] of microtubules are indicated). The plus-end directed motor Kin3 is given as an example. Local translation of septin mRNAs on the cytoplasmic surface of endosomes results the assembly of heteromeric septin complexes on endosomes. These heteromeric protein complexes are transported towards the growth pole to enable efficient formation of septin filaments forming a gradient emanating from the hyphal tip. The cytoplasmic surface of transport endosomes is enlarged in D. **(D)** Components of the endosomal RNA transport machinery. Rrm4 core mRNA-binding protein (green oval) and Pab1 poly(A)-binding protein (grey oval) are attached to the surface of Rab5a-positive transport endosomes via the adaptor protein Upa1. Upa1 is bound to the endosomal surface via a PI3P-binding FYVE domain and possesses PAM2L (P2L) and PAM2 (P2) domains to interact with MLLE domains (M) of Rrm4 and Pab1. Multi-PAM2 protein Upa2 (blue oval) presumably acts as a scaffold for Pab1 proteins on the poly(A) tail of cargo mRNAs, and its GWW motif (orange patch) is important for association of Pab1 on endosomal surface. The interaction partner of the GWW motif is currently unknown as indicated by a question mark. Rrm4 has three RRM domains (1, 2, 3), which notably bind septin mRNAs, and recognises the UAUG motif via the third RRM domain (3). Additional RNA-binding protein Grp1 (light blue oval) co-localises and shares mRNA targets with Rrm4, including septins. Bound mRNAs are translated during transport on endosomes and the translation products are co-transported, as exemplified by shuttling of partially assembled septin hetero-oligomers for increased efficiency.

Rrm4: a major RBP for mRNA transport on endosomes

An insightful addition to the picture of the endosomal distribution chain was the presence of the mRNA-binding protein Rrm4 on Rab5-positive endosomes, uncovering a novel mechanism of mRNA transport in polarised cells (Baumann et al., 2012; Jansen et al., 2014). Prior to this discovery, there was genetic evidence linking Rrm4 to endosomal function and cell polarity: loss of Rrm4 leads to the formation of aberrant bipolar hyphae, similar to those of *kin3Δ* strains (Fig. 1B; Becht et al., 2006).

Rrm4 contains three RRM domains for RNA binding at the N-terminus and two MLLE domains for protein–protein interaction at the C-terminus. A recent transcriptome-wide analysis mapped sequences bound by Rrm4 with single-nucleotide resolution. This showed groups of transcripts with different patterns of binding including precisely the start or stop codons, the ORF and, most prominently, the 3′ untranslated region (UTR) (Fig. 1C–D; Olgeiser et al., 2019). Differential binding specificities of the three RRM domains, in combination with other protein interactors, might bring about different binding patterns on the target mRNA. Supporting this notion, the third RRM domain recognises the sequence motif UAUG. Furthermore, the small glycine-rich RNA-binding protein Grp1 was found to share targets with Rrm4, particularly in 3′ UTRs (Fig. 1C–D; Olgeiser et al., 2019). In essence, the key RNA-binding protein of endosomal mRNA transport binds distinct translational landmark sites to orchestrate transport and translation.

On-the-go translation of mRNAs on shuttling endosomes

Evidence from RNA live imaging with *in vivo* UV crosslinking revealed that Rrm4 binds a distinct set of target mRNAs, including those encoding septins (König et al., 2009). Septins are cytoskeletal proteins that assemble into heteromeric building blocks, important for cell polarity and morphology (Mostowy and Cossart, 2012). In hyphae, septins form

higher-order structures, such as filaments, with a gradient emanating from the hyphal growth pole (Fig. 1C–D; Baumann et al., 2014; Zander et al., 2016).

Intriguingly, the septin proteins too were found to be present on Rrm4-positive transport endosomes, along with septin mRNA. Moreover, Rrm4-dependent shuttling of tagged ribosomes on these endosomes strongly suggests on-the-go translation of the cargo mRNA on the endosomal surface (Baumann et al., 2014; Higuchi et al., 2014). Consistently, all four septin mRNAs carry Rrm4 binding sites in their 3′ untranslated region (UTR), presumably so that the binding of Rrm4 does not interfere with translation during transport (Olgeiser et al., 2019). In the absence of Rrm4, shuttling of both septin mRNA and proteins was lost, as well as septin heteromer assembly and the formation of a gradient of higher order septin filaments (Fig. 1C–D; Baumann et al., 2014; Zander et al., 2016). Thus, a novel concept of endosomal transport-coupled translation was introduced (Baumann et al., 2014): local translation and assembly of protein complexes at the surface of motile endosomes allows the efficient delivery of ready-made products to the hyphal growth pole (Fig. 1C–D).

The endosomal RNA transport machinery

A major research question surrounding Rrm4-mediated endosomal mRNA transport is how the Rrm4-containing mRNPs are attached to endosomes. Initially, it was found that mutations in critical residues of the C-terminal MLLE domain caused loss of Rrm4 movement (Becht et al., 2006). The 70-amino-acid MLLE domain was first found in the human poly(A)-binding protein PABC1. It specifically interacts with the PAM2 peptide motif (PABP interacting motif 2), present in cognate protein interaction partners (Kozlov et al., 2010; Xie et al., 2014). Search for PAM2 motif proteins lead to Upa1 (*Ustilago* PAM2 protein 1; Pohlmann et al., 2015), which additionally contains a FYVE zinc finger for the interaction with PI3P lipids characteristic for early endosomes (Kutateladze, 2006; Stenmark et al., 2002). Indeed, Upa1 shuttles on almost all Rrm4-positive endosomes and the loss of Upa1 causes aberrant bipolar hyphal growth. Upa1 interacts with Rrm4 but unexpectedly, its PAM2 motif was dispensable for this function (Pohlmann et al., 2015). However, it was found to contain two PAM2-like sequences (PAM2L), which mediate the interaction with the MLLE domains of Rrm4 (Pohlmann et al., 2015). Taken together, Upa1 is the first example of a functionally important adaptor protein linking Rrm4-containing mRNPs to endosomes (Fig. 1D; Pohlmann et al., 2015). However, even in the absence of Upa1, residual endosomal shuttling of Rrm4 is observed, suggesting that there are additional factors involved.

Upa2, which exceptionally contains four PAM2 motifs, shuttles on almost all Rrm4-positive endosomes and is important for efficient unipolar hyphal growth (Jankowski et al., 2019). However, in contrast to Upa1 it requires Rrm4 to be present on endosomes, indicating that it most likely interacts with the components of the mRNP, rather than directly with the endosomal membrane. Also in this case, the PAM2 motifs were functionally dispensable. Instead, a novel functionally important effector domain at the N-terminus and a conserved GWW motif for endosomal mRNP attachment at the C-

terminus were discovered. Loss of Upa2 did not influence Rrm4, but shuttling of the poly(A)-binding protein Pab1 and specific target mRNAs was strongly reduced. Thus, Upa2 classifies as a novel core component of endosomal mRNA transport, which most likely serves as a scaffold protein for endosomal mRNP assembly or stability during transport (Fig. 1D; Jankowski et al., 2019).

To learn more about the identity of the transport endosomes, the conserved factor Did2 was studied. It regulates the ESCRT machinery (endosomal sorting complex required for transport) for endosomal maturation (Hurley, 2015; Teis et al., 2009). Loss of Did2 caused aberrant bipolar hyphal growth, suggesting a link to endosomal mRNA transport. Closer inspection revealed that maturation of shuttling endosomes was indeed disturbed, since marker proteins Rab7 or vacuolar cargo proteins were present on shuttling endosomes in *did2Δ* hyphae (Haag et al., 2015). The altered identity of the shuttling endosomes causes reduced attachment of the motor Kin3 as well as less FYVE protein Upa1. Consequently, mRNPs were transported less efficiently, explaining the phenotype. Thus, the ESCRT regulator orchestrates the balance of early endosomes functioning in long-distance transport and endocytic maturation (Haag et al., 2017).

Membrane-associated RNA transport as a widespread concept

Membrane-associated RNA transport appears to be a common theme in biology (Béthune et al., 2019). Within the fungal kingdom, a detailed phylogenetic analysis of the core endosomal RNA transport machinery components revealed its conservation across Basidiomycota and the distantly related Mucoromycota (Müller et al., 2019). Endosomal shuttling of the heterologously expressed Rrm4 orthologue from fungi as distant as *Rhizophagus irregularis* in *U. maydis*, suggests a high degree of functional conservation (Müller et al., 2019). By contrast, potential homologues of components of the core endosomal transport machinery like Rrm4, Upa1 and Upa2 were not found in Ascomycota. However, microtubule-dependent shuttling of the RNA-binding protein Gul1 was recently reported in hyphae of the ascomycete *Neurospora crassa* (Herold et al., 2019). Hence, long-distance transport of mRNAs along microtubules might be operational also in ascomycetes, however the core machinery appears to be different.

Comparable to endosomal mRNA transport in *U. maydis,* neuronal endosomes were discovered to deliver mRNAs and promote mitochondrial targeting of nuclear encoded proteins by local translation at the surface of late endosomes (Cioni et al., 2019). Furthermore, the mammalian RNA-binding protein ANXA11 links RNA granules to moving lysosomes for long-distance mRNA transport in neurons (Liao et al., 2019). In essence, endosomal mRNA transport is not an exceptional invention in basidiomycete smut fungi, but a widespread trafficking process.

On a wider scale, membrane-associated RNA-binding proteins (memRBPs) coordinate membrane-coupled local translation, not only at endosomes or the ER but most likely at all internal membranes including those of mitochondria, peroxisomes and vacuoles (Béthune et al., 2019). This brings us to hypothesise that such memRBPs would also facilitate specific

loading of various RNA cargo from intercommunicating intracellular organelles into secreted extracellular membrane structures, which can be considered "extended" organelles that can bring about extended phenotypes (Dawkins, 1982).

3. Extracellular vesicle-mediated RNA transport

Extracellular vesicles

Extracellular vesicles (EVs) are membranous nano-sized particles secreted by organisms representing the kingdoms of life. Despite initial disregard as being cell debris or disposals, cumulative evidence clearly indicates biological functionality of EVs, particularly in intercellular and inter-organismal communication (Deatherage and Cookson, 2012; Maas et al., 2017; Meldolesi, 2018; Mittelbrunn and Sanchez-Madrid, 2012). EVs are now recognised as common vehicles that deliver molecules such as RNAs and proteins to instigate physiological changes in recipient cells. Already observed in early ultrastructural studies, EVs have only recently begun to gain increasing attention from plant scientists and microbiologists. EVs are proposed to play pivotal roles in cross-kingdom communication between microbial pathogens and their hosts (Bielska et al., 2019; Bielska and May, 2019; Kuipers et al., 2018; Rutter and Innes, 2018; Rybak and Robatzek, 2019; Samuel et al., 2015; Soares et al., 2017). In this part, we summarise the state of the-art in fungal EVs, their protein and RNA cargos as well as their potential function in intra-species to cross-kingdom communication.

EV biogenesis in fungi

EVs are a collective term for a very heterogeneous group of lipid bilayer particles varying in size, composition and cargo. Such high level of heterogeneity suggests that distinct EV biogenesis pathways must exist in cells (Mathieu et al., 2019; van Niel et al., 2018). In mammalian cell types, two major EV secretion mechanisms have been described. On the one hand, intraluminal vesicles in multivesicular endosomes (MVEs) are released as exosomes upon fusion of MVEs with the plasma membrane (Fig. 2). On the other hand, microvesicles bud directly off the plasma membrane, which explains the overlap in molecular contents in this type of EVs with the local cytoplasm at the cell periphery. In both EV secretion pathways, conserved ESCRT components and accessory proteins are involved (Colombo et al., 2013). Furthermore, various proteins that are linked to endomembrane systems, such as small GTPases (Muralidharan-Chari et al., 2009), SNAREs (Fader et al., 2009; Koles et al., 2012), syntenins (Baietti et al., 2012) and tetraspanins (van Niel et al., 2011), are relevant for EV biogenesis and cargo loading. Homologous proteins and similar secretory pathways are likely to participate in fungal EV biogenesis as well, but their relative contribution and biological significance remain to be clarified (Oliveira et al., 2013). In this regard, genetic evidence suggests involvement of both the conventional secretory pathway and the ESCRT-mediated MVE pathway in fungal EV biogenesis and cargo loading. For instance, *Saccharomyces cerevisiae* mutants of both the exocytic Rab GTPase *Sec4*, required for post-Golgi
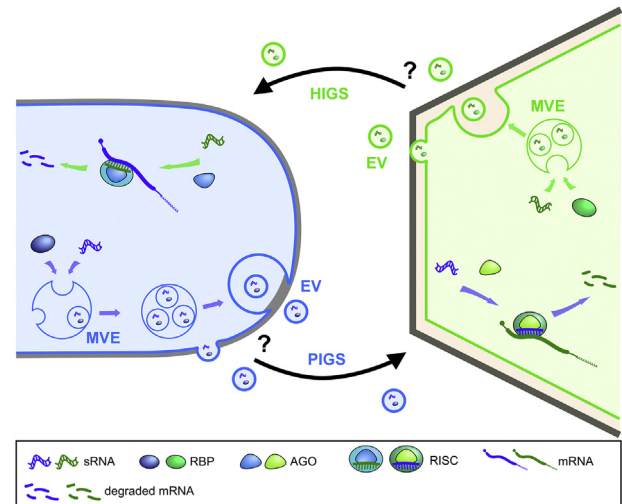

Fig. 2 − **Cross-kingdom RNAi at the fungus−plant interface mediated by extracellular vesicles (EVs). During infection, both the fungus and the plant deploy small RNAs (sRNAs) to silence target genes in the interaction partner, as virulence and defence strategies, respectively. Silencing of fungal pathogen genes by plant host sRNAs is termed host-induced gene silencing (HIGS) and *vice versa*, pathogen-induced gene silencing (PIGS) is brought about by fungal sRNAs in plants. EVs are one of the ways in which sRNAs are transferred between interacting organisms. EVs can be derived from multivesicular endosomes (MVEs) or from budding at the plasma membrane. Endosomes bud inwards during maturation to form intraluminal vesicles, incorporating contents from the cytosol, notably sRNAs and proteins. RNA-binding proteins are thought to be key determinants of RNA loading into EVs. Intraluminal vesicles are released as exosomes upon fusion of the MVE with the plasma membrane. Precisely how EVs cross the cell walls and deliver their contents to the recipient cell are currently undetermined.**

secretory vesicle formation, and the ESCRT component *Snf7,* show altered EV protein composition (Oliveira et al., 2010b). Furthermore, knocking down the exocyst component *Sec6* in the fungus *Cryptococcus neoformans* led to a dramatic reduction in EV secretion (Panepinto et al., 2009), presumably by affecting MVE fusion with the plasma membrane. Obviously, disruption of individual genes involved in EV biogenesis does not completely abolish EV formation, implying a certain level of functional redundancy of genes and pathways in EV formation.

Proteins and RNAs in fungal EVs

To gain further insights into the biogenesis of fungal EVs and their potential roles in fungal biology and pathogenicity, several studies have examined the EV protein and RNA cargos (Rodrigues et al., 2014). Commonly, many proteins found in EVs indeed lack classical signal peptides, supporting their

cellular release via unconventional secretion mechanisms (Rodrigues et al., 2008). Comparative proteomics of fungal EVs displayed not only high diversity, but also revealed core sets of cargo proteins, indicating some degree of conservation in EV biogenesis, cargo loading and function (Rodrigues et al., 2014; Vallejo et al., 2012). These EV core proteins were predicted to function in translation, carbohydrate and protein metabolism, oxidation/reduction, transport, stress response and signalling functions (Vallejo et al., 2012). Of note, several virulence factors have been found in EVs of pathogenic fungal species, suggesting a role of EVs in pathogenesis (Bleackley et al., 2019).

Beside proteins, a number of RNA species have been identified in fungal EVs. To date, studies on various fungal species have predominantly focused on smaller non-coding RNAs (<200 nt), including potential gene-regulatory small RNAs, such as miRNA-like RNAs (milRNAs) and tRNA fragments (tRFs) (Fig. 2; Alves et al., 2019; Peres da Silva et al., 2019; Peres da Silva et al., 2015; Rayner et al., 2017). The detection of small RNAs in fungal EVs supports their proposed role in RNA-mediated intra- or interspecific communication. Moreover, full-length mRNAs have also been found in fungal EVs (Alves et al., 2019; Peres da Silva et al., 2019), but it needs to be clarified whether EV mRNAs are translated into functional peptides in recipient cells. Beside detection, enrichment of certain RNA species and sequence motifs has been reported in plant and animal EVs (Villarroya-Beltri et al., 2014). Indeed, there seems to be clear differences between cellular and EV abundance of transcripts (Alves et al., 2019; Peres da Silva et al., 2019) implying the existence of active, yet unknown RNA sorting mechanisms into EVs. In this regard, RNA-binding proteins that form ribonucleoprotein complexes were found to facilitate loading of specific microRNAs into mammalian exosomes (Statello et al., 2018; Villarroya-Beltri et al., 2014). Similarly, ribonucleoprotein complexes are prime suspects to mediate RNA sorting into fungal EVs (Fig. 2). Accordingly, candidate RBPs have been detected in fungal EV proteome studies (Alves et al., 2019), thus waiting to be studied for their role in EV RNA sorting.

EVs in human-pathogenic fungi

Fungal EVs are thought to participate in intercellular communication regarding host-fungal or fungal–microbial interactions. Indeed, fungal EVs released from different pathogenic species can either support host infection (Bielska et al., 2018; Ikeda et al., 2018) or stimulate immune responses in their mammalian host cells (Oliveira et al., 2010a; Vargas et al., 2015). For instance, EVs isolated from the culture supernatant of *Candida albicans* or *Cryptococcus neoformans* have immuno-modulatory effects on macrophages and other immune cells (Joffe et al., 2016; Zamith-Miranda et al., 2018). Known virulence-associated proteins, such as laccases and ureases, were found in *C. neoformans* and *C. albicans* EVs, suggesting vesicular transport of such virulence factors towards host cells for infection (Oliveira et al., 2010b; Rodrigues et al., 2008). Other non-proteinaceous compounds were also detected in fungal EVs that are known to contribute to pathogenicity and virulence, such as melanin and the polysaccharide glucuronoxylomannan (Eisenman et al., 2009; Rodrigues et al.,

2007). Interestingly, fungi do not only secrete EVs for pathogenesis, but eventually also for defence against predators. For instance, *C. neoformans* was reported to release EVs for protection against the predatory amoeba *Acanthamoeba castellanii*. The fungal EVs are internalised by the amoeba cells and are suggested to suppress predatory activity that result in increased fungal survival rates (Rizzo et al., 2017).

An interesting function of fungal EVs has been proposed in regard to intraspecific, intercellular communication at the population level (Bielska and May, 2019). Virulence of the *Cryptococcus gattii* outbreak lineage R265 is attributed to an explosive proliferative ability through "division of labour" between fungal cells co-infecting a macrophage (Voelz et al., 2014). In this context, EVs isolated from axenic culture of the outbreak strain are sufficient to trigger rapid proliferation of a recipient non-outbreak strain inside macrophages in cell culture. Noteworthy, both the EV protein and RNA cargoes are essential for this effect. Proliferation of the non-outbreak strain in macrophages in the presence of other macrophages infected with the outbreak strain further supports EV-mediated long-distance communication (Bielska et al., 2018). Similarly, bacterial outer membrane vesicles were also reported to transport quorum sensing molecules (Toyofuku, 2019), indicating that EVs may be a common means of microbial communication at population level.

EVs in plant–fungal interactions

EV- and MVE-like structures have also been observed in plants by microscopic techniques at infection sites of fungal pathogens (Fig. 2; An et al., 2007; Snetselaar and Mims, 1994). Ultrastructural examination of non-host interaction between the barley powdery mildew fungus *Blumeria graminis* f.sp. *hordei* and *Arabidopsis thaliana* revealed plant MVEs and syntaxin PEN1-positive exosomes accumulating around the fungal infection structures (An et al., 2006; Böhlenius et al., 2010; Meyer et al., 2009). Intriguingly, an antimicrobial capacity of infection-induced PEN1-positive EVs was proposed recently; EVs isolated from leaf apoplastic wash fluids of *Arabidopsis* plants challenged with the bacterial pathogen *Pseudomonas syringae* showed enrichment of antimicrobial peptides, such as Pathogenesis-Related (PR) proteins (Hansen and Nielsen, 2017; Rutter and Innes, 2017). Plant EVs were also found to supress fungal pathogens. For instance, incubation of *Sclerotinia sclerotiorum* liquid culture with EVs isolated from sunflower apoplastic wash fluid led to uptake of plant EVs by the fungus and subsequent growth inhibition (Regente et al., 2017). However, the identity of the components of plant EVs inhibiting fungal proliferation remains unknown. *Arabidopsis* EVs also contain different types of small and tiny RNAs (Baldrich et al., 2019) that might mediate plant-pathogen crosstalk. The phenomenon, whereby plant host-derived sRNA silences genes in the pathogen, is known as host-induced gene silencing (HIGS; Fig. 2; Nowara et al., 2010). Recently, it was demonstrated for the first time in *Arabidopsis,* that HIGS is mediated by EVs for plant defence (Huang et al., 2019). *Arabidopsis* delivers miRNAs and trans-acting siRNAs (tasiRNAs) via exosome-like EVs into cells of the fungal plant pathogen *Botrytis cinerea* during infection. EV sRNAs were found to suppress fungal virulence genes putatively involved in

Table 1 — Comparison of intra- and extracellular membrane-associated RNA transport.		
	Intracellular RNA transport	Extracellular RNA transport
Organelle	Rab5-positive early endosomes	Extracellular vesicles (EVs)
Origin	Endocytic pathway, ESCRT	Endocytic pathway, ESCRT, MVEs
Function	Spatiotemporal regulation of 2mRNA translation during polar growth	Cross kingdom RNAi, intercellular communication
RNA-binding proteins	Rrm4, Grp1, Pab1 (*U. maydis*) Gul1 (*N. crassa*)	Several uncharacterized RBPs found in EVs with currently unknown function in RNA transport
Cargo RNAs	mRNAs	Small regulatory RNAs, tRNA halves, other types of RNAs

intracellular transport and pathogenesis (Cai et al., 2018). Along the same lines, *Arabidopsis* EVs are proposed to also deliver siRNAs into the oomycete plant pathogen *Phytophthora capsici*, possibly to silence virulence genes (Hou et al., 2019). Likewise, cotton plants also deliver miRNAs to the fungal pathogen *Verticillium dahliae* to inhibit virulence gene expression and to promote disease resistance (Zhang et al., 2016), but participation of cotton EVs in miRNA transport has so far not been examined.

Cross-kingdom RNAi in plant–fungal interaction is bidirectional (Wang et al., 2016). Pathogen-induced gene silencing (PIGS; Fig. 2) by a fungal pathogen was initially discovered as a virulence strategy for *B. cinerea*. This fungal pathogen delivers sRNAs into plant cells during infection, which hijack the plant RNAi machinery to silence host immunity genes (Weiberg et al., 2013). Similarly, sRNAs of the fungal plant pathogen *Verticillium dahliae* were found associated with the plant RNAi machinery during infection (Wang et al., 2016). Moreover, miRNA-like RNAs of the wheat pathogens *Puccinia striiformis f.sp. tritici* and *Fusarium graminearum* were suggested to target host plant genes for infection (Wang et al., 2017, Jian and Liang, 2019). Other types of plant pathogens, parasites or symbionts are proposed to deliver sRNAs into their host plants to manipulate gene expression (Weiberg et al., 2015). Indeed interspecies and cross-kingdom RNAi has been discovered in the parasitic plant *Cuscuta* spp. (Johnson and Axtell, 2019) and the nitrogen-fixing bacteria *Sinorhizobium meliloti* (Ren et al., 2019). Whether fungi and other microbes deliver sRNAs and other types of virulence factors (effectors) into host cells via EVs, needs to be resolved.

Another type of membranous structure, called membrane tubules ("memtubs"), has been described at the interface between the arbuscular mycorrhizal fungus *Rhizophagus irregularis* and its plant host (Ivanov et al., 2019; Roth et al., 2019). Memtubs seem to be generally conserved in plant–fungus

interaction, and have also been observed in the pathogen *U. maydis* (Roth et al., 2019). Consistent with the hypothesis, memtubs might be produced to increase surface areas for exchange of signals and nutrients at the fungus–plant interface. However, any functional role of memtubs and whether RNAs and proteins can be transported via this route between fungi and plants needs to be investigated.

How EVs of 50–500 nm in diameter can traverse the cell wall of bacteria, fungi or plants is currently poorly understood. Different models of vesicular trans-cell wall shuttling have been postulated (Brown et al., 2015; Wolf and Casadevall, 2014). One hypothesis is that EVs cross the cell wall via pores or channels (Brown et al., 2015 Walker et al., 2018). However, electron microscopy studies of EV interaction with the fungal cell wall in *C. neoformans* suggest direct vesicular exit through mechanisms that depend on cell wall melanisation (Wolf et al., 2014), indicating that cell wall composition matters. Similarly, the viscoelastic properties of *C. albicans* cell walls seem to influence the traffic of liposomes (Walker et al., 2018). Higher cell wall plasticity at the site of cell separation, hyphal branching or actively growing daughter cells and hyphal tips may facilitate EV release as well. Interestingly, many putative cell wall remodelling enzymes, such as glucanases and pectinases were identified in EVs, suggesting cell wall modifying activity by EVs may promote their cell wall passage (Nimrichter et al., 2016; Rodrigues et al., 2014).

4.   Concluding remarks

In this review article, we describe how two major membrane-associated RNA transport mechanisms - endosomal and EV-mediated RNA trafficking - function in fungi. Although these two modes of transport seem to lack an obvious connection, there are most likely linked at the subcellular level by sharing components of the endosomal pathway from which they origin. In Table 1, we compare key features of intracellular and extracellular RNA transport.

During endocytosis, endosomes mature by forming MVEs to target protein cargo for degradation or for recycling towards the plasma membrane (Huotari and Helenius, 2011). However, early endosomes also function as multipurpose platforms in long-distance intracellular mRNA transport. They deliver mRNAs and cognate translation products for spatio-temporal regulation of protein expression within fungal hyphae, for example during polar growth (Baumann et al., 2014). Interestingly, also in the case of extracellular RNA transport, the endocytic formation of MVEs starting with maturing early endosomes has been proposed to be one important pathway that leads to the formation of EVs (Fig. 2).

We envision that key factors of both intra- and extracellular RNA transport are RBPs as they constitute key regulatory elements for RNA selection, stabilisation and transport. They form higher-order RNPs and link these transport units physically to membranes, for example, by direct interaction of RBPs with specific lipid structures. Alternatively, adaptor proteins, such as Upa1, connect cargo RNPs with transport membranes via lipid-binding domains (Pohlmann et al.,

2015). Loading of MVEs with cargo RNAs for extracellular transport is likely mediated by transport RBPs, too, although their identities are not known in fungi, yet (Table 1). Hence, studying and comparing these seemingly different RNA transport processes is very informative and highly rewarding to understand the various facets of RNA and membrane trafficking. As so often, fungi could serve as excellent model systems to advance this emerging research area.

Declaration of Competing Interest

All authors agree with the submission and declare no conflict of interest.

Acknowledgements

R E F E R E N C E S

Alves, L.R., Peres da Silva, R., Sanchez, D.A., Zamith-Miranda, D., Rodrigues, M.L., Goldenberg, S., Puccia, R., Nosanchuk, J.D., 2019. Extracellular vesicle-mediated RNA release in *Histoplasma capsulatum*. mSphere 4 e00176-00119.

An, Q., Huckelhoven, R., Kogel, K.H., van Bel, A.J., 2006. Multivesicular bodies participate in a cell wall-associated defence response in barley leaves attacked by the pathogenic powdery mildew fungus. Cell Microbiol. 8, 1009−1019.

An, Q., van Bel, A.J., Huckelhoven, R., 2007. Do plant cells secrete exosomes derived from multivesicular bodies? Plant Signal. Behav. 2, 4−7.

Baietti, Maria Francesca, Zhang, Zhe, Mortier, Eva, Melchior, Aurélie, Degeest, Gisèle, Geeraerts, Annelies, Ivarsson, Ylva, Depoortere, Fabienne, Coomans, Christien, Vermeiren, Elke, Zimmermann, Pascale, David, Guido, 2012. Syndecan−syntenin−ALIX regulates the biogenesis of exosomes. Nat. Cell Biol. 14, 677.

Baldrich, P., Rutter, B.D., Karimi, H.Z., Podicheti, R., Meyers, B.C., Innes, R.W., 2019. Plant extracellular vesicles contain diverse small RNA species and are enriched in 10- to 17-nucleotide "tiny" RNAs. Plant Cell 31, 315−324.

Baumann, S., König, J., Koepke, J., Feldbrügge, M., 2014. Endosomal transport of septin mRNA and protein indicates local translation on endosomes and is required for correct septin filamentation. EMBO Rep. 15, 94−102.

Baumann, S., Pohlmann, T., Jungbluth, M., Brachmann, A., Feldbrügge, M., 2012. Kinesin-3 and dynein mediate microtubule-dependent co-transport of mRNPs and endosomes. J. Cell Sci. 125, 2740−2752.

Becht, P., König, J., Feldbrügge, M., 2006. The RNA-binding protein Rrm4 is essential for polarity in *Ustilago maydis* and shuttles along microtubules. J. Cell Sci. 119, 4964−4973.

Béthune, J., Jansen, R.P., Feldbrügge, M., Zarnack, K., 2019. Membrane-associated RNA-binding proteins orchestrate organelle-coupled translation. Trends Cell Biol. 29, 178−188.

Bielska, E., Birch, P.R.J., Buck, A.H., Abreu-Goodger, C., Innes, R.W., Jin, H., Pfaffl, M.W., Robatzek, S., Regev-Rudzki, N., Tisserant, C., Wang, S., Weiberg, A., 2019. Highlights of the mini-symposium on extracellular vesicles in inter-organismal communication, held in Munich, Germany, August 2018. J. Extracell. Vesicles 8, 1590116.

Bielska, E., Higuchi, Y., Schuster, M., Steinberg, N., Kilaru, S., Talbot, N.J., Steinberg, G., 2014. Long-distance endosome trafficking drives fungal effector production during plant infection. Nat. Commun. 5, 5097.

Bielska, E., May, R.C., 2019. Extracellular vesicles of human pathogenic fungi. Curr. Opin. Microbiol. 52, 90−99.

Bielska, E., Sisquella, M.A., Aldeieg, M., Birch, C., O'Donoghue, E.J., May, R.C., 2018. Pathogen-derived extracellular vesicles mediate virulence in the fatal human pathogen *Cryptococcus gattii*. Nat. Commun. 9, 1556.

Bleackley, M.R., Dawson, C.S., Anderson, M.A., 2019. Fungal extracellular vesicles with a focus on proteomic analysis. Proteomics 19e1800232.

Böhlenius, H., Morch, S.M., Godfrey, D., Nielsen, M.E., Thordal-Christensen, H., 2010. The multivesicular body-localized GTPase ARFA1b/1c is important for callose deposition and ROR2 syntaxin-dependent preinvasive basal defense in barley. Plant Cell 22, 3831−3844.

Bologna, N.G., Voinnet, O., 2014. The diversity, biogenesis, and activities of endogenous silencing small RNAs in Arabidopsis. Annu. Rev. Plant Biol. 65, 473−503.

Brachmann, A., Weinzierl, G., Kämper, J., Kahmann, R., 2001. Identification of genes in the bW/bE regulatory cascade in *Ustilago maydis*. Mol. Microbiol. 42, 1047−1063.

Brambilla, M., Martani, F., Bertacchi, S., Vitangeli, I., Branduardi, P., 2019. The *Saccharomyces cerevisiae* poly (A) binding protein (Pab1): Master regulator of mRNA metabolism and cell physiology. Yeast 36, 23−34.

Brown, L., Wolf, J.M., Prados-Rosales, R., Casadevall, A., 2015. Through the wall: extracellular vesicles in Gram-positive bacteria, mycobacteria and fungi. Nat. Rev. Microbiol. 13, 620−630.

Cai, Q., Qiao, L., Wang, M., He, B., Lin, F.M., Palmquist, J., Huang, S.D., Jin, H., 2018. Plants send small RNAs in extracellular vesicles to fungal pathogen to silence virulence genes. Science 360, 1126−1129.

Chang, S.S., Zhang, Z., Liu, Y., 2012. RNA interference pathways in fungi: mechanisms and functions. Annu. Rev. Microbiol. 66, 305−323.

Cioni, J.M., Lin, J.Q., Holtermann, A.V., Koppers, M., Jakobs, M.A.H., Azizi, A., Turner-Bridger, B., Shigeoka, T., Franze, K., Harris, W.A., Holt, C.E., 2019. Late endosomes act as mRNA translation platforms and sustain mitochondria in axons. Cell 176, 56−72 e15.

Colombo, M., Moita, C., van Niel, G., Kowal, J., Vigneron, J., Benaroch, P., Manel, N., Moita, L.F., Thery, C., Raposo, G., 2013. Analysis of ESCRT functions in exosome biogenesis, composition and secretion highlights the heterogeneity of extracellular vesicles. J. Cell Sci. 126, 5553−5565.

Dawkins, R., 1982. The Extended Phenotype. Oxford University Press, Oxford, UK.

Deatherage, B.L., Cookson, B.T., 2012. Membrane vesicle release in bacteria, eukaryotes, and archaea: a conserved yet underappreciated aspect of microbial life. Infect. Immun. 80, 1948−1957.

Eisenman, H.C., Frases, S., Nicola, A.M., Rodrigues, M.L., Casadevall, A., 2009. Vesicle-associated melanization in *Cryptococcus neoformans*. Microbiology 155, 3860–3867.

Eliscovich, C., Singer, R.H., 2017. RNP transport in cell biology: the long and winding road. Curr. Opin. Cell Biol. 45, 38–46.

Fader, C.M., Sanchez, D.G., Mestre, M.B., Colombo, M.I., 2009. TI-VAMP/VAMP7 and VAMP3/cellubrevin: two v-SNARE proteins involved in specific steps of the autophagy/multivesicular body pathways. Biochim. Biophys. Acta 1793, 1901–1916.

Gibbings, D.J., Ciaudo, C., Erhardt, M., Voinnet, O., 2009. Multivesicular bodies associate with components of miRNA effector complexes and modulate miRNA activity. Nat. Cell Biol. 11, 1143–1149.

Haag, C., Pohlmann, T., Feldbrugge, M., 2017. The ESCRT regulator Did2 maintains the balance between long-distance endosomal transport and endocytic trafficking. PLoS Genet. 13e1006734.

Haag, C., Steuten, B., Feldbrügge, M., 2015. Membrane-coupled mRNA trafficking in fungi. Annu. Rev. Microbiol. 69, 265–281.

Hansen, L.L., Nielsen, M.E., 2017. Plant exosomes: using an unconventional exit to prevent pathogen entry? J. Exp. Bot. 69, 59–68.

Harris, S.D., 2019. Hyphal branching in filamentous fungi. Dev. Biol. 451, 35–39.

Hentze, M.W., Castello, A., Schwarzl, T., Preiss, T., 2018. A brave new world of RNA-binding proteins. Nat. Rev. Mol. Cell Biol. 19, 327–341.

Herold, I., Kowbel, D., Delgado-Alvarez, D.L., Garduno-Rosales, M., Mourino-Perez, R.R., Yarden, O., 2019. Transcriptional profiling and localization of GUL-1, a COT-1 pathway component, in *Neurospora crassa*. Fungal Genet. Biol. 126, 1–11.

Higuchi, Y., Ashwin, P., Roger, Y., Steinberg, G., 2014. Early endosome motility spatially organizes polysome distribution. J. Cell Biol. 204, 343–357.

Hogan, D.J., Riordan, D.P., Gerber, A.P., Herschlag, D., Brown, P.O., 2008. Diverse RNA-binding proteins interact with functionally related sets of RNAs, suggesting an extensive regulatory system. PLoS Biol. 6, e255.

Hou, Y., Zhai, Y., Feng, L., Karimi, H.Z., Rutter, B.D., Zeng, L., Choi, D.S., Zhang, B., Gu, W., Chen, X., Ye, W., Innes, R.W., Zhai, J., Ma, W., 2019. A *Phytophthora* effector suppresses trans-kingdom RNAi to promote disease susceptibility. Cell Host Microbe 25, 153–165 e155.

Huang, C.Y., Wang, H., Hu, P., Hamby, R., Jin, H., 2019. Small RNAs - Big players in plant-microbe interactions. Cell Host Microbe 26, 173–182.

Huotari, J., Helenius, A., 2011. Endosome maturation. EMBO J. 30, 3481–3500.

Hurley, J.H., 2015. ESCRTs are everywhere. EMBO J. 34, 2398–2407.

Ikeda, M.A.K., de Almeida, J.R.F., Jannuzzi, G.P., Cronemberger-Andrade, A., Torrecilhas, A.C.T., Moretti, N.S., da Cunha, J.P.C., de Almeida, S.R., Ferreira, K.S., 2018. Extracellular vesicles from *Sporothrix brasiliensis* are an important virulence factor that induce an increase in fungal burden in experimental sporotrichosis. Front. Microbiol. 9, 2286.

Ivanov, S., Austin 2nd, J., Berg, R.H., Harrison, M.J., 2019. Extensive membrane systems at the host-arbuscular mycorrhizal fungus interface. Nat. Plants 5, 194–203.

Jankowski, S., Pohlmann, T., Baumann, S., Müntjes, K.M., Devan, S.K., Zander, S., Feldbrügge, M., 2019. The multi PAM2 protein Upa2 functions as novel core component of endosomal mRNA transport. EMBO Rep. 24e47381.

Jansen, R.P., Niessing, D., Baumann, S., Feldbrügge, M., 2014. mRNA transport meets membrane traffic. Trends Genet. 30, 408–417.

Jian, J., Liang, X., 2019. One small RNA of *Fusarium graminearum* targets and silences CEBiP gene in common wheat. Microorganisms 7, 425.

Joffe, L.S., Nimrichter, L., Rodrigues, M.L., Del Poeta, M., 2016. Potential roles of fungal extracellular vesicles during infection. mSphere 1 e00099-00016.

Johnson, N.R., Axtell, M.J., 2019. Small RNA warfare: exploring origins and function of trans-species microRNAs from the parasitic plant *Cuscuta*. Curr. Opin. Plant Biol. 50, 76–81.

Koles, K., Nunnari, J., Korkut, C., Barria, R., Brewer, C., Li, Y., Leszyk, J., Zhang, B., Budnik, V., 2012. Mechanism of evenness interrupted (Evi)-exosome release at synaptic boutons. J. Biol. Chem. 287, 16820–16834.

König, J., Baumann, S., Koepke, J., Pohlmann, T., Zarnack, K., Feldbrügge, M., 2009. The fungal RNA-binding protein Rrm4 mediates long-distance transport of *ubi1* and *rho3* mRNAs. EMBO J. 28, 1855–1866.

Kozlov, G., Menade, M., Rosenauer, A., Nguyen, L., Gehring, K., 2010. Molecular determinants of PAM2 recognition by the MLLE domain of poly(A)-binding protein. J. Mol. Biol. 397, 397–407.

Kuipers, M.E., Hokke, C.H., Smits, H.H., Nolte-'t Hoen, E.N.M., 2018. Pathogen-derived extracellular vesicle-associated molecules that affect the host immune system: an overview. Front. Microbiol. 9, 2182.

Kutateladze, T.G., 2006. Phosphatidylinositol 3-phosphate recognition and membrane docking by the FYVE domain. Biochim. Biophys. Acta 1761, 868–877.

Lanver, D., Tollot, M., Schweizer, G., Lo Presti, L., Reissmann, S., Ma, L.S., Schuster, M., Tanaka, S., Liang, L., Ludwig, N., Kahmann, R., 2017. *Ustilago maydis* effectors and their impact on virulence. Nat. Rev. Microbiol. 15, 409–421.

Lee, Young Sik, Pressman, Sigal, Andress, Arlise P., Kim, Kevin, White, Jamie L., Cassidy, Justin J., Li, Xin, Lubell, Kim, Lim, Do Hwan, Cho, Ik Sang, Nakahara, Kenji, Preall, Jonathan B., Bellare, Priya, Sontheimer, Erik J., Carthew, Richard W., 2009. Silencing by small RNAs is linked to endosomal trafficking. Nat. Cell Biol. 11, 1150.

Liao, Y.C., Fernandopulle, M.S., Wang, G., Choi, H., Hao, L., Drerup, C.M., Patel, R., Qamar, S., Nixon-Abell, J., Shen, Y., Meadows, W., Vendruscolo, M., Knowles, T.P.J., Nelson, M., Czekalska, M.A., Musteikyte, G., Gachechiladze, M.A., Stephens, C.A., Pasolli, H.A., Forrest, L.R., St George-Hyslop, P., Lippincott-Schwartz, J., Ward, M.E., 2019. RNA granules hitchhike on lysosomes for long-distance transport, using annexin A11 as a molecular tether. Cell 179, 147–164 e120.

Maas, S.L.N., Breakefield, X.O., Weaver, A.M., 2017. Extracellular vesicles: Unique intercellular delivery vehicles. Trends Cell Biol. 27, 172–188.

Martin, K.C., Ephrussi, A., 2009. mRNA localization: gene expression in the spatial dimension. Cell 136, 719–730.

Mathieu, M., Martin-Jaular, L., Lavieu, G., Thery, C., 2019. Specificities of secretion and uptake of exosomes and other extracellular vesicles for cell-to-cell communication. Nat. Cell Biol. 21, 9–17.

Meldolesi, J., 2018. Exosomes and ectosomes in intercellular communication. Curr. Biol. 28, R435–R444.

Meyer, D., Pajonk, S., Micali, C., O'Connell, R., Schulze-Lefert, P., 2009. Extracellular transport and integration of plant secretory proteins into pathogen-induced cell wall compartments. Plant J. 57, 986–999.

Mittelbrunn, M., Sanchez-Madrid, F., 2012. Intercellular communication: diverse structures for exchange of genetic information. Nat. Rev. Mol. Cell Biol. 13, 328–335.

Mostowy, S., Cossart, P., 2012. Septins: the fourth component of the cytoskeleton. Nat. Rev. Mol. Cell Biol. 13, 183–194.

Müller, J., Pohlmann, T., Feldbrügge, M., 2019. Core components of endosomal mRNA transport are evolutionarily conserved in fungi. Fungal Genet. Biol. 126, 12–16.

Muralidharan-Chari, V., Clancy, J., Plou, C., Romao, M., Chavrier, P., Raposo, G., D'Souza-Schorey, C., 2009. ARF6-

regulated shedding of tumor cell-derived plasma membrane microvesicles. Curr. Biol. 19, 1875–1885.

Niessing, D., Jansen, R.P., Pohlmann, T., Feldbrügge, M., 2018. mRNA transport in fungal top models. Wiley Interdiscip. Rev. RNA 9, e1453.

Nimrichter, L., de Souza, M.M., Del Poeta, M., Nosanchuk, J.D., Joffe, L., Tavares Pde, M., Rodrigues, M.L., 2016. Extracellular vesicle-associated transitory cell wall components and their impact on the interaction of fungi with host cells. Front. Microbiol. 7, 1034.

Nowara, D., Gay, A., Lacomme, C., Shaw, J., Ridout, C., Douchkov, D., Hensel, G., Kumlehn, J., Schweizer, P., 2010. HIGS: host-induced gene silencing in the obligate biotrophic fungal pathogen *Blumeria graminis*. Plant Cell 22, 3130–3141.

Olgeiser, L., Haag, C., Boerner, S., Ule, J., Busch, A., Koepke, J., König, J., Feldbrügge, M., Zarnack, K., 2019. The key protein of endosomal mRNP transport Rrm4 binds translational landmark sites of cargo mRNAs. EMBO Rep. 20e46588.

Oliveira, D.L., Freire-de-Lima, C.G., Nosanchuk, J.D., Casadevall, A., Rodrigues, M.L., Nimrichter, L., 2010a. Extracellular vesicles from *Cryptococcus neoformans* modulate macrophage functions. Infect. Immun. 78, 1601–1609.

Oliveira, D.L., Nakayasu, E.S., Joffe, L.S., Guimaraes, A.J., Sobreira, T.J., Nosanchuk, J.D., Cordero, R.J., Frases, S., Casadevall, A., Almeida, I.C., Nimrichter, L., Rodrigues, M.L., 2010b. Characterization of yeast extracellular vesicles: evidence for the participation of different pathways of cellular traffic in vesicle biogenesis. PLoS One 5e11113.

Oliveira, D.L., Rizzo, J., Joffe, L.S., Godinho, R.M., Rodrigues, M.L., 2013. Where do they come from and where do they go: candidates for regulating extracellular vesicle formation in fungi. Int. J. Mol. Sci. 14, 9581–9603.

Panepinto, J., Komperda, K., Frases, S., Park, Y.D., Djordjevic, J.T., Casadevall, A., Williamson, P.R., 2009. Sec6-dependent sorting of fungal extracellular exosomes and laccase of *Cryptococcus neoformans*. Mol. Microbiol. 71, 1165–1176.

Peres da Silva, R., Longo, L.G.V., Cunha, Jpcd, Sobreira, T.J.P., Rodrigues, M.L., Faoro, H., Goldenberg, S., Alves, L.R., Puccia, R., 2019. Comparison of the RNA Content of Extracellular Vesicles Derived from *Paracoccidioides brasiliensis* and *Paracoccidioides lutzii*. Cells 8.

Peres da Silva, R., Puccia, R., Rodrigues, M.L., Oliveira, D.L., Joffe, L.S., Cesar, G.V., Nimrichter, L., Goldenberg, S., Alves, L.R., 2015. Extracellular vesicle-mediated export of fungal RNA. Sci. Rep. 5, 7763.

Pohlmann, T., Baumann, S., Haag, C., Albrecht, M., Feldbrügge, M., 2015. A FYVE zinc finger domain protein specifically links mRNA transport to endosome trafficking. Elife 4e06041.

Rayner, S., Bruhn, S., Vallhov, H., Andersson, A., Billmyre, R.B., Scheynius, A., 2017. Identification of small RNAs in extracellular vesicles from the commensal yeast *Malassezia sympodialis*. Sci. Rep. 7, 39742.

Regente, M., Pinedo, M., San Clemente, H., Balliau, T., Jamet, E., de la Canal, L., 2017. Plant extracellular vesicles are incorporated by a fungal pathogen and inhibit its growth. J. Exp. Bot. 68, 5485–5495.

Ren, B., Wang, X., Duan, J., Ma, J., 2019. Rhizobial tRNA-derived small RNAs are signal molecules regulating plant nodulation. Science 365, 919–922.

Riquelme, M., Aguirre, J., Bartnicki-Garcia, S., Braus, G.H., Feldbrügge, M., Fleig, U., Hansberg, W., Herrera-Estrella, A., Kämper, J., Kück, U., Mourino-Perez, R.R., Takeshita, N., Fischer, R., 2018. Fungal morphogenesis, from the polarized growth of hyphae to complex reproduction and infection structures. Microbiol. Mol. Biol. Rev. 82, 1–47.

Rizzo, J., Albuquerque, P.C., Wolf, J.M., Nascimento, R., Pereira, M.D., Nosanchuk, J.D., Rodrigues, M.L., 2017. Analysis

of multiple components involved in the interaction between *Cryptococcus neoformans* and *Acanthamoeba castellanii*. Fungal Biol 121, 602–614.

Rodrigues, M.L., Nakayasu, E.S., Almeida, I.C., Nimrichter, L., 2014. The impact of proteomics on the understanding of functions and biogenesis of fungal extracellular vesicles. J. Proteomics 97, 177–186.

Rodrigues, M.L., Nakayasu, E.S., Oliveira, D.L., Nimrichter, L., Nosanchuk, J.D., Almeida, I.C., Casadevall, A., 2008. Extracellular vesicles produced by *Cryptococcus neoformans* contain protein components associated with virulence. Eukaryot. Cell 7, 58–67.

Rodrigues, M.L., Nimrichter, L., Oliveira, D.L., Frases, S., Miranda, K., Zaragoza, O., Alvarez, M., Nakouzi, A., Feldmesser, M., Casadevall, A., 2007. Vesicular polysaccharide export in *Cryptococcus neoformans* is a eukaryotic solution to the problem of fungal trans-cell wall transport. Eukaryot. Cell 6, 48–59.

Roth, R., Hillmer, S., Funaya, C., Chiapello, M., Schumacher, K., Lo Presti, L., Kahmann, R., Paszkowski, U., 2019. Arbuscular cell invasion coincides with extracellular vesicles and membrane tubules. Nat. Plants 5, 204–211.

Rutter, B.D., Innes, R.W., 2017. Extracellular vesicles isolated from the leaf apoplast carry stress-response proteins. Plant Physiol. 173, 728–741.

Rutter, B.D., Innes, R.W., 2018. Extracellular vesicles as key mediators of plant-microbe interactions. Curr. Opin. Plant Biol. 44, 16–22.

Rybak, K., Robatzek, S., 2019. Functions of extracellular vesicles in immunity and virulence. Plant Physiol. 179, 1236–1247.

Samuel, M., Bleackley, M., Anderson, M., Mathivanan, S., 2015. Extracellular vesicles including exosomes in cross kingdom regulation: a viewpoint from plant-fungal interactions. Front. Plant Sci. 6, 766.

Schuster, M., Kilaru, S., Fink, G., Collemare, J., Roger, Y., Steinberg, G., 2011. Kinesin-3 and dynein cooperate in long-range retrograde endosome motility along a non-uniform microtubule array. Mol. Biol. Cell 22, 3645–3657.

Singh, G., Pratt, G., Yeo, G.W., Moore, M.J., 2015. The clothes make the mRNA: past and present trends in mRNP fashion. Annu. Rev. Biochem. 84, 325–354.

Snetselaar and Mims, 1994Snetselaar, K.M., Mims, C.W., 1994. Light and electron microscopy of *Ustilago maydis* hyphae in maize. Mycol. Res. 98, 347–355.

Soares, R.P., Xander, P., Costa, A.O., Marcilla, A., Menezes-Neto, A., Del Portillo, H., Witwer, K., Wauben, M., Nolte, T., Hoen, E., Olivier, M., Criado, M.F., da Silva, L.L.P., Abdel Baqui, M.M., Schenkman, S., Colli, W., Alves, M.J.M., Ferreira, K.S., Puccia, R., Nejsum, P., Riesbeck, K., Stensballe, A., Hansen, E.P., Jaular, L.M., Ovstebo, R., de la Canal, L., Bergese, P., Pereira-Chioccola, V., Pfaffl, M.W., Fritz, J., Gho, Y.S., Torrecilhas, A.C., 2017. Highlights of the Sao Paulo ISEV workshop on extracellular vesicles in cross-kingdom communication. J. Extracell. Vesicles 6, 1407213.

Statello, L., Maugeri, M., Garre, E., Nawaz, M., Wahlgren, J., Papadimitriou, A., Lundqvist, C., Lindfors, L., Collen, A., Sunnerhagen, P., Ragusa, M., Purrello, M., Di Pietro, C., Tigue, N., Valadi, H., 2018. Identification of RNA-binding proteins in exosomes capable of interacting with different types of RNA: RBP-facilitated transport of RNAs into exosomes. PLoS One 13e0195969.

Steinberg, G., 2012. The transport machinery for motility of fungal endosomes. Fungal Genet. Biol. 49, 675–676.

Steinberg, G., 2014. Endocytosis and early endosome motility in filamentous fungi. Curr. Opin. Microbiol. 20, 10–18.

Stenmark, H., Aasland, R., Driscoll, P.C., 2002. The phosphatidylinositol 3-phosphate-binding FYVE finger. FEBS Lett. 513, 77–84.

Teis, D., Saksena, S., Emr, S.D., 2009. SnapShot: the ESCRT machinery. Cell 137, 182–182 e181.

Toyofuku, M., 2019. Bacterial communication through membrane vesicles. Biosci. Biotechnol. Biochem. 83, 1599−1605.

Vallejo, M.C., Nakayasu, E.S., Matsuo, A.L., Sobreira, T.J., Longo, L.V., Ganiko, L., Almeida, I.C., Puccia, R., 2012. Vesicle and vesicle-free extracellular proteome of Paracoccidioides brasiliensis: comparative analysis with other pathogenic fungi. J. Proteome Res. 11, 1676−1685.

van Niel, G., Charrin, S., Simoes, S., Romao, M., Rochin, L., Saftig, P., Marks, M.S., Rubinstein, E., Raposo, G., 2011. The tetraspanin CD63 regulates ESCRT-independent and -dependent endosomal sorting during melanogenesis. Dev. Cell 21, 708−721.

van Niel, G., D'Angelo, G., Raposo, G., 2018. Shedding light on the cell biology of extracellular vesicles. Nat. Rev. Mol. Cell Biol. 19, 213−228.

Vargas, G., Rocha, J.D., Oliveira, D.L., Albuquerque, P.C., Frases, S., Santos, S.S., Nosanchuk, J.D., Gomes, A.M., Medeiros, L.C., Miranda, K., Sobreira, T.J., Nakayasu, E.S., Arigi, E.A., Casadevall, A., Guimaraes, A.J., Rodrigues, M.L., Freire-de-Lima, C.G., Almeida, I.C., Nimrichter, L., 2015. Compositional and immunobiological analyses of extracellular vesicles released by *Candida albicans*. Cell Microbiol. 17, 389−407.

Villarroya-Beltri, C., Baixauli, F., Gutierrez-Vazquez, C., Sanchez-Madrid, F., Mittelbrunn, M., 2014. Sorting it out: regulation of exosome loading. Semin. Cancer Biol. 28, 3−13.

Voelz, K., Johnston, S.A., Smith, L.M., Hall, R.A., Idnurm, A., May, R.C., 2014. 'Division of labour' in response to host oxidative burst drives a fatal *Cryptococcus gattii* outbreak. Nat. Commun. 5, 5194.

Vollmeister, E., Schipper, K., Baumann, S., Haag, C., Pohlmann, T., Stock, J., Feldbrügge, M., 2012. Fungal development of the plant pathogen *Ustilago maydis*. FEMS Microbiol. Rev. 36, 59−77.

Walker, L., Sood, P., Lenardon, M.D., Milne, G., Olson, J., Jensen, G., Wolf, J., Casadevall, A., Adler-Moore, J., Gow, N.A.R., 2018. The viscoelastic properties of the fungal cell wall allow traffic of AmBisome as intact liposome vesicles. mBio 9, e02383-17.

Wang, B., Sun, Y., Song, N., Zhao, M., Liu, R., Feng, H., Wang, X., Kang, Z., 2017. *Puccinia striiformis* f. sp. *tritici* microRNA-like RNA 1 (*Pst*-milR1), an important pathogenicity factor of *Pst*, impairs wheat resistance to *Pst* by suppressing the wheat pathogenesis-related 2 gene. New Phytol. 215, 338−350.

Wang, M., Weiberg, A., Lin, F.M., Thomma, B.P., Huang, H.D., Jin, H., 2016. Bidirectional cross-kingdom RNAi and fungal uptake of external RNAs confer plant protection. Nat. Plants 2, 16151.

Weiberg, A., Bellinger, M., Jin, H., 2015. Conversations between kingdoms: small RNAs. Curr. Opin. Biotechnol. 32, 207−215.

Weiberg, A., Wang, M., Lin, F.M., Zhao, H., Zhang, Z., Kaloshian, I., Huang, H.D., Jin, H., 2013. Fungal small RNAs suppress plant immunity by hijacking host RNA interference pathways. Science 342, 118−123.

Wilson, R.C., Doudna, J.A., 2013. Molecular mechanisms of RNA interference. Annu. Rev. Biophys. 42, 217−239.

Wolf, J.M., Casadevall, A., 2014. Challenges posed by extracellular vesicles from eukaryotic microbes. Curr. Opin. Microbiol. 22, 73−78.

Wolf, J.M., Espadas-Moreno, J., Luque-Garcia, J.L., Casadevall, A., 2014. Interaction of *Cryptococcus neoformans* extracellular vesicles with the cell wall. Eukaryot. Cell 13, 1484−1493.

Xie, J., Kozlov, G., Gehring, K., 2014. The "tale" of poly(A) binding protein: the MLLE domain and PAM2-containing proteins. Biochim. Biophys. Acta 1839, 1062−1068.

Zamith-Miranda, D., Nimrichter, L., Rodrigues, M.L., Nosanchuk, J.D., 2018. Fungal extracellular vesicles: modulating host-pathogen interactions by both the fungus and the host. Microbes Infect. 20, 501−504.

Zander, S., Baumann, S., Weidtkamp-Peters, S., Feldbrügge, M., 2016. Endosomal assembly and transport of heteromeric septin complexes promote septin cytoskeleton formation. J. Cell Sci. 129, 2778−2792.

Zhang, T., Zhao, Y.L., Zhao, J.H., Wang, S., Jin, Y., Chen, Z.Q., Fang, Y.Y., Hua, C.L., Ding, S.W., Guo, H.S., 2016. Cotton plants export microRNAs to inhibit virulence gene expression in a fungal pathogen. Nat. Plants 2, 16153.

2. Isolation of Extracellular Vesicles and Associated RNA from *Ustilago maydis*

Seomun Kwon[1] and Michael Feldbrügge[1,] *

[1]Institute for Microbiology, Heinrich Heine University Düsseldorf, Cluster of Excellence on Plant Sciences, 40225 Düsseldorf, Germany; *For correspondence: feldbrue@hhu.de
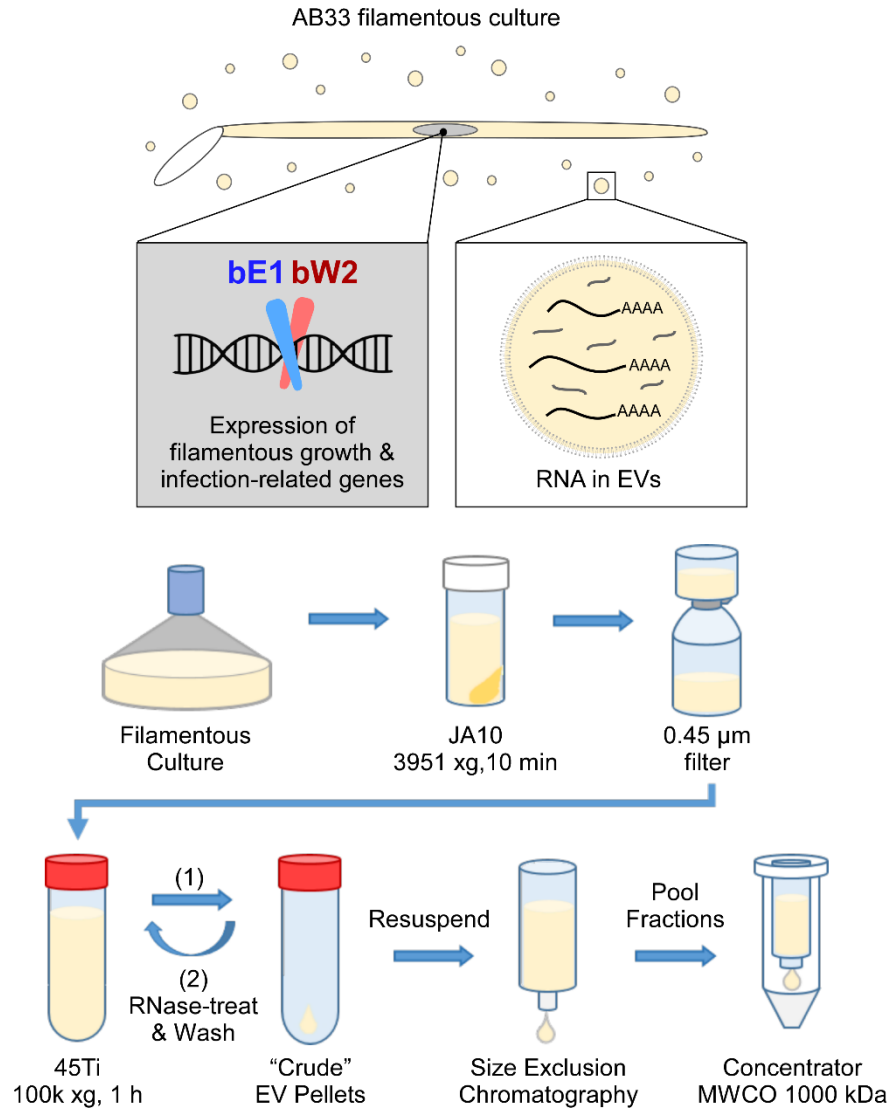
Disclaimer & Personal Contribution

This is a draft manuscript. All materials presented here were produced by Seomun Kwon. Additional authors may be added in the final manuscript with their permission, as per contribution.

Abstract

Extracellular vesicles (EVs) carry diverse cargo molecules and can mediate communication between host and pathogen cells. Here we detail a procedure for isolation of EVs from the maize smut fungus, *Ustilago maydis*, for analysis of EV-associated extracellular RNA. It is practically challenging to study EVs of pathogenic microbes *in planta*. Isolation of *U. maydis* EVs from the apoplastic washing fluid of infected maize plants is inherently destructive and ideally requires prior testing of suitable EV markers in both the fungus and the plant. Combining simplicity and relevance for plant infection, our approach is to induce infectious, filamentous development in axenic culture. Several genes relevant for infection are still expressed in axenic filaments and their transcripts can be detected in the culture EVs. The protocol presented here combines filtration, ultracentrifugation and size-exclusion chromatography to isolate EVs from the culture supernatant, followed by extraction of EV-associated RNA. Typical EV samples and the profile of EV-associated RNA are presented. EVs prepared using this protocol can be additionally used for examination of various cargos other than RNA, which may expand our current knowledge of phytopathogen effectors and PAMPs.

Graphic abstract:

AB33 filamentous culture

bE1 bW2

Expression of filamentous growth & infection-related genes

RNA in EVs

Filamentous Culture

JA10 3951 xg,10 min

0.45 µm filter

(1)

(2) RNase-treat & Wash

Resuspend

Pool Fractions

45Ti 100k xg, 1 h

"Crude" EV Pellets

Size Exclusion Chromatography

Concentrator MWCO 1000 kDa

Keywords: Extracellular vesicles, EVs, plant pathogen, smut fungus, *Ustilago maydis*

Background

Extracellular vesicle (EV)-mediated communication is an emerging topic in plant-microbe interactions. In phytopathology, effectors can be defined as molecules secreted by pathogens that bring about physiological changes in the plant host to support infection. For phytopathogens, EVs could be a means of effector delivery into plant cells to facilitate infection. While the search for effectors to date have predominantly focused on conventionally secreted proteins (Lanver et al., 2018, Toruño et al., 2016), effectors in the form of small RNAs (Weiberg et al., 2013) and unconventionally secreted proteins (Liu et al., 2014) are being discovered. Since EVs are a means of intercellular exchange of otherwise intracellular molecules, examination of cargos carried by phytopathogen EVs may expand our current scope of effectors. Here we detail the procedure for preparation of EVs from axenic filamentous cultures of the maize smut fungus *Ustilago maydis*, and extraction of extracellular RNA associated with the EVs.

U. maydis produces EVs and other EV-like structures, both in axenic culture (Kwon et al., 2021) and *in planta* (Ludwig et al., 2021). So far, EVs of phytopathogenic fungi have been isolated from axenic cultures (Hill and Solomon, 2020, Bleackley et al., 2020, Kwon et al., 2021). Analysis of pathogen EVs from infected plant samples would be ideal, but the available methods are inherently destructive, especially for maize leaves (Witzel et al., 2011). Therefore, reliable fungal EV markers and cell lysis markers would be required to isolate fungal EVs by immunoaffinity capture or to determine the degree of contamination from lysis. These are as yet lacking for *U. maydis*. While preparation of EVs from axenic cultures is simpler, the expression profile of the cells and the contents of the EVs are not so representative of the infection conditions.

To address these issues, our strategy is to isolate EVs from a *U. maydis* strain that developmentally and transcriptionally mimics infectious hyphae in axenic culture. In nature, yeast-like, haploid sporidia must mate to form a dikaryotic, infectious filament, where the bE and bW transcription factors from each sporidium can form an active heterodimer to trigger a transcriptional cascade for the infectious filamentous program (Brefort et al., 2009). In the laboratory strain AB33, bE and bW are both present under nitrate-inducible promoters (Figure 1A) (Brachmann et al., 2001). Thus their expression can be induced in sporidial culture (Figure 1B) by simply changing the nitrogen source from ammonium to nitrate. This allows facile, uniform switch to the filamentous program in axenic culture without mating (Figure 1C).

Indeed, several genes relevant for infection are expressed in AB33 induced filaments in axenic culture (Wahl et al., 2010). We have found that mRNAs of many such genes that are normally upregulated during

plant infection (Lanver et al., 2018), are associated with EVs from AB33 filament cultures (Kwon et al., 2021). These include mRNAs of some known effectors and virulence genes (Djamei et al., 2011, Ludwig et al., 2021).

We describe here the methods to prepare EVs from AB33 induced filaments and to extract the associated RNA. The EV preparations obtained can be also be used for proteomic, lipidomic, or metabolomic analyses. Thus, induced filamentous cultures of *U. maydis* can be used for initial identification of EV-associated effector candidates and EV-markers, prior to moving on to *in planta* EVs, or to complement future data from infected plant samples. Furthermore, using tagged lines or mutants in the AB33 background, specific mRNAs and protein cargos and the mechanism of EV loading could be studied.
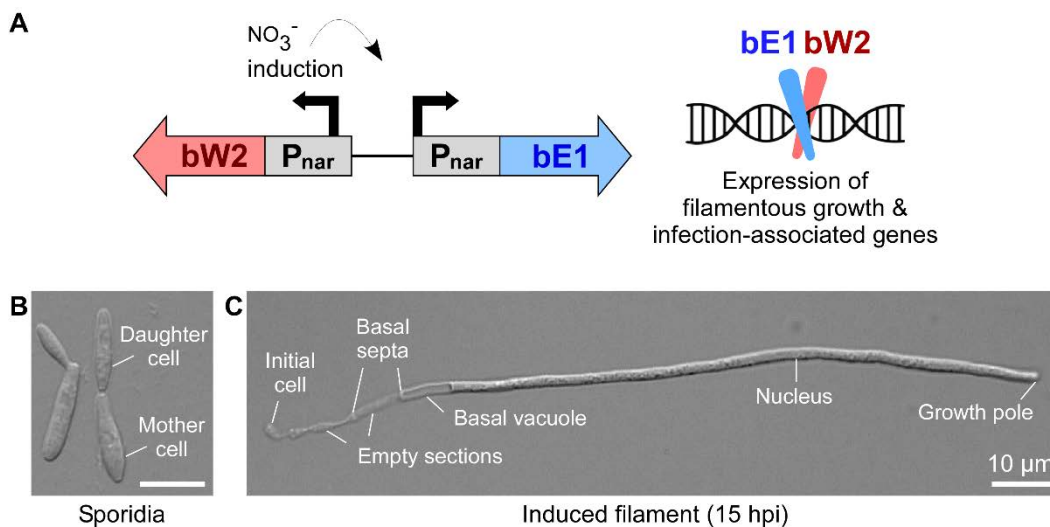

Figure 1. Induction of filamentous growth and infection-asssociated genes in axenic culture of the U. maydis synthetic strain AB33.
A. In the synthetic laboratory strain AB33, genes encoding compatible bE1 and bW2 homeodomain transcription factors are both placed under nitrate (NO_3^-)- inducible promoters (Pnar). Their expression can be induced by switching the nitrogen source to NO_3^-, as in the nitrate minimal medium (NM). bE1 and bW2 form active heterodimers and trigger a transcriptional cascade of filamentation- and infection-related genes. **B.** AB33 sporidia grown to OD_{600} = ~1.0 in complete medium (CM) + 1% glucose, from which filamentation is induced. **C.** AB33 filament at 15-16 hours post induction (hpi) in NM + 2% glucose, from which EVs are isolated.

Materials and Reagents

1. *U. maydis* laboratory strain AB33 (Brachmann et al., 2001) (available at Institute for Microbiology, Heinrich-Heine-University Düsseldorf and many other groups working on *U. maydis*)

2. 1 Plate solid complete medium + 1% glucose (w/v) (CM-glc agar; see Recipes) (Holliday, 1974). Unused plates can be stored at 4°C for up to 1 month.

3. 900 ml Complete medium (CM) + 1% glucose (see Recipes).
   All liquid media in this protocol can be stored for months at room temperature, protected from prolonged light exposure.

4. 200 ml CM + 2% glucose

5. 400 ml Nitrate minimal medium (NM) (see Recipes)

6. 900 ml NM with 2% glucose (see Recipes)

7. Clear plastic cuvettes (Sarstedt, catalog number: 67.742)

8. Sterile, autoclaved funnel lined with 2 layers of Miracloth (Fisher Scientific, Merck Millipore Calbiochem™, catalog number: 15802987). Funnel should fit the mouth of Schott bottles.

9. Filtropur BT50 Steritop filters, 0.45 µm, PES, 500 ml (Sarstedt, catalog number: 83.3941.100)

10. 1x PBS pH 7.2 (ThermoFisher Scientific, Gibco™, catalog number: 20012027), kept at 4°C or on ice throughout use.

11. 10 mg / ml RNase A stock solution (see Recipes; Merck, catalog number: R9009), kept at -20°C until use.

12. Sterile reaction tubes, 5 ml (Sarstedt, catalog number: 72.701)

13. VIVASPIN 500 MWCO 1000 kDa concentrator, PES (Sartorius, catalog number: VS0161)

14. Filtropur S 0.45 µm syringe filter (Sarstedt, catalog number: 83.1826)

15. Injekt® Luer Lock Solo single-use syringe without needle, 2ml (Braun, catalog number: 4606701V)

16. qEVoriginal / 70 nm Size-Exclusion Chromatography columns (IZON, catalog number: SP1)

17. Falcon tubes, 15 ml (Sarstedt, catalog number: 62.554.502)

18. DNA LoBind® Nuclease-free reaction tubes, 2 ml (Eppendorf, catalog number: 0030108078)

19. DNA LoBind® Nuclease-free reaction tubes, 1.5 ml (Eppendorf, catalog number: 0030108051)

20. Nuclease-free, filtered pipette tips (starlab, TipOne®, catalog number: S1126-7810, S1120-8810, S1120-2810, S1120-3810)

21. TRI Reagent® LS, for processing fluid samples (Sigma, catalog number: T3934)

22. Manual phase lock gel™, heavy (5 PRIME, catalog number: 2302830)

23. GlycoBlue™ Coprecipitant 15 mg / ml (Fisher Scientific, Invitrogen™, catalog number: 10301575)

24. Molecular biology grade Isopropanol (Fisher Scientific, catalog number: BP2618-1), pre-cooled in -20°C.

25. Molecular biology grade Ethanol (Merck, catalog number: 111727), pre-cooled in -20°C.

26. HPLC-grade or nuclease-free water (Fisher Scientific, catalog number: 10257243)

27. DNase I, RNase-free, 1 U / μl (ThermoFisher Scientific, catalog number: EN0521)

28. RNA Clean & Concentrator^{TM}-5 (Zymo Research, catalog number: R1015S)

29. Falcon tubes, 50 ml (Sarstedt, catalog number: 62.547.254)

30. Liquid nitrogen

31. Glass beads 0.25-0.5 mm (Roth, catalog number: A553.1)

32. Triton X-100, molecular biology grade (Merck, catalog number: T8787)

Equipment

1. Clean bench

2. A sterile test tube

3. Culture rotator for test tubes or equivalent

4. Spectrophotometer, able to measure optical density at λ = 600 nm (OD_{600}) (ThermoFisher Scientific, catalog number: 840-209800)

5. Sterilised baffled Erlenmeyer flask, 500 ml (Glassgerätebau Ochs Laborfachhandel e.K., catalog number: 110500)

6. 4x Sterilised Fernbach flasks, 1800 ml (VWR, Duran^{TM}, catalog number: 391-0310)

7. Culture shaker adjustable to 28°C and 200 rpm, large enough to fit 2 x Fernbach flasks above

8. Centrifuge with rotor for 500 ml bottles (Beckman Coulter, J2-21, Discontinued)

9. Angle rotor for 500 ml bottles (Beckman Coulter, JA-10, catalog number: 369687)

10. 4x Autoclaved centrifuge bottle with sealing cap, polycarbonate, 500 ml (ThermoFisher Scientific, Nalgene^{TM}, catalog number: 3140-0500)

11. 2x sterilised Schott bottles, 1 l (VWR, Duran^{TM}, catalog number: 215-1517P)

12. Centrifuge with rotor for 50 ml falcon tubes (Hettich, Rotanta 460-R, catalog number: 5660)

13. Angle rotor for 50 ml falcon tubes (Hettich, Angle rotor, 6-places, catalog number: 5615)

14. Vacuum pump

15. Precision balance that can measure to 0.001 g with maximum weighing capacity of at least 300 g

16. 6x or, if available,12x Ultracentrifuge bottles with cap assemblies, 38 x 102 mm, polycarbonate, 70 ml (Beckman Coulter, catalog number: 355622; see Note 1.).

17. Angle rotor for ultracentrifugation with 70 ml bottles (Beckman Coulter, Type 45 Ti rotor, catalog number: 339160), pre-cooled to 4°C.

18. Ultracentrifuge (Beckman Couter, L8-70M, discontinued)

19. Clamp stand

20. Cooling microfuge

21. Fume hood

22. Protection and gear for handling liquid nitrogen

23. Bead beater

24. Optional shaker at 4°C

Procedure

A. Culturing *U. maydis*

Always use sterile technique and work in a clean bench when handling cultures. *Ustilago maydis* is a pathogen of maize and AB33 is a genetically modified laboratory strain. Follow regulations and precautions for handling, propagation, and disposal of genetically modified organisms and pathogenic microorganisms as instructed by your institution.

1. **Preparing the inoculum**

   a) Take a small amount of inoculum from a frozen glycerol stock (see Note 2.) and streak out on CM-glc agar plate. Incubate at 28°C overnight or until off-white fungal growth is visible (see Note 3.).

   b) Scrape off a small amount of fungal material on the plate, enough to cover the end of a pipette tip, and transfer to a sterile test tube filled with 3 ml of liquid CM + 2% glucose. Incubate with rotation or shaking at 28°C for 24 hours.

   c) Transfer 100 µl of the test tube culture to a 500 ml baffled flask filled with 100 ml CM + 2% glucose. Incubate on a shaker set to 200 rpm, 28°C for 18 hours. This is the "pre-culture", which is grown to a high OD but not to reach stationary phase.

2. **Sporidial culture** (Figure 1B)

   a) Measure the optical density of the pre-culture at $\lambda = 600$ nm (OD_{600}), using unused CM as blank control. Dilute 8- to 10-fold in a cuvette with extra CM, depending on the accurate measuring range of the spectrophotometer available. Pipette up and down immediately

before OD measurement, avoiding air bubbles, to ensure even suspension of cells.

b) Calculate what volume of the pre-culture is needed to obtain 450 ml of sporidial culture with starting OD_{600} = 0.125.

c) Prepare two sterile 1800 ml volume Fernbach flasks. To each flask, add the required volume of pre-culture and CM + 1% glucose to 450 ml final volume. Hence the total volume of the sporidial culture is 2 x 450 = 900 ml. Check OD_{600} of cultures in both flasks.

d) Incubate on a shaker at 200 rpm, 28°C for 6 hours.

e) Measure OD_{600} of the sporidial cultures; OD_{600} values should be approximately 1.0.

3. **Induction of filamentous growth in NM** (Figure 1C)

Viability of induced AB33 filaments at 15-16 hpi is approximately 98 % (98.72 ± 1.28 %; Figure 2).

a) Transfer the sporidial cultures in two Fernbach flasks to two separate sterile 500 ml centrifuge bottles. Balance the bottles to 0.1 g of each other with leftover CM.

b) Centrifuge in JA-10 rotor or equivalent at 6000 rpm (3951 xg) for 5 minutes.
Discard the supernatant carefully, avoiding disruption of the cell pellet.

c) Resuspend each pellet in 100 ml NM. Balance bottles to 0.05 g with NM.

d) Centrifuge in JA-10 rotor at 6000 rpm (3951 xg) for 5 minutes.
Discard the supernatant carefully, avoiding disruption of the cell pellet.

e) Resuspend each pellet thoroughly in 100 ml NM + 2% glucose and transfer each to a new Fernbach flask. Rinse each bottle with additional 350 ml NM + 2% glucose and transfer to the flasks so that the total volume of the shifted cultures is 2 x 450 = 900 ml.

f) Measure OD_{600} of the cultures shifted to NM. Expect transfer losses of around 10%.

g) Incubate on a shaker at 200 rpm for 15 hours. Processing takes up to 1 hour so it can be 16 hours post induction by the time cell-free culture supernatant is obtained.
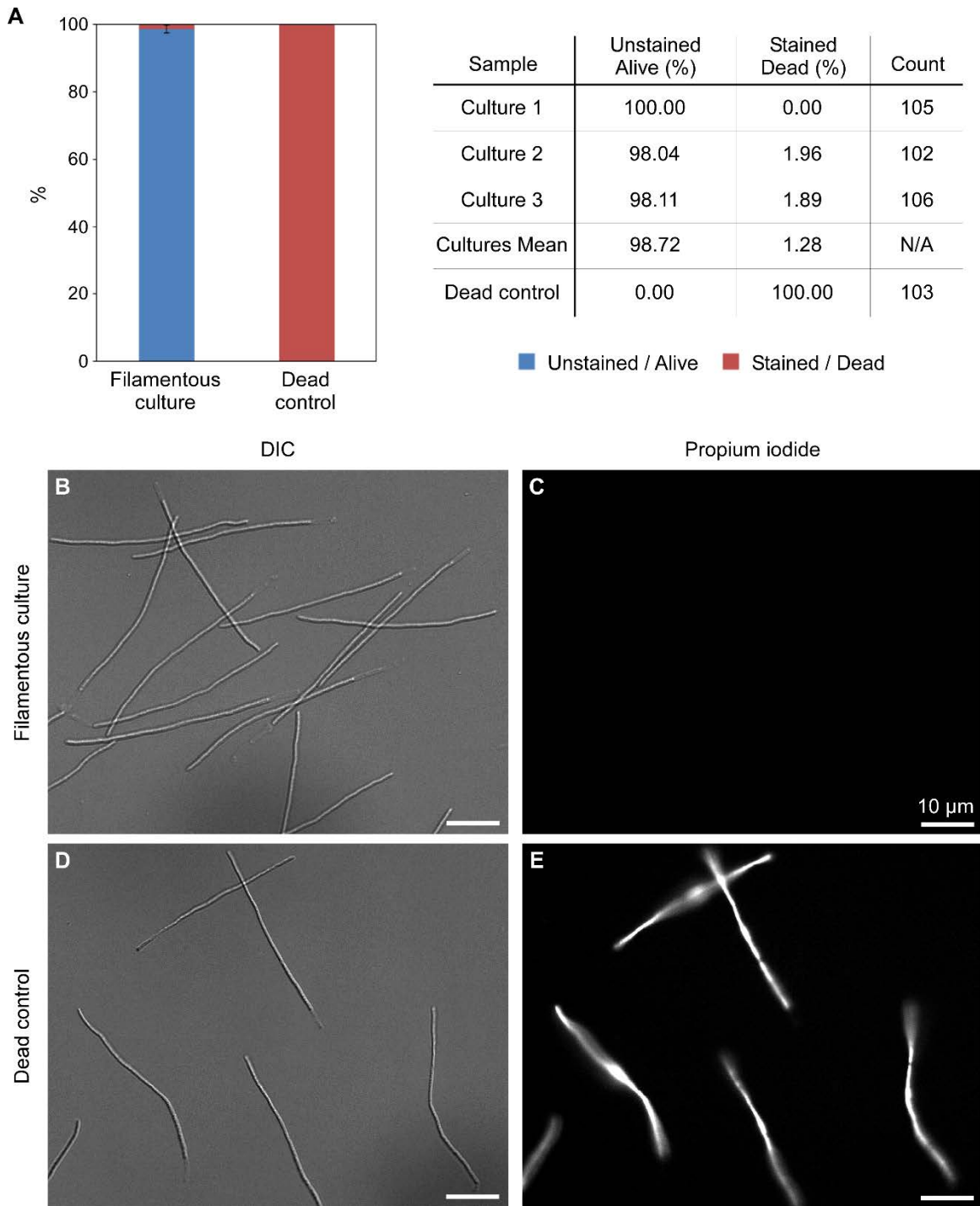
A

Sample	Unstained Alive (%)	Stained Dead (%)	Count
Culture 1	100.00	0.00	105
Culture 2	98.04	1.96	102
Culture 3	98.11	1.89	106
Cultures Mean	98.72	1.28	N/A
Dead control	0.00	100.00	103

■ Unstained / Alive   ■ Stained / Dead

DIC   Propium iodide

Figure 2. Viability of the AB33 induced filaments at the time point of EV isolation.
A. Percentage of filament cells unstained and stained with propium iodide (4 μg/ml final concentration) in 15-16 hpi cultures versus the dead control, incubated at 95°C for 5 minutes. Stained cells are considered dead. **B.** & **C.** Differential interference contrast (DIC) image and propium iodide-stained fluorescence microscopy images of AB33 induced filaments at 15-16 hpi. **D.** & **E.** DIC and propium-iodide stained images of the dead control.

B. Isolation of extracellular vesicles from the filamentous culture supernatant (Figure 3)

Optionally, the whole procedure can be carried out as sterile as possible by opening bottles and tubes only in the clean bench and using sterile equipment and reagents wherever possible.
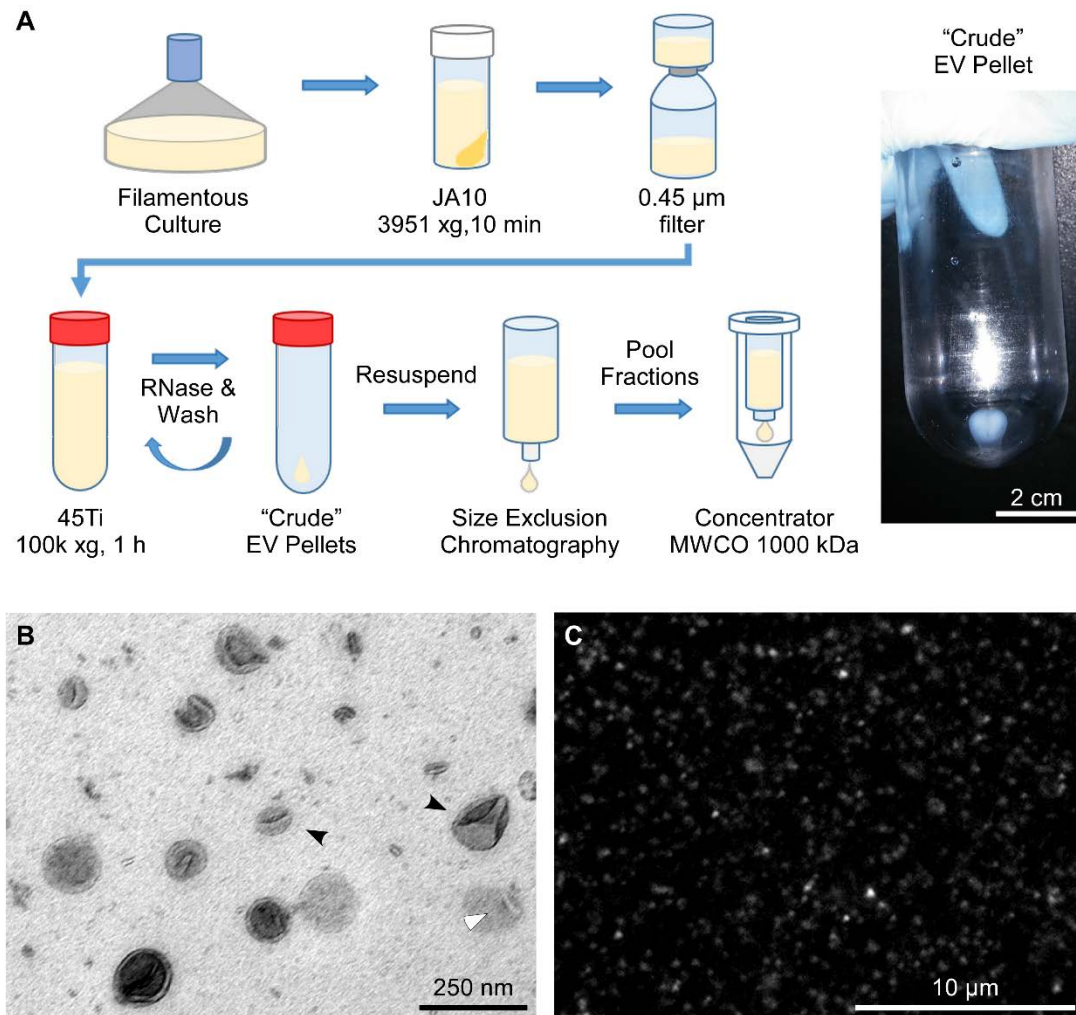

Figure 3. Overview of EV isolation from filamentous cultures of *U. maydis*.
A. Schematic for the EV isolation procedure. 15-16 hpi AB33 filament cultures are centrifuged to collect the supernatant. The culture supernatant is filtered to remove any cells and larger debris. The filtrate is ultracentrifuged to obtain "crude" EV pellets, which are resuspended in PBS and treated with RNase (for options, see section B3 and Figure 4. RNase treatment of EVs). Treated EVs are washed in additional PBS by another round of ultracentrifugation. The treated "crude" EV pellet (image to the right) is resuspended in PBS and passed through a simple size-exclusion chromatography column. EV-enriched fractions are pooled and concentrated for RNA extraction. **B.** Transmission electron micrograph of prepared EVs. Black arrowheads indicate typical cup-shaped morphology of fixed EVs and the white arrowhead indicates a lysed EV. **C.** EV preparation stained with the lipophilic dye FM4-64 (8 µM final concentration).

1. **Preparation of cell-free culture supernatant**

   a) Transfer the 15 hpi filamentous cultures to two 500 ml centrifuge bottles. Balance the bottles to 0.1 g of each other.

   Optionally, filament cell pellets may be saved for RNA extraction (see Note 4.).

   b) Pellet the cells in JA-10 rotor or equivalent at 6000 rpm (3951 xg) for 10 minutes. The supernatant should be completely clear after the run.

   c) Place the funnel lined with miracloth over a 1 l Schott bottle. Pour the supernatant carefully through the funnel, avoiding disruption of the cell pellet (see Note 5.).

   d) Pour the collected supernatant into a 0.45 μm steritop filter connected to a 1 l bottle and the vacuum pump. Filter gently by either turning on the pump in short bursts, or if adjustable, reduce pressure slowly until the supernatant comes through. In the end there should be at least ~820 ml left from 900 ml starting material, even with transfer losses.

2. **Ultracentrifugation to obtain "crude" pellets with EVs**

   a) Fill six 70 ml ultracentrifuge bottles with the filtered supernatant as much as possible without leaking (68-69 ml) and balance opposite bottles to 0.003 g including the cap assemblies. If two ultracentrifuges are available, it is possible to prepare 12 bottles and process the all of the filtered supernatant simultaneously. Otherwise, keep the remaining filtered supernatant at 4°C for the second ultracentrifuge run.

   b) Ultracentrifuge in Type 45 Ti rotor at 36,000 RPM (100,000 xg) at 4°C for 1 hour.

   c) At the end of the run, pale "crude" EV pellets should be visible (see Figure 3A). Mark the position of the pellets on the outside of the bottles with a marker pen.

   d) Discard the supernatant and resuspend the EV pellets in 500 μl PBS each. Keep samples at 4°C or on ice. If resuspending one pellet at a time, only discard the supernatant just before resuspending to prevent drying of the samples. Pipetting by hand is faster but tedious. Alternatively, fix the tubes securely on a shaker at 4°C to resuspend the pellets gently. Keep the tubes at an angle so that the pellets are always covered by 500 μl PBS. EV suspensions should look slightly milky.

   e) 2nd ultracentrifuge run: process the remaining filtered supernatant, repeating steps 2a) to 2c) above, ideally in fresh ultracentrifuge bottles, while the crude EV pellets from the first run in 2d) are being resuspended.

   f) Discard the supernatant from the 2nd ultracentrifuge run. Transfer onto each new EV pellet,

the resuspension from a single ultracentrifuge bottle in step 2d) i.e. ~ 500 μl. Resuspend the pellets as before.

3. **RNase treatment of EVs** (see Figure 4 for different options).

a) Pool together EV suspensions into a single 5ml tube. There should be slightly less than 3 ml (6x ~500 μl) due to transfer losses.

b) Adjust the volume of the EV suspension with extra PBS, up to the 3 ml mark on the 5 ml tube

   i. Option 1 (Figure 4a): To simply obtain EV-associated RNA for experiments such as RT-qPCR, carry on with RNase treatment in the 5 ml tube.

   ii. Option 2 (Figure 4b): To carry out control experiments, split the sample into 3x 1 ml in three separate 1.5 ml tubes for the following treatments: PBS (mock), RNase, and RNase with Triton X-100.
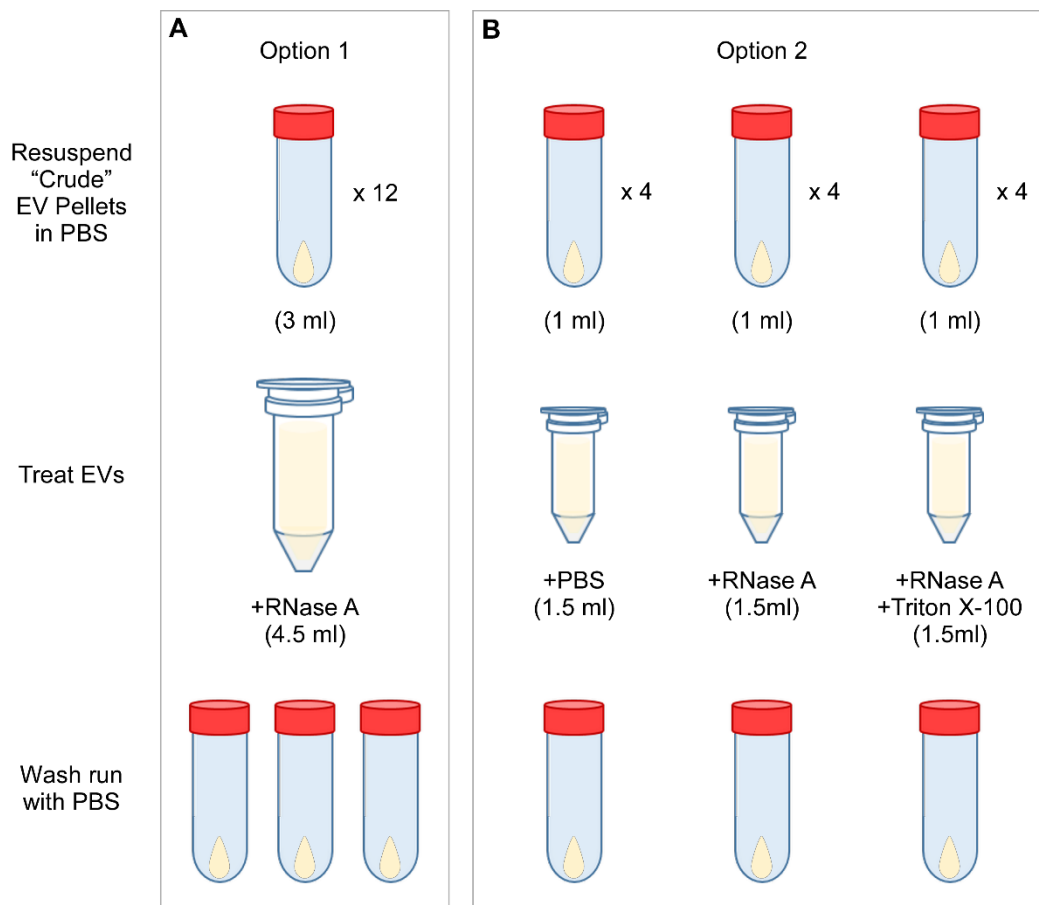

Figure 4. RNase treatment of EVs.
A. Option 1: treatment of EVs with RNase A for purposes that require as much RNA as possible, such as RT-qPCR. **B.** Option 2: mock (+PBS), RNase (+RNase A) and detergent control (+RNase A +Triton X-100).

c) Treat EVs

    i. Option 1: To 3 ml of EV suspension, add 1455 µl PBS and 45 µl of 10 mg / ml RNase A stock solution to obtain a final volume of 4.5 ml and final RNase A concentration of 0.1 µg / µl.

    ii. Option 2: To each 3x 1 ml EV suspension add PBS, RNase A, and Triton X-100 as in the following table:

	PBS (mock)	0.1 µg/µl RNase A	0.1 µg/µl RNase A, 0.1% Triton X-100
EV suspension	1000 µl	1000 µl	1000 µl
PBS	500 µl	485 µl	470 µl
10% Triton X-100	-	-	15 µl
RNase A 10 mg / ml	-	15 µl	15 µl
Total volume	1500 µl	1500 µl	1500 µl

d) Vortex gently on the lowest speed to mix thoroughly and incubate for 10 minutes on ice to degrade any unprotected extracellular RNA.

e) Transfer treated EVs to three ultracentrifuge bottles

    i. Option 1: Split and transfer 1.5 ml each to three separate ultracentrifuge bottles.

    ii. Option 2: Transfer the three differently treated samples into three separate ultracentrifuge bottles.

f) Increase the volume in each ultracentrifuge bottle to ~69 ml with PBS. Balance the opposite tubes to 0.001 g.

g) Ultracentrifuge 36,000 rpm at 4°C for 1 hour as before in 2b).

h) Resuspend the pellets in PBS

    i. Option 1: Resuspend all three EV pellets in 500 µl PBS in total.

    ii. Option 2: Resuspend each pellet in 500 µl PBS.

i) The final "crude" EV suspension can be snap-frozen and stored at -80°C then thawed on ice before proceeding to further purification.

4. Further purification of EVs with IZON qEV columns

This section is based on the manufacturer's instructions (IZON Science Ltd.), which may be updated over time. Cross-check with the instructions from the product purchased. From the TEM images of the particles in the fractions (Figure 5) and the RNA associated with them (Figure 6),

fractions 8-10 are generally the best suited for analysis, but due to some variability, EVs sometimes elute in earlier in fraction 7 also (see Note 6). The manufacturers recommend checking fractions 7-12 for EVs.

<u>Preparation of samples and column</u>

a) Filter 500 µl EV suspension with 0.45 µm syringe filter connected to a 2 ml syringe. There is always a volume retained in the filter. Disconnect the filter from the syringe, pull the piston back up, reconnect, and push to collect the retained EV suspension. Keep on ice until ready.

b) Leave column to equilibriate to room temperature (18-24°C)

c) Prepare 1x 15 ml falcon tube for rinsing, 1x 5 ml tube for void fractions (Fr. 1-6), 6x 1.5 ml Lo-bind tubes for EV-containing fractions (Fr. 7-12), 1x 5 ml tube for wash fractions (Fr. 13-18), 1x 15 ml falcon tubes for rinsing the column again.

d) Clamp the column vertically straight onto the stand. Set up tubes in sequence directly below the column to collect immediately.

e) Remove the top cap and then the bottom cap from the column.

f) Start collecting the flow-through in the first 15 ml falcon tube for rinsing.

g) Always keeping the top of the column submerged, add PBS 1ml at a time until 15 ml has passed through the column.

h) Measure the time it takes for 5 ml of PBS to pass through the column, so that the flow rate through the column can be checked after use and regeneration later in step 4o).

<u>Purification</u>

i) Let the PBS above the column bed flow through, as soon as the meniscus reaches the top of the column bed, add the filtered "crude" EV suspension from step 4a).

j) Immediately start collecting in the designated 5 ml tube for "void" fractions (Fr. 1-6).

k) As soon as the sample has entered the column bed, start adding another 10 ml of PBS, 1ml at a time. Add the first 1 ml very slowly to prevent the column from drying, but also not to dilute the EVs that have not yet entered the column.

l) Collect the "void" fractions (Fr. 1-6) altogether up to the 3 ml mark on the 5 ml tube. Place on ice.

m) Collect the six EV-containing fractions (Fr. 7-12) up to 0.5 ml mark in each 1.5 ml tube. Place on ice.

n) Collect the "wash" fractions (Fr. 13-18) up to 3 ml mark in the designated 5 ml tube. Place on ice.

Column regeneration

o) Rinse the column by passing through another 10 ml of PBS and measure the time it takes for the last 5 ml to come through. Compare the flow rate before and after the sample as an indication of whether the column has been sufficiently rinsed.

p) Close the bottom of the column and add PBS at the top so that there is 2ml above the column bed. Seal the column and store away at 4°C.

5. Concentration of EV-enriched fractions for RNA extraction

a) Precool the microfuge to 4°C

b) Pool fractions 7-10 (4 x 0.5 ml each, total 2 ml) into a single 2 ml tube. Keep on ice.

c) Load 500 µl at a time into VIVASPIN 500 MWCO 1000 kDa concentrator.

d) Spin at 15,000 xg for 2-5 minutes at a time and check the retained volume. If the membrane gets blocked, gently pipette up and down without touching the membrane to unblock or transfer to a new concentrator if necessary. Carry on until all of the 2 ml of pooled fractions is concentrated to 250 µl.

e) Transfer the sample concentrated to 250 µl to a clean 2 ml reaction tube, place on ice. Proceed with RNA extraction. Alternatively, samples may be snap-frozen and stored at -80°C then thawed on ice before RNA extraction.
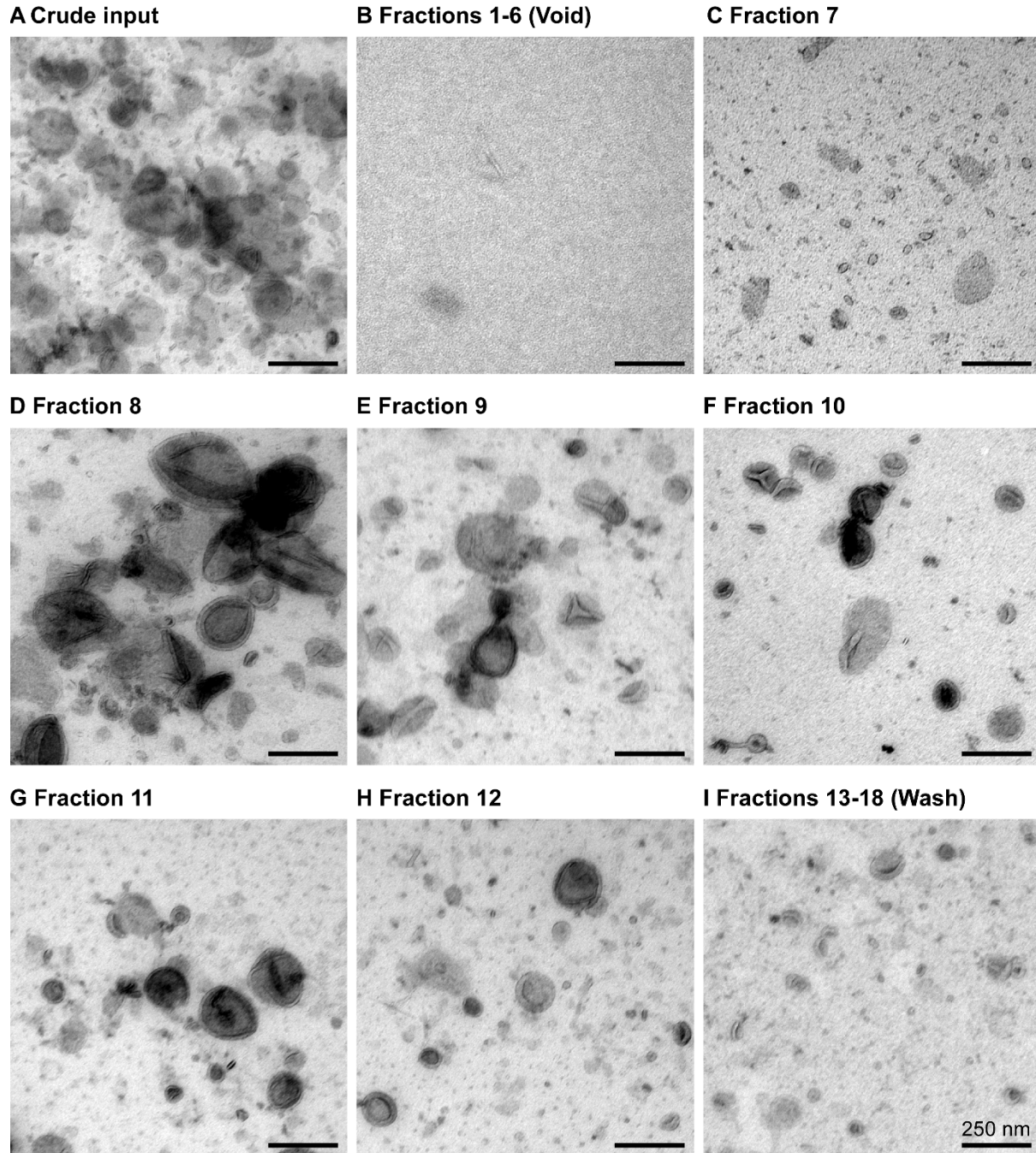
A Crude input

B Fractions 1-6 (Void)

C Fraction 7

D Fraction 8

E Fraction 9

F Fraction 10

G Fraction 11

H Fraction 12

I Fractions 13-18 (Wash)

250 nm

Figure 5. Transmission electron micrographs of fractions from size-exclusion chromatography (SEC).
A. The "crude" EV pellet from ultracentrifugation is resuspended and used as an input. **B.** Fractions 1-6 is the void volume of the column **C.-H.** EV-containing fractions 7-12. **I.** Wash fractions 13-18 where remaining particles are eluted from the column. Fractions 7-10 (**C.-F.**) are recommended for further analysis. In practice, EVs may be eluted later in fraction 8 as shown in this figure.
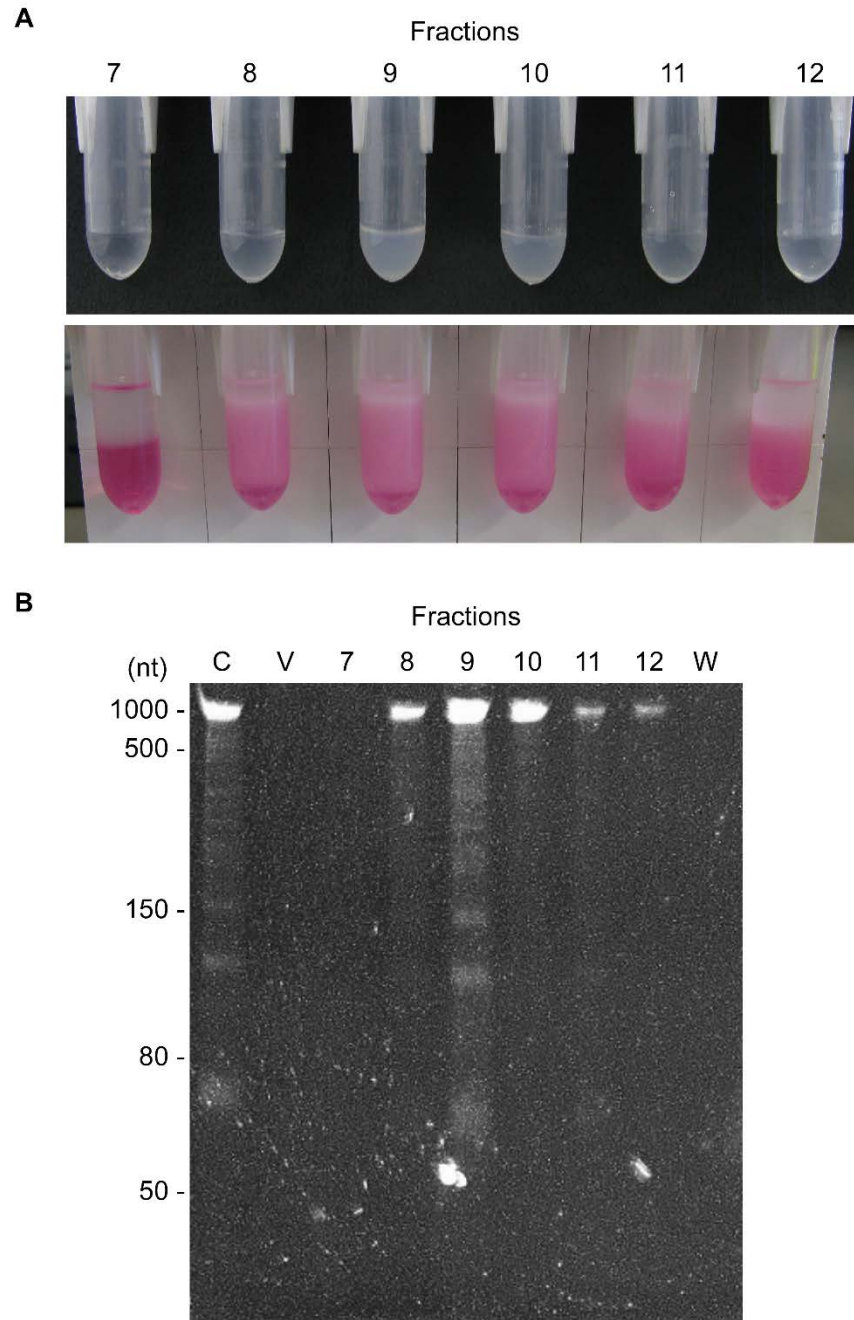
Figure 6. RNA extraction from SEC fractions.
A. EV-containing fractions (7-12) obtained from SEC (top) and RNA extraction using TRI reagent LS (bottom). Fractions 8-10 visibly contain more particles. **B.** RNA extracted from SEC fractions. From left to right: "Crude" EV suspension input (C), void volume (V; fractions 1-6), EV-containing fractions (7-12), wash volume (W; fractions 13-18). The 6% urea-PAGE gel stained with SYBR Green II was used here only to show which fractions contain the most RNA and does not resolve the full size range of RNA in the fractions.

C. RNA extraction from EV suspensions

Work under a fume hood and take precautions when handling TRI reagent LS and chloroform. RNA is extracted from EV samples with TRI reagent LS, treated with DNase and re-extracted with TRI reagent LS or cleaned up using RNA Clean & Concentrator™-5 (Zymo Research). Optionally, RNA can also be extracted from filament cell pellets saved in step B1a), using the normal TRI reagent (see Note 4.). For The extracted RNA is treated with DNase and can be re-extracted with TRI reagent LS or cleaned up using RNA Clean & Concentrator™-5 (Zymo Research).

1. RNA extraction with a modified TRI reagent LS protocol (SIGMA-ALDRICH)

a) Pre-cool the microfuge to 4°C.

b) Prepare two Phaselock gel Heavy tubes for every sample: spin down at 13000 RPM (~16,000 xg) for 30 seconds in the microfuge.

c) Add 750 µl TRI reagent LS per 250 µl EV suspension in a 2 ml reaction tube.

d) Shake vigorously for 15 seconds until homogenous, incubate for 2 minutes at room temperature.

e) Add 200µl Chloroform to each sample.

f) Shake vigorously for 15 seconds until homogenous, incubate 2 minutes at room temperature.

g) Transfer each sample to a pre-spun Phaselock gel tube prepared in 1b). Centrifuge 13000 RPM for 15 minutes, 4°C.

h) Transfer the top aqueous phase of each sample carefully to a new RNase-free 1.5 ml reaction tube, avoid touching the interphase and the Phaselock gel.

i) Add 400 µl chloroform to each sample

j) Shake vigorously for 15 seconds until homogenous, incubate 2 minutes at room temperature.

k) Transfer each sample to a pre-spun Phaselock gel tube prepared in 1b). Centrifuge 13000 RPM for 15 minutes, 4°C.

l) Transfer the top aqueous phase of each sample carefully to a new RNase-free 1.5 ml reaction tube, avoid touching the interphase and the Phaselock gel.

m) Add 1µl Glycoblue to each sample.

n) Add 500 µl ice-cold isopropanol from -20°C to each sample.

o) Mix by inverting ten times and allow to precipitate overnight in -20°C.

p) Centrifuge 13000 RPM for 30 minutes, 4°C.

q) Remove the supernatant with a pipette, taking care not to disturb the small, translucent, blue pellet containing RNA.

r) Add 1 ml ice-cold 75% EtOH from -20°C to each pellet.

s) Centrifuge 13000 RPM for 5 minutes, 4°C.

t) Remove the supernatant carefully as before.

u) Repeat steps r) to t).

v) Dry pellet by spinning down and pipetting away residual ethanol with fine 10μl tips, taking care not to disturb the pellet.

w) Resuspended all RNA pellets in 15 μl of HPLC H_2O each.

x) Treat with DNase as according to manufacturer's instructions.

y) Re-extract with TRI reagent LS (after increasing volume to 250 μl with nuclease-free water or nuclease-free PBS. Alternatively, use RNA Clean & Concentrator™-5 as according to manufacturer's instructions.

2. **Check quality of EV-associated RNA and filament RNA samples**

Use Bioanalyser™ Nano Chip as per manufacturer's instructions. Load 1μl of each RNA sample per lane and measure using the "Eukaryote" setting. Representative results are shown in Figure 7.
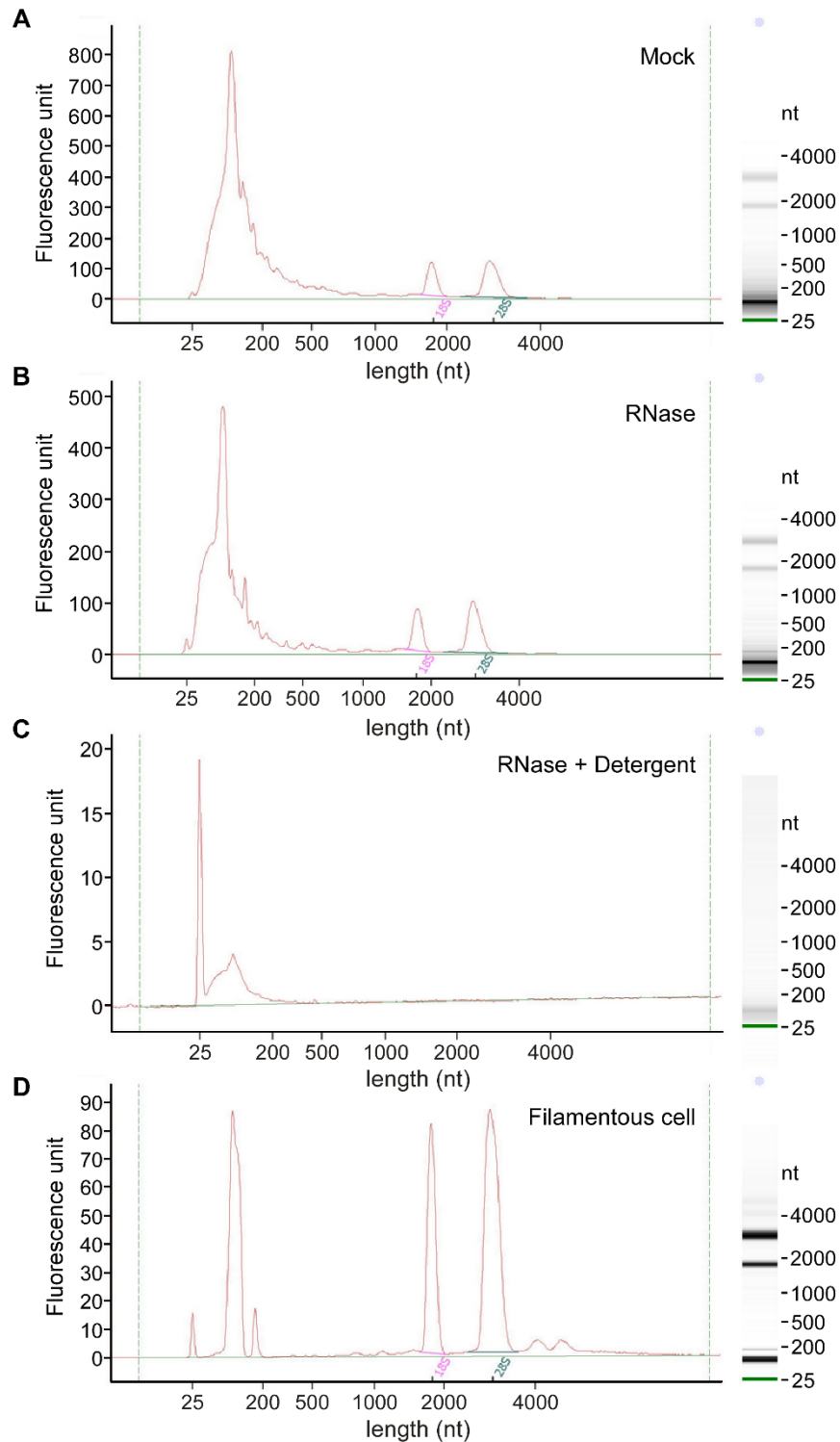
Figure 7. Bioanalyser profile of RNA extracted from EV samples and AB33 filaments.
Bioanalyser profiles of RNA extracted from **A.** EVs mock-treated with additional PBS, **B.** 0.1 µg / µL RNase A in PBS, and **C**. 0.1 µg / µL RNase A and 0.1% (v/v) triton X-100 in PBS. **D.** Total RNA of induced hyphal filament cells, from which above EV samples were derived. Original data and figure from (Kwon et al., 2021).

Notes

1. Polycarbonate ultracentrifuge bottles can be optionally sterilsed with 10% H_2O_2 in sterile distilled water for 10 minutes and rinsed thoroughly with sterile distilled water prior to use. Use personal protective equipment while handling. 10% H_2O_2 can cause burns.

2. How to prepare glycerol stocks is described elsewhere (Bösch et al., 2016).

3. The culture on the plate can be stored at 4°C and used for up to 3 weeks.

4. For comparison between EVs and filament cell RNA samples, save a cell pellet and extract RNA as below. If only one strain was used for EV isolation, then 2 cell pellets can be prepared for the sake of balancing. Use the following cell lysis step then use the standard TRI reagent method as according to the manufacturer:

   a) Prepare a 2 ml reaction tube filled with ~200 μl plastic beads

   b) Transfer 30 ml of culture to a 50 ml falcon tube and centrifuge at 6400 RPM (3871 xg; check specifications of own centrifuge) for 5 minutes.

   c) Combine the supernatant with the rest of culture supernatant in step B1c) for EV isolation.

   d) Resuspend the cell pellet in 2 ml PBS, and transfer to the 2 ml tube filled with ~200 μl of plastic beads prepared above.

   e) Snap freeze with liquid nitrogen and store at -80°C until RNA extraction.
   When ready, carry out steps f-h swiftly to avoid thawing and degradation of RNA.

   f) Take out the cell pellet from -80°C and put on ice.

   g) Add 1 ml TRI reagent.

   h) Beat in the Retsch mill for 5 minutes at 30/s, 4°C.

5. Filamentous cell pellets are less compact than sporidial ones and some carryover is unavoidable but can be minimized by pouring over the miracloth. The reason for excluding cells as much as possible before ultrafiltration is to prevent blockage of the filter and potential contamination from lysis of carried over cells under pressure. It is better to leave behind the last few ml of supernatant than to have more cells carried over; there is 70-80 ml excess supernatant so it's okay to lose some at this step.

6. There may be some variability in elution if the fractions are collected manually. Nonetheless, in differential gene expression analysis, there was very little variation and high correlation (6.6%; Pearson correlation = 0.96) between four biological replicates of PBS- and four biological replicates of RNase-treated EVs samples combined (Kwon et al., 2021). This is despite isolating EVs on four separate days and using different columns for differently treated samples. Although

Fraction 7 did not seem to contain appreciable amount of EVs (Figure 5) nor RNA (Figure 6), we isolated RNA from fractions 7-10 combined to create an inventory of mRNAs in EVs (Kwon et al., 2021). Theoretically, Fraction 7, which is eluted directly after the void volume of the column, should contain more particles in the size range of EVs than smaller protein aggregates or lipoproteins.

Recipes

The original recipes are described in an earlier study (Holliday, 1974) and reproduced here. Prepare all solutions and media in ddH$_2$O.

1. Trace element suspension. Shake well before use.

Ingredients	Per 1000 ml	Final concentration
H$_3$BO$_3$	60 mg	0.06 % (w/v)
MnCl*4H$_2$O	140 mg	0.14 % (w/v)
ZnCl$_2$	400 mg	0.4 % (w/v)
Na$_2$MoO$_4$*2H$_2$O	40 mg	0.4 % (w/v)
FeCl$_3$*6H2O	100 mg	0.1 % (w/v)
CuSO$_4$*5H2O	40 mg	0.04 % (w/v)

2. Salt solution

Ingredients	Per 1000 ml	Final concentration
KH$_2$PO$_4$	16 g	16 % (w/v)
Na$_2$SO$_4$	4 g	4 % (w/v)
KCl	8 g	8 % (w/v)
CaCl$_2$*2H2O	1.32 g	1.32 % (w/v)
Trace element suspension	8 ml	8 % (w/v)
MgSO$_4$*	2 g	2 % (w/v)

*dehydrated, water-free MgSO$_4$, not MgSO$_4$*7H$_2$O

3. Vitamin solution (store at -20°C)

Ingredients	Per 1000 ml	Final concentration
Thiamine	200 mg	0.1 % (w/v)
Riboflavin	100 mg	0.05 % (w/v)
Pyridoxine	100 mg	0.05 % (w/v)
Calcium-pantothenate	400 mg	0.2 % (w/v)
Aminobenzoic acid	100 mg	0.05 % (w/v)
Nicotinic acid	400 mg	0.2 % (w/v)
Choline chloride	400 mg	0.2 % (w/v)
Myo-inositol	2000 mg	1 % (w/v)

4. Complete medium (CM)

	Ingredients	Per 1000 ml	Final concentration
Dissolve all except agar completely in ddH$_2$O, adjust pH, then add agar only for solid medium; autoclave 5 min, 121°C	Casamino acids (Gibco, Bacto™, catalog number: 223050)	2.5 g	0.25 % (w/v)
	Yeast extract (Gibco, Bacto™, catalog number: 212750)	1 g	0.1 % (w/v)
	DNA degradation free acid (Sigma, D-3159)	0.5 g	0.05 % (w/v)
	NH$_4$NO$_3$	1.5 g	0.15 % (w/v)
	Vitamin solution	10 ml	1 % (v/v)
	Salt solution	62.5 ml	6.25 % (v/v)
	5 M NaOH	Adjust to pH 7.0	
	Bacto-Agar* (Gibco, Bacto™, catalog number: 214010)	20 g	2 % (w/v)
Add only after the medium has cooled below 60°C	50% Glucose solution; filter-sterilised	20 ml	1 % (w/v)

* For solid medium only

5. Nitrate minimal medium (NM)

	Ingredients	Per 1000 ml	Final concentration
Dissolve completely in ddH$_2$O, adjust pH; autoclave 5 min, 121°C	KNO$_3$	3.0 g	0.25 % (w/v)
	Salt solution	62.5 ml	6.25 % (v/v)
	5 M KOH	Adjust to pH 7.0	
Add only after the medium has cooled below 60°C	50% Glucose solution; filter-sterilised	20.0 ml	1.0 % (w/v)

6. 10 mg / ml RNase A stock solution

		Per 10 ml	Final concentration
Dissolve RNase A powder in 0.1M Sodium acetate buffer, boil at 100°C for 15 minutes	RNase A (Merck, catalog number: R9009)	100 mg	10 mg / ml
	0.1 M Sodium acetate (pH 5.2)	9 ml	
Allow to cool to room temperature and add Tris-HCl	Tris-HCl pH 7.4	1 ml	

Contributions & Acknowledgments

Competing interests

There are no competing interests. No funding or free products were acquired from vendors or advertisers.

Ethics

No human or animal subjects are used in the described protocol.

References

BLEACKLEY, M., SAMUEL, M., GARCIA-CERON, D., MCKENNA, J. A., LOWE, R. G. T., PATHAN, M., ZHAO, K. N., ANG, C. S., MATHIVANAN, S. & ANDERSON, M. A. 2020. Extracellular Vesicles From the Cotton Pathogen *Fusarium oxysporum* f. sp. *vasinfectum* Induce a Phytotoxic Response in Plants. *Frontiers in Plant Science,* 10.

BÖSCH, K., FRANTZESKAKIS, L., VRANES, M., KÄMPER, J., SCHIPPER, K. & GÖHRE, V. 2016. Genetic Manipulation of the Plant Pathogen Ustilago maydis to Study Fungal Biology and Plant Microbe Interactions. *J Vis Exp*.

BRACHMANN, A., WEINZIERL, G., KAMPER, J. & KAHMANN, R. 2001. Identification of genes in the bW/bE regulatory cascade in *Ustilago maydis*. *Molecular Microbiology,* 42**,** 1047-1063.

BREFORT, T., DOEHLEMANN, G., MENDOZA-MENDOZA, A., REISSMANN, S., DJAMEI, A. & KAHMANN, R. 2009. *Ustilago maydis* as a Pathogen. *Annual Review of Phytopathology,* 47**,** 423-445.

DJAMEI, A., SCHIPPER, K., RABE, F., GHOSH, A., VINCON, V., KAHNT, J., OSORIO, S., TOHGE, T., FERNIE, A. R., FEUSSNER, I., FEUSSNER, K., MEINICKE, P., STIERHOF, Y. D., SCHWARZ, H., MACEK, B., MANN, M. & KAHMANN, R. 2011. Metabolic priming by a secreted fungal effector. *Nature,* 478**,** 395-+.

HILL, E. H. & SOLOMON, P. S. 2020. Extracellular vesicles from the apoplastic fungal wheat pathogen *Zymoseptoria tritici*. *Fungal Biol Biotechnol,* 7**,** 13.

HOLLIDAY, R. 1974. *Ustilago maydis*. *In:* KING, R. C. (ed.) *Bacteria, Bacteriophages, and Fungi.* Boston, MA: Springer.

IZON SCIENCE LTD. *qEVoriginal User Manual* [Online]. https://support.izon.com/technical-note-qevoriginal. [Accessed 05.12.2021].

KWON, S., RUPP, O., BRACHMANN, A., BLUM, C. F., KRAEGE, A., GOESMANN, A. & FELDBRÜGGE, M. 2021. mRNA Inventory of Extracellular Vesicles from Ustilago maydis. *Journal of Fungi,* 7**,** 562.

LANVER, D., MULLER, A. N., HAPPEL, P., SCHWEIZER, G., HAAS, F. B., FRANITZA, M., PELLEGRIN, C., REISSMANN, S., ALTMULLER, J., RENSING, S. A. & KAHMANN, R. 2018. The Biotrophic Development of Ustilago maydis Studied by RNA-Seq Analysis. *Plant Cell,* 30**,** 300-323.

LIU, T., SONG, T., ZHANG, X., YUAN, H., SU, L., LI, W., XU, J., LIU, S., CHEN, L., CHEN, T., ZHANG, M., GU, L., ZHANG, B. & DOU, D. 2014. Unconventionally secreted effectors of two filamentous pathogens target plant salicylate biosynthesis. *Nature Communications,* 5**,** 4686.

LUDWIG, N., REISSMANN, S., SCHIPPER, K., GONZALEZ, C., ASSMANN, D., GLATTER, T., MORETTI, M., MA, L. S., REXER, K. H., SNETSELAAR, K. & KAHMANN, R. 2021. A cell surface-exposed protein complex with an essential virulence function in *Ustilago maydis*. *Nature Microbiology*.

SIGMA-ALDRICH. *T3934 TRI Reagent LS (T3934) - Technical Bulletin* [Online]. Available: https://www.sigmaaldrich.com/deepweb/assets/sigmaaldrich/product/documents/136/679/t3934bul.pdf [Accessed 05.12.2021].

TORUÑO, T. Y., STERGIOPOULOS, I. & COAKER, G. 2016. Plant-Pathogen Effectors: Cellular Probes Interfering with Plant Defenses in Spatial and Temporal Manners. *Annual Review of Phytopathology,* 54**,** 419-441.

WAHL, R., ZAHIRI, A. & KAMPER, J. 2010. The Ustilago maydis b mating type locus controls hyphal proliferation and expression of secreted virulence factors in planta. *Molecular Microbiology,* 75**,** 208-220.

WEIBERG, A., WANG, M., LIN, F. M., ZHAO, H. W., ZHANG, Z. H., KALOSHIAN, I., HUANG, H. D. & JIN, H. L. 2013. Fungal Small RNAs Suppress Plant Immunity by Hijacking Host RNA Interference Pathways. *Science,* 342**,** 118-123.

WITZEL, K., SHAHZAD, M., MATROS, A., MOCK, H.-P. & MÜHLING, K. H. 2011. Comparative evaluation of extraction methods for apoplastic proteins from maize leaves. *Plant methods* [Online], 7.

3. mRNA Inventory of Extracellular Vesicles from *Ustilago maydis*

<u>Disclaimer</u>

This manuscript has been published in Journal of Fungi (https://doi.org/10.3390/jof7070562). Author contributions are stated in the manuscript and all contents of the submission package and the final published materials have been confirmed by the authors. The latest published version of the manuscript is reproduced here with permissions according to the MDPI Open Access Policy.

<u>Personal Contribution</u>

I have conceptualised the project, designed the methodology, and carried out all experiments, except library generation and sequencing. I have performed all analyses except the RNA-seq data processing steps up to differential gene expression analysis, and the 3'UTR motif prediction. I have written the original manuscript and produced all the figures and tables except Figure S1 and S2. I have earned an independent scholarship from the Deutscher Akademischer Austausch Dienst with own proposal on EVs and participated in writing the grant proposal with Prof. Dr. Michael Feldbrügge to obtain DFG-FOR5116 subproject B3 (FE/448/15-1) to fund this project.

mRNA Inventory of Extracellular Vesicles from *Ustilago maydis*

Seomun Kwon [1], Oliver Rupp [2], Andreas Brachmann [3], Christopher Frederik Blum [4], Anton Kraege [1], Alexander Goesmann [2] and Michael Feldbrügge [1,*]

1   Institute for Microbiology, Cluster of Excellence on Plant Sciences, Heinrich Heine University Düsseldorf, 40225 Düsseldorf, Germany; Seomun.Kwon@hhu.de (S.K.); Anton.Kraege@hhu.de (A.K.)
2   Bioinformatics and Systems Biology, Justus-Liebig-Universität, 35392 Giessen, Germany; oliver.rupp@computational.bio.uni-giessen.de (O.R.); Alexander.Goesmann@computational.bio.uni-giessen.de (A.G.)
3   Biocenter of the LMU Munich, Genetics Section, Grosshaderner Str. 2-4, 82152 Planegg-Martinsried, Germany; brachmann@lmu.de
4   Institute for Mathematical Modelling of Biological Systems, Heinrich Heine University Düsseldorf, 40225 Düsseldorf, Germany; Christopher.Blum@hhu.de
*   Correspondence: feldbrue@hhu.de; Tel.: +49-211-81-14720

Abstract: Extracellular vesicles (EVs) can transfer diverse RNA cargo for intercellular communication. EV-associated RNAs have been found in diverse fungi and were proposed to be relevant for pathogenesis in animal hosts. In plant-pathogen interactions, small RNAs are exchanged in a cross-kingdom RNAi warfare and EVs were considered to be a delivery mechanism. To extend the search for EV-associated molecules involved in plant-pathogen communication, we have characterised the repertoire of EV-associated mRNAs secreted by the maize smut pathogen, *Ustilago maydis*. For this initial survey, we examined EV-enriched fractions from axenic filamentous cultures that mimic infectious hyphae. EV-associated RNAs were resistant to degradation by RNases and the presence of intact mRNAs was evident. The set of mRNAs enriched inside EVs relative to the fungal cells are functionally distinct from those that are depleted from EVs. mRNAs encoding metabolic enzymes are particularly enriched. Intriguingly, mRNAs of some known effectors and other proteins linked to virulence were also found in EVs. Furthermore, several mRNAs enriched in EVs are also upregulated during infection, suggesting that EV-associated mRNAs may participate in plant-pathogen interactions.

Keywords: extracellular vesicles (EVs); mRNA; fungal pathogen; plant pathogen; *Ustilago maydis*

1. Introduction

Extracellular vesicles (EVs) are ubiquitously secreted from cells, carrying a diverse array of molecular cargos. The role of EVs in intercellular signalling and communication is particularly interesting, as they can facilitate mass delivery of otherwise intracellular molecules across the extracellular space. EV-associated molecules can induce physiological changes in the recipient cells [1]. In pathogenic microbes, EVs can facilitate both intraspecies coordination of pathogen cells during infection [2], and broader cross-kingdom interaction with host cells [3,4].

Investigations on fungal EVs have identified associated proteins [5], RNAs [6], lipids [7], polysaccharides [8], and metabolites [9]. At the level of individual cells, EVs have been implicated in structural functions such as cell wall remodelling [10] and glucuronoxylomannan capsule formation [8]. At the population level, secretion of EVs in *Candida albicans* is important for biofilm formation and antifungal resistance [11]. Furthermore, EVs of *Cryptococcus gattii* effectuate long-distance coordination of virulence between fungal cells engulfed in different macrophages; EVs from a hypervirulent strain trigger rapid proliferation of less virulent strains in the phagosome [3]. While EVs of some clinically important

fungi carry virulence-associated molecules [12] and promote infection [3,13,14], many studies also indicate that fungal EVs stimulate host immune responses to the detriment of the pathogen [15].

The role of EVs in plant-pathogen interaction is not yet well understood, although they have been frequently observed at various plant-fungal interfaces [16–18] Biological significance of plant EVs and their cargos have been elucidated in only a few cases. For instance, EVs of the model plant *Arabidopsis thaliana* carry small RNAs (sRNAs) that silence virulence genes in the grey mould fungus *Botrytis cinerea* [19] and the oomycete pathogen *Phytophthora capsici* [20] during infection. *A. thaliana* EVs additionally contain "tiny RNAs" [21] and various defence-related proteins [22]. In another example, sunflower EVs inhibit spore germination and growth of the white mould pathogen, *Sclerotinia sclerotiorum* [23].

EVs of plant pathogenic fungi are only recently being characterised. So far, EV-associated proteomes of the wheat pathogen, *Zymoseptoria tritici* [24], and the cotton pathogen, *Fusarium oxysporum* f. sp. *vasinfectum* (*Fov*; [9]) have been examined. *Fov* secretes EVs with polyketide synthases and a purple pigment. The fractions containing these EVs trigger hypersensitive cell-death in plants, reflecting the necrotrophic lifestyle of this highly prolific mycotoxin producer [9]. While studies on plant pathogen effectors to date have primarily focused on conventionally secreted proteins, such efforts to examine EV cargos could broaden the spectrum of effector candidates, not only to include unconventionally secreted proteins, but also RNAs and metabolites.

Fungal EVs have been found to contain all types of RNA, the majority of the cargo being shorter sRNAs and tRNAs, but also mRNAs and rRNAs [6]. sRNA effectors have been discovered in at least five different filamentous phytopathogens to date [25–29]. These participate in the bidirectional, cross-kingdom RNAi warfare between plants and pathogens [26]. The diversity of RNAs associated with fungal EVs suggest that RNA species other than sRNAs could also be transferred from a pathogenic fungus to function as effectors in host cells. Particularly interesting would be the concept of effector delivery in the form of full-length mRNAs in pathogen EVs. Such mRNAs could theoretically be translated in the recipient host cells to yield multiple proteins and transfer the cost of effector protein production to the host.

Ustilago maydis is a biotrophic fungal pathogen of maize [30], which can cause up to 20% yield losses [31]. It is an established model organism for endosome-associated mRNA transport [32] and has secondarily lost the RNAi machinery, so it does not produce canonical sRNAs [33]. This makes it an interesting organism to examine the mRNA cargo of EVs. EV-like structures have long been observed at the interface between *U. maydis* and maize cells during biotrophic infection [16], suggesting their relevance in the interaction. Furthermore, engineered strains are available, where filamentous growth and the concomitant infection program can be induced in axenic culture [34].

In nature, the infectious form of *U. maydis* is the dikaryotic filament, formed by mating of compatible sporidia [30]. Filamentation is brought about by heterodimerisation of complementary bE and bW homeodomain transcription factors from each sporidium, which initiates a transcriptional cascade for infectious development [35,36]. Here we have taken advantage of a laboratory strain, AB33, where complementary bE and bW are both present in the same strain and are inducible by switching the nitrogen source, allowing facile and reproducible filamentation in culture [34]. AB33 induced filaments transcriptionally and developmentally mimic infectious dikaryotic filaments and have been used as a surrogate to study the initial stage of infection. Evidently, many effectors and genes relevant for infection are expressed in AB33 filaments in culture [35,36]. Hence, we have utilised *U. maydis* as an ideal system for an initial survey of EV cargo mRNAs in plant pathogens.

2. Materials and Methods

2.1. Culture Conditions and EV Isolation

Initial sporidial cultures of strain AB33 from Brachmann et al. [34] were grown to OD_{600} 1.0 ± 0.1 in complete medium [37], supplemented with 1% glucose. The cells were shifted to nitrate minimal medium [37] with 2% glucose (w/v) to induce filamentation as described previously [34]. Filament cells were pelleted between 15–16 h post induction (hpi) by centrifugation with JA10 rotor (Beckman Coulter, Krefeld, Germany) at 6000 rpm ($3951 \times g$) for 10 min. Cell pellets were snap-frozen and saved for RNA extraction. The supernatant was passed through 0.45 µm filter (Sarstedt, Nümbrecht, Germany). The filtrate was ultracentrifuged with 45 Ti rotor (Beckman Coulter) at 36,000 rpm ($100,000 \times g$), 4 °C, for 1 h. Resulting pellet was resuspended in phosphate buffered saline (GIBCO™ PBS; pH 7.2, ThermoFisher, Dreieich, Germany) and treated with PBS (mock), 0.1 µg/µL RNase A (ThermoFisher), or RNase A with 0.1% (v/v) Triton X-100 (Sigma, Darmstadt, Germany) at 4 °C for 10 min. Protease treatment was not included as incubation at the recommended temperature 37 °C alone compromised sample quality, while protease treatment itself did not produce a qualitative difference. The treated EVs were "washed" by adding PBS and repeating ultracentrifugation. The final pellets were resuspended in PBS and passed through qEVorginal/70 nm size exclusion chromatography columns (IZON, Lyon, France). Fractions enriched in EVs were collected and concentrated with Vivaspin-500 MWCO 1000 kDa concentrator (Sartorius, Göttingen, Germany). EVs were snap-frozen and stored at −80 °C until required.

2.2. Microscopy

Grids with EV samples for transmission electron microscopy (TEM) were prepared as previously described with a few modifications [38]. EVs in PBS were placed on 300 sq formvar/carbon grids (Plano, Wetzlar, Germany), fixed with 2% paraformaldehyde (v/v) in PBS, then 1% glutaraldehyde (v/v). Samples were contrasted with 4% uranyl acetate (w/v), 2% methylcellulose (w/v) and examined with an EM902 transmission electron microscope (Zeiss, Oberkochen, Germany). EVs in PBS were stained with 8 µM FM4-64 (final concentration; ThermoFisher) and examined with a Zeiss Axio Imager M1, equipped with a Spot Pursuit CCD camera (Diagnostic Instruments, Sterling Heights, MI, USA) and Plan Neofluar objective lens (100×, NA 1.3). FM4-64 was excited with an HXP metal halide lamp (LEj) in combination with filter set for mCherry (ET560/40BP, ET585LP, ET630/75BP; Chroma, Bellow Falls, VT, USA). Microscope operation and image processing were conducted with MetaMorph (version 7, Molecular Devices, San Jose, CA, USA). Differential interference contrast images of sporidia and filament cells were obtained with the same instrument with a 63× objective (NA 1.25).

2.3. RNA Extraction, Quality Control, and Sequencing

RNA was extracted from EVs and filament samples using standard methods for TRI-reagen LS (Sigma) and TRI-reagent (Sigma), respectively, with a few modifications. Extracted RNA was treated with DNase I (ThermoFisher) as per manufacturer's instructions and re-extracted with TRI-reagent LS. Coprecipitant GlycoBlue™ (ThermoFisher) was used for EV RNA samples for the first extraction and for all samples in the re-extraction. RNA quality was controlled with Bioanalyzer™ RNA 6000 Nano (Agilent, Santa Clara, CA, USA) assay using the eukaryote setting. Libraries for sequencing were generated with NEBNext® Ultra™ II Directional RNA Library Prep Kit for Illumina together with NEBNext® Poly(A) mRNA Magnetic Isolation Module according to the manufacturer's instructions (NEB, Frankfurt am Main, Germany). Libraries were quality controlled with High Sensitivity DNA Kit on Bioanalyzer (Agilent) and quantified on Qubit 2.0 Fluorometer (ThermoFisher) with ds HS Assay Kit. Sequencing was performed in the Genomics Service Unit of LMU Biocenter, on Illumina MiSeq with v3 chemistry with 2×150 bp paired-end reads (Illumina, San Diego, CA, USA).

2.4. Analysis of RNA-seq Data

Raw sequencing reads were quality checked with FastQC (November 2014) [39], adapter sequences and low quality regions (Q20) were trimmed at the end with Trimmomatic (August 2014) [40]. The reads were mapped to the *Ustilago maydis* genome (Umaydis521_2.0, ENSEMBL) [41,42], using HISAT2 (version 2.1.0) [43] with known splice-sites from the ENSEMBL annotation. The library degradation was checked using the geneBodyCoverage.py tool from RSeQC (August 2012) [44] using the BAM file with the mapped reads. Due to short reads, we first merged the paired-end reads using BBMerge (version 2019) [45] and then aligned the merged reads to the reference using HISAT2 [43]. To correct the read counts for potentially degraded transcripts we used the DegNorm tool (version 0.1.4) [46]. The DegNorm-corrected read counts were used for pair-wise differential expression analyses with DESeq2 (version 1.32.0) [47]. Raw reads, DegNorm-corrected counts file, and the DESeq2 results are available at NCBI's Gene Expression Omnibus [48] (accession number GSE176292).

Principal component analysis on DESeq2 results was visualised with PCAtools (version 2.2.0) [49] and the differentially expressed genes displayed using EnhancedVolcano [50]. Mapped reads were viewed on IGV (version 2.4.10) [51]. A given transcript was considered to have "full CDS coverage" if they meet the following criterion: the entire coding region is covered by at least one read per nucleotide position in at least one out of four biological replicates. GO term and KEGG pathway (version 98.1) [52] overrepresentation analyses were carried out following a published protocol [53], using g:Profiler (version e104_eg51_p15_3922dba) [54] and Cytoscape (version 3.8.2) [55]. On g:Profiler, an ordered gene set analysis was performed, where transcript/gene IDs were sorted with the most enriched in EVs at the top. Default multiple testing correction with g:SCS algorithm was used to test for significance [54]. To test for overrepresentation of KEGG pathways, a custom GMT file created from the KEGG pathway database was used [52]. Transcripts upregulated during infection were defined from a published infection time-course dataset [56] (n = 2316, log2 fold change $\geq$ 1, padj < 0.01), where a given transcript should be upregulated during at least one infection time-point (0.5–12 days post inoculation; dpi) compared to axenic sporidia, which is the starting inoculum at 0 dpi.

For comparison of 3′ untranslated regions (3′UTRs) of mRNAs enriched in EVs versus those depleted from EVs, UTRs were partially annotated based on the mapped RNA-seq reads. Reads with gaps larger than 10 kb were removed with BBMap (version 38.87 [57]). Reads that extend beyond but still overlap with the exon region of a given gene were selected for UTR annotation with SAMtools (version 1.11) [58]. The UTRs were defined with the following criteria using BEDtools (version 2.29.2) [59]: covered by at least 10 reads per position per sample, in at least three samples. Regions that did not meet these criteria were not annotated. The partially annotated 3′UTRs of transcripts enriched in EVs (n = 655, baseMean > 10, log2 fold change > 1, padj < 0.01) and depleted from EVs (n = 841, baseMean > 10, log2 fold change < −1, padj < 0.01) were compared. Single nucleotide and 4-mer frequencies were calculated for both classes and tested for difference using the normal approximation to the binomial difference.

2.5. Validation by RT and RT-qPCR

RNA extracted from RNase-treated EVs and filament cells were cleaned, concentrated with RNA Clean & Concentrator-5 (Zymo Research, Freiburg, Germany). 200 ng of cleaned RNA was used as template for first-strand cDNA synthesis with SuperScript™ IV First-Strand Synthesis System (ThermoFisher), with an inclusive RNase H treatment as according to the manufacturer's instructions. The first-strand reaction was 8-fold diluted and 1 μL was used as template for PCR with 100 nM primers, following an otherwise standard protocol for Phusion® High-Fidelity DNA Polymerase (NEB) with 35 cycles. Annealing temperature was 60 °C and extension time was 50 s for all reactions. For RT-qPCR, 100 ng of RNA was used as input for first-strand cDNA synthesis. The cDNA was diluted 16-fold and 2 μL was used per reaction in qPCR, following an otherwise standard Luna®

Universal qPCR Master Mix (NEB) protocol in Stratagene Mx3000P (Agilent). Relative gene expression analysis was carried out using the $2^{-\Delta\Delta CT}$ method [60], with UMAG_02361 as a reference gene between EVs and filament samples (Log2 fold change = −0.09 in RNA-seq; Table S1). Primers used for full-length RT-PCR and RT-qPCR are shown in Table S2.

3. Results

3.1. EVs from Axenic Filamentous Cultures of U. maydis Contain RNA

First, to check whether *U. maydis* hyphae secrete EVs with appreciable RNA cargo, we have developed a robust protocol for EV isolation (or enrichment) from *U. maydis* cultures. EVs were isolated from filaments of strain AB33 [34], induced from yeast-like, budding sporidia (Figure 1a) in axenic culture. Isolated particles were examined by TEM, which confirmed typical cup-shaped form of fixed EVs (Figure 1b). The samples were subjected to staining with the lipophilic dye FM4-64, which further verified the presence of lipid-containing particles (Figure 1c).

In order to determine the presence of extracellular RNA protected within EVs, Bioanalyzer™ profiles of EV-associated RNAs were examined following RNase treatment of EVs prior to RNA extraction. While RNA extracted from EVs treated with RNase alone (Figure 2b) still produced a profile comparable to mock-treated EVs (Figure 2a), RNase treatment in the presence of a detergent (Figure 2c) at a concentration that should disrupt EV membrane integrity [61], led to extensive degradation of EV-associated RNA. This supports that the extracellular RNA isolated is likely to be encased in EVs, protected from the RNase-rich culture environment.
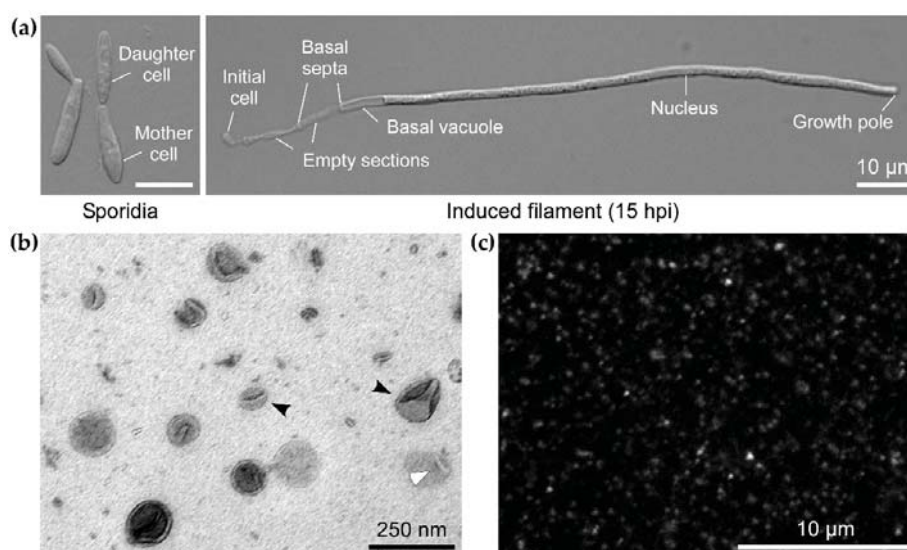

Figure 1. Extracellular vesicles (EVs) from axenic filamentous culture of *Ustilago maydis*. (**a**) Infectious filamentous development was induced in axenic culture using the laboratory strain AB33 [34]. In this strain, the transcriptional cascade of genes necessary for infection and dimorphic switch from yeast-like budding sporidia (left) to hyphal filament (right), can be induced by switching the nitrogen source (both scale bars = 10 μm). EVs were prepared from cultures of filaments between 15–16 h post induction as the one shown on the right. (**b**) Transmission electron micrograph of EVs from filamentous culture of AB33 (scale bar = 250 nm). Typical cup-shaped morphology of EVs is due to fixation. Examples of a smaller and a larger EV are indicated with black arrowheads and an EV lysed during sample preparation is marked with an empty arrowhead. (**c**) Staining of AB33 filament EVs with the lipophilic dye FM4-64 (scale bar = 10 μm). Larger brighter spots are most likely aggregates of EVs formed due to ultracentrifugation.
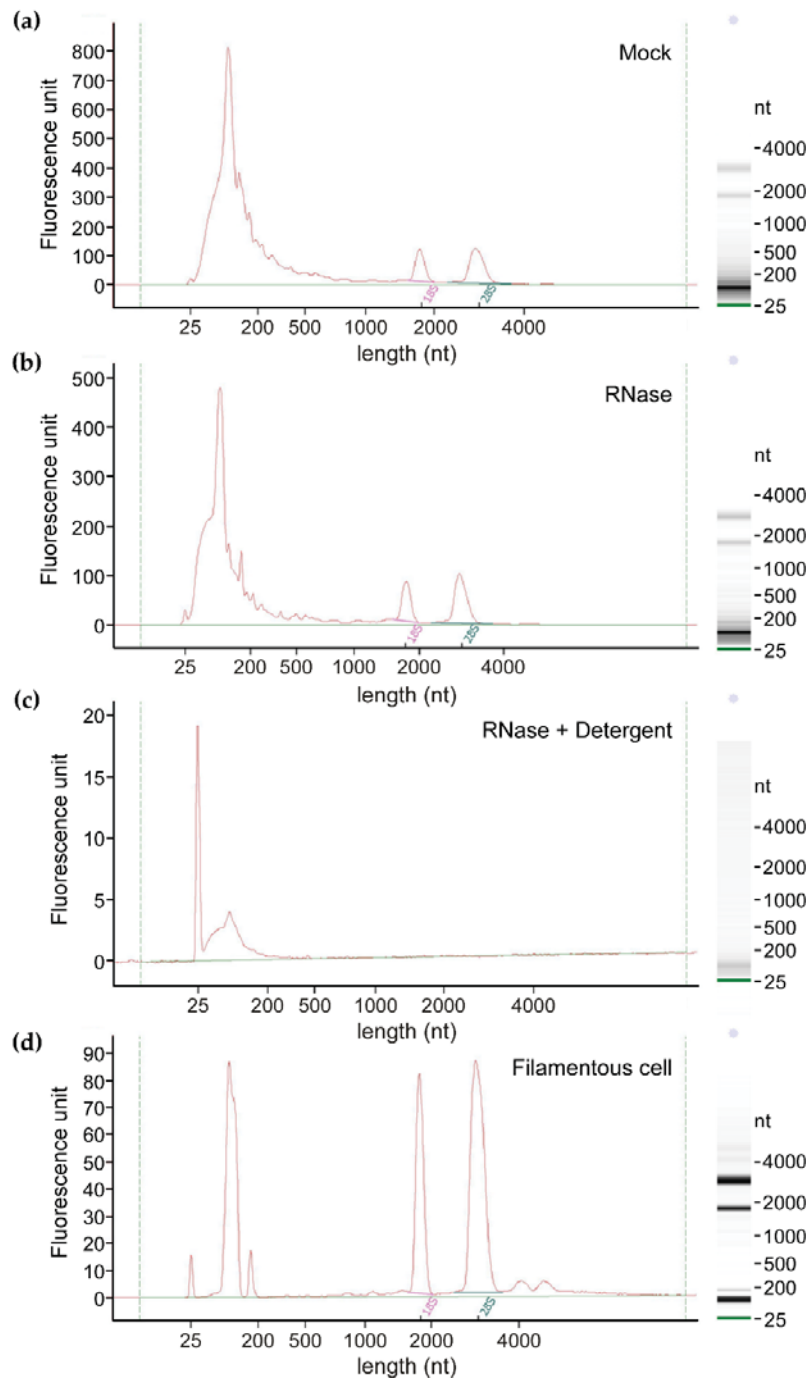
Figure 2. Extracellular RNA associated with *U. maydis* EVs. (**a**) Bioanalyzer profile of RNA extracted from EVs suspended in PBS, incubated with additional PBS as a mock treatment. (**b**) RNA from EVs treated with 0.1 µg/µL RNase A in PBS. (**c**) RNA from EVs treated with 0.1 µg/µL RNase A and 0.1% (*v/v*) triton X-100 in PBS. (**d**) Total RNA of induced hyphal filament cells, from which above EV samples were derived.

Bioanalyzer^{TM} profiles of EV-associated RNAs showed the presence of distinct 18S and 28S ribosomal RNA (rRNA) peaks and a larger, broader peak of less than 200 nt (Figure 2a,b). 18S and 28S rRNAs occupy a lesser proportion (7.3% ± 1.7; *n* = 4) in EV samples (Figure 2a) compared to total RNA samples of filamentous cells (45.2% ± 3.0;

n = 4; Figure 2d). Most EV-associated RNA molecules detected were under 200 nt in length. This is in the range of tRNAs and other non-coding RNAs in *U. maydis*, but probably also includes fragmented mRNAs and rRNAs.

Integrity of EV-associated RNAs seems lower, with a mean RNA integrity number (RIN) value of 3.6 $\pm$ 1.7, compared to 9.8 $\pm$ 0.1 for filament cell RNA (*n* = 4; Figure 2d). This is typical for EV-associated RNAs [62]. The consensus in the EV field is that the RNA integrity number (RIN) provided by the Bioanalyzer^{TM} is not appropriate for RNA from EVs, as shorter RNAs are typically predominant in EVs and relative proportions of different RNA species are likely to be different from total cell RNA [62,63]. The presence of distinct longer rRNA peaks and the absence of notable degradation signals between the major peaks suggest that the higher proportion of shorter RNAs may not simply be attributable to degradation alone, but rather a typical feature of EV-associated RNAs, where shorter transcripts or fragments are more abundant and rRNA is relatively depleted [62,63].

3.2. U. maydis EVs Carry a Distinct Pool of mRNAs Compared to Filaments

To create a catalogue of mRNAs in *U. maydis* EVs, sequencing was carried out on poly(A)-enriched libraries of RNA from mock-treated EVs, RNase-treated EVs, and the corresponding hyphal filaments (Figure 2). Reads mapping to rRNA and tRNA regions were also detected, albeit not as abundantly as expected from the Bioanalyser profiles, due to the poly(A)-enrichment method of library preparation. The exact proportions of different RNA species in *U. maydis* EVs remains to be determined.

To assess the variation between all the samples, principal component analysis was carried out following differential expression analysis (Figure 3a). The first principal component (PC1), corresponding to the sample type (EVs vs. filaments), represented 74.7% variance. The EV samples clustered together tightly, regardless of treatment, with their variation no greater than 6.6% (PC2), although the variability was greater among the RNase-treated samples. Mock-treated and RNase-treated EV samples showed a high correlation in read counts (Figure S1). The mean Pearson correlation between the replicates of mock- and RNase-treated EV samples combined is 0.96, while the correlation for replicates from the mock-treated samples alone is 0.97 and RNase-treated samples is 0.96. The mean correlation between EV and filament samples is lower at 0.83.

With the assumption that functionally important mRNA cargo would be selectively loaded and therefore relatively "enriched" inside EVs, differential expression analysis was carried out to identify transcripts differentially associated with EVs compared to filament cells. Transcripts from 1974 out of 6765 protein coding genes were differentially associated with EVs (Figure 3b; Bonferoni-Hochberg adjusted Wald test *p*-value, padj < 0.01, log2 fold change $\geq$ 1 or $\leq$ −1), of which 758 transcripts were $\geq$2-fold enriched within EVs and 1189 were depleted from EVs to the same extent (Table S1). This indicates selective loading instead of random bulk loading of RNA into EVs.

Following the observation that the proportion of shorter RNAs is increased in EVs compared to filaments (Figure 2), we analysed the length distribution of mRNAs in relation to their enrichment within EVs (Figure 3c). This revealed a bias for enrichment of shorter mRNAs; the median for mRNAs relatively enriched in EVs was 1.002 kb, compared to 1.962 kb for depleted transcripts (Wilcoxon rank sum test, W = 775,462, *p*-value = 3.77×10^{-108}), and 1.523 kb for those in neither category (Wilcoxon rank sum test, W = 1,109,078, *p*-value = 2.26×10^{-55}; Figure 3c). This is in agreement with the notion that larger size can hinder RNA loading into EVs [64]. In essence, RNA-seq of *U. maydis* EV samples has revealed the presence of thousands of mRNAs associated with EVs and relative enrichment of certain population of mRNAs in EVs compared to filament cells is the first indication that there might be specificity in loading of mRNAs into EVs.
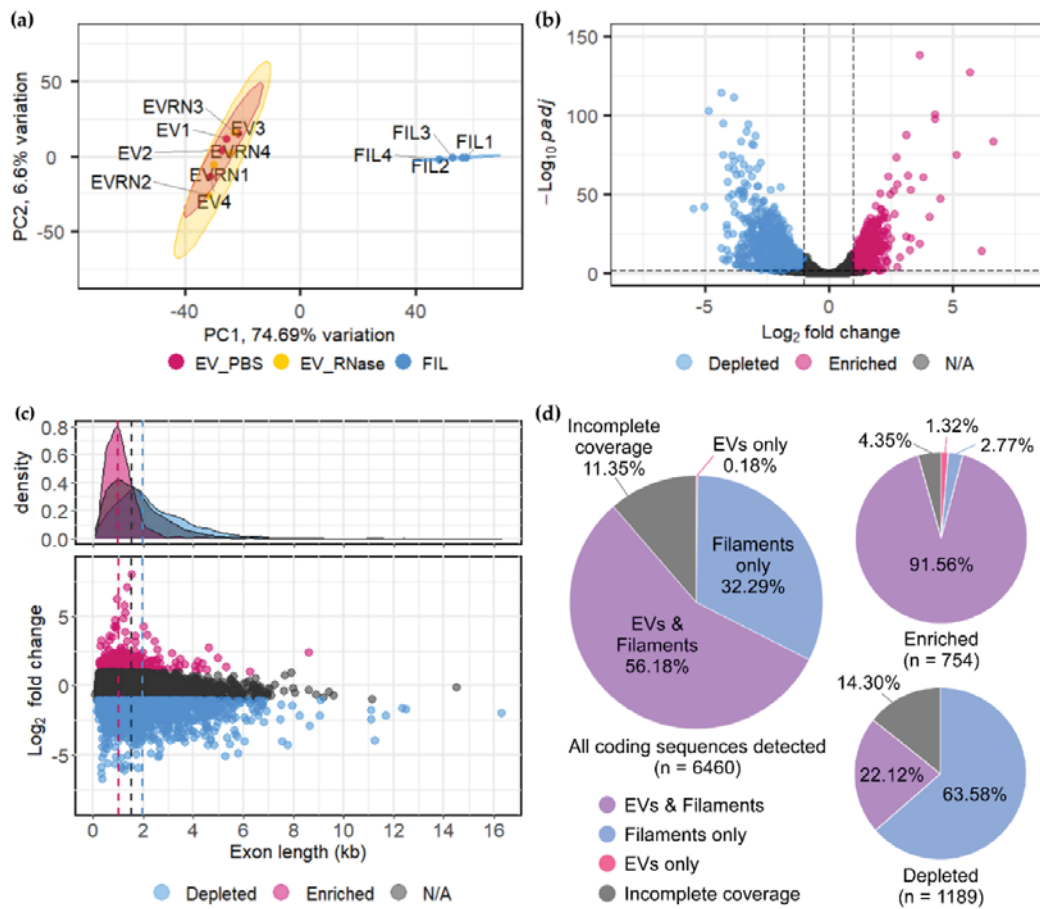
Figure 3. mRNA content of EVs is distinct from that of the hyphal filaments from which they originate. (**a**) Principal component analysis representing "differential expression" or differential presence of mRNAs in four corresponding sets of mock (EV_PBS; red) and RNase-treated (EV_RNase; yellow) EV samples and hyphal filament samples (FIL; blue). (**b**) Volcano plot of transcripts relatively enriched within EVs (red; n = 758, log2 fold change ≥ 1, padj < 0.01) and depleted from EVs (blue; n = 1189, log2 fold change ≤ -1, padj < 0.01) compared to hyphal filaments. (**c**) Effect of transcript length on mRNA enrichment in EVs (log2 fold change). The median length of enriched transcripts is 1.002 kb (red dotted line), is shorter compared to 2.082 kb for depleted transcripts (blue dotted line; Wilcoxon rank sum test, W = 775,462, *p*-value = 3.77×10^{-108}) and 1.523 kb for those neither enriched nor depleted (grey dotted line; log2 fold change > -1 and <1, Wilcoxon rank sum test, W = 1,109,078, *p*-value = 2.26×10^{-55}). (**d**) Percentage of transcripts with full read coverage of the coding sequences (CDS); the entire coding region should be covered by at least one read per nucleotide position in at least one out of four biological replicates. Pie charts are shown for all 6460 coding transcripts detected in EVs and for those relatively enriched in EVs and depleted from EVs.

3.3. Confirmation of Enriched mRNAs with Full-Length CDS in EVs

If mRNAs in EVs are transferred to recipient cells for a specific biological purpose, they could either be translated into functional proteins and/or be fed into the RNAi machinery to silence gene expression. Full-length mRNAs are prerequisite for the first scenario, while fragments should suffice for the latter. Hence, we have checked for the coverage of coding sequences (CDS) in our RNA-seq experiment. Annotations of untranslated regions (UTRs) are not available for *U. maydis*, but the read coverages continuously extending beyond the CDS indicates that the UTRs may be intact for several transcripts. Over half of all transcripts detected in the RNA-seq experiment had full CDS coverage in EVs (Figure 3d). Furthermore, 92.9% of transcripts significantly enriched in EVs (n = 758, log2 fold change $\geq$ 1, padj < 0.01), had full CDS coverage, suggesting the presence of full-length mRNAs in EVs (Figure 3d).

For verification, four enriched mRNA candidates, that have previously been shown to be upregulated during infection [56], were chosen to secondarily confirm the presence of full-length CDS and enrichment in EVs. Two candidates that encode putative oxidoreductases, UMAG_02984 and UMAG_04370, were chosen as they were among the most highly enriched mRNAs in EVs (Table S1). The other two candidates, UMAG_11400 and UMAG_01171, encode metabolic enzymes and were chosen among the less enriched mRNAs in EVs (log2 fold change ~1), in order to test a range of enrichment levels. Presence of full-length transcripts in EVs was checked first by RNA-seq read coverage (Figure 4a) and then by reverse-transcription with oligo-d(T) primers, followed by PCR with primers covering at least 90% of the coding region (Figure 4b). Hence, the intactness of the poly(A) tail and the exon region could be inferred. Relative enrichment of the candidate mRNAs in EVs versus filament cells was checked by RT-qPCR, which was in agreement with the RNA-seq results (Figure 4c). Thus, we have demonstrated that the presence of full-length mRNAs, enriched inside EVs is highly probable, opening up the possibility that fungal mRNAs might be translated in the host.

3.4. Functional Enrichment of mRNAs in EVs

With the notion that mRNAs enriched inside EVs are more likely to be functionally important, we carried out GO term overrepresentation analysis on transcripts differentially associated with EVs. Indeed, mRNAs relatively enriched in EVs showed overrepresentation of different functional GO terms from those that are depleted (Figure 5; Table S3). Transcripts enriched within EVs (log2 fold change $\geq$ 1, padj < 0.01, baseMean $\geq$ 10) showed significant overrepresentation of biological process GO terms for various metabolic processes, proteosomal protein degradation, vesicle-mediated transport, organisation of actin filaments, cytokinesis, and pathogenesis (Figure 5a; g:SCS padj < 0.05). Accordingly, overrepresented molecular function GO terms were mostly enzymatic activities or proteasome-related (Figure 5b). Although the GO term for "pathogenesis" was overrepresented (Figure 5a), the enriched mRNAs are mostly involved in iron uptake, and those that have been examined in *U. maydis* seem to play a role in nutrient acquisition rather than having a direct virulence function [65]. Overrepresented cellular compartment GO terms indicated that the protein products of mRNAs enriched in EVs localise to the cytosol, membranes of vacuoles and vesicles, the proteasome, and the septin complex (Figure 5c). Overrepresentation of GO terms related to intracellular vesicle transport and septins might reflect the link between endosomes and EVs [66], and septin mRNAs are confirmed cargos of endosome-associated mRNA transport in *U. maydis* [67,68].

Transcripts that are relatively depleted from EVs (log2 fold change $\leq$ −1, padj < 0.01) were involved in transmembrane transport, cell wall processes, signal transduction, and several ER-related process such as protein glycosylation, glycolipid metabolism, ER organisation, and the ER-associated protein degradation (ERAD) pathway (Figure 5a). Accordingly, these were predicted to function predominantly at the ER and the plasma membrane (Figure 5c). In agreement with the depletion of ER-targeted mRNAs, transcripts of conventionally secreted proteins were also generally depleted from EVs (n = 1113,

log2 fold change ≤ -1, padj < 0.01, baseMean ≥ 10, g:SCS padj $= 2.08 \times 10^{-13}$). These results suggest that subcellular localisation of mRNAs may affect their loading into EVs: mRNAs associated with intracellular vesicles are more likely to be loaded into EVs, while those that require translation at the rough ER are relatively depleted from EVs.

Since the 3′UTR region is particularly important for subcellular localisation of mRNAs [69], we have partially annotated the UTRs based on the mapped sequencing reads and carried out a preliminary analysis to test if there is a difference between the 3′UTRs of mRNAs enriched in EVs and those depleted from EVs. 3′UTRs of enriched mRNAs showed a higher frequency of adenine nucleotides ($p = 1.3 \times 10^{-19}$) and less cytosine ($p = 1.1 \times 10^{-7}$) and uridine ($p = 9.6 \times 10^{-3}$) compared to the depleted sequences. Accordingly, A-rich 4-mers were significantly increased in frequency among the enriched 3′UTR sequences compared to the depleted ($p < 0.05$; Figure S2b). This prompts deeper investigation into EV-targeting motifs in the future.
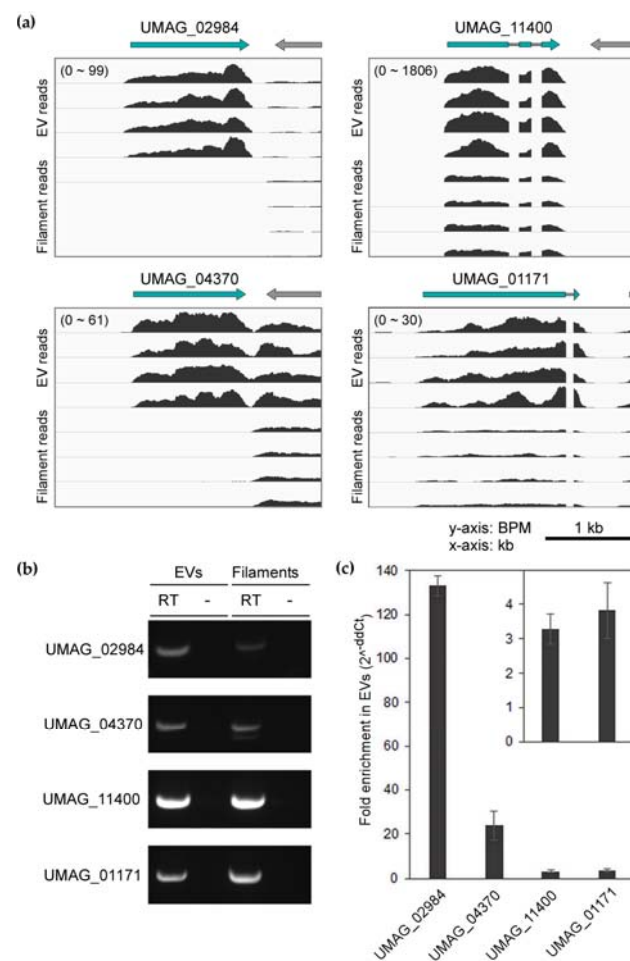

Figure 4. Presence of full-length mRNAs enriched within EVs. (**a**) RNA-seq read coverage of selected infection-relevant, EV-associated mRNA candidates in four biological replicates each of EV and filament samples. *Y*-axis shows normalised coverage in bases per million (bpm) and the range is indicated in brackets. *X*-axis is length in kb (scale bar = 1 kb). (**b**) Confirmation of full-length mRNA candidates by RT-PCR. Primers to yield amplicons covering $\geq 90\%$ of transcript coding region length were used. RT indicates that the reverse-transcribed first-strand cDNA was used as a template for PCR and "-" sign indicates a -RT negative control. (**c**) Confirmation of relative transcript enrichment in EVs compared to filaments by RT-qPCR. Fold relative enrichment within EVs calculated as 2^{-ddCt}. Inset shows fold enrichment of UMAG_11400 and UMAG_01171 with an adjusted *y*-axis.
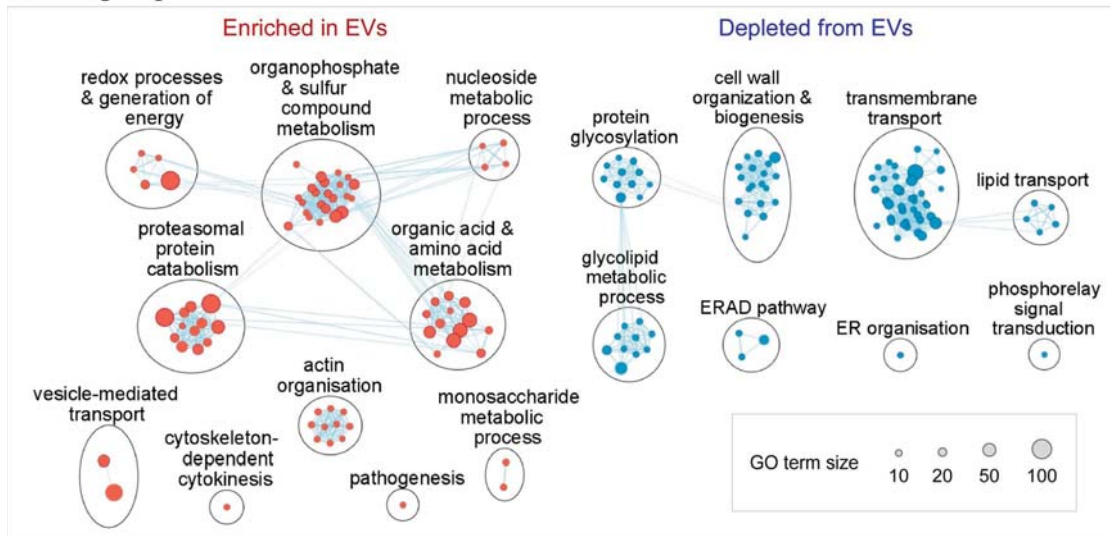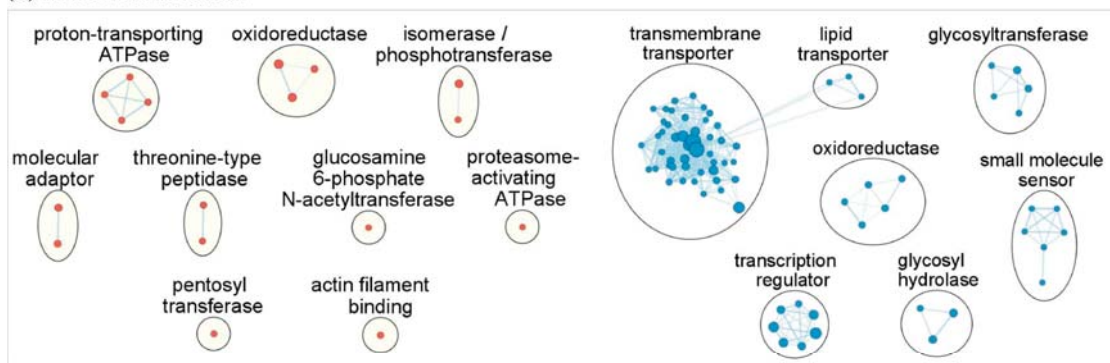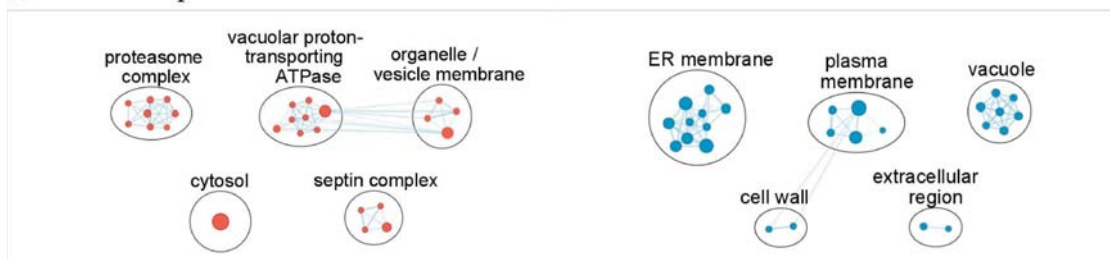
Figure 5. Gene ontology (GO) term analysis of mRNAs differentially loaded into EVs. Biological process (**a**), molecular function (**b**), cellular compartment (**c**). GO terms significantly overrepresented (g:SCS padj < 0.05) in sets of transcripts enriched (red clusters; n = 748, baseMean ≥ 10, log2 fold change ≥ 1, padj < 0.01) and depleted from EVs (blue clusters; n = 1113, baseMean ≥ 10, log2 fold change ≤ −1, padj < 0.01).

3.5. mRNAs Upregulated during Infection Are Present in EVs from Axenic Filaments

Since *U. maydis* is a plant pathogen, we asked whether a portion of EV-associated mRNAs are relevant for infection. Many genes pertinent for infection are expressed in AB33 filaments in culture due to the transcriptional cascade instigated by bE/bW [35]. Indeed, mRNAs of at least nine previously characterised *bona fide* effectors and secreted proteins linked to virulence were reliably detected in EVs: Stp2 [70], ApB73 [71], Scp2 [72], UMAG_01690 [73], Sta1 [74], Stp1 [75], Nuc1 [76], Cmu1 [77], and UmFly1 [78] (in the order of enrichment in EVs; Table S4).

Next, we searched for mRNAs enriched in EVs, that are also upregulated during plant infection. For this, we referred to the published time-course transcriptomic analysis of *U. maydis* infection [56]. 161 mRNAs were found to be both enriched in EVs and upregulated during infection compared to the axenic sporidia at 0 dpi (Figure 6a & Table S5). Over three-quarters of these were induced early on, during the first four days of infection (Figure 6b). GO term analysis of these 161 mRNAs found an overrepresentation of oxidoreductase and other catalytic enzyme activities, as well as functions linked to sulphur compound catabolism and homocysteine metabolism (g:SCS padj < 0.05; Figure 6c). We further examined KEGG pathways [52] and found significant overrepresentation of functions in metabolic pathways, including beta-alanine metabolism, aromatic amino acid biosynthesis, nitrogen metabolism, and glycerolipid metabolism (g:SCS padj < 0.05; Figure 6d). If pathogen EV-associated mRNAs can act as effectors, such metabolic enzymes may be relevant, as *U. maydis* is known to reprogram plant host metabolism [79].

We have examined the most highly enriched mRNAs ($n = 17$, Log2 fold change ≥ 3, padj < 0.01, baseMean ≥ 10), with the assumption that these are more likely to have been loaded in EVs to serve a biological function (Table 1). Many of the most enriched mRNAs encode oxidoreductases with similar annotations, suggesting related activities. This reflects the general overrepresentation of GO terms for oxidoreductases and metabolic enzymes (Figures 5 and 6). Secondly, 10 out of the 17 most enriched mRNAs are induced concomitant with filamentous growth (Log2 fold change ≥ 1, padj < 0.01; [80]), and are up-regulated during infection (Log2 fold change ≥ 1, padj < 0.01; [56]). Furthermore, with reference to the previously defined co-expression modules from an extensive infectious time-course study [56], we found an overrepresentation of the "magenta" infection-related expression module representative of biotrophic proliferation *in planta* (g:SCS padj = 1.43×10^{-4}). In essence, we observe an enrichment of mRNAs in EVs that can be linked to filament induction and infection.
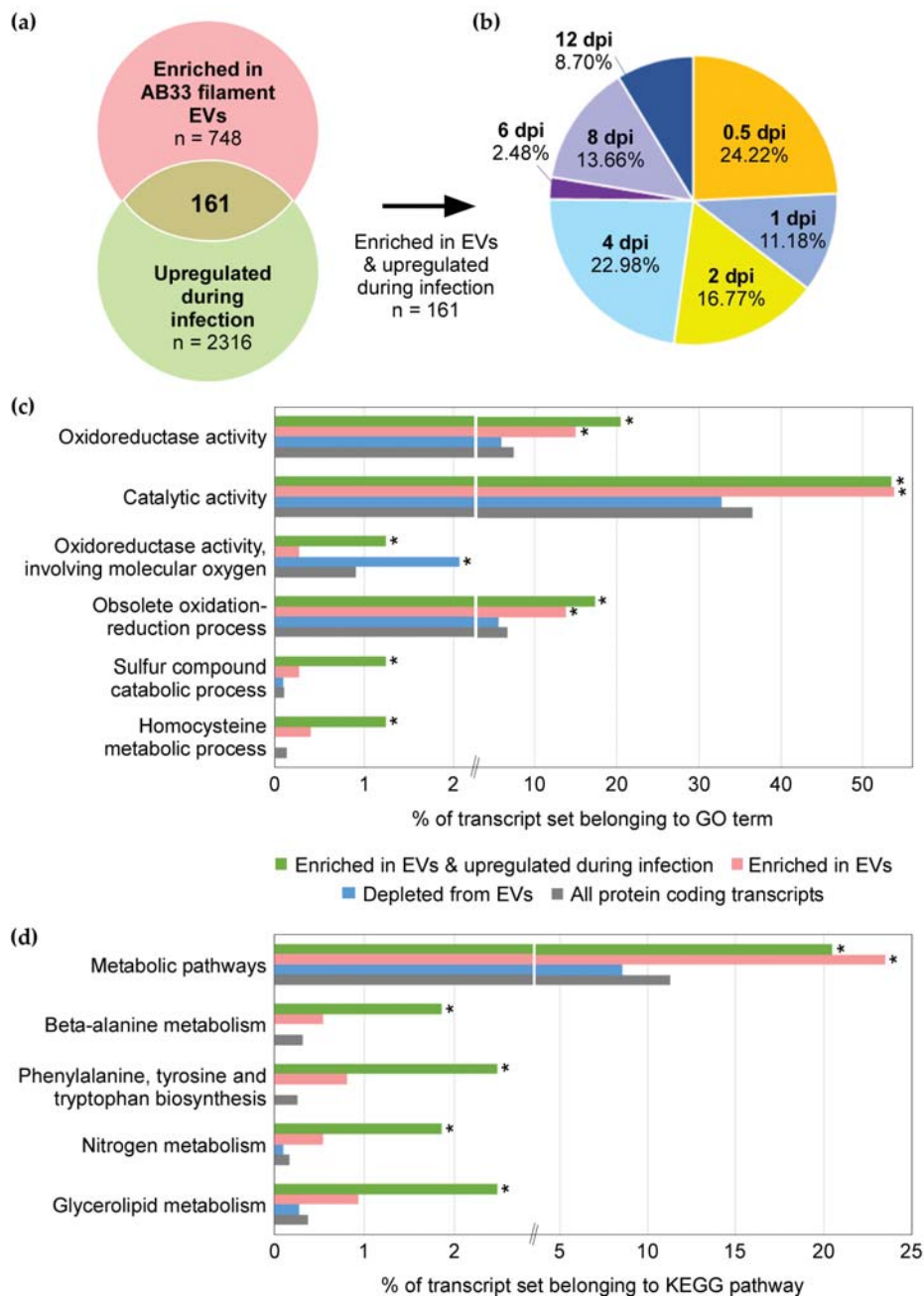
Figure 6. mRNAs enriched within EVs and upregulated during infection. (**a**) Overlap between transcripts enriched within EVs of induced filaments and those upregulated during plant infection. Pink circle represents mRNAs enriched in EVs relative to induced filaments are from this study (n = 748, Log2 fold change ≥ 1, padj < 0.01, baseMean ≥ 10). Green circle represents are mRNAs upregulated in infectious hyphae at 0.5–12 days post inoculation compared to axenic sporidia at 0 dpi (n = 2316, Log2 fold change ≥ 1, padj < 0.01; original data from Lanver et al. [56]). (**b**) Pie chart showing peak expression time-points of 161 mRNAs both upregulated during infection and enriched in EVs. (**c**) GO terms and (**d**) KEGG pathways overrepresented in sets of transcripts enriched in EVs and upregulated in plants (green; n = 161), all enriched in EVs (pink; n = 748, baseMean ≥ 10, Log2 fold change ≥ 1, padj < 0.01), all depleted from EVs (blue; n = 1113, baseMean ≥ 10, Log2 fold change ≤ −1, padj < 0.01), and all protein coding transcripts known in *U. maydis* (grey; n = 6765). Asterisk indicates significant overrepresentation compared to all protein coding transcripts (g:SCS padj < 0.05).

Table 1. mRNAs most highly enriched in EVs of induced filaments (Log2 fold change ≥ 3, padj < 0.01, baseMean ≥ 10). The 5th column from the left contains values obtained by analysing the raw data from Olgeiser et al. [80]. The 6th and 7th columns contain values from the supplementary dataset published by Lanver et al. [56].

GeneID	Uniprot Annotation	TPM in EVs	Enrichment in EVs vs. Filaments (Log2FC)	Induction in Filaments vs. Sporidia (Log2FC) [80]	Induction during Infection 0.5–12 dpi vs. 0 dpi Sporidia (Largest Log2FC) [56]	Infection Time Course Co-Expression Module [56]
UMAG_02215	flavin-binding monoxygenase	63	8.01	3.31	10.53 (2 dpi)	Magenta (biotrophy)
UMAG_02984	acyl-CoA dehydrogenase	335	7.08	5.70	12.46 (4 dpi)	Magenta (biotrophy)
UMAG_03995	TauD family 2-oxoglutarate-dependent taurine dioxygenase	575	5.78	3.44	8.11 (4 dpi)	Magenta (biotrophy)
UMAG_04370	TauD family 2-oxoglutarate-dependent taurine dioxygenase	256	5.25	3.55	11.21 (2 dpi)	Magenta (biotrophy)
UMAG_06042	2-oxoglutarate/Fe(II)-dependent dioxygenase	185	4.87	4.03	7.71 (4 dpi)	Magenta (biotrophy)
UMAG_00145	serine/threonine protein kinase	827	4.28	0.06	0.54 (12 dpi)	Cyan (tumour)
UMAG_01433	enoyl-CoA isomerase/hydratase fer4 in siderophore ferrichrome A biosynthesis	267	4.26	−0.09	−4.21 (8 dpi)	Burlywood
UMAG_02006	secreted peptidase	498	4.24	4.61	8.29 (1 dpi)	Red (Plant surface)
UMAG_11874	uncharacterised protein	57	4.14	5.30	7.66 (12 dpi)	Cyan (tumour)
UMAG_01432	acyltransferase fer5	524	3.85	−0.24	−4.39 (8 dpi)	Burlywood
UMAG_00133	1-alkyl-2-acetylglycero-phosphocholine esterase	20	3.66	−7.08	−2.58 (8 dpi)	Dark-green
UMAG_06404	peroxiredoxin	7147	3.61	0.35	1.50 (2 dpi)	Light-green (early biotrophy)
UMAG_02803	glycosyl hydrolases family 16 (GH16) domain-containing protein	68	3.59	−2.29	−6.04 (4 dpi)	Burlywood
UMAG_10260	peptide-methionine (S)-S-oxide reductase	352	3.26	−0.25	1.41 (2 dpi)	Cyan (tumour)
UMAG_03524	copper amine oxidase	29	3.22	2.76	5.29 (0.5 dpi)	Light-cyan
UMAG_05581	bifunctional cysteine synthase /	1183	3.20	1.28	2.58 (1 dpi)	Magenta (biotrophy)
UMAG_01232	O-acetylhomoserine aminocarboxypropyltransferase	1383	3.16	2.93	1.25 (0.5 dpi)	Light-cyan

4. Discussion

EVs are emerging as mediators of plant-pathogen communication, particularly as vehicles for transfer of RNA (reviewed in [81]). On the plant side, studies to date have mostly focused on the role of sRNAs [19,20] and proteins [22,23,82] in EVs, while only protein cargos have been examined in EVs of phytopathogenic fungi [9,24]. To extend the search for EV cargo molecules in plant-pathogen communication, we have characterised the repertoire of mRNAs associated with EVs of the fungus *U. maydis*.

For this purpose, we developed a robust EV isolation (or enrichment) protocol and examined EVs produced in axenic cultures of *U. maydis* filaments, used as a surrogate for infectious hyphae *in planta* (Figure 1). Omics studies on EVs of phytopathogenic fungi have so far examined EVs from axenic cultures [9,24]. While there are limitations to using axenic cultures of pathogenic fungi to identify EV cargos linked to virulence, isolation of fungal EVs from apoplastic washing fluid of maize plants is inherently destructive [83,84] and would first require development of markers for *U. maydis* EVs. Induced filaments of the lab strain AB33 in axenic culture mimic the morphology and, partially, the gene expression of infectious filaments [34–36] Therefore, we have used these cultures for an initial survey of EV-associated mRNAs in *U. maydis*.

We have reliably detected transcripts of *bona fide* effectors and several secreted proteins linked to virulence in AB33 filaments and their EVs (Table S4), which supports that our system has the potential to lead to discovery of novel EV-associated effectors. Thousands of mRNAs were detected in association with *U. maydis* EVs, the majority of which have full-length coverage (Figures 3d and 4) and are protected from external RNases (Figure 2). Protease activity in *U. maydis* cultures is high, requiring deletion of multiple proteases to obtain intact secreted proteins from *U. maydis* cultures [85]. Likewise, *U. maydis* secretes RNases in culture [76]. Therefore, it is unlikely that so many mRNAs can preserve integrity in the culture medium, unless they are protected inside EVs. Over 90% of the mRNAs enriched inside EVs are likely to be full-length (Figure 3d), suggesting that there is a biological reason for loading these mRNAs into EVs.

mRNA loading into EVs may be determined by the intracellular location of the mRNAs inside the fungal filament. The two most relevant EV subtypes are exosomes and microvesicles. Exosomes are originally intraluminal vesicles (ILVs) in multivesicular endosomes (MVEs) that are released upon fusion with the plasma membrane, while microvesicles are formed by direct budding from the plasma membrane [66]. Hence, localisation on the surface of maturing endosomes or at the cell periphery would increase the likelihood of being loaded into exosomes and microvesicles, respectively. This might explain why mRNAs encoding proteins linked to intracellular vesicles and vacuoles are enriched in EVs of *U. maydis* (Figure 5). Discovery of EV-associated RNA-binding proteins should help elucidate the mechanism of mRNA loading.

Since mRNAs enriched within EVs encode proteins with functions distinct from those that are depleted, we suspect a biological reason for preferentially exporting these mRNAs. Since several transcripts upregulated during infection are enriched in *U. maydis* EVs (Table 1; Figure 6a), such mRNAs could be studied further as effector candidates. There are two non-mutually exclusive hypotheses for the role of EV cargo mRNAs in *U. maydis*-maize interaction: (1) fungal mRNA fragments lead to silencing of maize genes or (2) full-length fungal mRNAs are translated into multiple effector proteins in maize cells.

Bidirectional, cross-kingdom RNA interference (RNAi) is a widespread mechanism of plant-pathogen interaction [86]. Diverse fungal and oomycete pathogens send sRNA effectors that hijack the plant RNAi machinery to silence host defence genes [20,25–29] As is the case for plant sRNAs that target pathogen genes [19], EVs are thought to be the vehicles of pathogen sRNA effector delivery to host plant cells. *U. maydis* has lost the conventional RNAi machinery [33]. Therefore, it might employ other RNA species, such as mRNA or tRNA fragments for the same purpose. For example, tRNA-fragments of the

bacterial symbiont *Bradyrhizobium japonicum* participate in silencing of plant genes involved in root hair development to promote nodulation [87].

Effector delivery in the form of mRNA could be highly cost-effective for the pathogen, if they can be translated in the correct location at required amplitude in the host cell. In support of this hypothesis, proof of principle studies using elegant reporter systems have demonstrated that EV-associated mRNAs are transferred and translated de novo in the recipient cells [88,89]. A recent in vivo study has shown that mRNAs in glioblastoma EVs are most likely translated in recipient astrocytes and lead to metabolic reprogramming [90]. Also, in the medically important *Paracoccidioides* spp., mRNA cargos of EVs were found to be translation-competent in a heterologous, in vitro system [91]. Given these examples and the evidence for full-length EV cargo mRNAs from this study (Figures 3d and 4b), translation of EV-associated fungal mRNAs into functional proteins in recipient cells seems possible.

It is interesting that the set of mRNAs enriched in EVs and upregulated during infection are overrepresented in metabolic enzymes and oxidoreductases (Figure 6). Biotrophic colonisation by *U. maydis* is accompanied by extensive reprogramming of metabolism, redox status, and hormone signalling in the infected plant tissues [79]. The fungus deploys effectors to divert metabolites away from biosynthesis of lignin [92] and salicylic acid (SA; [77]), and induces the jasmonate/ethylene signalling pathway to counter SA-mediated defence [93]. *U. maydis* also harbours metabolic enzymes lacking signal peptides that can synthesise [94,95], degrade [96], or potentially alter metabolic flux into biosynthesis of plant hormones [41]. Intriguingly, isochorismatases, which divert isochorismate away from SA biosynthesis in the host cell, are unconventionally secreted effectors of the filamentous phytopathogens, *Verticillium dahliae* and *Phytophthora sojae* [97]. Similarly, fungal metabolic and redox enzymes, that are upregulated during infection and loaded into EVs in the form of mRNA or protein, have the potential to "moonlight" as effectors if delivered to the host cell. Thus, the presence of intact, enriched mRNAs in EVs of *U. maydis* present an opportunity to discover novel RNA effectors in plant pathogenic fungi.

5. Conclusions

We have isolated EVs from the phytopathogenic fungus *U. maydis* and identified mRNAs that are enriched within EVs compared to the cells. Many of the highly enriched mRNAs are also upregulated during infection and are likely to be full-length. The inventory of these mRNAs now forms the foundation for future research addressing the mechanism of mRNA loading into EVs and their function in a recipient cell.

References

1. Tkach, M.; Thery, C. Communication by extracellular vesicles: Where we are and where we need to go. *Cell* **2016**, *164*, 1226–1232. [CrossRef]
2. Regev-Rudzki, N.; Wilson, D.W.; Carvalho, T.G.; Sisquella, X.; Coleman, B.M.; Rug, M.; Bursac, D.; Angrisano, F.; Gee, M.; Hill, A.F.; et al. Cell-cell communication between malaria-infected red blood cells via exosome-like vesicles. *Cell* **2013**, *153*, 1120–1133. [CrossRef] [PubMed]
3. Bielska, E.; Sisquella, M.A.; Aldeieg, M.; Birch, C.; O'Donoghue, E.J.; May, R.C. Pathogen-derived extracellular vesicles mediate virulence in the fatal human pathogen *Cryptococcus gattii*. *Nat. Commun.* **2018**, *9*, 1556. [CrossRef] [PubMed]
4. Kuipers, M.E.; Hokke, C.H.; Smits, H.H. Pathogen-derived extracellular vesicle-associated molecules that affect the host immune system: An overview. *Front. Microbiol.* **2018**, *9*, 2182. [CrossRef] [PubMed]
5. Bleackley, M.R.; Dawson, C.S.; Anderson, M.A. Fungal extracellular vesicles with a focus on proteomic analysis. *Proteomics* **2019**, *19*, 1800232. [CrossRef] [PubMed]
6. Peres da Silva, R.; Puccia, R.; Rodrigues, M.L.; Oliveira, D.L.; Joffe, L.S.; César, G.V.; Nimrichter, L.; Goldenberg, S.; Alves, L.R. Extracellular vesicle-mediated export of fungal RNA. *Sci. Rep.* **2015**, *5*, 7763. [CrossRef] [PubMed]
7. Vallejo, M.C.; Nakayasu, E.S.; Longo, L.V.G.; Ganiko, L.; Lopes, F.G.; Matsuo, A.L.; Almeida, I.C.; Puccia, R. Lipidomic analysis of extracellular vesicles from the pathogenic phase of *Paracoccidioides brasiliensis*. *PLoS ONE* **2012**, *7*, e39463. [CrossRef]
8. Rodrigues, M.L.; Nimrichter, L.; Oliveira, D.L.; Frases, S.; Miranda, K.; Zaragoza, O.; Alvarez, M.; Nakouzi, A.; Feldmesser, M.; Casadevall, A. Vesicular polysaccharide export in *Cryptococcus neoformans* is a eukaryotic solution to the problem of fungal trans-cell wall transport. *Eukaryot. Cell* **2007**, *6*, 48–59. [CrossRef]
9. Bleackley, M.; Samuel, M.; Garcia-Ceron, D.; Mckenna, J.A.; Lowe, R.G.T.; Pathan, M.; Zhao, K.N.; Ang, C.S.; Mathivanan, S.; Anderson, M.A. Extracellular vesicles from the cotton pathogen *Fusarium oxysporum* f. sp. vasinfectum induce a phytotoxic response in plants. *Front. Plant Sci.* **2020**, *10*, 1610. [CrossRef]
10. Zhao, K.N.; Bleackley, M.; Chisanga, D.; Gangoda, L.; Fonseka, P.; Liem, M.; Kalra, H.; Al Saffar, H.; Keerthikumar, S.; Ang, C.S.; et al. Extracellular vesicles secreted by *Saccharomyces cerevisiae* are involved in cell wall remodelling. *Commun. Biol.* **2019**, *2*, 305. [CrossRef]
11. Zarnowski, R.; Sanchez, H.; Covelli, A.S.; Dominguez, E.; Jaromin, A.; Bernhardt, J.; Mitchell, K.F.; Heiss, C.; Azadi, P.; Mitchell, A.; et al. *Candida albicans* biofilm-induced vesicles confer drug resistance through matrix biogenesis. *PLoS Biol.* **2018**, *16*, e2006872. [CrossRef]
12. Rodrigues, M.L.; Nakayasu, E.S.; Oliveira, D.L.; Nimrichter, L.; Nosanchuk, J.D.; Almeida, I.C.; Casadevall, A. Extracellular vesicles produced by *Cryptococcus neoformans* contain protein components associated with virulence. *Eukaryot. Cell* **2008**, *7*, 58–67. [CrossRef]
13. Hai, T.P.; Tuan, T.L.; Van Anh, D.; Mai, T.N.; Phu Huong, L.N.; Thwaites, G.; Johnson, E.; Van Vinh Chau, N.; Baker, S.; Ashton, P.; et al. The virulence of the *Cryptococcus neoformans* vnia-5 lineage is highly plastic and associated with isolate background. *bioRxiv* **2020**. [CrossRef]
14. Ikeda, M.A.K.; de Almeida, J.R.F.; Jannuzzi, G.P.; Cronemberger-Andrade, A.; Torrecilhas, A.C.T.; Moretti, N.S.; da Cunha, J.P.C.; de Almeida, S.R.; Ferreira, K.S. Extracellular vesicles from *Sporothrix brasiliensis* are an important virulence factor that induce an increase in fungal burden in experimental sporotrichosis. *Front. Microbiol.* **2018**, *9*, 2286. [CrossRef] [PubMed]

15. Freitas, M.S.; Bonato, V.L.D.; Pessoni, A.M.; Rodrigues, M.L.; Casadevall, A.; Almeidaa, F. Fungal extracellular vesicles as potential targets for immune interventions. *Msphere* **2019**, *4*, e00747-19. [CrossRef] [PubMed]

16. Snetselaar, K.M.; Mims, C.W. Light and electron-microscopy of *Ustilago maydis* hyphae in maize. *Mycol. Res.* **1994**, *98*, 347–355. [CrossRef]

17. An, Q.; Ehlers, K.; Kogel, K.H.; van Bel, A.J.; Hückelhoven, R. Multivesicular compartments proliferate in susceptible and resistant *MLA12*-barley leaves in response to infection by the biotrophic powdery mildew fungus. *New Phytol.* **2006**, *172*, 563–576. [CrossRef] [PubMed]

18. Roth, R.; Hillmer, S.; Funaya, C.; Chiapello, M.; Schumacher, K.; Lo Presti, L.; Kahmann, R.; Paszkowski, U. Arbuscular cell invasion coincides with extracellular vesicles and membrane tubules. *Nat. Plants* **2019**, *5*, 204–211. [CrossRef]

19. Cai, Q.; Qiao, L.; Wang, M.; He, B.; Lin, F.M.; Palmquist, J.; Huang, S.D.; Jin, H. Plants send small RNAs in extracellular vesicles to fungal pathogen to silence virulence genes. *Science* **2018**, *360*, 1126–1129. [CrossRef]

20. Hou, Y.; Zhai, Y.; Feng, L.; Karimi, H.Z.; Rutter, B.D.; Zeng, L.; Choi, D.S.; Zhang, B.; Gu, W.; Chen, X.; et al. A *Phytophthora* effector suppresses trans-kingdom rnai to promote disease susceptibility. *Cell Host Microbe* **2019**, *25*, 153–165.e155. [CrossRef]

21. Baldrich, P.; Rutter, B.D.; Karimi, H.Z.; Podicheti, R.; Meyers, B.C.; Innes, R.W. Plant extracellular vesicles contain diverse small RNA species and are enriched in 10-to 17-nucleotide "tiny" rnas. *Plant Cell* **2019**, *31*, 315–324. [CrossRef]

22. Rutter, B.D.; Innes, R.W. Extracellular vesicles isolated from the leaf apoplast carry stress-response proteins. *Plant Physiol.* **2017**, *173*, 728–741. [CrossRef]

23. Regente, M.; Pinedo, M.; San Clemente, H.; Balliau, T.; Jamet, E.; de la Canal, L. Plant extracellular vesicles are incorporated by a fungal pathogen and inhibit its growth. *J. Exp. Bot.* **2017**, *68*, 5485–5495. [CrossRef] [PubMed]

24. Hill, E.H.; Solomon, P.S. Extracellular vesicles from the apoplastic fungal wheat pathogen *Zymoseptoria tritici*. *Fungal Biol. Biotechnol.* **2020**, *7*, 13. [CrossRef] [PubMed]

25. Weiberg, A.; Wang, M.; Lin, F.M.; Zhao, H.W.; Zhang, Z.H.; Kaloshian, I.; Huang, H.D.; Jin, H.L. Fungal small RNAs suppress plant immunity by hijacking host RNA interference pathways. *Science* **2013**, *342*, 118–123. [CrossRef] [PubMed]

26. Wang, M.; Weiberg, A.; Lin, F.M.; Thomma, B.P.H.J.; Huang, H.D.; Jin, H.L. Bidirectional cross-kingdom RNAi and fungal uptake of external rnas confer plant protection. *Nat. Plants* **2016**, *2*, 16151. [CrossRef]

27. Wang, B.; Sun, Y.; Song, N.; Zhao, M.; Liu, R.; Feng, H.; Wang, X.; Kang, Z. *Puccinia striiformis* f. sp. *tritici* microRNA-like rna 1 (*Pst*-milR1), an important pathogenicity factor of *Pst*, impairs wheat resistance to *Pst* by suppressing the wheat pathogenesis-related 2 gene. *New Phytol.* **2017**, *215*, 338–350. [CrossRef]

28. Jian, J.; Liang, X. One small RNA of *Fusarium graminearum* targets and silences cebip gene in common wheat. *Microorganisms* **2019**, *7*, 425. [CrossRef] [PubMed]

29. Dunker, F.; Trutzenberg, A.; Rothenpieler, J.S.; Kuhn, S.; Prols, R.; Schreiber, T.; Tissier, A.; Kemen, A.; Kemen, E.; Huckelhoven, R.; et al. Oomycete small RNAs bind to the plant RNA-induced silencing complex for virulence. *eLife* **2020**, *9*, e56096. [CrossRef]

30. Brefort, T.; Doehlemann, G.; Mendoza-Mendoza, A.; Reissmann, S.; Djamei, A.; Kahmann, R. *Ustilago maydis* as a pathogen. *Annu. Rev. Phytopathol.* **2009**, *47*, 423–445. [CrossRef]

31. Fisher, M.C.; Henk, D.A.; Briggs, C.J.; Brownstein, J.S.; Madoff, L.C.; McCraw, S.L.; Gurr, S.J. Emerging fungal threats to animal, plant and ecosystem health. *Nature* **2012**, *484*, 186–194. [CrossRef]

32. Haag, C.; Steuten, B.; Feldbrügge, M. Membrane-coupled mRNA trafficking in fungi. *Annu. Rev. Microbiol.* **2015**, *69*, 265–281. [CrossRef]

33. Laurie, J.D.; Linning, R.; Bakkeren, G. Hallmarks of RNA silencing are found in the smut fungus *Ustilago hordei* but not in its close relative *Ustilago maydis*. *Curr. Genet.* **2008**, *53*, 49–58. [CrossRef] [PubMed]

34. Brachmann, A.; Weinzierl, G.; Kamper, J.; Kahmann, R. Identification of genes in the bW/bE regulatory cascade in *Ustilago maydis*. *Mol. Microbiol.* **2001**, *42*, 1047–1063. [CrossRef] [PubMed]

35. Wahl, R.; Zahiri, A.; Kamper, J. The Ustilago maydis b mating type locus controls hyphal proliferation and expression of secreted virulence factors in planta. *Mol. Microbiol.* **2010**, *75*, 208–220. [CrossRef] [PubMed]

36. Heimel, K.; Scherer, M.; Vranes, M.; Wahl, R.; Pothiratana, C.; Schuler, D.; Vincon, V.; Finkernagel, F.; Flor-Parra, I.; Kamper, J. The transcription factor Rbf1 is the master regulator for b-mating type controlled pathogenic development in *Ustilago maydis*. *PLoS Pathog.* **2010**, *6*, e1001035. [CrossRef] [PubMed]

37. Holliday, R. Ustilago maydis. In *Bacteria, Bacteriophages, and Fungi: Volume 1*; King, R.C., Ed.; Springer US: Boston, MA, USA, 1974; pp. 575–595.

38. Cicero, A.L.; Delevoye, C.; Gilles-Marsens, F.; Loew, D.; Dingli, F.; Guéré, C.; André, N.; Vié, K.; van Niel, G.; Raposo, G. Exosomes released by keratinocytes modulate melanocyte pigmentation. *Nat. Commun.* **2015**, *6*, 7506. [CrossRef] [PubMed]

39. Andrews, S. FastQC: A Quality Control Tool for High Throughput Sequence Data. Available online: http://www.bioinformatics. babraham.ac.uk/projects/fastqc/ (accessed on 10 November 2014).

40. Bolger, A.M.; Lohse, M.; Usadel, B. Trimmomatic: A flexible trimmer for Illumina sequence data. *Bioinformatics* **2014**, *30*, 2114–2120. [CrossRef]

41. Kämper, J.; Kahmann, R.; Bölker, M.; Ma, L.-J.; Brefort, T.; Saville, B.J.; Banuett, F.; Kronstad, J.W.; Gold, S.E.; Müller, O.; et al. Insights from the genome of the biotrophic fungal plant pathogen *Ustilago maydis*. *Nature* **2006**, *444*, 97–101. [CrossRef]

42. Howe, K.L.; Contreras-Moreira, B.; De Silva, N.; Maslen, G.; Akanni, W.; Allen, J.; Alvarez-Jarreta, J.; Barba, M.; Bolser, D.M.; Cambell, L.; et al. Ensembl genomes 2020-enabling non-vertebrate genomic research. *Nucleic Acids Res.* **2020**, *48*, D689–D695. [CrossRef]
43. Kim, D.; Paggi, J.M.; Park, C.; Bennett, C.; Salzberg, S.L. Graph-based genome alignment and genotyping with HISAT2 and HISAT-genotype. *Nat. Biotechnol.* **2019**, *37*, 907–915. [CrossRef]
44. Wang, L.; Wang, S.; Li, W. Rseqc: Quality control of RNA-seq experiments. *Bioinformatics* **2012**, *28*, 2184–2185. [CrossRef]
45. Bushnell, B.; Rood, J.; Singer, E. BBMerge—Accurate paired shotgun read merging via overlap. *PLoS ONE* **2017**, *12*, e0185056. [CrossRef]
46. Xiong, B.; Yang, Y.; Fineis, F.R.; Wang, J.-P. DegNorm: Normalization of generalized transcript degradation improves accuracy in RNA-seq analysis. *Genome Biol.* **2019**, *20*, 75. [CrossRef]
47. Love, M.I.; Huber, W.; Anders, S. Moderated estimation of fold change and dispersion for RNA-seq data with DESeq2. *Genome Biol.* **2014**, *15*, 550. [CrossRef] [PubMed]
48. Edgar, R.; Domrachev, M.; Lash, A.E. Gene expression omnibus: NCBI gene expression and hybridization array data repository. *Nucleic Acids Res.* **2002**, *30*, 207–210. [CrossRef] [PubMed]
49. Blighe, K.L.A. PCAtools: Everything Principal Component Analysis. R Package Version 2.2.0. Available online: https://bioconductor.org/packages/release/bioc/vignettes/PCAtools/inst/doc/PCAtools.html (accessed on 18 March 2021).
50. Blighe, K.R.S.; Lewis, M. EnhancedVolcano: Publication-Ready Volcano Plots with Enhanced Colouring and Labeling. R Package Version 1.8.0. Available online: https://github.com/kevinblighe/EnhancedVolcano (accessed on 18 March 2021).
51. Robinson, J.T.; Thorvaldsdóttir, H.; Winckler, W.; Guttman, M.; Lander, E.S.; Getz, G.; Mesirov, J.P. Integrative genomics viewer. *Nat. Biotechnol.* **2011**, *29*, 24–26. [CrossRef]
52. Kanehisa, M.; Goto, S. Kegg: Kyoto encyclopedia of genes and genomes. *Nucleic Acids Res.* **2000**, *28*, 27–30. [CrossRef] [PubMed]
53. Reimand, J.; Isserlin, R.; Voisin, V.; Kucera, M.; Tannus-Lopes, C.; Rostamianfar, A.; Wadi, L.; Meyer, M.; Wong, J.; Xu, C.; et al. Pathway enrichment analysis and visualization of omics data using g:Profiler, GSEA, Cytoscape and EnrichmentMap. *Nat. Protoc.* **2019**, *14*, 482–517. [CrossRef]
54. Raudvere, U.; Kolberg, L.; Kuzmin, I.; Arak, T.; Adler, P.; Peterson, H.; Vilo, J. G:Profiler: A web server for functional enrichment analysis and conversions of gene lists (2019 update). *Nucleic Acids Res.* **2019**, *47*, W191–W198. [CrossRef]
55. Shannon, P.; Markiel, A.; Ozier, O.; Baliga, N.S.; Wang, J.T.; Ramage, D.; Amin, N.; Schwikowski, B.; Ideker, T. Cytoscape: A software environment for integrated models of biomolecular interaction networks. *Genome Res.* **2003**, *13*, 2498–2504. [CrossRef]
56. Lanver, D.; Muller, A.N.; Happel, P.; Schweizer, G.; Haas, F.B.; Franitza, M.; Pellegrin, C.; Reissmann, S.; Altmuller, J.; Rensing, S.A.; et al. The biotrophic development of *Ustilago maydis* studied by RNA-seq analysis. *Plant Cell* **2018**, *30*, 300–323. [CrossRef]
57. Bushnell, B. BBMap Short Read Aligner, and Other Bioinformatic Tools. Available online: https://sourceforge.net/projects/bbmap/ (accessed on 5 November 2020).
58. Li, H.; Handsaker, B.; Wysoker, A.; Fennell, T.; Ruan, J.; Homer, N.; Marth, G.; Abecasis, G.; Durbin, R.; Genome Project Data Processing, S. The sequence alignment/map format and Samtools. *Bioinformatics* **2009**, *25*, 2078–2079. [CrossRef]
59. Quinlan, A.R.; Hall, I.M. BEDtools: A flexible suite of utilities for comparing genomic features. *Bioinformatics* **2010**, *26*, 841–842. [CrossRef]
60. Livak, K.J.; Schmittgen, T.D. Analysis of relative gene expression data using real-time quantitative PCR and the 2(-Delta Delta C(T)) method. *Methods* **2001**, *25*, 402–408. [CrossRef]
61. Osteikoetxea, X.; Sodar, B.; Nemeth, A.; Szabo-Taylor, K.; Paloczi, K.; Vukman, K.V.; Tamasi, V.; Balogh, A.; Kittel, A.; Pallinger, E.; et al. Differential detergent sensitivity of extracellular vesicle subpopulations. *Org. Biomol. Chem.* **2015**, *13*, 9775–9782. [CrossRef] [PubMed]
62. Mateescu, B.; Kowal, E.J.K.; van Balkom, B.W.M.; Bartel, S.; Bhattacharyya, S.N.; Buzas, E.I.; Buck, A.H.; de Candia, P.; Chow, F.W.N.; Das, S.; et al. Obstacles and opportunities in the functional analysis of extracellular vesicle RNA—An ISEV position paper. *J. Extracell. Vesicles* **2017**, *6*, 1286095. [CrossRef]
63. O'Brien, K.; Breyne, K.; Ughetto, S.; Laurent, L.C.; Breakefield, X.O. RNA delivery by extracellular vesicles in mammalian cells and its applications. *Nat. Rev. Mol. Cell Biol.* **2020**, *21*, 585–606. [CrossRef] [PubMed]
64. Wei, Z.; Batagov, A.O.; Schinelli, S.; Wang, J.; Wang, Y.; El Fatimy, R.; Rabinovsky, R.; Balaj, L.; Chen, C.C.; Hochberg, F.; et al. Coding and noncoding landscape of extracellular RNA released by human glioma stem cells. *Nat. Commun.* **2017**, *8*, 1145. [CrossRef] [PubMed]
65. Eichhorn, H.; Lessing, F.; Winterberg, B.; Schirawski, J.; Kämper, J.; Müller, P.; Kahmann, R. A ferroxidation/permeation iron uptake system is required for virulence in *Ustilago maydis*. *Plant Cell* **2006**, *18*, 3332–3345. [CrossRef]
66. van Niel, G.; D'Angelo, G.; Raposo, G. Shedding light on the cell biology of extracellular vesicles. *Nat. Rev. Mol. Cell Biol.* **2018**, *19*, 213–228. [CrossRef] [PubMed]
67. Baumann, S.; Konig, J.; Koepke, J.; Feldbrügge, M. Endosomal transport of septin mRNA and protein indicates local translation on endosomes and is required for correct septin filamentation. *EMBO Rep.* **2014**, *15*, 94–102. [CrossRef]
68. Zander, S.; Baumann, S.; Weidtkamp-Peters, S.; Feldbrügge, M. Endosomal assembly and transport of heteromeric septin complexes promote septin cytoskeleton formation. *J. Cell Sci.* **2016**, *129*, 2778–2792. [CrossRef] [PubMed]
69. Andreassi, C.; Riccio, A. To localize or not to localize: mRNA fate is in 3′UTR ends. *Trends Cell Biol.* **2009**, *19*, 465–474. [CrossRef]

70. Ludwig, N.; Reissmann, S.; Schipper, K.; Gonzalez, C.; Assmann, D.; Glatter, T.; Moretti, M.; Ma, L.S.; Rexer, K.H.; Snetselaar, K.; et al. A cell surface-exposed protein complex with an essential virulence function in *Ustilago maydis*. *Nat. Microbiol.* **2021**, *6*, 722–730. [CrossRef] [PubMed]

71. Stirnberg, A.; Djamei, A. Characterization of ApB73, a virulence factor important for colonization of *Zea mays* by the smut *Ustilago maydis*. *Mol. Plant Pathol.* **2016**, *17*, 1467–1479. [CrossRef]

72. Krombach, S.; Reissmann, S.; Kreibich, S.; Bochen, F.; Kahmann, R. Virulence function of the *Ustilago maydis* sterol carrier protein 2. *New Phytol.* **2018**, *220*, 553–566. [CrossRef]

73. Schilling, L.; Matei, A.; Redkar, A.; Walbot, V.; Doehlemann, G. Virulence of the maize smut *Ustilago maydis* is shaped by organ-specific effectors. *Mol. Plant Pathol.* **2014**, *15*, 780–789. [CrossRef] [PubMed]

74. Tanaka, S.; Gollin, I.; Rossel, N.; Kahmann, R. The functionally conserved effector Sta1 is a fungal cell wall protein required for virulence in *Ustilago maydis*. *New Phytol.* **2020**, *227*, 185–199. [CrossRef]

75. Schipper, K. *Charakterisierung Eines Ustilago Maydis Genclusters, das für Drei Neuartige Sekretierte Effektoren Kodiert*; Philipps-Universität Marburg: Marburg, Germany, 2009.

76. Mukherjee, D.; Gupta, S.; Ghosh, A.; Ghosh, A. *Ustilago maydis* secreted T2 ribonucleases, Nuc1 and Nuc2 scavenge extracellular RNA. *Cell Microbiol.* **2020**, *22*, e13256. [CrossRef]

77. Djamei, A.; Schipper, K.; Rabe, F.; Ghosh, A.; Vincon, V.; Kahnt, J.; Osorio, S.; Tohge, T.; Fernie, A.R.; Feussner, I.; et al. Metabolic priming by a secreted fungal effector. *Nature* **2011**, *478*, 395–398. [CrossRef] [PubMed]

78. Ökmen, B.; Kemmerich, B.; Hilbig, D.; Wemhoner, R.; Aschenbroich, J.; Perrar, A.; Huesgen, P.F.; Schipper, K.; Doehlemann, G. Dual function of a secreted fungalysin metalloprotease in *Ustilago maydis*. *New Phytol.* **2018**, *220*, 249–261. [CrossRef]

79. Doehlemann, G.; Wahl, R.; Horst, R.J.; Voll, L.M.; Usadel, B.; Poree, F.; Stitt, M.; Pons-Kuhnemann, J.; Sonnewald, U.; Kahmann, R.; et al. Reprogramming a maize plant: Transcriptional and metabolic changes induced by the fungal biotroph *Ustilago maydis*. *Plant J.* **2008**, *56*, 181–195. [CrossRef]

80. Olgeiser, L.; Haag, C.; Boerner, S.; Ule, J.; Busch, A.; Koepke, J.; König, J.; Feldbrügge, M.; Zarnack, K. The key protein of endosomal mRNP transport Rrm4 binds translational landmark sites of cargo mRNAs. *EMBO Rep.* **2019**, *20*, e46588. [CrossRef] [PubMed]

81. Kwon, S.; Tisserant, C.; Tulinski, M.; Weiberg, A.; Feldbrügge, M. Inside-out: From endosomes to extracellular vesicles in fungal RNA transport. *Fungal Biol. Rev.* **2020**, *34*, 89–99. [CrossRef]

82. De Palma, M.; Ambrosone, A.; Leone, A.; Del Gaudio, P.; Ruocco, M.; Turiák, L.; Bokka, R.; Fiume, I.; Tucci, M.; Pocsfalvi, G. Plant roots release small extracellular vesicles with antifungal activity. *Plants* **2020**, *9*, 1777. [CrossRef] [PubMed]

83. Witzel, K.; Shahzad, M.; Matros, A.; Mock, H.P.; Muhling, K.H. Comparative evaluation of extraction methods for apoplastic proteins from maize leaves. *Plant Methods* **2011**, *7*, 48. [CrossRef]

84. Gentzel, I.; Giese, L.; Zhao, W.Y.; Alonso, A.P.; Mackey, D. A simple method for measuring apoplast hydration and collecting apoplast contents. *Plant Physiol.* **2019**, *179*, 1265–1272. [CrossRef]

85. Terfrüchte, M.; Wewetzer, S.; Sarkari, P.; Stollewerk, D.; Franz-Wachtel, M.; Macek, B.; Schleputz, T.; Feldbrügge, M.; Buchs, J.; Schipper, K. Tackling destructive proteolysis of unconventionally secreted heterologous proteins in *Ustilago maydis*. *J. Biotechnol.* **2018**, *284*, 37–51. [CrossRef]

86. Huang, C.-Y.; Wang, H.; Hu, P.; Hamby, R.; Jin, H. Small RNAs—Big players in plant-microbe interactions. *Cell Host Microbe* **2019**, *26*, 173–182. [CrossRef]

87. Ren, B.; Wang, X.; Duan, J.; Ma, J. Rhizobial tRNA-derived small RNAs are signal molecules regulating plant nodulation. *Science* **2019**, *365*, 919–922. [CrossRef] [PubMed]

88. Ridder, K.; Sevko, A.; Heide, J.; Dams, M.; Rupp, A.K.; Macas, J.; Starmann, J.; Tjwa, M.; Plate, K.H.; Sultmann, H.; et al. Extracellular vesicle-mediated transfer of functional RNA in the tumor microenvironment. *Oncoimmunology* **2015**, *4*, e1008371. [CrossRef]

89. Lai, C.P.; Kim, E.Y.; Badr, C.E.; Weissleder, R.; Mempel, T.R.; Tannous, B.A.; Breakefield, X.O. Visualization and tracking of tumour extracellular vesicle delivery and RNA translation using multiplexed reporters. *Nat. Commun.* **2015**, *6*, 7029. [CrossRef]

90. Zeng, A.; Wei, Z.; Rabinovsky, R.; Jun, H.J.; El Fatimy, R.; Deforzh, E.; Arora, R.; Yao, Y.; Yao, S.; Yan, W.; et al. Glioblastoma-derived extracellular vesicles facilitate transformation of astrocytes via reprogramming oncogenic metabolism. *iScience* **2020**, *23*, 101420. [CrossRef] [PubMed]

91. Peres da Silva, R.; Longo, L.G.V.; Cunha, J.; Sobreira, T.J.P.; Rodrigues, M.L.; Faoro, H.; Goldenberg, S.; Alves, L.R.; Puccia, R. Comparison of the RNA content of extracellular vesicles derived from *Paracoccidioides brasiliensis* and *Paracoccidioides lutzii*. *Cells-Basel* **2019**, *8*, 765. [CrossRef]

92. Tanaka, S.; Brefort, T.; Neidig, N.; Djamei, A.; Kahnt, J.; Vermerris, W.; Koenig, S.; Feussner, K.; Feussner, I.; Kahmann, R. A secreted *Ustilago maydis* effector promotes virulence by targeting anthocyanin biosynthesis in maize. *eLife* **2014**, *3*, e01355. [CrossRef]

93. Darino, M.; Chia, K.-S.; Marques, J.; Aleksza, D.; Soto-Jiménez, L.M.; Saado, I.; Uhse, S.; Borg, M.; Betz, R.; Bindics, J.; et al. *Ustilago maydis* effector Jsi1 interacts with topless corepressor, hijacking plant jasmonate/ethylene signaling. *New Phytol.* **2021**, *229*, 3393–3407. [CrossRef]

94. Reineke, G.; Heinze, B.; Schirawski, J.; Buettner, H.; Kahmann, R.; Basse, C.W. Indole-3-acetic acid (IAA) biosynthesis in the smut fungus *Ustilago maydis* and its relevance for increased IAA levels in infected tissue and host tumour formation. *Mol. Plant Pathol.* **2008**, *9*, 339–355. [CrossRef] [PubMed]

95. Bruce, S.A.; Saville, B.J.; Neil Emery, R.J. *Ustilago maydis* produces cytokinins and abscisic acid for potential regulation of tumor formation in maize. *J. Plant Growth Regul.* **2011**, *30*, 51–63. [CrossRef]

96. Rabe, F.; Ajami-Rashidi, Z.; Doehlemann, G.; Kahmann, R.; Djamei, A. Degradation of the plant defence hormone salicylic acid by the biotrophic fungus *Ustilago maydis*. *Mol. Microbiol.* **2013**, *89*, 179–188. [CrossRef] [PubMed]

97. Liu, T.; Song, T.; Zhang, X.; Yuan, H.; Su, L.; Li, W.; Xu, J.; Liu, S.; Chen, L.; Chen, T.; et al. Unconventionally secreted effectors of two filamentous pathogens target plant salicylate biosynthesis. *Nat. Commun.* **2014**, *5*, 4686. [CrossRef] [PubMed]

4. Exploration of mRNA Effector Candidates and Development of Methods to Investigate *Ustilago maydis* EVs during Infection

4.1. Background to mRNA effector candidates

In the previous chapters, I have described the EV isolation method specifically developed for induced filamentous cultures of the *U. maydis* strain AB33 (Chapter 2) and characterised the repertoire of mRNAs associated with the EVs prepared using this method (Chapter 3; (Kwon et al., 2021)). AB33 filament cultures were used in order to bypass the technical complications in examining fungal EVs from infected tissues. Transcriptomic analysis of AB33 filaments in Chapter 3 have re-confirmed that AB33 filaments are indeed a partial transcriptional mimic of infectious hyphae *in planta*. So it was possible to identify from these cultures EV cargos that are relevant for infection, particularly mRNAs that could potentially act as effectors when delivered and translated in plant cells. The success of this strategy to discover EV-associated mRNA effectors depends on how representative the AB33 induced filaments are of infectious hyphae (discussed in Chapter 5.1.) and the correctness of the assumptions behind the selection criteria.

The list of 161 candidate mRNA effectors (Chapter 3, Table S5; (Kwon et al., 2021)) were selected based on the following <u>criteria</u>:

1. Relative enrichment in EVs compared to filaments (log2FC ≥ 1; padj < 0.01; baseMean ≥ 10)
2. Upregulation during plant infection compared to the starting inoculum ((log2FC ≥ 1; padj < 0.01; (Lanver et al., 2018))

The <u>assumptions</u> behind the selection criteria were:

1. Relative enrichment of a given mRNA in EVs indicates selective secretion for functionality.
2. Upregulation during infection indicates potential infection-related function.
3. If a given transcript is enriched in EVs produced by AB33 filaments in culture, it is also enriched in EVs of infectious hyphae *in planta*.
4. Therefore, if a transcript is enriched in culture EVs and upregulated during infection, they would be even more abundant in EVs of infectious hyphae.

Here, relative "enrichment" of an mRNA in EVs means that it is differentially detected in EVs compared to the mRNA population in filamentous cells, comparable to the concept of differential gene expression between different cellular samples and measured as log2 fold change.

In addition to enrichment, abundance and intactness of mRNAs in EVs are factors pertinent for my hypothesis that fungal EV-associated mRNAs are translated in maize. Incidentally, the set of mRNAs enriched in EVs (log2FC ≥ 1; padj < 0.01) are more abundant and more likely to be full-length in EVs compared to non-enriched sets (Table 4-1; (Kwon et al., 2021)). Hence it seems to have been a sound decision to select mRNA effector candidates among the mRNAs relatively enriched in AB33 filament EVs.

Table 4-1. Comparison of differentially detected versus non-differentially sorted transcripts in EVs

Group	Count	Median exon length (nt)	Median TPM*	% transcript IDs with full coverage
Total detected in EVs	6460	1512	44.75	56.36
≥ 2-fold Enriched (log2FC ≥ 1; padj < 0.01)	758	1002	211.27	92.88
≥ 2-fold Depleted (log2FC ≤ -1; padj < 0.01)	1189	2082	14.84	22.12
Not differentially loaded	4513	1523	47.58	45.89

*TPM = Transcripts per million; transcript abundance normalised for transcript length, sequencing depth, and scaled to per million for within sample comparison and between biological replicates.

4.2. mRNA effector candidates for testing transfer and translation in plant cells

Among the 161 infection-relevant EV-associated mRNAs above, the top candidates for testing the hypothesis of fungal mRNA transfer and translation in maize cells were selected with the following additional criteria (darker blue boxes, Figure 4-1):

1. Easily detectable in EVs of AB33 induced filaments (≥ 50 TPM)

2. Upregulated at 4 days post inoculation (dpi) *in planta* compared to the starting inoculum (log2FC ≥ 1; padj < 0.01; (Lanver et al., 2018))

3. Highly abundant at 4 dpi (≥ 1000 normalised baseMean counts; (Lanver et al., 2018))

4. The most enriched in AB33 induced filament EVs or the most abundant at 4 dpi *in planta*

4 dpi is the stage when the infectious hyphae are still proliferating biotrophically both within the paramural space and in the apoplast of maize plants. At this stage, the hyphae are not yet forming a protective matrix, which may be a physical barrier that limits EV-mediated communication with the plant.

mRNA effector candidate selection criteria

| Enriched in EV vs. Fil |
| log2FC ≥ 1, padj < 0.01, baseMean ≥ 10 (748) |

| Upregulated during any infection stage* |
| log2FC ≥ 1, padj < 0.01 (161) |

Infection-relevant mRNAs enriched in EVs from Table S5, Kwon et al. (2021), Chapter 3

| Easily detectable in EVs |
| ≥ 50 TPM in EVs (126) |

| Upregulated at 4 dpi* |
| log2FC ≥ 1, padj < 0.01 (108) |

| Highly abundant at 4 dpi* |
| baseMean ≥ 1000 (14) |

Candidate selection for testing fungal mRNA transfer via EVs and translation in plant cells

| Most enriched in AB33 induced filament EVs: UMAG_02984 | Most abundant at 4 dpi*: UMAG_11400 |

Figure 4-1. mRNA effector candidate selection strategy for hypothesis testing.
Candidates were further narrowed down from the 161 infection-relevant mRNAs enriched in EVs as defined in Table S5 of the published manuscript in Chapter 3 (Kwon et al., 2021). The list was narrowed down to 14 candidates based on their detectability in EVs and high upregulation at 4 dpi *in planta* (Lanver et al., 2018). Asterisk indicates selection based on data from Lanver et al. (2018). Of the 14 candidates, the most enriched mRNA in AB33 filament EVs and the most abundant mRNA at 4 dpi during infection were chosen for testing mRNA transfer via EVs and translation in plant cells.

Applying the selection criteria in Figure 4-1 narrowed down the list to 14 candidates (Table 4-2). Most of these are predicted to encode metabolic enzymes with oxidoreductase activities. As discussed in the manuscript in Chapter 3, *U. maydis* modulates metabolism of maize plants (Doehlemann et al., 2008), so it is fitting that many mRNA effector candidates encode metabolic enzymes. For hypothesis testing, I have selected the most enriched mRNA in EVs, UMAG_02984, and the most abundantly expressed mRNA at 4 dpi, UMAG_11400. UMAG_02984 is a putative "dibenzothiaprene desulfurizing enzyme" according to the MIPS *Ustilago maydis* database (Mewes et al., 2010), or an "acyl-coA dehydrogenase" according to Uniprot (The UniProt Consortium, 2020), while UMAG_11400 is a probable thiamine thiazole synthase (Table 4-2).

Table 4-2. 14 mRNA effector candidates enriched in EVs of AB33 induced filaments and highly upregulated at 4 dpi *in planta*

GeneID	Annotation (The Uniprot Consortium, 2020; Mewes et al., 2010)	EVs from AB33 induced filament culture		Infected maize leaves 4 dpi (Lanver et al., 2018)		Co-expression module*
		Log2FC EVs vs. Filaments	TPM in EVs	Log2FC 4 dpi vs. inoculum	4 dpi base mean	
UMAG_02984	acyl-CoA dehydrogenase; related to dibenzothiophene desulfurization enzyme C	**7.08**	334.61	12.46	2527.96	Biotrophy
UMAG_03995	TauD family 2-oxoglutarate-dependent taurine dioxygenase	5.78	575.13	8.11	2279.92	Biotrophy
UMAG_04370	TauD family 2-oxoglutarate-dependent taurine dioxygenase	5.25	256.17	10.70	2245.69	Biotrophy
UMAG_06042	2-oxoglutarate/Fe(II)-dependent dioxygenase; clavaminate synthase-like protein	4.87	184.82	7.71	1249.97	Biotrophy
UMAG_06404	Thioredoxin peroxidase	3.61	7146.74	1.17	1587.61	Early biotrophy
UMAG_05581	bifunctional cysteine synthase; O-acetylhomoserine (thiol)-lyase	3.20	1183.08	2.42	1095.38	Biotrophy
UMAG_01171	related to 4-coumarate-CoA ligase	1.74	95.17	3.40	3597.81	Tumour
UMAG_10596	aldehyde dehydrogenase	1.57	210.09	3.53	1172.65	Tumour
UMAG_00816	NMT1 Hydroxymethylpyrimidine phosphate synthase in thiamine biosynthesis	1.52	2252.86	6.03	3346.13	Biotrophy
UMAG_00304	TRP2 anthranilate synthase component I	1.35	211.55	2.61	1431.48	Tumour
UMAG_11078	RmlC-like cupin domain-containing protein	1.32	166.47	3.36	1275.83	Tumour
UMAG_11400	Thiamine thiazole synthase	1.17	7715.00	6.84	**6597.22**	Biotrophy
UMAG_11610	Aldolase II	1.08	228.33	2.49	2052.40	Biotrophy
UMAG_12178	related to 5-carboxyvanillate decarboxylase; Amidohydrohydrolase domain-containing protein	1.02	200.14	8.41	1730.38	Biotrophy

* Colouring is according to the names of the co-expression modules that represent the corresponding infection stages: magenta, light green, and cyan (Lanver et al., 2018).

To gather more information on the functionality of the two mRNA effector candidates selected for hypothesis testing, domain annotations (Blum et al., 2021), predicted subcellular localisation (Almagro Armenteros et al., 2017), and orthologs (Boratyn et al., 2012) were examined (Table 4-3). Orthologs were searched in *Zea mays*, *A. thaliana*, and *S. cerevisiae* (Boratyn et al., 2012). The reason for searching in the two plant species is to infer the function and subcellular localisation if the candidates really were to act as effectors in plant cells. The budding yeast was included for comparison within the fungal kingdom.

Based on homology, UMAG_02984 may encode a cytosolic isovaleryl-CoA dehydrogenase, whose orthologs in plants are targeted to the mitochondria and are involved in degradation of branched-chain amino acids (leucine, isoleucine, and valine) and phytol (Araújo et al., 2010). Phytol is a constituent of chlorophyll, which has been linked to ethylene signalling-dependent resistance against root knot nematodes (Fujimoto et al., 2021). If phytol is also important for defence against *U. maydis* in maize, and if the UMAG_02984 proteins can localise correctly in the plant cell to degrade phytol, they could dampen ethylene signalling.

Interestingly, the putative thiamine thiazole synthase UMAG_11400 was unanimously predicted to localise to chloroplasts like the plant orthologs using three different subcellular localisation prediction programs, while the yeast ortholog was not (Almagro Armenteros et al., 2017, Sperschneider et al., 2017, Almagro Armenteros et al., 2019). This could be reflecting the lifestyle of the plant pathogen *U. maydis*, hinting that if UMAG_11400 protein acts as an effector, it may do so in chloroplasts. Notably, among the 14 candidates in Table 4-2, UMAG_11400 and UMAG_00816 are both predicted to be involved in thiamine biosynthesis and very highly upregulated at 4 dpi (Lanver et al., 2018). Intriguingly, thiamine is required for proliferation and maintenance of meristematic stem cells in maize (Woodward et al., 2010) and human cancer cells (Liu et al., 2010). UMAG_11400 encodes a thiamine thiazole synthase and its ortholog in maize, *thi2*, is necessary for maintenance of the shoot apical meristem (Woodward et al., 2010). Based on this, I speculate that UMAG_11400 could locally increase thiamine levels in infected tissues to support host cell proliferation during tumorigenesis.

Table 4-3. Predicted domain architecture, subcellular localisation and orthologs of top mRNA effector candidates for hypothesis testing

GeneID	Putative function (The Uniprot Consortium, 2020)	InterPro domain (Blum et al., 2020)	Deeploc 1.0* (Almagro Armenteros et al., 2017)	Orthologs found by DELTA-BLAST (Boratyn et al., 2012)
UMAG_02984	Acyl-coA dehydrogenase	• IPR009100 Acyl-CoA dehydrogenase/oxidase, N-terminal and middle domain superfamily (52-255) • IPR013107 Acyl-CoA dehydrogenase, C-terminal domain (274-413)	Cytosol	• [Z. mays] isovaleryl-CoA dehydrogenase, mitochondrial; score = 326 • [A. thaliana] isovaleryl-CoA-dehydrogenase, mitochondrial; score = 299 • [S. cerevisiae] acyl-CoA oxidase, peroxisomal; score = 106
UMAG_11400	Thiamine thiazole synthase	• IPR002922 Thiazole biosynthetic enzyme Thi4 family (2-335)	Chloroplast	• [A. thaliana] thiazole biosynthetic enzyme, chloroplastic; score = 260 • [S. cerevisiae] thiamine thiazole synthase, cytosolic; score = 249 • [Z. mays] thiamine thiazole synthase 2, chloroplastic; score = 246

*Deeploc 1.0 was run with plant setting to predict subcellular localization *in planta*

4.3. Testing mRNA transfer into plant cells

The simplest way of testing EV-associated mRNA delivery and translation in recipient cells is using mRNAs encoding fluorescent or luminescent reporters (Lai et al., 2015). Following this strategy, constructs were created for each of the top two mRNA effector candidates with the following features:

1. Translational fusion with mVenus for detection of the protein via microscopy
2. Nuclear localisation signal (NLS) to sequester the protein in the nucleus, thus reducing protein loading into EVs
3. To be inserted into the native locus of the mRNA effector candidates to maintain the same promoter, 5', and 3' untranslated regions (UTRs) for original expression profile and localisation

Thus, using these constructs, it was anticipated that the mRNA would be produced and loaded into EVs normally, while the protein is not loaded into EVs to a level detectable by microscopy. So any mVenus signal that is detected in the maize cells would be most likely from *de novo* translated mRNA effectors delivered via EVs (Figure 4-2).
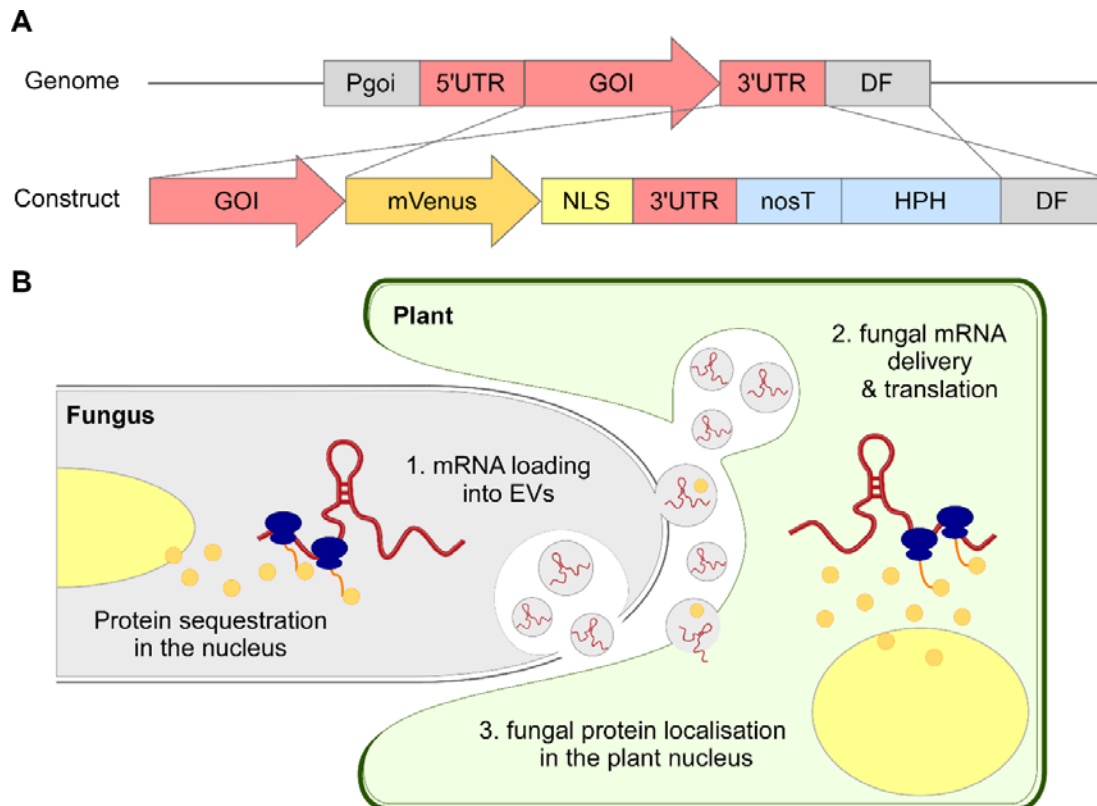
Figure 4-2. Strategy to test the fungal EV-associated mRNA delivery and translation in plant cells.

A. Design of *U. maydis* strains to test the hypothesis of EV-mediated mRNA transfer and translation in plant cells. In the transformation construct, candidate mRNA effector gene of interest (GOI) is translationally fused to the fluorescent marker mVenus for visualisation, and a nuclear localisation signal from (NLS) for nuclear targeting of the translated protein (Collas and Aleström, 1996). This is followed by the nopaline synthase terminator (nosT) (Bevan et al., 1983), and the hygromycin B phosphotransferase cassette (HPH) as an antibiotic resistance marker for selection of transformants (Blochlinger and Diggelmann, 1984). The construct was designed for integration into the native locus of the candidate mRNA effector by homologous recombination at the GOI sequence and the downstream flank (DF). Thus, the fusion mRNAs produced from transformants are expressed under the native promoter of GOI (Pgoi), with native 5' and 3'UTR sequences. **B.** Strategy to detect mRNA transfer and translation.
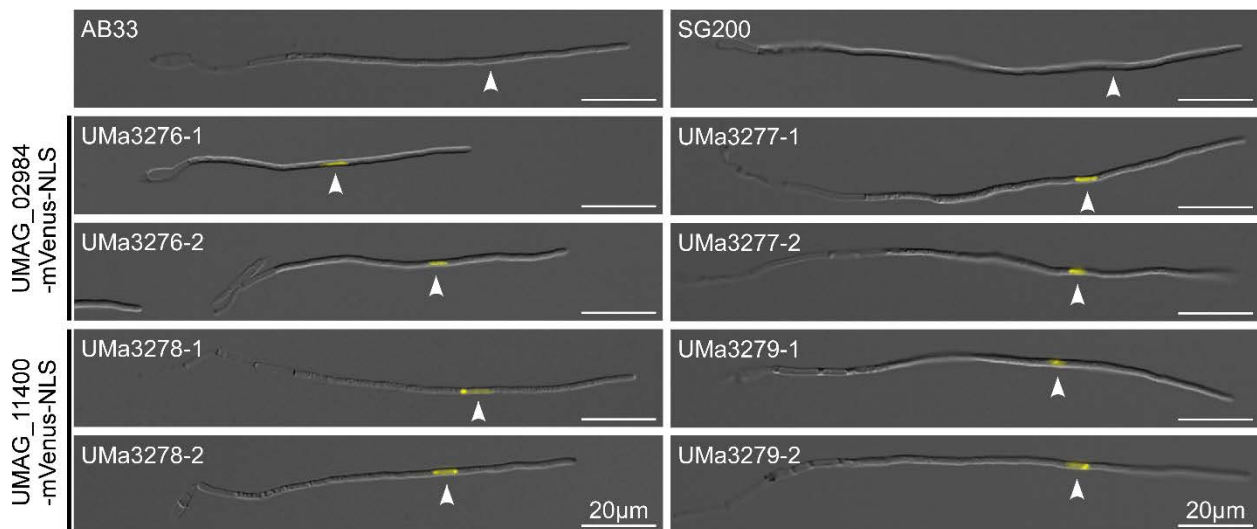
Figure 4-3. Nuclear localisation of proteins encoded by mRNA effector candidates fused to mVenus-NLS. Strains were made in AB33 and SG200 background (top row). Strains UMa3276 and UMa3277 express UMAG_02984-mVenus-NLS. UMa3278 and UMa3279 express UMAG_11400-mVenus-NLS. Two independent transformants are shown per strain. mVenus signals are pseudocoloured yellow. Nuclei are indicated with arrowheads. Scale bars = 20 μm.

For each of the two mRNA effector candidates, the test constructs were used to transform two different progenitor strains, AB33 and SG200 (Figure 4-3; list of strains in Table 4-4, Appendix to Chapter 4). This is because AB33 filament cultures are suitable for isolation of large amounts of EVs but AB33 cannot infect the plant due to repression of the promoter controlling bE/bW expression by ammonium ions *in planta* (Brachmann et al., 2001). On the other hand, SG200 also harbours bE/bW heterodimer and can infect plants as a haploid without mating (solopathogenic) but is not suitable for culture EV isolation (Bölker et al., 1995, Kämper et al., 2006). The mVenus-NLS-tagged strains showed correct localisation of the protein in the nucleus during filamentous growth as expected (Figure 4-3).

Next, enrichment of the tagged mRNAs in EVs versus filaments were checked by RT-qPCR (Figure 4-4). For this purpose, the AB33-background strains (UMa3276 and UMa3278) were used. Relative fold enrichment ($2^{\wedge-ddCT}$) of the tagged mRNA effector candidates, UMAG_02984 and UMAG_11400, were calculated using two different reference genes. UMAG_02361 had previously been used as a reference gene between EVs and filaments in the manuscript in Chapter 3 (Kwon et al., 2021) and UMAG_01054 was additionally chosen based on the low Log2FC value in the RNA-seq data (Table S1 in Kwon et al., 2021) and stable expression across infection stages (Lanver et al., 2018). Depending on the reference gene, UMAG_02984 should be 70- to 120-fold, and UMAG_11400 1.4 to 3-fold enriched in EVs according to previous experiments comparing AB33 EVs and filaments. Unfortunately, in the single experiment presented in Figure 4-4, the fold change for UMAG_02984 was not as high as in the previous experiments, even for the untagged mRNAs (Figure 4-4A). Nonetheless, the tagged UMAG_02984 mRNA was still enriched in EVs, even more4 so than the untagged versions in AB33 and UMa3278. However, the tagged UMAG_11400 mRNA was not as enriched as expected (Figure 4-4B). Since the tagged UMAG_02984 mRNA was still enriched and UMAG_11400 mRNA is highly abundant anyway, the strains were still used to test for mRNA transfer.
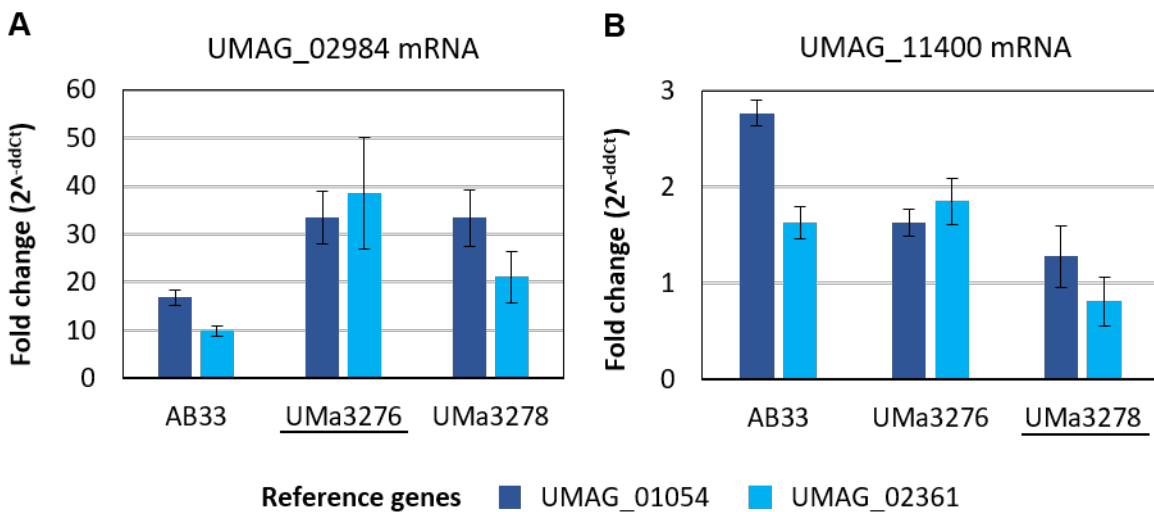
Figure 4-4. Effect of tagging mRNA effector candidates with mVenus-NLS on their enrichment in EVs versus filaments. A. Fold enrichment of UMAG_02984 mRNA. **B.** Fold enrichment of UMAG_11400 mRNA. Fold changes were calculated by the $2^{\wedge-ddCt}$ method using two reference genes, UMAG_01054 (dark blue) and UMAG_02361 (light blue). The strain where the native gene is replaced by the mVenus-NLS tagged version is underlined. These are the results from only one experiment.

As a final check before using the mVenus-NLS-tagged strains to test mRNA transfer into maize cells, EVs were isolated from the AB33-background strains (UMa3276 and UMa3278) and checked for mVenus signal by microscopy. It was expected that NLS tagging would be sufficient to minimise tagged protein loading into EVs. While UMAG_02984-mVenus-NLS produced fluorescence only marginally above the AB33 background, signals from UMAG_11400-mVenus-NLS proteins were easily detectable, indicating abundant protein loading into EVs (Figure 4-5). This meant that for UMAG_11400, if there is any mVenus signal detected in the recipient cell, the contribution of proteins *de novo* synthesised from delivered mRNAs cannot be easily distinguished from the signals produced by those delivered already in the protein form. Since it would be useful to know if at least the EV cargo proteins can be delivered to plant cells, the UMAG_11400-mVenus-NLS strains were still included in further experiments.
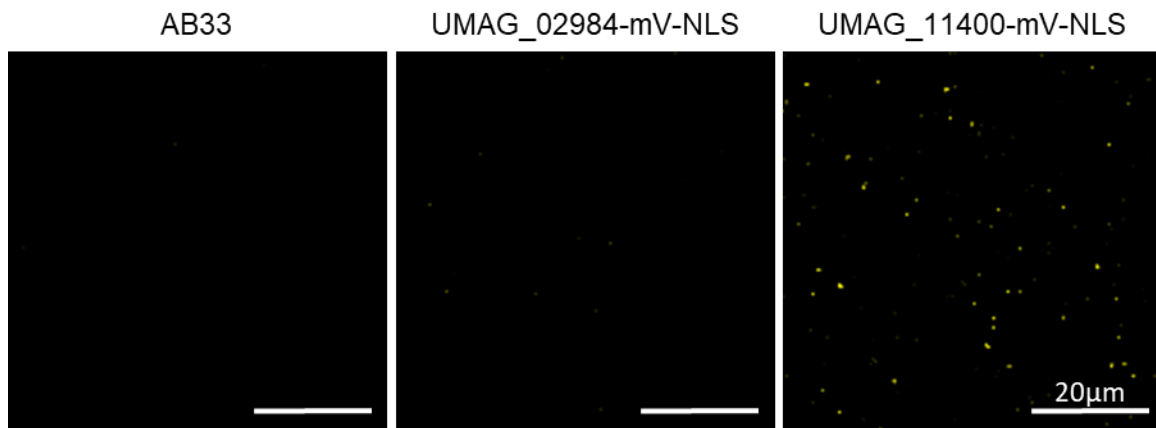
Figure 4-5. Detectability of the mVenus-NLS-tagged proteins in EVs. EVs isolated from induced filaments of AB33 (negative control) and AB33-background strains expressing UMAG_02984-mV-NLS (UMa3276) and UMAG_11400-mV-NLS (UMa3278). mVenus signals are pseudocoloured yellow. Scale bars = 20 μm.

The SG200 background strains (UMa3277 and UMa3279) were used to infect maize and infected samples were examined by microscopy at 4 dpi (Figure 4-6). Cells where the colonising fungal hyphae were in the vicinity of the plant nuclei were examined closer. While the mVenus signal was strongly detected in the hyphal nuclei of the tagged strains, indicating robust expression *in planta* as anticipated, no signal above background could be discerned in the plant nuclei. This is despite having tried to increase sensitivity and visibility by sectioning and focusing on locations where hyphae are traversing through plant cells with Hoechst-stained nuclei.
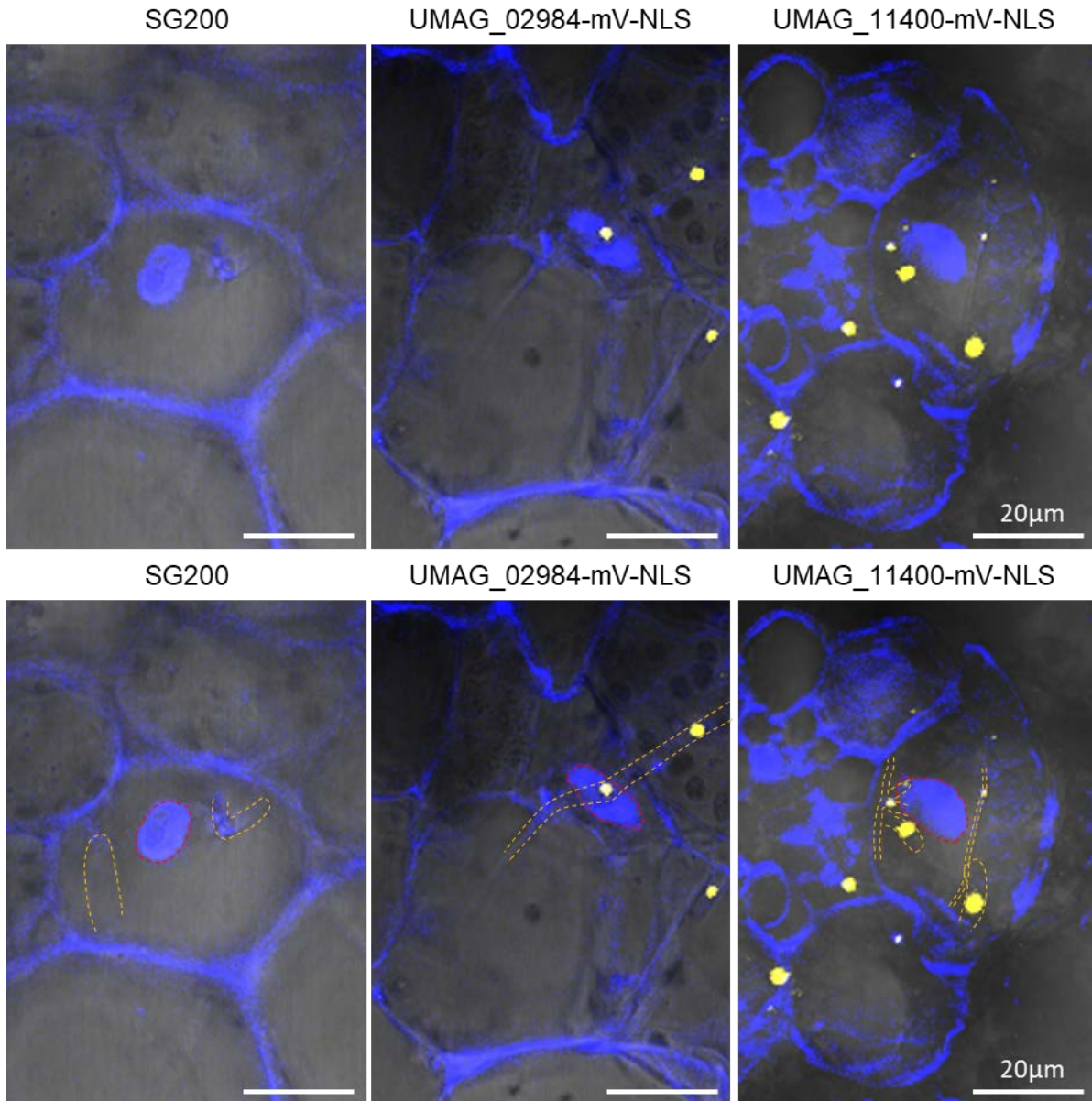
Figure 4-6. Localisation of mVenus-NLS-tagged proteins during plant infection. Maximum intensity projection images of maize cells colonised with SG200-background strains expressing UMAG_02984-mV-NLS (UMa3277) and UMAG_11400-mV-NLS (UMa3279) were sampled at 4 dpi and stained with Hoechst 33342. Plant nuclei and cell walls are stained with Hoechst 33342 (blue). mVenus signal (yellow) can be seen in the nuclei of *U. maydis* hyphae. Original images are shown at the top and images with marked outlines of plant nuclei (red dotted lines) and hyphae (yellow dotted lines) are shown below them. Scale bars = 20 μm.
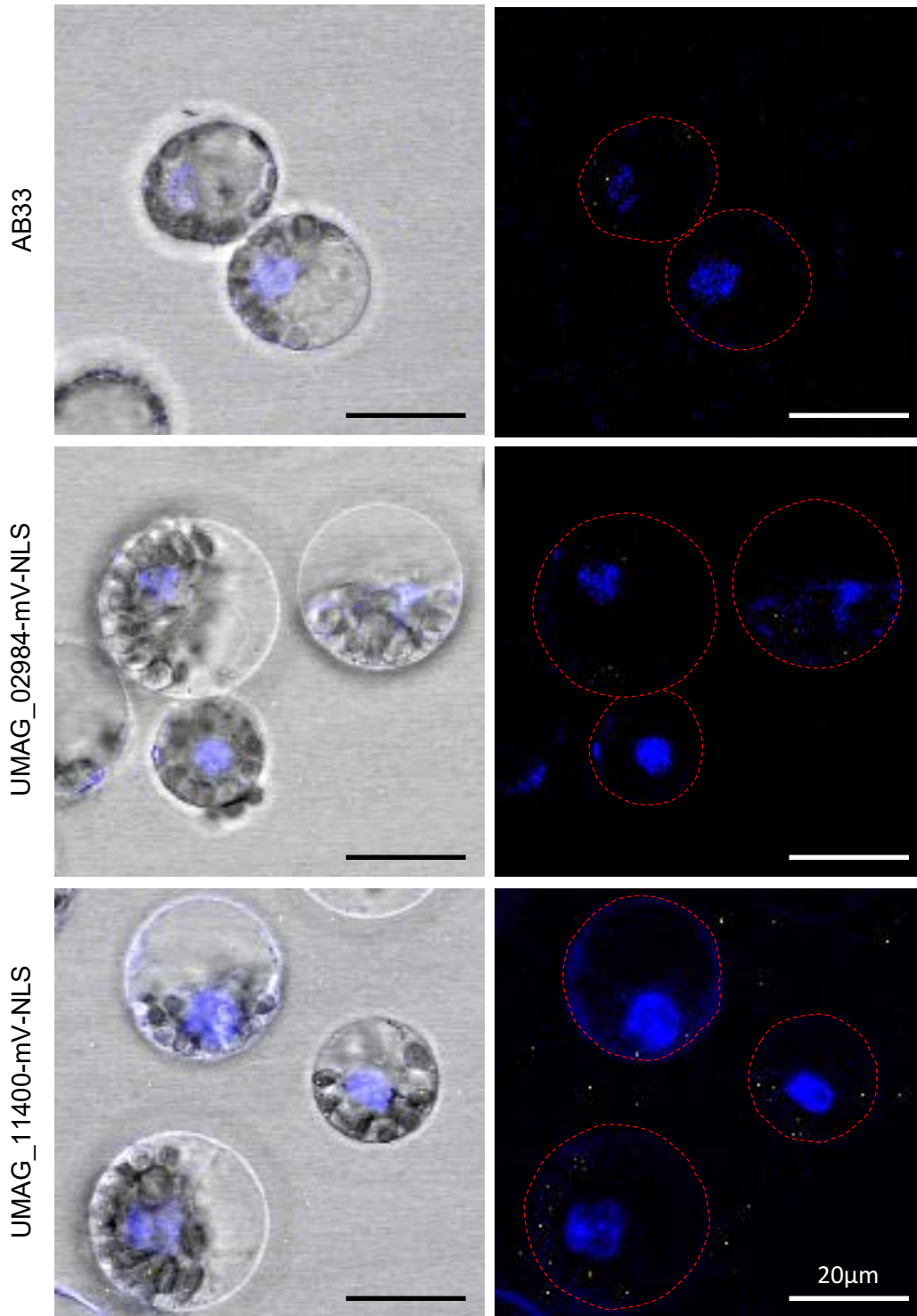
Figure 4-7. Maize protoplasts incubated with *U. maydis* induced filament EVs.
Maize protoplasts incubated with EVs from AB33-background strains expressing UMAG_02984-mV-NLS (UMa3276) and UMAG_11400-mV-NLS (UMa3278) for approximately 6 hours. Nuclei are stained with Hoechst 33342 and pseudocoloured blue. mVenus signals are pseudocoloured yellow. Scale bars = 20 μm.

Since no mVenus signal that is clearly distinguishable from the autofluorescence could be detected in the plant nuclei, the experimental setup was simplified further to increase the chances of fungal EV cargo uptake. EVs isolated from induced filamentous cultures of AB33-background strains (UMa3276 and UMa3278) were added to maize leaf protoplasts and examined after 6 hours (Figure 4-7). Even with protoplasts, uptake of *U. maydis* EVs and their cargos was unclear. There seemed to be more yellow speckles associated with protoplasts incubated with EVs carrying UMAG_11400-mVenus-NLS. However, it could not be properly determined whether the signal was from EVs on the surface of the protoplasts or from the inside because the fragile protoplasts burst while obtaining Z-stacks. In any case, there was no clear mVenus signal observed in the nuclei of maize protoplasts. Furthermore, there was a high level of autofluorescence from the stressed protoplasts, which overlaps with the mVenus emission spectrum. Although it was possible to set a threshold based on protoplasts treated with AB33 EVs, this rendered it difficult to distinguish the already weak mVenus signal, if any. The results of these experiments to test fungal mRNA transfer via EVs and translation in plant cells are thus inconclusive due to technical limitations.

4.4.   EV isolation from apoplastic washing fluid of infected maize

While generating a list of mRNA effector candidates from EVs of AB33 filament cultures is informative, combining this list with a catalogue of *U. maydis* EV-associated RNA from infected plants would allow selection of more promising candidates. This is particularly important as it is laborious and technically challenging to test transfer and translation of individual candidates. The most commonly used approach for isolating EVs from plant materials is apoplastic washing fluid (AWF) extraction (Rutter et al., 2017). I have adopted parts of existing protocols for maize AWF extraction (Dr. Kerstin Schipper, personal communication; (Witzel et al., 2011)) and plant EV isolation (Rutter et al., 2017) to develop a protocol for apoplastic EV isolation from infected maize leaves (Figure 4-8).

| Collect infected parts | Vacuum infiltrate with Buffer | 700 xg 20 mins | Filter 0.45µm | 100,000 xg 60 mins |
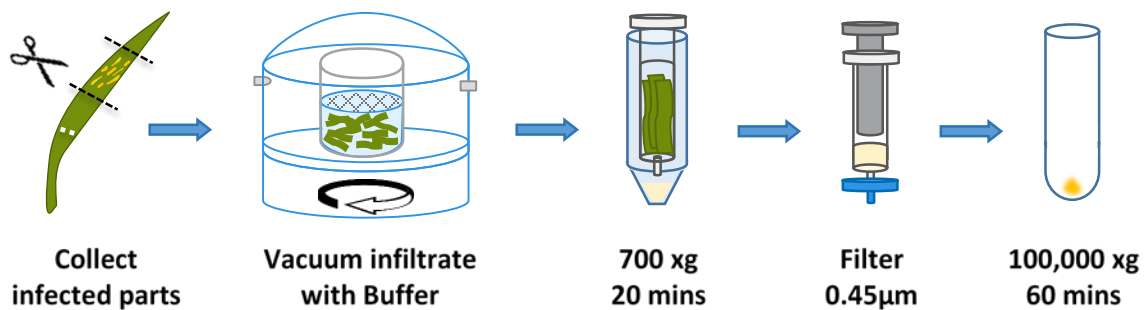
Figure 4-8. Schematic of EV isolation procedure from apoplastic washing fluid of infected plants.
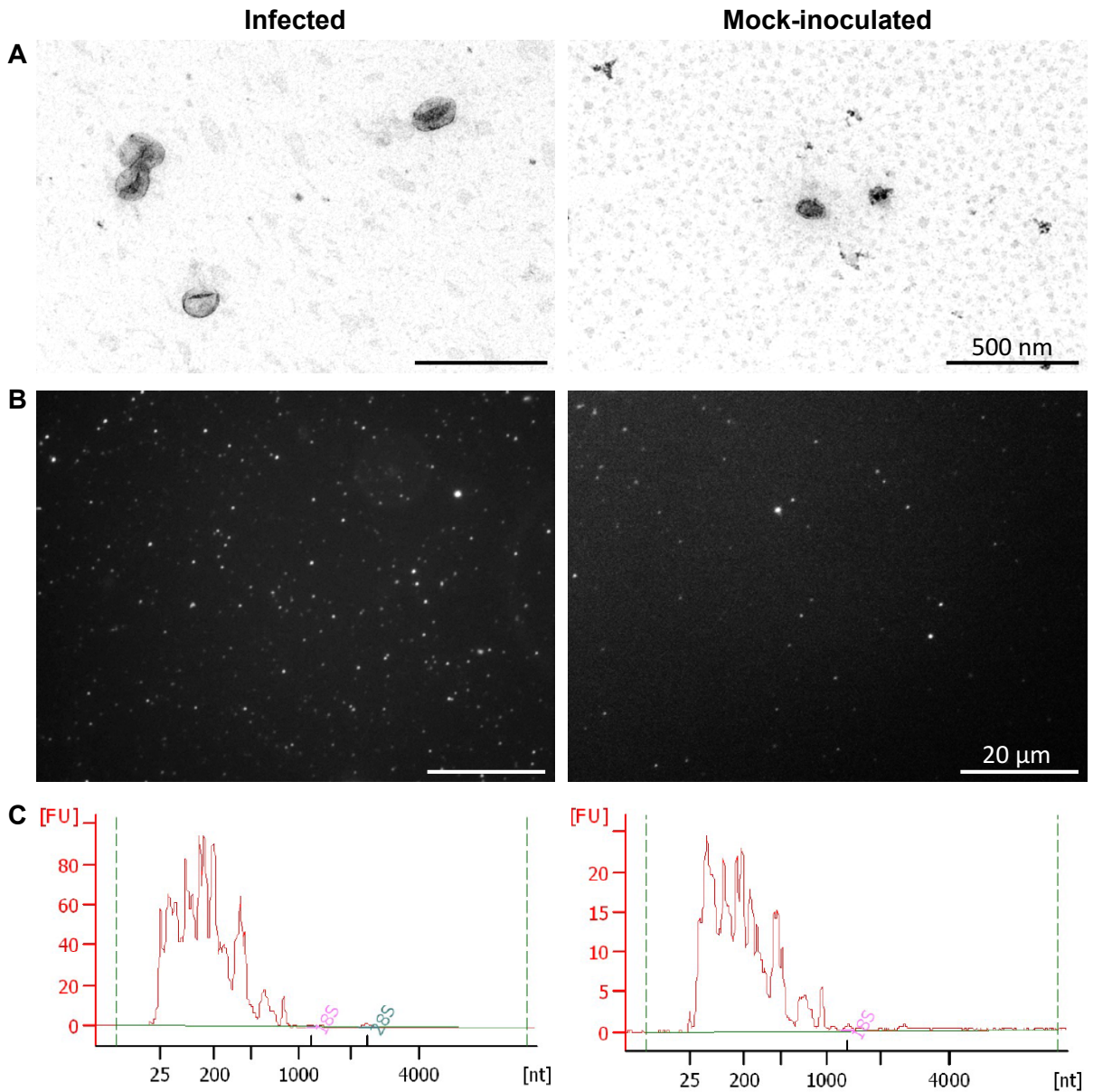
Figure 4-9. Comparison of EVs isolated from infected versus mock-inoculated maize plants.
A. Transmission electron micrographs of EV-like particles prepared from apoplastic washing fluid (AWF). Scale bars = 500 μm. **B.** Lipophilic dye FM4-64 stained particles isolated from AWF. Scale bars = 20 μm. **C.** Bioanalyser profile of RNA extracted from the same AWF EV preparation as in B. Images and graph on the right are from infected maize plants and those to the left are from mock-inoculated plants, all from 6 dpi.

The EVs isolated using this method up to the concentration step was examined by transmission electron microscopy and stained with the lipophilic dye FM4-64 (Figure 4-9). Under TEM, typical cup-shaped EV-like structures could be found easily in the infected sample but difficult to find in mock-inoculated samples (Figure 4-9A). There were more lipophilic dye-stained particles isolated from infected plants compared to mock-inoculated plants, although the particles could not be quantified (Figure 4-9B). Accordingly, a greater amount of RNA could be isolated from the EV preparations from infected plants compared to mock-inoculated (Figure 4-9). Although it was possible to normalise the mass of starting maize leaf material prior to infiltration but the volume of AWF obtained from infected samples were always greater than mock-infected, possibly due to proliferation of infectious hyphae in the apoplastic space at 6 dpi. Number of particles in the size range of EVs per ml of AWF obtained can be quantified by nanoparticle tracking analysis or dynamic light scattering in the future. It is still unknown if EVs from *U. maydis* are also present among the AWF EVs from infected maize leaves. A marker for *U. maydis* EVs would be useful to confirm the presence of and to isolate fungal EVs from AWF.

4.5.   Syntaxin Sso1 as a potential EV marker

EV membrane-resident marker proteins with fluorescent and affinity tags are required for visualisation and purification of *U. maydis* EVs from infected plant materials. Tetraspanins are the most commonly used exosome markers conserved in animals (Witwer et al., 2013), plants (Cai et al., 2018), and fungi (Lambou et al., 2008). Unfortunately, tetraspanins are absent in *U. maydis* (Kämper et al., 2006). Therefore, I searched for orthologs of known EV markers in *U. maydis* and selected the syntaxin (t-SNARE; target-Soluble NSF Attachment Protein Receptor) protein Sso1, which has also been used previously as a plasma membrane marker in *U. maydis* (Treitschke et al., 2010). In *Arabidopsis thaliana*, syntaxin PEN1 is linked to plant vesicle-related defence against invading fungal pathogens (Collins et al., 2003) and has been used as an EV marker (Rutter et al., 2017).

The N-terminal portion of a syntaxin is on the cytosolic side, anchored to the plasma membrane via a single transmembrane domain (Liang et al., 2013), followed by extracellular hydrophilic residues in the C-terminus (Yuan and Jäntti, 2010). Sso1 in *U. maydis* is predicted to have a slightly longer extracellular C-terminal tail than syntaxins from other organisms (Appendix to Chapter 4, Figure 4-12; (Sievers et al., 2011, Tsirigos et al., 2015)). For imaging and purification of EVs, EV marker constructs were designed so that Sso1 is fused on the cytosolic N-terminus to triple fluorescent proteins and the extracellular C-terminus to an affinity tag (Figure 4-10). Strains were generated where these marker constructs are integrated in

multiple copies in the *ip* locus and expressed constitutively in both AB33 and SG200 backgrounds (list of strains in Appendix to Chapter 4, Table 4-4).

Microscopic examination of an AB33 background strain constitutively expressing the tagged Sso1 revealed plasma membrane localisation as expected in both sporidia and induced filaments (Figure 4-10A & B). It was promising that the GFP signal was clearly detectable in EVs isolated from induced filament cultures of this strain without staining with a fluorescent lipophilic dye (Figure 4-10C). Attempts were made to confirm the presence of full-length EV marker fusion proteins in EVs by Western blot. Unfortunately, buffer conditions must still be optimised for complete solubilisation of membrane proteins. The presence of the fluorescent protein signal at the plasma membrane and the EVs suggests that at least the N-terminus of the EV marker is intact. If the external tag is also intact, it should be possible to purify fungal EVs from apoplastic washing fluid of infected maize (Schematic shown in Figure 4-10F), or perform immunogold to follow the fate of fungal EVs in planta.
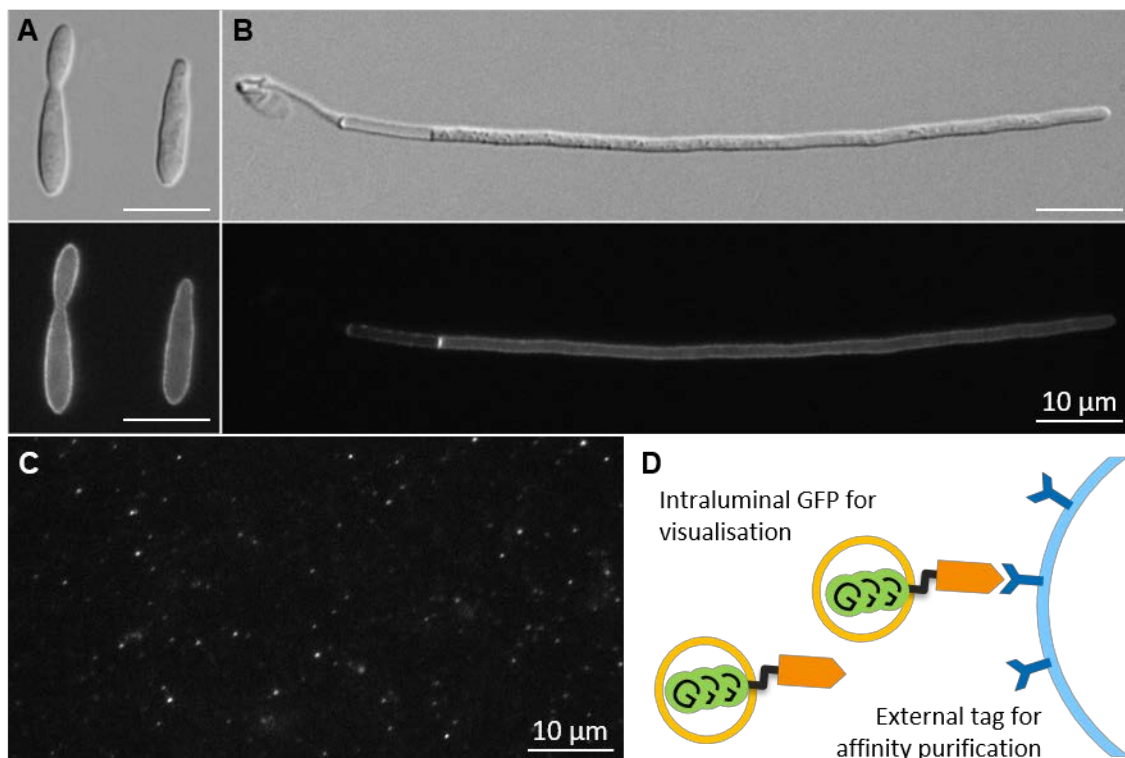
Figure 4-10. Membrane localisation of the tagged Sso1 and their detection in EVs.
A. & **B.** Plasma membrane localisation of the eGFP-tagged Sso1 signal in sporidia and induced filaments of an AB33 background strain expressing 3xeGFP-Sso1-3xHA (UMa2864-1). **C.** eGFP signal in EVs isolated from induced filaments of the same strain expressing the tagged Sso1 marker. Scale bars = 10μm. **D.** Schematic showing the design of the Sso1 fusion proteins as EV markers, with the fluorescent protein for visualisation on the intraluminal side, and an external affinity tag for purification or immunogold labelling.
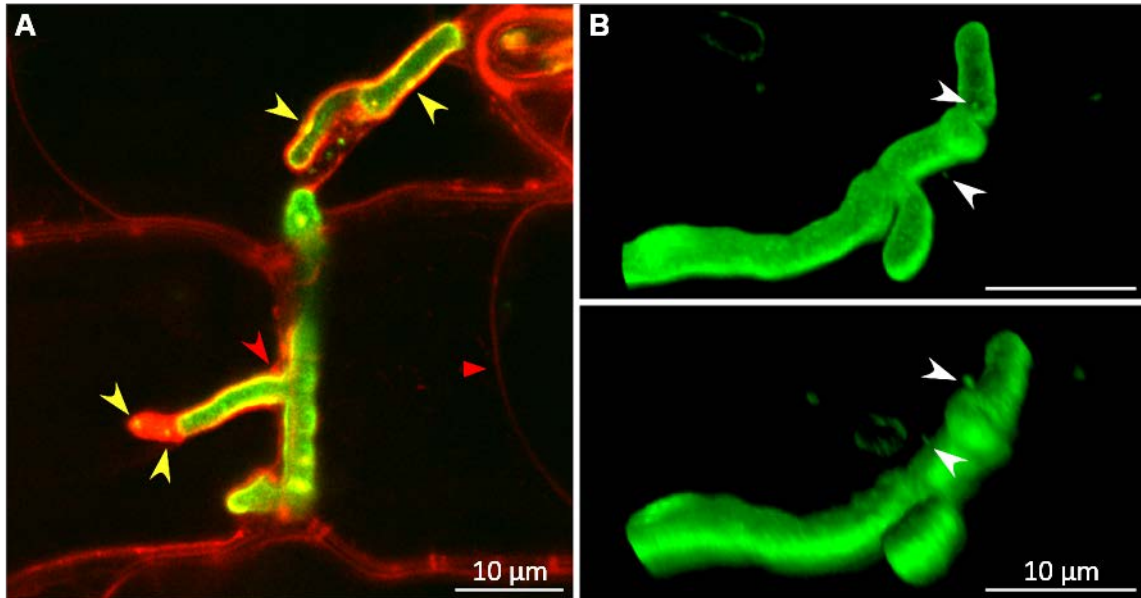
Figure 4-11. Potential to use the tagged Sso1 marker to visualise EV-like membrane structures produced by *U. maydis* hyphae during infection. A. Maize tissue infected with a strain expressing 3xGFP-Sso1-2xStrepII (UMa2863-1), plasmolysed and stained with the lipophilic dye FM4-64 at 4 dpi. The plasma membrane of the maize cell is stained red and that of the fungus is green from the GFP-tagged marker and yellow if stained with FM4-64. Sso1 accumulations are visible as puncta on the hyphal plasma membrane (yellow arrowheads), where the hypha is encased by the plant plasma membrane (red arrowhead). The maize cell on the right is plasmolysed (red triangle). **B.** 3D reconstruction of the GFP signals from a hypha of the same strain (UMa2836-1) at 4 dpi. EV-like structures are visible as bumps on the fungal plasma membrane (white arrowheads). The image above shows a bird's eye view of the 3D reconstructed hypha and the image below is the same hypha rotated. Scale bars = 10 μm.

Initial attempts were made to use the tagged Sso1 EV marker (3xeGFP-Sso1-2xStrepII) to observe fungal EV secretion and uptake into plant cells during infection (Figure 4-11). Infected maize tissues were stained with the lipophilic dye FM4-64 so that the plant plasma membrane would be red and if stained, the fungal plasma membrane would be yellow due to overlap with the GFP-tagged Sso1 (Figure 4-11A). In addition to staining, the plant cells were plasmolysed to pull away the plant plasma membrane from infectious hyphae, in order to check for fungal EVs in the paramural space (Figure 4-11A). So far, no clear GFP signal from the Sso1 marker could be observed in the paramural space of plasmolysed cells. Where the plant plasma membrane is surrounding the fungal hypha, Sso1 puncta were visible on the fungal plasma membrane. These Sso1 puncta may be sites of active effector secretion as described in *Magnaporthe oryzae* (Giraldo et al., 2013) or there may be EV release at these intimate contact points with the plant plasma membrane (Figure 4-11A). To examine the hyphal plasma membrane more closely, a 3D reconstruction of the GFP signals from an *in planta* hypha expressing 3xeGFP-Sso1-2xStrepII was

generated (Figure 4-11B & C). Small bumps that seem continuous with the fungal plasma membrane could be observed (Figure 4-11B). However, uptake of such fungal EV-like structures into the plant cell could not be captured. It remains to be determined whether the bumps on the plasma membrane extend beyond the fungal cell wall, and whether these are EVs or simply plasma membrane extensions as proposed previously (Roth et al., 2019, Ludwig et al., 2021).

4.6. Materials and Methods

Use of online bioinformatic databases and tools

Annotations for the mRNA effector candidate genes were retrieved from UniProt (The UniProt Consortium, 2020) and the MIPS Ustilago maydis database (Mewes et al., 2010). Domain or protein family annotations were searched in InterPro release 87.0 (Blum et al., 2021). Subcellular localisation of the protein product was predicted with Deeploc 1.0 (Almagro Armenteros et al., 2017), LOCALIZER 1.0.4 (Sperschneider et al., 2017), and TargetP-2.0 (Almagro Armenteros et al., 2019), using the plant option if available. Orthologs were searched by DELTA-BLAST (Domain Enhanced Lookup Time Accelerated BLAST) with default settings in the NCBI blastp suite (Boratyn et al., 2012). Syntaxin sequences were aligned using CLUSTAL O version 1.2.4 (Sievers et al., 2011).

Generation of *U. maydis* strains and cultivation

U. maydis strains were generated by introducing genetic constructs into progenitor strains AB33 (Brachmann et al., 2001) and SG200 (Bölker et al., 1995) for stable integration into the genome by homologous recombination at target loci, as described previously (Bösch et al., 2016). Constructs for testing mRNA effector candidate delivery were integrated into the native gene loci of the candidates, UMAG_02984 and UMAG_11400, to replace the original gene with one fused to mVenus (Kremers et al., 2006), SV40 NLS (Collas and Aleström, 1996), original 3'UTR, followed by *Agrobacterium tumefaciens nos* (nopaline synthase) terminator (Bevan et al., 1983), and a hygromycin phosphotransferase cassette (Blochlinger and Diggelmann, 1984). For EV marker constructs, *sso1* gene (UMAG_04228) fused to *3xegfp* (Cormack et al., 1996) and either *2xstrep-tagII* or *3xHA* (Schmidt and Skerra, 2007) were placed under the *Potef* overexpression promoter (Spellig et al., 1996, Zarnack et al., 2006). The EV marker construct was ectopically inserted in multiple copies into the *ip* (iron-sulphur protein subunit of succinate dehydrogenase) locus, replacing the native carboxin-sensitive allele with a carboxin resistant one (Broomfield and Hargreaves, 1992). *U. maydis* strains generated and used here are listed in Table 4-4, Appendix to Chapter 4.

Culture conditions and media are detailed in Chapter 2. Sporidial cultures were grown at 28°C in complete medium (CM) + 1% (w/v) glucose. Filamentation was induced in AB33 background strains by shifting the sporidia to nitrate minimal medium (NM) + 2% glucose for 15-16 hours for EV isolation or +1% glucose for 6-8 hours for microscopy. For SG200 background strains, filamentation was induced by shifting to ammonium minimal medium (Holliday, 1974) + 1% glucose + 0.1% (w/v) charcoal for 6-8 hours for microscopy.

qPCR confirmation of mRNA effector candidate loading into EVs

RNA was extracted and cDNA synthesised from AB33, UMa3276-1 and UMa3278-1 filaments harvested at 15-16 hpi and their EVs as described in Chapter 2 and Chapter 3 (Kwon et al., 2021). qPCR was carried out as in detailed in Chapter 3 (Kwon et al., 2021), using specific primers in Table 4-5, Appendix to chapter 4).

Microscopy of *U. maydis* cells and EVs from culture

Cultured *U. maydis* cells and EVs isolate from both axenic cultures and apoplastic washing fluids were examined with Zeiss Axio Imager M1 (Zeiss, Oberkochen) widefield microscope, Plan Neofluar 40x (NA 1.3) and 63x (NA 1.25) objectives, and a Spot Pursuit CCD camera (Diagnostic Instruments, Sterling Heights, MI). Fluorescence proteins or dyes were excited with an HXP metal halide lamp (LEj, Jena) in combination with filter sets for GFP (ET470/40BP, ET495LP, ET525/50BP) and mCherry (ET560/40BP, ET585LP, ET630/75BP, Chroma, Bellow Falls, VT). Microscope operation and image processing was performed on MetaMorph (Molecular Devices, version 7, Sunnyvale, CA). Cultured *U. maydis* cells were imaged without staining. EVs were observed with or without 8 µM FM4-64 (ThermoFisher Scientific, Waltham, MA).

Microscopy of infected maize leaves or maize protoplasts incubated with EVs

Maize seedlings of cultivar Early Golden Bantam were infected with SG200 background strains as described previously (Bösch et al., 2016). All maize samples were imaged with Zeiss LSM 880 Airyscan (Zeiss, Oberkochen) fitted with C-Apochromat 40x (NA 1.2) and Plan-Apochromat 63x (NA 1.4) objectives, Airyscan detector (32x GaAsP), PMT and T-PMT detectors.

For testing transfer of mVenus-NLS-tagged effector candidates during infection, 4 dpi maize leaves infected with strains UMa3277-1 and UMa3279-1 were hand-sectioned into thin cross-sections and stained with 5 µg/ml Hoechst 33342 (ThermoFisher Scientific, Waltham, MA) with 0.05% (v/v) Triton X-100 (Merck, Darmstadt) in PBS for 15 minutes followed by incubation in PBS alone for 30 minutes. To test uptake of *U. maydis* EVs carrying mVenus-NLS-tagged effector candidates by plant protoplasts, maize leaf

protoplasts were prepared according to a published protocol (Gomez-Cano et al., 2019), only with the pH of the protoplast buffer adjusted to pH 7 instead of pH 5.7. This modification was made due to relatively diminished mVenus signal in pH 5.7. EVs were prepared as detailed in Chapter 2 from induced filament cultures of UMa3276-1 and UMa3278-1, but resuspended in maize protoplast buffer pH 7 instead of PBS. Maize protoplasts were incubated with *U. maydis* EVs for 4-5 hours and briefly stained with 5 µg/ml Hoechst 33342 without Triton X-100 for imaging. mVenus signals in *U. maydis* EVs and hyphae were imaged using 514 nm laser (5 %) with beam splitters (MBS: 458/514, MBS_InVis: -405, DBS1: Mirror), and GaAsP detector (pinhole 47 µm, filter 520-551, master gain 697, digital gain 1.0). For Hoechst 33342, 405 nm laser (5%), same beam splitters as above, and PMT detector (pinhole 47 µm, filter 413-460, master gain 750, digital gain 1.0) were used.

To check for *U. maydis* EV production during infection, maize leaves infected with eGFP-tagged EV marker strain UMa2863-1 were imaged. For imaging eGFP signals in hyphae alone, 488 nm laser (3 %), beam splitters (MBS: 488, MBS_Invis: Plate, DBS1 plate), emission filters BP 495-550 + BP 570-620, and Airyscan detector array (pinhole 125 µm, superresoution mode, Airyscan parameter 7.8 3D, master gain 950, digital gain 1.00) were used. To examine contact sites between the maize plasma membrane and *U. maydis* hyphae, infected leaf pieces were vacuum infiltrated for 30 minutes with 1 M sorbitol and 10 µM FM4-64 for plasmolysis and membrane staining. eGFP was imaged using 488 nm laser (10 %), beam splitters (MBS: 488, MBS_Invis: Plate, DBS1 plate), emission filters (BP 420-480 + BP 495-550), and Airyscan detector array (pinhole 94 µm, superresoution mode, Airyscan parameter 7.3 2D, master gain 950, digital gain 1.00). FM4-64 fluorescence was imaged using 561 nm laser (3%), beam splitters (MBS 458/561, MBS_InVis: Plate, DBS1: Plate), emission filters (BP 570-620 + LP 645), and Airyscan detector array (pinhole 94 µm, superresoution mode, Airyscan parameter 6.6 2D, master gain 900, digital gain 1.00).

Isolation and examination of EVs from maize apoplastic washing fluid

Approximately 10 cm pieces of leaves with visible lesions were harvested from 6 dpi maize plants infected with SG200 and equivalent parts were collected from mock inoculated plants. Leaf pieces were collected in a beaker of ice-cold tap water, briefly shaken and patted dry in a sieve lined with paper towels, then weighed before and after infiltration. Leaf pieces were submerged and infiltrated with ice-cold vesicle isolation buffer (20 mM MES, 2 mM CaCl₂, 0.1 M NaCl pH 6) for 30 minutes at 150-200 mbar. Infiltrated leaf pieces were shaken and patted dry and weighed to estimate infiltration volume. Leaf pieces were stacked, rolled up in Nescofilm (Fisher Scientific, Schwerte), inserted into 50 ml volume syringes (Carl Roth, Karlsruhe) in 500 ml centrifuge bottles (ThermoFisher Scientific, Waltham, MA), and centrifuged for 700

xg for 20 minutes in JA-10 rotor to collect the AWF. AWF was filtered with 0.45 µm syringe filter (Sarstedt, Nümbrecht) and centrifuged at 100,000 xg in 45 Ti rotor (Beckman Coulter, Brea, CA). Resulting pellet was resuspended in PBS and subjected to FM4-64 staining, TEM, and RNA extraction as detailed in Chapter 2.

4.7.   Appendix to Chapter 4

```
HsSTX1A    ------------------------------------------------------------     0
UmSso1     MARDRLAAMRAQQAGGYGGYGGGNNGYGDHSYPTQQQGNAQGGYAQQHQQSGYAYNHASY    60
ScSSO1     ------------------------------------------------------------     0


HsSTX1A    ------------------MKDRTQE---LRTAKDSD-DDDDVAVTVDRDRFMDEFFEQVE    38
UmSso1     DSQPQAGYAPPQPTGYGQMPQPQSAGYAATGGAPPNSYEMQSVTTEKPAGDMNSFFSDIS   120
ScSSO1     -----MSYNNPY-----QLETPFEESYELDEGS---------SAIGAEGHDFVGFMNKIS    41
                             :      .       .             .    : *:..:.

HsSTX1A    EIRGFIDKIAENVEEVKRKHSAILASPNPDEKTKEELEELMSDIKKTANKVRSKLKSIEQ    98
UmSso1     EIQDTIRLIDENVNKISDLHSRSLNNMDEAS--AQYAEQQLASIQQETSSLTNGVKNRIK   178
ScSSO1     QINRDLDKYDHTINQVDSLHKRLLTEVNEEQ--ASHLRHSLDNFVAQATDLQFKLKNEIK    99
           :*.  :     ..:::.  *.  * *  . .   . ..:  .:    :..:    :*. :

HsSTX1A    SIEQEEGLNRSSADLRIRKTQHSTLSRKFVEVMSEYNATQSDYRERCKGRIQRQLEITGR   158
UmSso1     LLESQNKRVPAGGDKNVRNTQIGAVKNRFKETIQRYQQVEQSYRQKYRARAERQFRIVKP   238
ScSSO1     SAQ------RDGIHDTNKQAQAENSRQRFLKLIQDYRIVDSNYKEENKEQAKRQYMIIQP   153
             :        .  .  :::*      .:* : :. *. .:..*::. : : :** *

HsSTX1A    TTTSEELEDMLE-SGNPAIFASGIIMD--SSISKQALSEIETRHSEIIKLENSIRELHDM   215
UmSso1     DATQQEIKAALDDDQNGQIFSQALLNSNRHGEAKGALREVQERHEDIKRIERTITELAQL   298
ScSSO1     EATEDEVEAAISDVGGQQIFSQALLNANRRGEAKTALAEVQARHQELLKLEKSMAELTQL   213
            :*.:*::  :.   .   **:..::     . :* ** *:: **.:: ::*.:: ** ::

HsSTX1A    FMDMAMLVESQGEMIDRIEYNVEHAVDYVERAVSDTKKAVKYQSKARRKKIMIIICCVIL   275
UmSso1     FNEMSILVDEQDDALNVIQEQGAQVETDMNQGLQHTNKAVDSARKARKKRWICFWIIVIL   358
ScSSO1     FNDMEELVIEQQENVDVIDKNVEDAQLDVEQGVGHTDKAVKSARKARKNKIRCWLIVFAI   273
           * :*  **  .* : :: *: :  ..   :::.: .*.***.   ***::      . :

HsSTX1A    GIVIASTVG--GIFA---------------------------------------------   288
UmSso1     IIVIAAIIV--AVICTRPGNCGQSNGNGNARRSLITRAVQYGHGLLIEKKDARAYLLPDL   416
ScSSO1     IVVVVVVVVVPAVVKTR-------------------------------------------   290
            :*:.  :    .:.

HsSTX1A    --  288
UmSso1     GM  418
ScSSO1     --  290
```

```
Habc domain        H3 domain        Transmembrane helix        Extracellular portion
```

Figure 4-12. Amino acid sequence alignment of the syntaxin Sso1 in *U. maydis* (*Um*Sso1) with its orthologs in human (*Hs*STX1A) and yeast (*Sc*SSO1) (Sievers et al., 2011). For the human and yeast orthologs, the domains have been experimentally determined (Liang et al., 2013, Yuan and Jäntti, 2010). The domains indicated in the *U. maydis* Sso1 sequence are only predictions based on the characterised orthologs and a membrane protein topology prediction tool (Tsirigos et al., 2015). The Habc and H3 domains are indicated in light and dark grey, respectively. The transmembrane helix is marked in yellow. The extracellular portion is indicated in red letters and the rest of the protein is intracellular.

Table 4-4. *U. maydis* strains used in this thesis

Purpose	Strain name	Plasmid used	Genetic background	Description	Produced by
Progenitor strains for the strains generated in this thesis	AB33	-	*a2 P_nar:bW2 P_nar:bE1 ble^R*	Filamentation inducible in culture by switching N source	(Brachmann et al., 2001)
	SG200	-	*a1 mfa2 bE1 bW2 ble^R*	Solopathogenic	(Kämper et al., 2006)
For visualisation and purification of EVs	UMa 2863	pUMa 3847	*a1 mfa2 bE1 bW2 ble^R ip^S [P_otef:3xegfp:sso1:2xstrepII:T_nos] ip^R (cbx^R)*	Expresses 3xeGFP-Sso1-2xStrepII in SG200 background, in addition to the native Sso1 (UMAG_04228)	This study
	UMa 2864	pUMa 3848	*a2 P_nar:bW2 P_nar:bE1 ble^R ip^S [P_otef:3xegfp:sso1:2xstrepII:T_nos] ip^R (cbx^R)*	Expresses 3xeGFP-Sso1-3xHA in AB33 background, in addition to the native Sso1 (UMAG_04228)	This study
For testing transfer and translation of mRNA effectors in plant cells	UMa 3276	pUMa 4573	*a2 P_nar:bW2 P_nar:bE1 ble^R UMAG_02984:mVenus:NLS:T_nos:3'UTR:hyg^R*	Expresses of UMAG_02984-mVenus-NLS from the native locus	This study
	UMa 3277	pUMa 4573	*a1 mfa2 bE1 bW2 ble^R UMAG_02984:mVenus:NLS:T_nos:3'UTR:hyg^R*	Expresses of UMAG_02984-mVenus-NLS from the native locus	This study
	UMa 3278	pUMa 4574	*a2 P_nar:bW2 P_nar:bE1 ble^R UMAG_11400:mVenus:NLS:T_nos:3'UTR:hyg^R*	Expresses of UMAG_11400-mVenus-NLS from the native locus	This study
	UMa 3279	pUMa 4574	*a1 mfa2 bE1 bW2 ble^R UMAG_11400:mVenus:NLS:T_nos:3'UTR:hyg^R*	Expresses of UMAG_11400-mVenus-NLS from the native locus	This study

All listed strains and plasmids used for strain generation are available at the Institute for Microbiology.

a2, a2: alleles of mating-type locus *a* (Banuett and Herskowitz, 1989)

bE1, bW2: compatible alleles of homeodomain transcription factor genes in mating-type locus b
(Kronstad and Leong, 1990)

ble^R: bleomycin/phleomycin resistance cassette (Punt and van den Hondel, 1992)

cbx^R: carboxin resistance (due to *ip^R* allele) (Broomfield and Hargreaves, 1992)

hyg^R: hygromycin resistance cassette (Blochlinger and Diggelmann, 1984)

ip^R: carboxin-resistant allele of the *ip* (iron-sulphur protein subunit of succinate dehydrogenase) gene

ip^S: carboxin-sensitive allele of the *ip* gene

mfa2: allele of the *mfa* gene in mating locus *a* (Bölker et al., 1992)

NLS: nuclear localization signal from SV40 (Collas and Aleström, 1996)

P_nar: nitrate reductase nar1 promoter (Brachmann et al., 2001)

P_otef: strong hybrid promoter with *tetO* (tetracyclin operator) binding sites fused to *tef1* (translation
elongation factor 1) promoter (Zarnack et al., 2006)

Tnos: *nos* (nopaline synthase) terminator from *Agrobacterium tumefaciens* (Bevan et al., 1983)

3'UTR: 3'untranslated region of the gene of interest

Table 4-5. Primers for qPCR

Target transcript	Primer name	Primer sequence
UMAG_02984	AB581	GCCTACATCCAGATTGGCTATG
	AB582	GTTGTTCTTCCGTGATTGCTTG
UMAG_11400	AB688	GGTCTCACTTGCGCTTACA
	AB689	GATCACCATTCCGCTCATCA
UMAG_02361	AB599	CGCCTTTGTCATGGCTACT
	AB600	GCTGAACGTACTGGTTCTCTT
UMAG_01054	AB601	TCTGCGCAAGATCCGAAAG
	AB602	GTTGTCGGGATAAGCAGTGTAG

4.8. References

ALMAGRO ARMENTEROS, J. J., SALVATORE, M., EMANUELSSON, O., WINTHER, O., VON HEIJNE, G., ELOFSSON, A. & NIELSEN, H. 2019. Detecting sequence signals in targeting peptides using deep learning. *Life Science Alliance,* 2**,** e201900429.

ALMAGRO ARMENTEROS, J. J., SØNDERBY, C. K., SØNDERBY, S. K., NIELSEN, H. & WINTHER, O. 2017. DeepLoc: prediction of protein subcellular localization using deep learning. *Bioinformatics,* 33**,** 3387-3395.

ARAÚJO, W. L., ISHIZAKI, K., NUNES-NESI, A., LARSON, T. R., TOHGE, T., KRAHNERT, I., WITT, S., OBATA, T., SCHAUER, N., GRAHAM, I. A., LEAVER, C. J. & FERNIE, A. R. 2010. Identification of the 2-Hydroxyglutarate and Isovaleryl-CoA Dehydrogenases as Alternative Electron Donors Linking Lysine Catabolism to the Electron Transport Chain of Arabidopsis Mitochondria *The Plant Cell,* 22**,** 1549-1563.

BANUETT, F. & HERSKOWITZ, I. 1989. Different a alleles of Ustilago maydis are necessary for maintenance of filamentous growth but not for meiosis. *Proc Natl Acad Sci U S A,* 86**,** 5878-82.

BEVAN, M., BARNES, W. M. & CHILTON, M. D. 1983. Structure and transcription of the nopaline synthase gene region of T-DNA. *Nucleic acids research,* 11**,** 369-385.

BLOCHLINGER, K. & DIGGELMANN, H. 1984. Hygromycin B phosphotransferase as a selectable marker for DNA transfer experiments with higher eucaryotic cells. *Molecular and cellular biology,* 4**,** 2929-2931.

BLUM, M., CHANG, H.-Y., CHUGURANSKY, S., GREGO, T., KANDASAAMY, S., MITCHELL, A., NUKA, G., PAYSAN-LAFOSSE, T., QURESHI, M., RAJ, S., RICHARDSON, L., SALAZAR, G. A., WILLIAMS, L., BORK, P., BRIDGE, A., GOUGH, J., HAFT, D. H., LETUNIC, I., MARCHLER-BAUER, A., MI, H., NATALE, D. A., NECCI, M., ORENGO, C. A., PANDURANGAN, A. P., RIVOIRE, C., SIGRIST, C. J. A., SILLITOE, I., THANKI, N., THOMAS, P. D., TOSATTO, S. C. E., WU, C. H., BATEMAN, A. & FINN, R. D. 2021. The InterPro protein families and domains database: 20 years on. *Nucleic acids research,* 49**,** D344-D354.

BÖLKER, M., GENIN, S., LEHMLER, C. & KAHMANN, R. 1995. Genetic regulation of mating and dimorphism in Ustilago maydis. *Canadian Journal of Botany,* 73**,** 320-325.

BÖLKER, M., URBAN, M. & KAHMANN, R. 1992. The a mating type locus of U. maydis specifies cell signaling components. *Cell,* 68**,** 441-50.

BORATYN, G. M., SCHÄFFER, A. A., AGARWALA, R., ALTSCHUL, S. F., LIPMAN, D. J. & MADDEN, T. L. 2012. Domain enhanced lookup time accelerated BLAST. *Biology Direct,* 7**,** 12.

BÖSCH, K., FRANTZESKAKIS, L., VRANES, M., KÄMPER, J., SCHIPPER, K. & GÖHRE, V. 2016. Genetic Manipulation of the Plant Pathogen Ustilago maydis to Study Fungal Biology and Plant Microbe Interactions. *J Vis Exp*.

BRACHMANN, A., WEINZIERL, G., KAMPER, J. & KAHMANN, R. 2001. Identification of genes in the bW/bE regulatory cascade in *Ustilago maydis*. *Molecular Microbiology,* 42**,** 1047-1063.

BROOMFIELD, P. L. E. & HARGREAVES, J. A. 1992. A single amino-acid change in the iron-sulphur protein subunit of succinate dehydrogenase confers resistance to carboxin in Ustilago maydis. *Current Genetics,* 22**,** 117-121.

CAI, Q., QIAO, L., WANG, M., HE, B., LIN, F. M., PALMQUIST, J., HUANG, S. D. & JIN, H. 2018. Plants send small RNAs in extracellular vesicles to fungal pathogen to silence virulence genes. *Science,* 360**,** 1126-1129.

COLLAS, P. & ALESTRÖM, P. 1996. Nuclear localization signal of SV40 T antigen directs import of plasmid DNA into sea urchin male pronuclei in vitro. *Mol Reprod Dev,* 45**,** 431-8.

COLLINS, N. C., THORDAL-CHRISTENSEN, H., LIPKA, V., BAU, S., KOMBRINK, E., QIU, J.-L., HÜCKELHOVEN, R., STEIN, M., FREIALDENHOVEN, A., SOMERVILLE, S. C. & SCHULZE-LEFERT, P. 2003. SNARE-protein-mediated disease resistance at the plant cell wall. *Nature,* 425**,** 973-977.

CORMACK, B. P., VALDIVIA, R. H. & FALKOW, S. 1996. FACS-optimized mutants of the green fluorescent protein (GFP). *Gene,* 173**,** 33-38.

DOEHLEMANN, G., WAHL, R., HORST, R. J., VOLL, L. M., USADEL, B., POREE, F., STITT, M., PONS-KUHNEMANN, J., SONNEWALD, U., KAHMANN, R. & KAMPER, J. 2008. Reprogramming a maize plant: transcriptional and metabolic changes induced by the fungal biotroph *Ustilago maydis*. *Plant Journal,* 56**,** 181-195.

FUJIMOTO, T., ABE, H., MIZUKUBO, T. & SEO, S. 2021. Phytol, a Constituent of Chlorophyll, Induces Root-Knot Nematode Resistance in Arabidopsis via the Ethylene Signaling Pathway. *Molecular Plant-Microbe Interactions®,* 34**,** 279-285.

GIRALDO, M. C., DAGDAS, Y. F., GUPTA, Y. K., MENTLAK, T. A., YI, M., MARTINEZ-ROCHA, A. L., SAITOH, H., TERAUCHI, R., TALBOT, N. J. & VALENT, B. 2013. Two distinct secretion systems facilitate tissue invasion by the rice blast fungus Magnaporthe oryzae. *Nature Communications,* 4**,** 1996.

GOMEZ-CANO, L., YANG, F. & GROTEWOLD, E. 2019. Isolation and Efficient Maize Protoplast Transformation. *Bio-protocol,* 9**,** e3346.

HOLLIDAY, R. 1974. Ustilago maydis. *In:* KING, R. C. (ed.) *Bacteria, Bacteriophages, and Fungi: Volume 1.* Boston, MA: Springer US.

KÄMPER, J., KAHMANN, R., BÖLKER, M., MA, L.-J., BREFORT, T., SAVILLE, B. J., BANUETT, F., KRONSTAD, J. W., GOLD, S. E., MÜLLER, O., PERLIN, M. H., WÖSTEN, H. A. B., DE VRIES, R., RUIZ-HERRERA, J., REYNAGA-PEÑA, C. G., SNETSELAAR, K., MCCANN, M., PÉREZ-MARTÍN, J., FELDBRÜGGE, M., BASSE, C. W., STEINBERG, G., IBEAS, J. I., HOLLOMAN, W., GUZMAN, P., FARMAN, M., STAJICH, J. E., SENTANDREU, R., GONZÁLEZ-PRIETO, J. M., KENNELL, J. C., MOLINA, L., SCHIRAWSKI, J., MENDOZA-MENDOZA, A., GREILINGER, D., MÜNCH, K., RÖSSEL, N., SCHERER, M., VRANEŠ, M., LADENDORF, O., VINCON, V., FUCHS, U., SANDROCK, B., MENG, S., HO, E. C. H., CAHILL, M. J., BOYCE, K. J., KLOSE, J., KLOSTERMAN, S. J., DEELSTRA, H. J., ORTIZ-CASTELLANOS, L., LI, W., SANCHEZ-ALONSO, P., SCHREIER, P. H., HÄUSER-HAHN, I., VAUPEL, M., KOOPMANN, E., FRIEDRICH, G., VOSS, H., SCHLÜTER, T., MARGOLIS, J., PLATT, D., SWIMMER, C., GNIRKE, A., CHEN, F., VYSOTSKAIA, V., MANNHAUPT, G., GÜLDENER, U., MÜNSTERKÖTTER, M., HAASE, D., OESTERHELD, M., MEWES, H.-W., MAUCELI, E. W., DECAPRIO, D., WADE, C. M., BUTLER, J., YOUNG, S., JAFFE, D. B., CALVO, S., NUSBAUM, C., GALAGAN, J. & BIRREN, B. W. 2006. Insights from the genome of the biotrophic fungal plant pathogen Ustilago maydis. *Nature,* 444**,** 97-101.

KREMERS, G. J., GOEDHART, J., VAN MUNSTER, E. B. & GADELLA, T. W., JR. 2006. Cyan and yellow super fluorescent proteins with improved brightness, protein folding, and FRET Förster radius. *Biochemistry,* 45**,** 6570-80.

KRONSTAD, J. W. & LEONG, S. A. 1990. The b mating-type locus of Ustilago maydis contains variable and constant regions. *Genes Dev,* 4**,** 1384-95.

KWON, S., RUPP, O., BRACHMANN, A., BLUM, C. F., KRAEGE, A., GOESMANN, A. & FELDBRÜGGE, M. 2021. mRNA Inventory of Extracellular Vesicles from Ustilago maydis. *Journal of Fungi,* 7**,** 562.

LAI, C. P., KIM, E. Y., BADR, C. E., WEISSLEDER, R., MEMPEL, T. R., TANNOUS, B. A. & BREAKEFIELD, X. O. 2015. Visualization and tracking of tumour extracellular vesicle delivery and RNA translation using multiplexed reporters. *Nature Communications,* 6.

LAMBOU, K., THARREAU, D., KOHLER, A., SIRVEN, C., MARGUERETTAZ, M., BARBISAN, C., SEXTON, A. C., KELLNER, E. M., MARTIN, F., HOWLETT, B. J., ORBACH, M. J. & LEBRUN, M.-H. 2008. Fungi have three tetraspanin families with distinct functions. *BMC Genomics,* 9**,** 63.

LANVER, D., MULLER, A. N., HAPPEL, P., SCHWEIZER, G., HAAS, F. B., FRANITZA, M., PELLEGRIN, C., REISSMANN, S., ALTMULLER, J., RENSING, S. A. & KAHMANN, R. 2018. The Biotrophic Development of Ustilago maydis Studied by RNA-Seq Analysis. *Plant Cell,* 30**,** 300-323.

LIANG, B., KIESSLING, V. & TAMM, L. K. 2013. Prefusion structure of syntaxin-1A suggests pathway for folding into neuronal trans-SNARE complex fusion intermediate. *Proceedings of the National Academy of Sciences,* 110**,** 19384-19389.

LIU, S., MONKS, N. R., HANES, J. W., BEGLEY, T. P., YU, H. & MOSCOW, J. A. 2010. Sensitivity of breast cancer cell lines to recombinant thiaminase I. *Cancer Chemother Pharmacol,* 66**,** 171-9.

LUDWIG, N., REISSMANN, S., SCHIPPER, K., GONZALEZ, C., ASSMANN, D., GLATTER, T., MORETTI, M., MA, L. S., REXER, K. H., SNETSELAAR, K. & KAHMANN, R. 2021. A cell surface-exposed protein complex with an essential virulence function in *Ustilago maydis*. *Nature Microbiology*.

MEWES, H. W., RUEPP, A., THEIS, F., RATTEI, T., WALTER, M., FRISHMAN, D., SUHRE, K., SPANNAGL, M., MAYER, K. F. X., STÜMPFLEN, V. & ANTONOV, A. 2010. MIPS: curated databases and comprehensive secondary data resources in 2010. *Nucleic Acids Research,* 39**,** D220-D224.

PUNT, P. J. & VAN DEN HONDEL, C. A. M. J. J. 1992. Transformation of filamentous fungi based on hygromycin b and phleomycin resistance markers. *Methods in Enzymology.* Academic Press.

ROTH, R., HILLMER, S., FUNAYA, C., CHIAPELLO, M., SCHUMACHER, K., LO PRESTI, L., KAHMANN, R. & PASZKOWSKI, U. 2019. Arbuscular cell invasion coincides with extracellular vesicles and membrane tubules. *Nat Plants,* 5**,** 204-211.

RUTTER, B. D., RUTTER, K. L. & INNES, R. W. 2017. Isolation and Quantification of Plant Extracellular Vesicles. *Bio-protocol,* 7**,** e2533.

SCHMIDT, T. G. M. & SKERRA, A. 2007. The Strep-tag system for one-step purification and high-affinity detection or capturing of proteins. *Nature Protocols,* 2**,** 1528-1535.

SIEVERS, F., WILM, A., DINEEN, D., GIBSON, T. J., KARPLUS, K., LI, W., LOPEZ, R., MCWILLIAM, H., REMMERT, M., SÖDING, J., THOMPSON, J. D. & HIGGINS, D. G. 2011. Fast, scalable generation of high-quality protein multiple sequence alignments using Clustal Omega. *Molecular Systems Biology,* 7**,** 539.

SPELLIG, T., BOTTIN, A. & KAHMANN, R. 1996. Green fluorescent protein (GFP) as a new vital marker in the phytopathogenic fungusUstilago maydis. *Molecular and General Genetics MGG,* 252**,** 503-509.

SPERSCHNEIDER, J., CATANZARITI, A.-M., DEBOER, K., PETRE, B., GARDINER, D. M., SINGH, K. B., DODDS, P. N. & TAYLOR, J. M. 2017. LOCALIZER: subcellular localization prediction of both plant and effector proteins in the plant cell. *Scientific Reports,* 7**,** 44598.

THE UNIPROT CONSORTIUM 2020. UniProt: the universal protein knowledgebase in 2021. *Nucleic Acids Research,* 49**,** D480-D489.

TREITSCHKE, S., DOEHLEMANN, G., SCHUSTER, M. & STEINBERG, G. 2010. The myosin motor domain of fungal chitin synthase V is dispensable for vesicle motility but required for virulence of the maize pathogen Ustilago maydis. *The Plant cell,* 22**,** 2476-2494.

TSIRIGOS, K. D., PETERS, C., SHU, N., KÄLL, L. & ELOFSSON, A. 2015. The TOPCONS web server for consensus prediction of membrane protein topology and signal peptides. *Nucleic acids research,* 43**,** W401-W407.

WITWER, K. W., BUZÁS, E. I., BEMIS, L. T., BORA, A., LÄSSER, C., LÖTVALL, J., NOLTE-'T HOEN, E. N., PIPER, M. G., SIVARAMAN, S., SKOG, J., THÉRY, C., WAUBEN, M. H. & HOCHBERG, F. 2013. Standardization of sample collection, isolation and analysis methods in extracellular vesicle research. *Journal of Extracellular Vesicles,* 2**,** 20360.

WITZEL, K., SHAHZAD, M., MATROS, A., MOCK, H. P. & MUHLING, K. H. 2011. Comparative evaluation of extraction methods for apoplastic proteins from maize leaves. *Plant Methods,* 7.

WOODWARD, J. B., ABEYDEERA, N. D., PAUL, D., PHILLIPS, K., RAPALA-KOZIK, M., FREELING, M., BEGLEY, T. P., EALICK, S. E., MCSTEEN, P. & SCANLON, M. J. 2010. A Maize Thiamine Auxotroph Is Defective in Shoot Meristem Maintenance *The Plant Cell,* 22**,** 3305-3317.

YUAN, Q. & JÄNTTI, J. 2010. Functional Analysis of Phosphorylation on Saccharomyces cerevisiae Syntaxin 1 Homologues Sso1p and Sso2p. *PLOS ONE,* 5**,** e13323.

ZARNACK, K., MAURER, S., KAFFARNIK, F., LADENDORF, O., BRACHMANN, A., KÄMPER, J. & FELDBRÜGGE, M. 2006. Tetracycline-regulated gene expression in the pathogen Ustilago maydis. *Fungal Genetics and Biology,* 43**,** 727-738.

5. Discussion and Perspectives

Presented in this thesis are the pioneering efforts to investigate EVs and the associated RNA cargo secreted by the phytopathogenic fungus *Ustilago maydis*. The project was driven by the hypothesis that intact fungal mRNAs can be delivered to plant cells via EVs, where they are translated to produce effector proteins using host resources. As a first step, I have developed a highly reproducible EV isolation method for axenic cultures of induced filaments, which partially mimic infectious hyphae (Chapter 2). Applying this method, an inventory of EV-associated mRNAs was generated, from which we gained valuable insight into selective loading and functionality of mRNAs enriched in EVs (Chapter 3). Several functionally interesting candidate mRNA effectors were identified, that are both enriched in EVs and highly upregulated during infection. These endeavours culminated in an initial attempt to test the above hypothesis with individual candidates (Chapter 4). However, inconclusive results were obtained due to technical limitations. Since testing several candidates in this way is not feasible, the list of promising candidates should be narrowed down further by examining EVs from infected plant samples using high-throughput approaches. Hence I have developed a method to isolate EVs from apoplastic washing fluid (AWF) of infected maize plants and a marker to distinguish *U. maydis* EVs from plant-derived particles (Chapter 4). The two methods developed here can now be used further to investigate EV-mediated interaction between *U. maydis* and maize, since the data from EVs of induced filament cultures and infected plants should complement each other. The implications, usefulness, and limitations of the work presented in the previous chapters will be discussed below. Opportunities and challenges in studying EVs in *U. maydis*-maize pathosystem will be addressed, together with suggestions for future investigation.

5.1. AB33 filaments in culture as mimic of infectious hyphae

The relevance and usefulness of the EV cargo mRNA data obtained in Chapter 3 depends on how effectively AB33 b-induced filaments serve as a proxy for infectious hyphae *in planta* (Chapters 2 & 3). Of course it is neither feasible nor necessary to have a perfect mimic of a certain infection stage in culture. What is important is that a substantial set of infection-associated transcripts is selectively enriched in the culture EVs, so that mRNA effector candidates can be identified. Since I am primarily interested in the role of EVs at the intimate plant-fungus interfaces during establishment of biotrophy, infectious hyphae to 6 dpi in maize would be relevant for comparison (Lanver et al., 2018). Then to what extent are the AB33 induced filaments representative of such biotrophic infectious hyphae?

Developmentally, AB33 filaments in culture are equivalent to mated, infectious, dikaryotic filaments before plant penetration (0.5-1 dpi), that are unicellular and arrested at G2 phase of the cell cycle as a result of bE/bW activity (Brachmann et al., 2001, García-Muse et al., 2003, Heimel et al., 2010b). Upon detecting plant surface cues, infectious filaments begin to express a subset effector proteins and form appressorium-like structures to penetrate the plant (Lanver et al., 2014). Until this stage, infectious filaments are G2-arrested. But to proliferate *in planta*, nuclear proteins Clp1 and Cib1 are essential to negatively regulate the processes required up to penetration and switch to a biotrophic infection program (Schmitz et al., 2019, Heimel et al., 2013). Inside the plant, the fungus experiences ER stress, presumably stemming from the high secretory burden for establishing biotrophy (Heimel et al., 2013). ER stress leads to splicing of the unfolded protein response (UPR) regulator Cib1 mRNA into the form which, when translated, is able to stabilise Clp1 for UPR activation and cell cycle release (Heimel et al., 2010a, Heimel et al., 2013). In summary, AB33 filaments in culture are representative of the pre-penetration stage: they lack plant signals and ER-stress, so they are not proliferating like true multicellular hyphae *in planta*.

To address how transcriptionally representative AB33 filaments are of infectious hyphae, their transcriptome can be examined in light of previous transcriptomic studies in *U. maydis*. In these studies, gene sets relevant for infection have been defined as follows: infection stage-associated "coexpression modules" (Lanver et al., 2018), plant surface signal-induced (Lanver et al., 2014), and UPR-induced (Pinter et al., 2019). I have set 50 transcripts per million (TPM) as an arbitrary threshold for "reasonable" expression in AB33 filaments, given the median for all reliably detected transcripts is 65 TPM. Over half of the transcripts that belong to the pre-defined infection stage-associated "coexpression modules" (Lanver et al., 2018) were expressed above this threshold in AB33 filaments. Similarly, around 60% of plant surface signal-induced (Lanver et al., 2014) and UPR-induced transcripts were also above the threshold (Pinter et al., 2019). So over half of the genes relevant for infection are expressed in AB33 filaments, albeit not as strongly as during infection.

However, it must be noted that certain plant surface signal- (Lanver et al., 2014) and UPR-induced (Pinter et al., 2019) effectors are hardly expressed in AB33 (Chapter 3 table S4). These effector genes harbour UPR-responsive elements in the promoter, which make them direct targets for induction via the Cib1 transcription factor (Hampel et al., 2016). Examples of such conventionally secreted effectors are Pit2, Pep1, and the Tin proteins (Doehlemann et al., 2011, Doehlemann et al., 2009, Brefort et al., 2014). Nevertheless, mRNAs targeted to the ER for translation, including those of conventionally secreted proteins, are generally depleted from AB33 filament EVs (Chapter 3, Figure 5). Also, it does not make

sense for the fungus to send mRNAs of conventionally secreted proteins to the plant via EVs (Chapter 3, Figure 5). So ER stress-induced effector mRNAs may not necessarily be pertinent EV cargos. Rather, the main purpose of examining EVs is to search for novel effectors in the form of RNA or unconventionally secreted proteins.

Overall, given that a majority of genes relevant for infection are expressed, AB33 filament cultures are suitable for the purpose of identifying infection-relevant EV cargo mRNAs, as done so in Chapters 3 and 4. It was indeed possible to identify a considerable set of 161 infection-associated transcripts (Lanver et al., 2018) that are selectively enriched in EVs using AB33 filament cultures (Chapters 3 & 4). The potential to discover mRNA effectors using this system is further supported by the fact that the top most EV-enriched mRNAs are highly upregulated during infection and mostly belong to the infection-associated modules (Lanver et al., 2018) (Chapter 3, Table 1). In summary, although AB33 filaments in culture are an imperfect transcriptional mimic of infectious hyphae, they have been instrumental to selection of promising mRNA effector candidates.

5.2. A case for mRNAs as true cargos of *U. maydis* EVs

It is practically challenging to obtain EVs without co-purifying extracellular protein complexes and lipoproteins (Chapter 2). Then how likely it is that the RNA identified are truly inside EVs rather than in co-purified free ribonucleoprotein (RNP) complexes? This is a highly debated question in EVs of plants and their pathogens (Rutter and Innes, 2020). To address this question, RNase protection assay was carried out (Chapter 3, Figure 2). The RNA associated with *U. maydis* EVs were clearly protected from RNase treatment, while co-treatment with the detergent Triton X-100 led to near-complete degradation, only leaving behind traces of short residues (Chapter 3, Figure 2). The concentration of Triton X-100 (0.1% v/v) that was used here as an EV membrane lysis control, is at least 10-fold lower than the concentrations typically used for isolating intact membrane-associated protein complexes (Lautz et al., 2019) or RNPs (Fuentes-Iglesias et al., 2020). Hence the detergent treatment used here should only disrupt EV membranes but leave any complexes intact. As there is no appreciable RNA surviving detergent and RNase co-treatment, one can infer that for *U. maydis*, the contribution of free RNPs in extracellular RNA transport is minimal. So the results indicate that the RNA associated with *U. maydis* EVs identified in Chapter 3 are protected within EV membranes.

The EV samples used for RNA sequencing in Chapter 3 have not been treated with both protease and RNase. Protease treatment of EVs has been recommended (Rutter and Innes, 2020) but not always done

in studying EV-associated RNAs in plant-microbe interactions (Cai et al., 2018). It seems unlikely from the reasoning above that an additional protease treatment would make a great difference but it remains to be tested in the future. In any case, *U. maydis* is a highly prolific secretor of proteases and RNases in culture (Terfruchte et al., 2018, Mukherjee et al., 2020), so 15-16 hours of cultivation with a high starting cell density (detailed methods in Chapter 2) may have a similar effect to a standard protease treatment. Protease treatment may be especially important when investigating EV-associated sRNAs, because sRNAs are also commonly found in free RNPs (Arroyo et al., 2011) and lipoproteins (Michell and Vickers, 2016). But it may not be so critical for investigating longer EV-associated mRNAs for the following reason. According to a thorough comparison of extracellular fractions from human glioma stem cells, longer intact mRNAs (≥ 1000 nt) can only be detected in EVs, while only traces of shorter mRNAs of up to a few hundred nucleotides are detectible in RNPs (Wei et al., 2017). The median CDS length of mRNAs detected in EVs is 1181 nt. Over half of all transcripts detected in EVs have full CDS coverage and all four mRNA effector candidates tested (≥ 1000 nt) were confirmed to be intact and correctly spliced (Chapter 3, Figure 3 & 4). Taken together, intact mRNAs are very likely to be *bona fide* cargos of *U. maydis* EVs.

Having established that *U. maydis* secretes EVs with mRNAs, the next step is to rule out that these are cellular garbage. If *U. maydis* EVs were mere disposal mechanisms, one would expect to find enriched in AB33 filament EVs the transcripts that must be discarded (i.e. downregulated) during switch from sporidia to filaments (Olgeiser et al., 2019). This is certainly not the case (Appendix to Chapter 5, Figure 5-1). Rather, mRNAs relevant for infection are highly enriched and intact in EVs, which further support that the mRNA cargos are neither garbage nor randomly loaded (Chapter 3, Figure 4 & Table 1). Contamination from dead cells has been minimised by ensuring that the viability is as high as possible (Chapter 2). Even though minimal cell death is inevitable, dead fungal cells have been demonstrated to not yield appreciable EV-like structures since EV secretion is an active process (Rodrigues et al., 2007). Hence, mRNAs secreted in *U. maydis* EVs are more likely to be functional cargos than cellular waste.

5.3.   Are mRNA effectors theoretically probable?

The main working hypothesis is that *U. maydis* secretes EVs with mRNA effectors that are <u>delivered and translated</u> in maize cells to produce functional effector proteins. Having established that indeed there are promising, intact mRNAs in *U. maydis* EVs, there are additional pre-requisites that need to be met for mRNA effectors to be at least theoretically possible:

A. mRNA secretion should be a frequent phenomenon in fungal cells

B. A given mRNA species should be secreted frequently and/or abundantly via EVs

C. Fungal EVs must deliver mRNAs cargos to the cytosol of plant cells

D. Fungal mRNA should be compatible with the plant translation machinery

Points A and B on mRNA secretion can be addressed based on the findings of Chapter 3 and a few assumptions from literature. Attempts to test points C and D on mRNA delivery and translation *in planta* were inconclusive so these will be discussed based on literature alone (Chapter 4).

mRNA secretion: points A & B

As a reference, one study on cancer stem cell EVs provided an estimate of mRNA copy number per EVs (Wei et al., 2017). According to their estimate, there is only a single copy of mRNA per ~ 10 EVs, and the most abundant mRNA is only present one copy per ~ 1000 EVs (Wei et al., 2017). For such an estimate, one would need the following data:

1. Particle counts of the EV sample for RNA extraction e.g. by nanoparticle tracking analysis

2. Quantification of the total RNA extracted for the given number of particles

3. An estimate of the proportion of mRNAs, ideally by sequencing without any enrichment or depletion steps during library preparation and with a spike-in for absolute quantification, or by quantification of 1st strand cDNA products of reverse-transcription using oligo-d(T).

Since my experimental design for EV RNA sequencing had a poly(A)-enrichment step, no spike-in was used, and there is no corresponding EV count data, mRNA copy number per EV cannot be estimated (Chapter 3, Materials and Methods). Instead, it was possible to calculate how many EV-associated mRNAs are secreted per number of AB33 filament cells during culture (for detailed calculations, see Appendix to Chapter 5, Table 1). The following values were used for this estimation:

1. Number of cells from which EVs were isolated: ~ 10^{10} cells (Bösch et al., 2016)

2. Total amount of RNA isolated from EVs secreted by above number of cells: 1067 ± 721 ng

3. Assumed percentage of mRNAs in total EV RNA: 5% (Warner, 1999)

4. Median exon length of EV cargo mRNAs: 1181 nt

Based on these values, <u>0.3 to 1.4 mRNAs are secreted per cell, over 15-16 hours of culture</u>. For the most abundant mRNA effector candidate UMAG_11400, <u>one copy is secreted every 91 to 472 cells</u> over the same culture period (Appendix to Chapter 5, Table 1). As UMAG_11400 is continuously upregulated during

biotrophy, peaking at 8 dpi, it may be secreted more frequently *in planta*. Furthermore, there are usually several hyphal cells colonising a single plant cell by 4-6 dpi, so many copies of an mRNA effector could be secreted at the level of hyphal population colonising a single leaf during biotrophic infection. In my opinion, both calculations in cancer cell EVs (Wei et al., 2017) and my own calculations for *U. maydis* presented here are vast underestimates because material losses at each step and the biases introduced by the methods are difficult to account for and have been ignored for practicality.

The economic advantage of transferring effectors in the form of mRNAs instead of proteins would be realised if the delivered mRNAs are sufficiently translated in the host cell, using host resources. If *U. maydis* hyphae are able to secrete and deliver 1 mRNA per cell, every 16 hours, during infection, it could potentially have profound consequences. On average, 2800-9800 protein molecules are produced per mRNA molecule in mammalian cells (Schwanhäusser et al., 2013, Li et al., 2014), and 4800-5600 per mRNA in yeast (Ghaemmaghami et al., 2003, Lu et al., 2007). Hence, a single intact fungal mRNA delivered could theoretically produce thousands of protein molecules in the plant cell, and their physiological effects can be amplified further if they encode enzymes, signalling proteins, or transcription factors. Therefore, the frequency of mRNA secretion via EVs should be sufficient to uphold the hypothesis.

Delivery and translation: points C & D

The intimate contact sites between intramural *U. maydis* hyphae and the maize plasma membrane is the most likely site of EV-mediated exchange. Multiple EV-like structures have been routinely observed at these interfaces but moments of EV secretion or uptake have not been captured so far (Snetselaar and Mims, 1994, Roth et al., 2019, Ludwig et al., 2021). Although direct evidence for EV secretion and uptake during infection is missing, cross-kingdom exchange of EVs between plants and pathogens is a strong possibility, as detailed in the Introduction (Chapter 1). Furthermore, results from applying isolated fungal EVs on plants and vice versa support that cross-kingdom EV uptake may be possible in both directions (Regente et al., 2017, Cai et al., 2018, Bleackley et al., 2020, De Palma et al., 2020).

mRNA cargos in EVs can be delivered to the cytosol of the recipient cell in two major ways: direct fusion of EV and recipient cell plasma membrane, or by endocytosis followed by endosomal escape (van Niel et al., 2018). Both of these delivery routes require interaction of molecules on the EV surface and the plasma membrane of the recipient cell (van Niel et al., 2018). Recently in *U. maydis*, the Stp protein complex found on EV-like membrane "protrusions" that extend beyond the fungal cell wall, was discovered to interact tightly with maize plasma membrane proteins such as aquaporins (Ludwig et al., 2021). This

complex was proposed to form a translocon-like structure akin to the bacterial Type III secretion system (T3SS), through which effectors can be passed directly into the maize cell (Ludwig et al., 2021). The idea of a "translocon" in *U. maydis* was inspired by the interaction of rice aquaporin with the T3SS component Hpa1 in *Xanthomonas oryzae* pv. *oryzae*, which facilitates bacterial effector delivery (Zhang et al., 2019b, Li et al., 2019).

Intriguingly, in *A. thaliana*, aquaporins are internalised by endocytosis upon SA-induced ROS stress (Boursiac et al., 2008) and in metazoan cells, binding of interacting proteins can trigger internalisation of aquaporins (Zhang et al., 2019a). Based on this information, one can speculate the following: *U. maydis* EVs harbouring the "translocon" are endocytosed together with maize aquaporin, then the translocon allows endosomal escape of the intraluminal EV cargo by forming a conduit or by fusion of the EV with the plant endosomal membrane. Hence the idea of a fungal "translocon" complex, is compatible with the concept of effector delivery via EVs and could be a mechanism of mRNA cargo release into the maize cytosol. It would be fascinating to test these hypotheses in the future and their contributions in delivery of effectors in diverse forms.

If mRNA cargos of *U. maydis* EVs are delivered to the maize cytosol, these should theoretically be translatable using the maize translation machinery, given the codon usage of both organisms (Roy and van Staden, 2019, Liu et al., 2009). So far, transfer and translation of EV cargo mRNAs in recipient cells have only been demonstrated between metazoan cells (Ridder et al., 2015, Zomer et al., 2015, Lai et al., 2015), but not at the cross-kingdom level. Still, supporting this possibility, EV-associated mRNAs from the clinically important fungus *Paracoccidioides brasiliensis* could be translated in a rabbit reticulocyte system *in vitro* (Peres da Silva et al., 2019).

In summary, *U. maydis* EV secretion during infection and uptake by maize cells still need to be demonstrated, as well as the mechanism of mRNA release into the maize cytosol. There are interacting fungal and plant membrane proteins that might facilitate uptake and fungal EV cargo release into plant cells. In the future it will be interesting to use the tagged EV marker developed in Chapter 4 in combination with the tagged "translocon" complex to test and track EV secretion and uptake *in planta*. As long as delivered to the correct subcellular location in the plant cell, intact fungal mRNAs could theoretically be translated. So all in all, mRNA effectors can theoretically exist and the hypothesis of fungal mRNA translation in plant cells is still worth pursuing.

5.4.   The next steps for EV cargo mRNA effector candidates

In this thesis, only the mRNA inventory of EVs secreted by AB33 filament cultures have been examined in detail and used for selection of mRNA effector candidates (Chapters 3 & 4). Examining culture EVs have been informative, provided clues to selective loading of mRNAs, and inspired hypotheses for potential function of the mRNAs if delivered to the plant (see discussion of Chapter 3). Unfortunately, relying on culture EV RNA-seq data alone for mRNA effector candidate selection and then testing the candidates one by one proved to be an impractical strategy (Chapter 4). In future, mRNA effector candidates should be narrowed down further to optimal, high-confidence candidates for proof of concept (PoC) experiments to demonstrate fungal mRNA effector transfer and translation in plant cells.

How should we select optimal mRNA effector candidates for PoC? First, we need to characterise RNA and protein cargos of EVs from both cultures and AWF. A critical point for PoC is to distinguish the protein translated *de novo* from the mRNA effector in the plant cell from the protein produced in the fungus and then delivered via EVs. Therefore, an optimal candidate should be enriched and abundant as mRNA in EVs from both sources, but have low protein abundance in EVs. For such future endeavours, I have developed complementary methods to isolate and investigate *U. maydis* EVs from both cultures and AWF of infected plants (Chapters 2 & 4).

Why would we utilise EVs from culture when EVs can be isolated directly from infected leaves? Isolation of EVs from AWF of infected maize is not trivial (Chapter 4, Figure 4-8), let alone purification of fungal EVs from this mixed sample. AWF extraction method is especially destructive for maize (Witzel et al., 2011), which makes it difficult to exclude contamination. The amount of EV-associated RNA that can be obtained from hundreds of infected plants is already very low and only a fraction of that would be from the fungus (Chapter 4). Hence I am of the opinion that AWF EVs are valuable for cross-checking the mRNA effector candidates identified in culture EVs but is impractical to use for other purposes.

The benefit of using cultures for EV isolation is that a relatively large amount of EVs can be obtained from the fungus only. Culture conditions can be controlled to ensure viability (Chapter 2, Figure 2), and it is much easier to apply treatments as necessary. An added advantage of using AB33 is the possibility to synchronously induce several genes relevant for pathogenic, filamentous development in culture as detailed in Chapter 2 and section 5.1. (Brachmann et al., 2001). Main limitations are that AB33 filaments are not developmentally representative of hyphae proliferating *in planta*, they do not express all genes important for infection, and cannot infect plants beyond the first cell (Brachmann et al., 2001).

It may be possible to increase expression of some more infection-relevant genes in culture by using other strains and additional treatments to better mimic hyphae *in planta*. Filamentation can be induced in culture using other infection-competent strains, such as the solopathogenic SG200 or the mating-compatible pair FB1 and FB2, by addition of charcoal (Bölker et al., 1995, Banuett and Herskowitz, 1994). However, EVs can bind to the hydrophobic surface of charcoal particles, which may complicate EV isolation. Treatment with cutin monomers and ER stress-inducing agents such as dithiothreitol or tunicamycin may also enable identification of additional mRNA effector candidates (Bölker et al., 1995, Lanver et al., 2014, Hampel et al., 2016).

Once ideal mRNA effector candidates have been narrowed down, uptake of fungal EVs and translation of their mRNA cargo in plant cells must be demonstrated. EV markers developed for *U. maydis* could be used to show uptake (Chapter 4). PoC for translation of fungal mRNAs in plant cells, however artificial, is required for the hypothesis of mRNA effector to hold. And ultimately, virulence functions must be demonstrated for the translation products of mRNA effector candidates. To the best of my knowledge, all demonstrations of EV cargo mRNA translation in recipient cells have been made using transgenes rather than translational reporter fusions with native EV cargo mRNAs (Lai et al., 2015, Ridder et al., 2015, Zomer et al., 2015). So if the existence of mRNA effectors can be discovered and proven, they may be the first naturally occurring examples.

For the PoC experiments, *U. maydis* culture EVs could be applied to various plant samples. The attempts at PoC experiments using mRNA effector candidates translationally fused to mVenus were hindered by the strong autofluorescence of maize leaves (Figures 4-6 & 4-7). In hindsight, according to the autofluorescence emission spectra of maize leaf tissue when excited with lasers of various wavelengths, mVenus was not the best choice (Cheng, 2006). Tagging with a fluorescent protein better distinguishable from autofluorescence, such as CyOFP1 (Chu et al., 2016), may improve detection (Cheng, 2006). Tissues with less autofluorescence, such as etiolated seedlings or roots, could also be used for infection and EV-uptake experiments, respectively.

Alternatively, generating translational fusions of the mRNA effector candidates with an enzyme such as luciferase or GUS should allow amplification of the signal for improved detection. Furthermore, proteasome inhibitors can be added to accumulate the translation products of mRNA effector candidates. Previously, to demonstrate that in the recipient cells, luciferase proteins are newly translated from mRNAs delivered by EVs, luminescence signals were compared between cells in the presence versus absence of

the translation inhibitor cycloheximide (Lai et al., 2015). A similar strategy could be used to demonstrate translation of *U. maydis* mRNA effectors in plant cells.

Other less biased, high-throughput methods could be used in parallel to the targeted testing of individual candidates for PoC. Adapting methods originally developed for single cell RNA-seq of maize leaf tissues (Bezrutczyk et al., 2021, Marchant et al., 2021), cells that are in intimate contact with intramural fungal hyphae, can be fixed, protoplasted to separate from the fungus, and then cell-sorted for enrichment. RNA sequencing and proteomics of these infected protoplasts could detect fungal mRNAs and proteins that are taken up into plant cells. For testing the hypothesis of fungal mRNA translation using host machinery, ribosome profiling (Chotewutmontri et al., 2018) can be carried out on the infected maize protoplasts. For sorting and enrichment of maize protoplasts, it would be ideal to use a maize line with a fluorescently tagged marker gene especially upregulated when directly colonised by an intramural hypha. This may be a PR gene or even metabolic enzyme based on previous transcriptomic studies of infected maize cell types (Villajuana-Bonequi et al., 2019, Matei et al., 2018). Alternatively, tumour cells could be sorted by nuclear size (hyperplasic bundle sheath cells) or cell size (hypertrophic mesophyll cells) (Matei et al., 2018). So all in all, there are many possibilities and room for improvement in testing transfer and translation of fungal mRNAs in plant cells.

5.5.   Perspectives and additional research questions for *U. maydis* EVs

This thesis has very much focused on the mRNA cargo of *U. maydis* EVs and the hypothesis of effectors transferred in the form of mRNAs. But there are many other types of cargo molecules and interesting research questions regarding EVs in *U. maydis*. In this final section, I will address some basic questions in studying fungal EVs and EV-mediated plant-pathogen interactions and how to approach them using *U. maydis*.

How are EVs produced in *U. maydis*?

Some molecular components involved in biogenesis of exosomes and microvesicles in mammalian cells seem to be conserved in fungi also (van Niel et al., 2018, Rizzo et al., 2021). For example, reverse genetic studies have shown that as in mammalian cells (van Niel et al., 2018), the role of the ESCRT complex in EV production is conserved in various fungi (Oliveira et al., 2010, Zarnowski et al., 2018, Park et al., 2020). It is intriguing that in *U. maydis*, overexpression of the Stp complex in AB33 leads to increased formation of EV-like structures on the cell surface (Ludwig et al., 2021). Furthermore, treatment of *U. maydis* with chitosan induces membrane blebbing beyond the cell wall (Olicón-Hernández et al., 2015). It remains to

be confirmed whether such structures observed on the cell surface are truly EVs and compositionally equivalent to the EVs isolated in culture. So it would be interesting to elucidate mechanisms of EV biogenesis by the means of gene deletion and overexpression strains in *U. maydis,* in combination with stressor or inhibitor treatments. For this purpose, culture EV isolation method developed in Chapter 2 can be utilised, followed by quantitative and qualitative examination of EVs from these strains. Then the strains affected in EV biogenesis can be used in pathogenicity assays to link EVs with a virulence function. Examination of the EV biogenesis mutants throughout the lifecycle stages of *U. maydis* could reveal additional roles such as quorum sensing of sporidia or coordination of spore formation in tumours at the population level.

How are EVs secreted past the fungal cell wall?

How precisely EVs are secreted past the fungal cell wall is a question that remains to be answered. A convincing idea is that cell wall modifying enzymes are associated with the surface of EVs and pave their way through the cell wall. In ultrastructural observations of *U. maydis* hyphae in plants, the fungal cell wall is more diffuse at sites where EV-like structures accumulate (Snetselaar and Mims, 1994). Supporting this idea, cell wall modifying enzymes have been found in proteomes of fungal EVs (Nimrichter et al., 2016, Zhao et al., 2019), as well as in EVs of plants and bacteria that also have cell walls (de la Canal and Pinedo, 2018, Lee et al., 2009). Whether such cell wall-related enzymes are associated with *U. maydis* EVs can be revealed by proteomic investigations in the future and it would be possible to test if EV secretion is affected in cell wall-related mutants in *U. maydis* (Robledo-Briones and Ruiz-Herrera, 2013, Langner et al., 2015, Tanaka et al., 2020).

What factors allow selective loading of EV cargos?

According to the data presented in Chapter 3, the mRNAs enriched in EVs relative to filament cells seem to differ in subcellular localisation and functionality from those that are depleted from EVs. Factors that mediate targeting of a given molecule to the sites of EV biogenesis, such as surface of endosomes or in the cell periphery would be interesting to examine. Deletion of membrane-associated proteins in fungi have been shown to affect mRNA cargo composition of EVs; for example, the Golgi reassembly stacking protein (GRASP) (Peres da Silva et al., 2018) in *C. neoformans* and the endocytic adaptor protein Cin1 in *C. deneoformans* (Liu et al., 2020). However, RBPs would be more relevant for elucidating the specificity of mRNA loading into EVs. In *U. maydis*, one could investigate the potential role of the endosome-associated mRNA transport machinery and its core RBP Rrm4 in loading of mRNAs into EVs (Baumann et al., 2014,

Pohlmann et al., 2015). For future analyses it would be interesting to see if targets of previously characterised *U. maydis* RBPs such as Rrm4, Grp1 (Olgeiser et al., 2019), and Khd4 ((Vollmeister et al., 2009); personal communication Srimeenakshi Sankaranarayanan) in *U. maydis* are enriched in EVs.

Are fungal EVs taken up into plant cells and what is the fate of their cargos?

Currently there is no mechanistic explanation for how plants take up EVs. Where the biotrophic hyphae of *U. maydis* are within the plant cell walls, growing in intimate contact with the plant plasma membrane, is a likely site of EV-mediated exchange. As discussed above in 5.3., interaction between molecules on fungal EVs with plant plasma membrane proteins could mediate endocytosis of fungal EVs into plant cells (Boursiac et al., 2008, Ludwig et al., 2021). Since more diverse genetic resources and experimental tools are available in model plant species than in maize, it may be easier to track the uptake and fate of *U. maydis* culture EVs in non-host systems such as *A. thaliana* or tobacco. For example, the necrosis-inducing effects of EVs from the cotton pathogen *F. oxysporum* f.sp. *vasinfectum* have been demonstrated by infiltration into both the natural host as well as tobacco, although the mechanism of EV uptake or necrosis-inducing cargo delivery is as yet unknown (Bleackley et al., 2020).

To study the fate of RNA cargos of *U. maydis* EVs in maize, it would be worth checking whether there are *U. maydis* RNAs bound to not only maize ribosomes but also Argonaute proteins. If fungal mRNAs are detected in ribosome profiling of infected maize, it would support the hypothesis of mRNA effectors. If *U. maydis* RNA fragments are detected in AGO proteins of maize, it would support the hypothesis of pathogen-induced gene silencing instead. Such experiments could discover novel *U. maydis* RNA effectors in the form of both mRNAs and non-canonical sRNA effectors comparable to the conventional tasiRNA or miRNA effectors in other fungi that harbour RNAi machineries (Weiberg et al., 2013, Wang et al., 2017, Jian and Liang, 2019, Dunker et al., 2020, Ji et al., 2021).

Concluding remarks

In this thesis, I have presented the first characterisation of mRNA cargos of EVs from a phytopathogenic fungus and laid the foundation for investigation of EVs in *U. maydis*. Based on the findings of this work and others, the novel idea of pathogen effector transfer in the form of mRNAs and their translation in the host cell seems theoretically plausible. With the tools and methods developed here, it will be possible to discover and examine in depth novel forms of EV-associated effectors and study basic questions regarding EVs in the archetypal smut pathogen *U. maydis*.

5.6. Appendix to Chapter 5

Table 5-1 Calculating mRNA secretion from AB33 filaments	
Explanation	**Calculation**
Mean mass of total EV RNA from 4x biological replicates	1067 ± 721 ng
Mass of mRNAs assuming ~5% of total EV RNA are mRNAs (Warner, 1999)	0.05 * (1067 ± 721 ng total RNA) = **53.35 ± 36.05 ng mRNA**
Copies of mRNA given the median length of mRNAs in *U. maydis* EVs (1181 nt) calculated with NEBioCalculator® version 1.15.0 Formula for RNA copy number: (6.022×10^{23}) * (mass of ssRNA (g)) / ((length of ssRNA (nt) x 321.47 g/mol) + 18.02 g/mol)	(6.022×10^{23}) * (53.35 ± 36.05 ng mRNA * 10^{-9}) / ((1181 nt * 321.47 g/mol) + 18.02 g/mol) = **8.46 ± 5.72 x 10^{10} copies of mRNA**
Cell concentration when OD_{600} = 1 (Bösch et al., 2016) multiplied by the volume of culture supernatant from which EVs were isolated	(1 to 2 x 10^7 cells per ml) * 816 ml = 8.16 x 10^9 ~ 1.63 x 10^{10} cells **assumed to be ~10^{10} cells**
Number of mRNAs secreted per cell	8.46 ± 5.72 x 10^{10} copies of mRNA / 10^{10} cells = **0.85 ± 0.57 mRNAs** **ie. 0.27 to 1.41 mRNAs secreted per cell,** **over 15-16 hour culture period**
Number of mRNAs secreted per cell corrected for losses after two rounds of RNA extraction with TRI-reagent® LS, assuming ~60% RNA recovery in each round	0.85 ± 0.57 mRNAs / (0.6^2) = 2.35 ± 1.59 mRNAs **ie. 0.76 to 3.94 mRNAs secreted per cell,** **over 15-16 hour culture period**
Copy of UMAG_11400 mRNA (7715 TPM) per number of cells	$(7715 / 10^6)$ * 8.46 ± 5.72 x 10^{10} mRNAs in total = 6.53 ± 4.41 x 10^8 copies ie. 2.12 x 10^8 to 1.09 x 10^9 copies of UMAG_11400 mRNA secreted in total 1 / (2.12 x 10^8 / 10^{10}) = 472.02 1 / (1.09 x 10^9 / 10^{10}) = 91.430 **ie. 1 copy of UMAG_11400 mRNA in** **every 91 to 472 cells** Alternatively, factoring in losses from RNA extraction: 2.12 x 10^8 to 1.09 x 10^9 copies / (0.6^2) = 5.88 x 10^8 to 3.04 x 10^9 copies of UMAG_11400 mRNA secreted in total 1 / (5.88 x 10^8 / 10^{10}) = 169.93 1 / (3.04 x 10^9 / 10^{10}) = 32.92

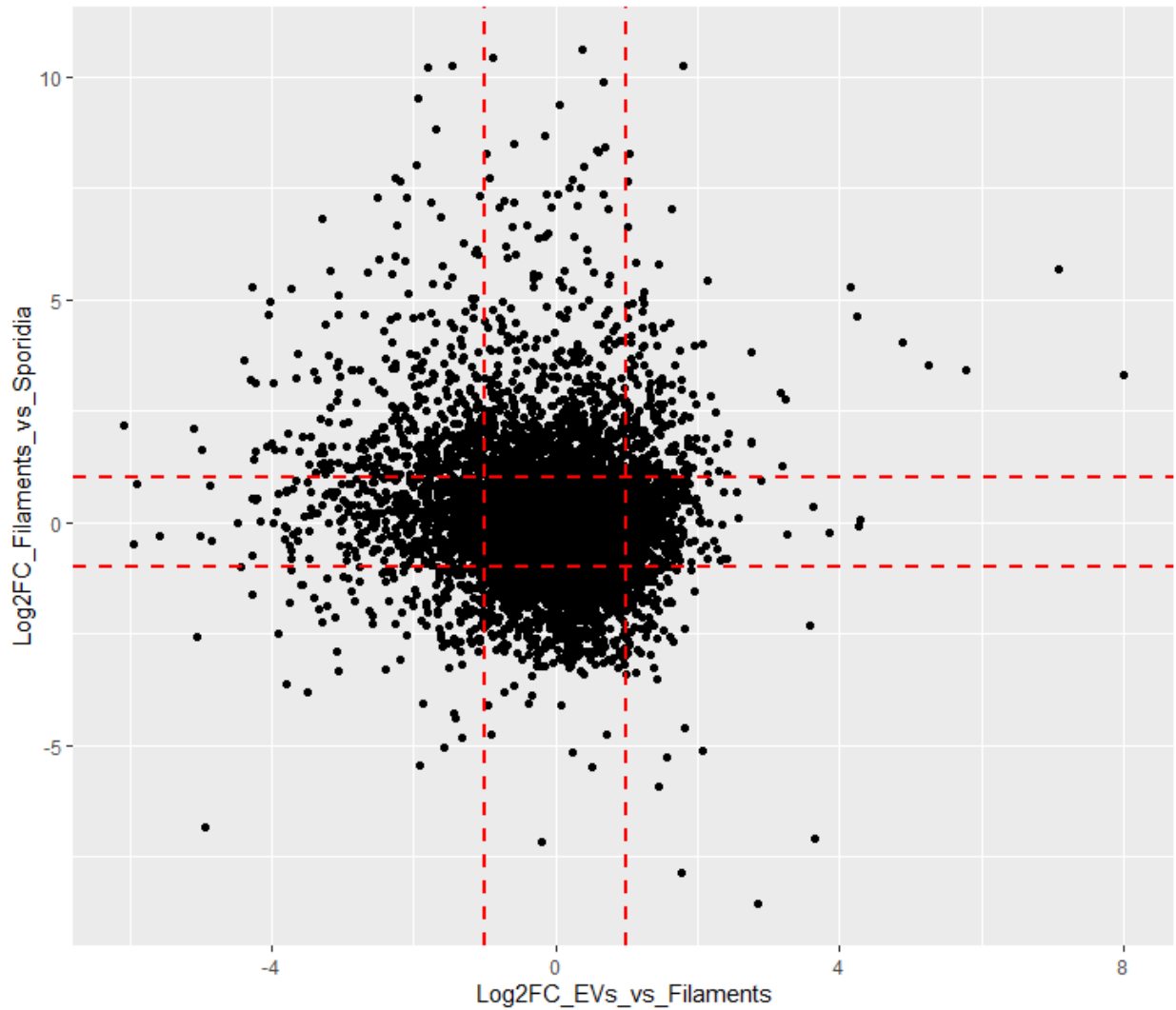|	ie. 1 copy of UMAG_11400 mRNA in every 33 to 167 cells, over 15-16 hour culture period

Figure 5-1. Correlation between enrichment in EVs and differential expression during developmental switch from sporidia to filaments. Transcripts that are downregulated in AB33 filaments versus sporidia are not more enriched in EVs.

5.7. References

ARROYO, J. D., CHEVILLET, J. R., KROH, E. M., RUF, I. K., PRITCHARD, C. C., GIBSON, D. F., MITCHELL, P. S., BENNETT, C. F., POGOSOVA-AGADJANYAN, E. L., STIREWALT, D. L., TAIT, J. F. & TEWARI, M. 2011. Argonaute2 complexes carry a population of circulating microRNAs independent of vesicles in human plasma. *Proceedings of the National Academy of Sciences,* 108**,** 5003-5008.

BANUETT, F. & HERSKOWITZ, I. 1994. Morphological Transitions in the Life Cycle of Ustilago maydis and Their Genetic Control by the a and b Loci. *Experimental Mycology,* 18**,** 247-266.

BAUMANN, S., KONIG, J., KOEPKE, J. & FELDBRUGGE, M. 2014. Endosomal transport of septin mRNA and protein indicates local translation on endosomes and is required for correct septin filamentation. *Embo Reports,* 15**,** 94-102.

BEZRUTCZYK, M., ZÖLLNER, N. R., KRUSE, C. P. S., HARTWIG, T., LAUTWEIN, T., KÖHRER, K., FROMMER, W. B. & KIM, J.-Y. 2021. Evidence for phloem loading via the abaxial bundle sheath cells in maize leaves. *The Plant Cell,* 33**,** 531-547.

BLEACKLEY, M., SAMUEL, M., GARCIA-CERON, D., MCKENNA, J. A., LOWE, R. G. T., PATHAN, M., ZHAO, K. N., ANG, C. S., MATHIVANAN, S. & ANDERSON, M. A. 2020. Extracellular Vesicles From the Cotton Pathogen *Fusarium oxysporum* f. sp. *vasinfectum* Induce a Phytotoxic Response in Plants. *Frontiers in Plant Science,* 10.

BÖLKER, M., GENIN, S., LEHMLER, C. & KAHMANN, R. 1995. Genetic regulation of mating and dimorphism in Ustilago maydis. *Canadian Journal of Botany,* 73**,** 320-325.

BÖSCH, K., FRANTZESKAKIS, L., VRANES, M., KÄMPER, J., SCHIPPER, K. & GÖHRE, V. 2016. Genetic Manipulation of the Plant Pathogen Ustilago maydis to Study Fungal Biology and Plant Microbe Interactions. *J Vis Exp*.

BOURSIAC, Y., BOUDET, J., POSTAIRE, O., LUU, D. T., TOURNAIRE-ROUX, C. & MAUREL, C. 2008. Stimulus-induced downregulation of root water transport involves reactive oxygen species-activated cell signalling and plasma membrane intrinsic protein internalization. *Plant J,* 56**,** 207-218.

BRACHMANN, A., WEINZIERL, G., KAMPER, J. & KAHMANN, R. 2001. Identification of genes in the bW/bE regulatory cascade in *Ustilago maydis*. *Molecular Microbiology,* 42**,** 1047-1063.

BREFORT, T., TANAKA, S., NEIDIG, N., DOEHLEMANN, G., VINCON, V. & KAHMANN, R. 2014. Characterization of the largest effector gene cluster of Ustilago maydis. *PLoS pathogens,* 10**,** e1003866-e1003866.

CAI, Q., QIAO, L., WANG, M., HE, B., LIN, F. M., PALMQUIST, J., HUANG, S. D. & JIN, H. 2018. Plants send small RNAs in extracellular vesicles to fungal pathogen to silence virulence genes. *Science,* 360**,** 1126-1129.

CHENG, P.-C. 2006. Interaction of Light with Botanical Specimens. *In:* PAWLEY, J. B. (ed.) *Handbook Of Biological Confocal Microscopy.* Boston, MA: Springer US.

CHOTEWUTMONTRI, P., STIFFLER, N., WATKINS, K. P. & BARKAN, A. 2018. Ribosome Profiling in Maize. *Methods Mol Biol,* 1676**,** 165-183.

CHU, J., OH, Y., SENS, A., ATAIE, N., DANA, H., MACKLIN, J. J., LAVIV, T., WELF, E. S., DEAN, K. M., ZHANG, F., KIM, B. B., TANG, C. T., HU, M., BAIRD, M. A., DAVIDSON, M. W., KAY, M. A., FIOLKA, R., YASUDA, R., KIM, D. S., NG, H. L. & LIN, M. Z. 2016. A bright cyan-excitable orange fluorescent protein facilitates dual-emission microscopy and enhances bioluminescence imaging in vivo. *Nat Biotechnol,* 34**,** 760-7.

DE LA CANAL, L. & PINEDO, M. 2018. Extracellular vesicles: a missing component in plant cell wall remodeling. *Journal of Experimental Botany,* 69**,** 4655-4658.

DE PALMA, M., AMBROSONE, A., LEONE, A., DEL GAUDIO, P., RUOCCO, M., TURIÁK, L., BOKKA, R., FIUME, I., TUCCI, M. & POCSFALVI, G. 2020. Plant Roots Release Small Extracellular Vesicles with Antifungal Activity. *Plants,* 9**,** 1777.

DOEHLEMANN, G., REISSMANN, S., ASSMANN, D., FLECKENSTEIN, M. & KAHMANN, R. 2011. Two linked genes encoding a secreted effector and a membrane protein are essential for Ustilago maydis-induced tumour formation. *Mol Microbiol,* 81**,** 751-66.

DOEHLEMANN, G., VAN DER LINDE, K., ASSMANN, D., SCHWAMMBACH, D., HOF, A., MOHANTY, A., JACKSON, D. & KAHMANN, R. 2009. Pep1, a secreted effector protein of Ustilago maydis, is required for successful invasion of plant cells. *PLoS Pathog,* 5**,** e1000290.

DUNKER, F., TRUTZENBERG, A., ROTHENPIELER, J. S., KUHN, S., PROLS, R., SCHREIBER, T., TISSIER, A., KEMEN, A., KEMEN, E., HUCKELHOVEN, R. & WEIBERG, A. 2020. Oomycete small RNAs bind to the plant RNA-induced silencing complex for virulence. *Elife,* 9.

FUENTES-IGLESIAS, A., GARCIA-OUTEIRAL, V., PARDAVILA, J. A., WANG, J., FIDALGO, M. & GUALLAR, D. 2020. An Optimized Immunoprecipitation Protocol for Assessing Protein-RNA Interactions In Vitro. *STAR Protocols,* 1**,** 100093.

GARCÍA-MUSE, T., STEINBERG, G. & PÉREZ-MARTÍN, J. 2003. Pheromone-induced G2 arrest in the phytopathogenic fungus Ustilago maydis. *Eukaryot Cell,* 2**,** 494-500.

GHAEMMAGHAMI, S., HUH, W.-K., BOWER, K., HOWSON, R. W., BELLE, A., DEPHOURE, N., O'SHEA, E. K. & WEISSMAN, J. S. 2003. Global analysis of protein expression in yeast. *Nature,* 425**,** 737-741.

HAMPEL, M., JAKOBI, M., SCHMITZ, L., MEYER, U., FINKERNAGEL, F., DOEHLEMANN, G. & HEIMEL, K. 2016. Unfolded Protein Response (UPR) Regulator Cib1 Controls Expression of Genes Encoding Secreted Virulence Factors in Ustilago maydis. *PLOS ONE,* 11**,** e0153861.

HEIMEL, K., FREITAG, J., HAMPEL, M., AST, J., BÖLKER, M. & KÄMPER, J. 2013. Crosstalk between the Unfolded Protein Response and Pathways That Regulate Pathogenic Development in Ustilago maydis *The Plant Cell,* 25**,** 4262-4277.

HEIMEL, K., SCHERER, M., SCHULER, D. & KAMPER, J. 2010a. The Ustilago maydis Clp1 Protein Orchestrates Pheromone and b-Dependent Signaling Pathways to Coordinate the Cell Cycle and Pathogenic Development. *Plant Cell,* 22**,** 2908-2922.

HEIMEL, K., SCHERER, M., VRANES, M., WAHL, R., POTHIRATANA, C., SCHULER, D., VINCON, V., FINKERNAGEL, F., FLOR-PARRA, I. & KAMPER, J. 2010b. The Transcription Factor Rbf1 Is the Master Regulator for b-Mating Type Controlled Pathogenic Development in *Ustilago maydis*. *Plos Pathogens,* 6.

JI, H.-M., MAO, H.-Y., LI, S.-J., FENG, T., ZHANG, Z.-Y., CHENG, L., LUO, S.-J., BORKOVICH, K. A. & OUYANG, S.-Q. 2021. Fol-milR1, a pathogenicity factor of Fusarium oxysporum, confers tomato wilt disease resistance by impairing host immune responses. *New Phytologist,* n/a.

JIAN, J. & LIANG, X. 2019. One Small RNA of *Fusarium graminearum* Targets and Silences CEBiP Gene in Common Wheat. *Microorganisms,* 7.

LAI, C. P., KIM, E. Y., BADR, C. E., WEISSLEDER, R., MEMPEL, T. R., TANNOUS, B. A. & BREAKEFIELD, X. O. 2015. Visualization and tracking of tumour extracellular vesicle delivery and RNA translation using multiplexed reporters. *Nature Communications,* 6.

LANGNER, T., ÖZTÜRK, M., HARTMANN, S., CORD-LANDWEHR, S., MOERSCHBACHER, B., WALTON, J. D. & GÖHRE, V. 2015. Chitinases Are Essential for Cell Separation in Ustilago maydis. *Eukaryotic cell,* 14**,** 846-857.

LANVER, D., BERNDT, P., TOLLOT, M., NAIK, V., VRANES, M., WARMANN, T., MÜNCH, K., RÖSSEL, N. & KAHMANN, R. 2014. Plant Surface Cues Prime Ustilago maydis for Biotrophic Development. *PLOS Pathogens,* 10**,** e1004272.

LANVER, D., MULLER, A. N., HAPPEL, P., SCHWEIZER, G., HAAS, F. B., FRANITZA, M., PELLEGRIN, C., REISSMANN, S., ALTMULLER, J., RENSING, S. A. & KAHMANN, R. 2018. The Biotrophic Development of Ustilago maydis Studied by RNA-Seq Analysis. *Plant Cell,* 30**,** 300-323.

LAUTZ, J. D., GNIFFKE, E. P., BROWN, E. A., IMMENDORF, K. B., MENDEL, R. D. & SMITH, S. E. P. 2019. Activity-dependent changes in synaptic protein complex composition are consistent in different detergents despite differential solubility. *Scientific reports,* 9**,** 10890-10890.

LEE, E.-Y., CHOI, D.-Y., KIM, D.-K., KIM, J.-W., PARK, J. O., KIM, S., KIM, S.-H., DESIDERIO, D. M., KIM, Y.-K., KIM, K.-P. & GHO, Y. S. 2009. Gram-positive bacteria produce membrane vesicles: Proteomics-based characterization of Staphylococcus aureus-derived membrane vesicles. *PROTEOMICS,* 9**,** 5425-5436.

LI, J. J., BICKEL, P. J. & BIGGIN, M. D. 2014. System wide analyses have underestimated protein abundances and the importance of transcription in mammals. *PeerJ,* 2**,** e270-e270.

LI, P., ZHANG, L., MO, X., JI, H., BIAN, H., HU, Y., MAJID, T., LONG, J., PANG, H., TAO, Y., MA, J. & DONG, H. 2019. Rice aquaporin PIP1;3 and harpin Hpa1 of bacterial blight pathogen cooperate in a type III effector translocation. *Journal of Experimental Botany,* 70**,** 3057-3073.

LIU, H., HE, R., ZHANG, H., HUANG, Y., TIAN, M. & ZHANG, J. 2009. Analysis of synonymous codon usage in Zea mays. *Molecular Biology Reports,* 37**,** 677.

LIU, M., ZHANG, Z., DING, C., WANG, T., KELLY, B. & WANG, P. 2020. Transcriptomic Analysis of Extracellular RNA Governed by the Endocytic Adaptor Protein Cin1 of Cryptococcus deneoformans. *Frontiers in Cellular and Infection Microbiology,* 10.

LU, P., VOGEL, C., WANG, R., YAO, X. & MARCOTTE, E. M. 2007. Absolute protein expression profiling estimates the relative contributions of transcriptional and translational regulation. *Nature Biotechnology,* 25**,** 117-124.

LUDWIG, N., REISSMANN, S., SCHIPPER, K., GONZALEZ, C., ASSMANN, D., GLATTER, T., MORETTI, M., MA, L. S., REXER, K. H., SNETSELAAR, K. & KAHMANN, R. 2021. A cell surface-exposed protein complex with an essential virulence function in *Ustilago maydis*. *Nature Microbiology*.

MARCHANT, D. B., NELMS, B. & WALBOT, V. 2021. Quantitative cell release from plant tissues for single-cell genomics. *bioRxiv***,** 2021.10.11.463960.

MATEI, A., ERNST, C., GÜNL, M., THIELE, B., ALTMÜLLER, J., WALBOT, V., USADEL, B. & DOEHLEMANN, G. 2018. How to make a tumour: cell type specific dissection of Ustilago maydis-induced tumour development in maize leaves. *New Phytologist,* 217**,** 1681-1695.

MICHELL, D. L. & VICKERS, K. C. 2016. Lipoprotein carriers of microRNAs. *Biochimica et biophysica acta,* 1861**,** 2069-2074.

MUKHERJEE, D., GUPTA, S., GHOSH, A. & GHOSH, A. 2020. *Ustilago maydis* secreted T2 ribonucleases, Nuc1 and Nuc2 scavenge extracellular RNA. *Cellular Microbiology,* 22**,** e13256.

NIMRICHTER, L., DE SOUZA, M. M., DEL POETA, M., NOSANCHUK, J. D., JOFFE, L., TAVARES, P. D. M. & RODRIGUES, M. L. 2016. Extracellular Vesicle-Associated Transitory Cell Wall Components and Their Impact on the Interaction of Fungi with Host Cells. *Frontiers in Microbiology,* 7.

OLGEISER, L., HAAG, C., BOERNER, S., ULE, J., BUSCH, A., KOEPKE, J., KONIG, J., FELDBRUGGE, M. & ZARNACK, K. 2019. The key protein of endosomal mRNP transport Rrm4 binds translational landmark sites of cargo mRNAs. *Embo Reports,* 20.

OLICÓN-HERNÁNDEZ, D. R., HERNÁNDEZ-LAUZARDO, A. N., PARDO, J. P., PEÑA, A., VELÁZQUEZ-DEL VALLE, M. G. & GUERRA-SÁNCHEZ, G. 2015. Influence of chitosan and its derivatives on cell development and physiology of Ustilago maydis. *Int J Biol Macromol,* 79**,** 654-60.

OLIVEIRA, D. L., NAKAYASU, E. S., JOFFE, L. S., GUIMARÃES, A. J., SOBREIRA, T. J. P., NOSANCHUK, J. D., CORDERO, R. J. B., FRASES, S., CASADEVALL, A., ALMEIDA, I. C., NIMRICHTER, L. & RODRIGUES, M. L. 2010. Characterization of Yeast Extracellular Vesicles: Evidence for the Participation of Different Pathways of Cellular Traffic in Vesicle Biogenesis. *PLOS ONE,* 5**,** e11113.

PARK, Y.-D., CHEN, S. H., CAMACHO, E., CASADEVALL, A., WILLIAMSON, P. R. & NOVERR, M. C. 2020. Role of the ESCRT Pathway in Laccase Trafficking and Virulence of Cryptococcus neoformans. *Infection and Immunity,* 88**,** e00954-19.

PERES DA SILVA, R., LONGO, L. G. V., CUNHA, J., SOBREIRA, T. J. P., RODRIGUES, M. L., FAORO, H., GOLDENBERG, S., ALVES, L. R. & PUCCIA, R. 2019. Comparison of the RNA Content of Extracellular Vesicles Derived from *Paracoccidioides brasiliensis* and *Paracoccidioides lutzii*. *Cells,* 8.

PERES DA SILVA, R., MARTINS, S. D. T., RIZZO, J., DOS REIS, F. C. G., JOFFE, L. S., VAINSTEIN, M., KMETZSCH, L., OLIVEIRA, D. L., PUCCIA, R., GOLDENBERG, S., RODRIGUES, M. L. & ALVES, L. R. 2018. Golgi Reassembly and Stacking Protein (GRASP) Participates in Vesicle-Mediated RNA Export in Cryptococcus Neoformans. *Genes,* 9**,** 400.

PINTER, N., HACH, C. A., HAMPEL, M., REKHTER, D., ZIENKIEWICZ, K., FEUSSNER, I., POEHLEIN, A., DANIEL, R., FINKERNAGEL, F. & HEIMEL, K. 2019. Signal peptide peptidase activity connects the unfolded protein response to plant defense suppression by Ustilago maydis. *PLOS Pathogens,* 15**,** e1007734.

POHLMANN, T., BAUMANN, S., HAAG, C., ALBRECHT, M. & FELDBRUGGE, M. 2015. A FYVE zinc finger domain protein specifically links mRNA transport to endosome trafficking. *Elife,* 4.

REGENTE, M., PINEDO, M., SAN CLEMENTE, H., BALLIAU, T., JAMET, E. & DE LA CANAL, L. 2017. Plant extracellular vesicles are incorporated by a fungal pathogen and inhibit its growth. *J Exp Bot,* 68**,** 5485-5495.

RIDDER, K., SEVKO, A., HEIDE, J., DAMS, M., RUPP, A. K., MACAS, J., STARMANN, J., TJWA, M., PLATE, K. H., SULTMANN, H., ALTEVOGT, P., UMANSKY, V. & MOMMA, S. 2015. Extracellular vesicle-mediated transfer of functional RNA in the tumor microenvironment. *Oncoimmunology,* 4.

RIZZO, J., TAHERALY, A. & JANBON, G. 2021. Structure, composition and biological properties of fungal extracellular vesicles. *microLife,* 2.

ROBLEDO-BRIONES, M. & RUIZ-HERRERA, J. 2013. Regulation of genes involved in cell wall synthesis and structure during Ustilago maydis dimorphism. *FEMS Yeast Research,* 13**,** 74-84.

RODRIGUES, M. L., NIMRICHTER, L., OLIVEIRA, D. L., FRASES, S., MIRANDA, K., ZARAGOZA, O., ALVAREZ, M., NAKOUZI, A., FELDMESSER, M. & CASADEVALL, A. 2007. Vesicular polysaccharide export in *Cryptococcus neoformans* is a eukaryotic solution to the problem of fungal trans-cell wall transport. *Eukaryotic Cell,* 6**,** 48-59.

ROTH, R., HILLMER, S., FUNAYA, C., CHIAPELLO, M., SCHUMACHER, K., LO PRESTI, L., KAHMANN, R. & PASZKOWSKI, U. 2019. Arbuscular cell invasion coincides with extracellular vesicles and membrane tubules. *Nat Plants,* 5**,** 204-211.

ROY, A. & VAN STADEN, J. 2019. Comprehensive profiling of codon usage signatures and codon context variations in the genus Ustilago. *World Journal of Microbiology and Biotechnology,* 35**,** 118.

RUTTER, B. D. & INNES, R. W. 2020. Growing pains: addressing the pitfalls of plant extracellular vesicle research. *New Phytologist,* 228**,** 1505-1510.

SCHMITZ, L., SCHWIER, M. A., HEIMEL, K. & LIN, X. 2019. The Unfolded Protein Response Regulates Pathogenic Development of Ustilago maydis by Rok1-Dependent Inhibition of Mating-Type Signaling. *mBio,* 10**,** e02756-19.

SCHWANHÄUSSER, B., BUSSE, D., LI, N., DITTMAR, G., SCHUCHHARDT, J., WOLF, J., CHEN, W. & SELBACH, M. 2013. Corrigendum: Global quantification of mammalian gene expression control. *Nature,* 495**,** 126-7.

SNETSELAAR, K. M. & MIMS, C. W. 1994. Light and Electron-Microscopy of *Ustilago maydis* Hyphae in Maize. *Mycological Research,* 98**,** 347-355.

TANAKA, S., GOLLIN, I., ROSSEL, N. & KAHMANN, R. 2020. The functionally conserved effector Sta1 is a fungal cell wall protein required for virulence in *Ustilago maydis*. *New Phytologist,* 227**,** 185-199.

TERFRUCHTE, M., WEWETZER, S., SARKARI, P., STOLLEWERK, D., FRANZ-WACHTEL, M., MACEK, B., SCHLEPUTZ, T., FELDBRUGGE, M., BUCHS, J. & SCHIPPER, K. 2018. Tackling destructive proteolysis of unconventionally secreted heterologous proteins in *Ustilago maydis*. *Journal of Biotechnology,* 284**,** 37-51.

VAN NIEL, G., D'ANGELO, G. & RAPOSO, G. 2018. Shedding light on the cell biology of extracellular vesicles. *Nature Reviews Molecular Cell Biology,* 19**,** 213-228.

VILLAJUANA-BONEQUI, M., MATEI, A., ERNST, C., HALLAB, A., USADEL, B. & DOEHLEMANN, G. 2019. Cell type specific transcriptional reprogramming of maize leaves during Ustilago maydis induced tumor formation. *Scientific Reports,* 9**,** 10227.

VOLLMEISTER, E., HAAG, C., ZARNACK, K., BAUMANN, S., KÖNIG, J., MANNHAUPT, G. & FELDBRÜGGE, M. 2009. Tandem KH domains of Khd4 recognize AUACCC and are essential for regulation of morphology as well as pathogenicity in Ustilago maydis. *Rna,* 15**,** 2206-18.

WANG, M., WEIBERG, A., DELLOTA, E., YAMANE, D. & JIN, H. L. 2017. Botrytis small RNA Bc-siR37 suppresses plant defense genes by cross-kingdom RNAi. *Rna Biology,* 14**,** 421-428.

WARNER, J. R. 1999. The economics of ribosome biosynthesis in yeast. *Trends in Biochemical Sciences,* 24**,** 437-440.

WEI, Z., BATAGOV, A. O., SCHINELLI, S., WANG, J., WANG, Y., EL FATIMY, R., RABINOVSKY, R., BALAJ, L., CHEN, C. C., HOCHBERG, F., CARTER, B., BREAKEFIELD, X. O. & KRICHEVSKY, A. M. 2017. Coding and noncoding landscape of extracellular RNA released by human glioma stem cells. *Nature Communications,* 8**,** 1145.

WEIBERG, A., WANG, M., LIN, F. M., ZHAO, H. W., ZHANG, Z. H., KALOSHIAN, I., HUANG, H. D. & JIN, H. L. 2013. Fungal Small RNAs Suppress Plant Immunity by Hijacking Host RNA Interference Pathways. *Science,* 342**,** 118-123.

WITZEL, K., SHAHZAD, M., MATROS, A., MOCK, H. P. & MUHLING, K. H. 2011. Comparative evaluation of extraction methods for apoplastic proteins from maize leaves. *Plant Methods,* 7.

ZARNOWSKI, R., SANCHEZ, H., COVELLI, A. S., DOMINGUEZ, E., JAROMIN, A., BERNHARDT, J., MITCHELL, K. F., HEISS, C., AZADI, P., MITCHELL, A. & ANDES, D. R. 2018. *Candida albicans* biofilm-induced vesicles confer drug resistance through matrix biogenesis. *Plos Biology,* 16.

ZHANG, L., CHEN, L. & DONG, H. 2019a. Plant Aquaporins in Infection by and Immunity Against Pathogens – A Critical Review. *Frontiers in Plant Science,* 10.

ZHANG, L., HU, Y., LI, P., WANG, X. & DONG, H. 2019b. Silencing of an aquaporin gene diminishes bacterial blight disease in rice. *Australasian Plant Pathology,* 48**,** 143-158.

ZHAO, K. N., BLEACKLEY, M., CHISANGA, D., GANGODA, L., FONSEKA, P., LIEM, M., KALRA, H., AL SAFFAR, H., KEERTHIKUMAR, S., ANG, C. S., ADDA, C. G., JIANG, L. Z., YAP, K., POON, I. K., LOCK, P., BULONE, V., ANDERSON, M. & MATHIVANAN, S. 2019. Extracellular vesicles secreted by *Saccharomyces cerevisiae* are involved in cell wall remodelling. *Communications Biology,* 2.

ZOMER, A., MAYNARD, C., VERWEIJ, F. J., KAMERMANS, A., SCHÄFER, R., BEERLING, E., SCHIFFELERS, R. M., DE WIT, E., BERENGUER, J., ELLENBROEK, S. I. J., WURDINGER, T., PEGTEL, D. M. & VAN RHEENEN, J. 2015. In Vivo imaging reveals extracellular vesicle-mediated phenocopying of metastatic behavior. *Cell,* 161**,** 1046-1057.

Acknowledgements

First and foremost, I would like to thank my PhD supervisor, Prof. Dr. Michael Feldbrügge, for a rather unique PhD experience with an unusual amount of intellectual freedom to explore. Looking back, all the frustrations and lack of positive results aside, I still couldn't have chosen a better place and organism for the "crazy" project I had designed. The last 5 years or so have certainly been a challenge and pushed me to grow both intellectually and personally. Although I never got the publication of my dreams, you let me learn to be independent and resourceful, taught me how to navigate through academia, and write a successful grant proposal. There were many valuable life lessons. Thank you.

I am grateful to all our collaborators for helping us embark on our journey with EVs, without whose support and goodwill, this project would never have gotten off the ground: Dr. Libera Lo Presti, a brilliant mind and a kind soul, without whom I would have been very, very lost and alone in the first years of the PhD; Dr. Andreas Brachmann, for all the sound advice, reliable support, and intellectual energy; Oliver Rupp, Dr. Christopher Blum, and Anton Kraege for their computer wizardry; Dr. Jafargholi Imani and Christina Birkenstock for propagating the maize seeds; Dr. Sebastian Hänsch and Marion Nissen at the CAi for helping me with the microscopes; Sachiko Kolar for technical support with strain generation.

A great thank you to members of the iGRAD-Plant graduate school for kindly letting me use equipment and reagents in your labs, and for all the good times with PBS pizza; Prof. Dr. Laura Rose for being my mentor; Dr. Vera Göhre for being my resident mentor at the institute, painstakingly guiding me through the thesis writing period; Dr. Petra Fackendahl and Dr. Sigrun Wegener-Feldbrügge for all the organisational matters.

All my colleagues/former colleagues at the institute, thank you for being there, for all the discussions, and for putting up with me. Thanks for all the moments of kindness, shared laughter, and commiseration. Katie, Marta, Diana, and Ute, thanks for helping me feel settled down in the lab. the overzealous, desperate night-/weekend-/lockdown-shifters, we have been a family during the pandemic, hope you all get a life soon. Special thanks to Vera, Kai, Sri, Lesley, Minerva, Trusha, Lilli, and Magnus for helping me with various parts of the thesis and the submission procedure. Thank you so much Uli for solving so many day-to-day problems.

Finally, I would like to thank all my friends and family who have supported me throughout these trying times. Thank you for lending an ear, a shoulder to cry/lean on, for food and hugs. Sarah, Chris, and Cora, thanks for being my extended family here, Diana, Peter & Raphaela, Michèle & André for helping me feel at home in Düsseldorf. Sri, Senthil, Summia, Minerva, you are my heroes, thanks for all the discussions, encouragement, and inspiration. Pietro, 이용환 선생님, 이인원 선생님, 박숙영 선생님, 성범이형, 기태형, thank you for motivating me and for all the moral support. I thank my cousins and friends outside the university for reminding me there's more to life. Last but certainly not least, 사랑하는 우리 엄마, 항상 기다려줘서 고마워요.